KU LEUVEN

ARENBERG DOCTORAL SCHOOL
Faculty of Engineering Science

Machine Learning on Belgian Health Expenditure Data

Data-driven screening for type 2 diabetes

Marc Claesen

Supervisor:
Prof. dr. ir. Bart De Moor

Co-supervisor:
Prof. dr. ir. dr. Frank De Smet

Dissertation presented in partial fulfillment of the requirements for the degree of Doctor in Engineering Science

December 2015

Machine Learning on Belgian Health Expenditure Data

Data-driven screening for type 2 diabetes

Marc CLAESEN

Examination committee:
Prof. dr. ir. Paul Sas, chair
Prof. dr. ir. Bart De Moor, supervisor
Prof. dr. ir. dr. Frank De Smet, co-supervisor
Prof. dr. ir. Johan Suykens
Prof. dr. Chantal Mathieu
Prof. dr. ir. Hendrik Blockeel
Prof. dr. ir. Jesse Davis
Prof. dr. Marco Loog
(TU Delft)

Dissertation presented in partial fulfillment of the requirements for the degree of Doctor in Engineering Science

December 2015

© 2015 KU Leuven – Faculty of Engineering Science
Uitgegeven in eigen beheer, Marc Claesen, Kasteelpark Arenberg 10, bus 2446, B-3001 Leuven (Belgium)

Alle rechten voorbehouden. Niets uit deze uitgave mag worden vermenigvuldigd en/of openbaar gemaakt worden door middel van druk, fotokopie, microfilm, elektronisch of op welke andere wijze ook zonder voorafgaande schriftelijke toestemming van de uitgever.

All rights reserved. No part of the publication may be reproduced in any form by print, photoprint, microfilm, electronic or any other means without written permission from the publisher.

Preface

Ever since I was little, I have been fascinated with computers and programming. I started my journey in the digital realm as an avid *Digger* player on a now-prehistoric 8086 MS-DOS PC, moved on to study computer science and mathematical modelling and finally ended up specializing in machine learning to design a screening tool for diabetes. What a long, strange trip it's been ...

Before I started my Master's, I never anticipated becoming a PhD student, at least partly due to my ignorance about what scientific research actually means. Now, at the end of my doctoral studies, I am happy to reflect on one of the best choices of my life. The past five years were inspiring, challenging and rewarding. I am proud to have worked on various meaningful projects and of the promising results we obtained through joint efforts involving many intelligent, creative and fun researchers. I feel priviliged to be a small cog in the giant machine that is scientific research along with so many talented, passionate people.

This thesis summarizes my research work as a PhD student at the STADIUS lab of the Dept. of Electrical Engineering (ESAT) of KU Leuven. My work was done in close collaboration with the National Alliance of Christian Mutualities (NACM), the Dept. of Clinical and Experimental Endocrinology of UZ Leuven and the Dept. of Computer Science of KU Leuven.

First, I want to thank my promotors Bart De Moor and Frank De Smet for making the project happen and for giving me the freedom to explore different avenues and to define my own research focus. In particular, Frank's help and guidance throughout the project has been invaluable, especially during the initial phases. Secondly, I am grateful to all my supervisors for their guidance and input in the project. Finally, I want to thank all jury members for their highly constructive comments on my work and for their suggestions on how to improve it further. I have learned so much from all of you.

My research would have been impossible without the medical expertise of Profs. Chantal Mathieu and Pieter Gillard. Thank you for all your input and for

patiently teaching me about the key aspects of diabetes and its treatment. I am proud to have collaborated with you, and I have always felt flattered by your enthusiasm about the project and the results we obtained.

I am grateful to have been able to learn about machine learning from many talented professors and colleagues. First, I would like to thank Prof. Johan Suykens for his invaluable input in various machine learning aspects and especially for helping me get on track during the initial phase of the project. Thanks to Prof. Yves Moreau for organizing group meetings which taught me a great deal about bioinformatics and for involving me in various projects. Finally, I feel blessed by the collaboration with Prof. Jesse Davis, which taught me a lot about expressing complex ideas and the importance of rewriting until an idea is explained just right.

I want to thank everyone at STADIUS for making the lab an inspiring workplace. Thanks to all my current and former office buddies for the friendships, collaborations and (most importantly?) the lunch breaks! First, thanks to Jaak and Dusan for being such productive coauthors. Next, thanks to Nico, Dusan, Arnaud and Yousef for all the interesting discussions, Gorana for (force?) feeding me cookies and Oliver for his endless supply of bad puns. Thanks to all BIOI members for making the past few years a fantastic experience. I am also grateful to Inge for her help in writing and managing project proposals. The administrative support of Ida, Elsy, John and Wim has been fantastic, as was the technical support by Maarten and Liesbeth.

I received a lot of help from many people at CM and hence I want to thank everyone there for the pleasant and productive collaboration. I would like to specifically show my appreciation to Michael Callens for coordinating the project and advocating in its favor. Thanks also to Koen Cornelis, Bernard Debbaut and Frie Niesten for enlightening me about different aspects of Belgian health insurance and the database infrastructure of CM.

I am grateful to the Flemish Institute of Science and Innovation (IWT) for granting me a doctoral scholarship. Additionally, I feel priviliged to have been able to take part in various workshops and entrepeneurial training sessions organized by iMinds and KU Leuven Research & Development.

I want to thank all fellow teaching assistants of courses I've been involved in for the nice teamwork. I specifically want to thank Devy for the fun collaboration on the control theory sessions and Nico for making the management of an army of job students enjoyable. Finally, kudos to Mauricio for his incredible dedication to teaching, evidenced by his excellent coordination of the course of CACSD and all the effort that went into setting up the online learning platform.

I owe a debt of gratitude to all my friends, and specifically to Alexander Vandersmissen for showing interest in whatever I do and patiently listening to various rants when their time is due. Thank you for only making moderate amounts of fun of me. Your understanding, support and advice have been extremely motivating and inspiring.

I want to thank my parents for their incessant patience, support and trust throughout my life. I am grateful to my entire family, which has recently expanded into a global conglomerate.

In closing, I would like to express my deepest gratitude to my *maganda* wife Joanne. Thank you for your patience and continuous support through the difficult and busy phases of my doctoral studies. You have always kept your faith in me, even when I doubted myself. You are my rock.

Marc

Diepenbeek
December 2015

Abstract

Diabetes mellitus is a metabolic disorder characterized by chronic hyperglycemia, which may cause serious harm to many of the body's systems. Diabetes is a deadly pandemic which presents a significant burden on healthcare systems worldwide, and will continue to do so as its global prevalence rises rapidly (particularly type 2 diabetes). In developed countries, the rising prevalence is primarily driven by population aging, lifestyle changes and greater longevity of diabetes patients. Diabetes can be managed effectively when detected early. Unfortunately, early detection proves difficult as the time between onset and clinical diagnosis may span several years. Furthermore, estimates indicate that over one third of diabetes patients in developed countries are undiagnosed.

We investigated the potential of Belgian health expenditure data as a basis to build a cost-effective population-wide screening approach for (type 2) diabetes mellitus, aspiring to improve secondary prevention by speeding up the diagnosis of patients in order to initiate treatment before the disease has caused irrevocable damage. We used health expenditure data collected by the National Alliance of Christian Mutualities – the largest social health insurer in Belgium. This data comprises basic biographic information and records of all refunded medical interventions and drug purchases, thus providing a long-term longitudinal overview of over 4 million individuals' medical expenditure histories.

Screening was formulated as a binary classification task, in which diabetes patients represent the positive class. Due to the nature of the problem and limitations of health expenditure data, we were unable to identify a set of known negatives (patients without diabetes). Hence, we had to learn classifiers from positive and unlabeled data. During this project we made two contributions to this subdomain of semi-supervised learning: (i) a novel learning method which is robust to false positives and (ii) an approach to evaluate classifiers using traditional metrics without known negatives in the test set. Additionally, we mapped the survival of patients starting various antidiabetic pharmacotherapies and developed two open-source machine learning packages: one for ensemble

learning and another to automate hyperparameter search.

We built a screening method with competitive performance to existing state-of-the-art approaches. This exceeded our expectations, since health expenditure data omits most info about the typical risk factors used by other screening methods (BMI, lifestyle, genetic predisposition, ...). As such, the combination of health expenditure data and additional information about risk factors is a promising avenue for future research in screening for diabetes mellitus. Finally, our approach has a very low operational cost since we only used readily-available data, which effectively removes one of the key barriers of population-wide screening for diabetes.

Beknopte samenvatting

Diabetes mellitus is een metabolische stoornis die gekarakteriseerd wordt door chronische hyperglycemie, hetgeen zware schade kan veroorzaken aan verschillende biologische systemen in het lichaam. Diabetes is een dodelijke pandemie die leidt tot een enorme belasting op de wereldwijde gezondheidszorg. De impact van diabetes zal verder toenemen in de komende jaren aangezien de globale prevalentie nog steeds stijgt, in het bijzonder deze van type 2 diabetes. In ontwikkelde landen is de stijgende prevalentie voornamelijk te wijten aan vergrijzing, veranderingen in levensstijl en langere overleving van diabetespatiënten. Wanneer diabetes vroeg gedetecteerd wordt, kan de ziekte goed behandeld worden, maar vroegtijdige detectie blijkt problematisch aangezien de periode tussen de ontwikkeling en diagnose van diabetes verschillende jaren kan duren. Verder is naar schatting één derde van de type 2 diabetes-patiënten niet gediagnosticeerd in Westerse landen.

Wij hebben het potentieel onderzocht om een kosteneffectieve, nationale screening-methode voor (type 2) diabetes mellitus te ontwikkelen op basis van Belgische ziekenfondsgegevens. Dit zou een meerwaarde kunnen betekenen in secundaire preventie als we hiermee sneller patiënten kunnen diagnosticeren en vervolgens behandelen voor de ziekte onherroepelijke schade heeft aangericht. We maakten gebruik van ziekenfondsgegevens die verzameld werden door de Landsbond der Christelijke Mutualiteiten (CM) – het grootste ziekenfonds in België. Deze data omvat simpele biografische informatie en records van alle terugbetaalde medische interventies en aankopen van medicijnen, wat in zijn geheel een longitudinaal overzicht over lange termijn geeft van de medische uitgaven van de meer dan 4 miljoen CM-leden.

Screening werd geformuleerd als een binaire klassificatie-taak, waarin diabetespatiënten de positieve klasse voorstellen. Door de aard van het probleem en beperkingen van ziekenfondsgegevens konden we geen verzameling van gekende negatieven bekomen (dit zijn mensen die zeker geen diabetes hebben). Daarom hebben we modellen moeten opstellen op basis van positieve en niet-

gelabelde data. Tijdens dit project hebben we twee bijdragen geleverd aan dit subdomein van semi-supervised learning: (i) een nieuwe leermethode die robuust is tegen valse positieven en (ii) een aanpak om de performantie van modellen te evalueren via traditionele metrieken zonder gekende negatieven in de test set. Verder hebben we de overleving van patiënten die startten met verscheidene glucoseverlagende farmacotherapiëen in kaart gebracht en twee open source pakketten ontwikkeld voor machine learning: één voor ensemble learning en één om hyperparameter-optimalisatie te automatiseren.

De ontwikkelde screening-methode is qua performantie competitief met de beste bestaande alternatieven. Dit overtrof onze verwachtingen, aangezien ziekenfondsgegevens weinig tot geen informatie bevatten over een aantal typische risicofactoren die aan de basis liggen van de meeste bestaande screening-methodes (BMI, levensstijl, genetische aanleg, ...). Hieruit volgt dat de combinatie van ziekenfondsgegevens en bijkomende informatie over risicofactoren een interessante piste is voor toekomstig onderzoek in screening voor diabetes mellitus. Tenslotte heeft onze aanpak een zeer lage operationele kost omdat de methode volledig gebaseerd is op gegevens die reeds ter beschikking staan, hetgeen een oplossing biedt aan één van de belangrijkste barrières voor nationale screening-methodes voor diabetes.

Abbreviations

A1C	glycated hemoglobin
ADA	American Diabetes Association
ATC	anatomical therapeutic chemical
AUC	area under the curve
AUPR	area under the PR curve
AUROC	area under the ROC curve
BAG	bagging SVM
BMI	body mass index
CDF	cumulative distribution function
CI	confidence interval
CMA-ES	covariance matrix adaptation evolutionary strategy
CVD	cardiovascular disease
CWSVM	class-weighted support vector machine
DDD	defined daily dose
DPP-4	dipeptidyl peptidase-4
ECDF	empirical cumulative distribution function
FN	false negative
FP	false positive
FPR	false positive rate
GA	genetic algorithm
gcc	GNU compiler collection
GLA	glucose lowering agent
GLP-1	glucagon-like peptide-1

GP	general practitioner
HR	hazard ratio
IDDM	insulin-dependent diabetes mellitus
IDF	International Diabetes Federation
IFG	impaired fasting glucose
IGT	impaired glucose tolerance
JSON	Javascript object notation
NACM	National Alliance of Christian Mutualities
NIDDM	noninsulin-dependent diabetes mellitus
NIHDI	National Institute for Health and Disability Insurance
NNT	number needed to treat
OAD	oral antidiabetic drug
OGTT	oral glucose tolerance test
PR	precision-recall
PSO	particle swarm optimization
PU learning	learning from positive and unlabeled data
RBF	radial basis function
RBM	restricted Boltzmann machine
RESVM	robust ensemble of support vector machines
ROC	receiver operating characteristic
SU	sulfonylurea (anti-diabetic medication)
SV	support vector
SVC	support vector classifier
SVM	support vector machine
T2D	type 2 diabetes mellitus
TN	true negative
TP	true positive
TPE	tree-structured Parzen estimators
TPR	true positive rate
TZD	thiazolidinediones (anti-diabetic medication)
WHO	World Health Organization

List of Symbols

Ω	Asymptotic lower bound on (time) complexity
τ	Bound on rank cumulative distribution function
$\mathcal{C}$	Classifier, e.g. trained SVM model
$\mathbf{X}^{(te)}$	Data set for testing
$\mathbf{X}^{(tr)}$	Data set for training
$\mathbf{X}$	Data set
$\mathcal{U}$	Data without label (unlabeled)
$\mathcal{R}$	Data, ranked based on model output
$\hat{\beta}$	Fraction of positives in the unlabeled set (estimated)
β	Fraction of positives in the unlabeled set (truth)
λ	Hyperparameters of a learning/modeling method
φ	Kernel embedding function (input space $\rightarrow$ kernel feature space)
κ	Kernel function: $\kappa(\mathbf{u}, \mathbf{v}) = \langle \varphi(\mathbf{u}), \varphi(\mathbf{v}) \rangle$
$\mathcal{N}$	Negative class
$\mathcal{N}_L$	Negatives with known label (known negatives)
$\mathcal{P}$	Positive class
$\mathcal{P}_U^\star$	Positive surrogates, unlabeled instances treated as positives
$\mathcal{P}_L$	Positives with known label (known positives)
$\mathcal{P}_U$	Positives without known label (latent positives)

$\mathcal{P}_\Omega$	Positives (all): set union of known and latent positives
$\mathcal{P}^\star_\Omega$	Positives: union of known and surrogate positives ($\approx \mathcal{P}_\Omega$)
$C_\mathcal{P}$	SVM hyperparameter: misclassification penalty on positives
$C_\mathcal{U}$	SVM hyperparameter: misclassification penalty on unlabeled data
C	SVM hyperparameter: misclassification penalty
ρ	SVM model bias
$\mathbf{w}$	SVM model separating hyperplane

Contents

Abstract v

Contents xiii

List of Figures xxi

List of Tables xxv

1 Introduction 1

1.1 Diabetes mellitus 2

1.2 Early detection and intervention in type 2 diabetes 2

1.2.1 Diagnosis of diabetes 5

1.2.2 Existing screening and prescreening approaches 6

1.2.3 Situation in Belgium 7

1.3 Belgian mutual health insurance 7

1.3.1 Data related to medical interventions 9

1.3.2 Data related to drug purchases 10

1.3.3 Quality of health expenditure data 11

1.4 Machine learning challenges and contributions 12

1.4.1 Learning from positive and unlabeled data 13

1.4.2 Automated hyperparameter optimization 15
1.4.3 Open-source software 16
1.5 Structure of the thesis 17

Appendices **18**

1.A Regulation of blood glucose levels 18
1.B Complications and comorbidities of diabetes 18
1.C Classification of diabetes mellitus 19
1.D Prevalence and burden of diabetes 20
1.E Treatment of diabetes mellitus 21

2 Mortality in individuals treated with glucose lowering agents: a large, controlled cohort study **25**

2.1 Introduction 27
2.2 Research design and methods 28
2.2.1 Study cohort selection 28
2.2.2 Control cohort selection 31
2.2.3 Therapy changes within cohorts 31
2.2.4 Censoring 33
2.2.5 Statistical analysis 33
2.3 Results 34
2.3.1 Baseline cohort characteristics 34
2.3.2 Five-year survival in individuals on different glucose lowering agents 34
2.3.3 Age-dependent 5-year survival of individuals on different glucose lowering agents 37
2.3.4 Statins and survival in individuals on different glucose lowering therapy 41
2.4 Conclusions 42

3 EnsembleSVM: A Library for Ensemble Learning Using SVMs 46

3.1 Introduction 47

3.2 Software Description 48

3.2.1 Implementation 48

3.2.2 Tools 49

3.3 Benchmark Results 49

3.4 Conclusions 51

4 SVM Ensemble Learning from Positive and Unlabeled Data 53

4.1 Introduction 54

4.2 Related work 55

4.2.1 Class-weighted SVM 55

4.2.2 Bagging SVM 56

4.3 Robust Ensemble of SVMs 57

4.3.1 Bootstrap resampling contaminated sets 57

4.3.2 Bagging predictors 58

4.3.3 Justification of the RESVM algorithm 59

4.3.4 RESVM training 60

4.3.5 RESVM prediction 61

4.4 Experimental setup 62

4.4.1 Simulation setup 62

4.4.2 Data sets 65

4.5 Results and discussion 68

4.5.1 Results for supervised classification 68

4.5.2 Results for PU learning 68

4.5.3 Results of semi-supervised classification 70

4.5.4 A note on the number of repetitions per experiment . . 72

4.5.5 Trend across data sets . . . 73
4.5.6 Effect of contamination . . . 74
4.5.7 RESVM optimal parameters . . . 76
4.6 Conclusion . . . 77

5 Hyperparameter Search in Machine Learning 79
5.1 Introduction . . . 80
5.1.1 Example: controlling model complexity . . . 80
5.1.2 Formalizing hyperparameter search . . . 81
5.2 Challenges in hyperparameter search . . . 81
5.2.1 Costly objective function evaluations . . . 81
5.2.2 Randomness . . . 82
5.2.3 Complex search spaces . . . 82
5.3 Current approaches . . . 83
5.4 Conclusion . . . 83

6 Easy Hyperparameter Search Using Optunity 85
6.1 Introduction . . . 86
6.2 Optunity . . . 86
6.2.1 Functional Overview . . . 87
6.2.2 Available Solvers . . . 88
6.2.3 Software Design and Implementation . . . 88
6.2.4 Development and Documentation . . . 88
6.3 Related Work . . . 89
6.4 Solver Benchmark . . . 89

Appendices 91
6.A Survey of hyperparameter optimization in NIPS 2014 . . . 91

6.B Performance benchmark 92
6.B.1 Setup 92
6.B.2 Results & Discussion 93

7 Assessing Binary Classifiers Using Only Positive and Unlabeled Data 97

7.1 Introduction 98
7.2 Background and definitions 99
7.2.1 Rank distributions and contingency tables 99
7.2.2 ROC and PR curves 100
7.2.3 Evaluation with partially labeled data 101
7.3 Relationship between the rank CDF of positives and contingency tables 101
7.3.1 Rank distributions and contingency tables based on subsets of positives within a ranking 102
7.3.2 Contingency tables based on partially labeled data . . . 103
7.4 Efficiently computing the bounds 104
7.4.1 Computing the contingency table with greatest-lower bound on FPR at given rank r 105
7.4.2 Bounds on the rank distribution of $\mathcal{P}_U$ 106
7.5 Constructing ROC and PR curve estimates 107
7.6 Discussion and Recommendations 108
7.6.1 Determining $\hat{\beta}$ and its effect 108
7.6.2 Model selection 110
7.6.3 Empirical quality of the estimates 111
7.6.4 Relative importance of known negatives compared to known positives 112
7.7 Conclusion 113

Appendices 114

7.A Effect of $\hat{\beta}$ on contingency table entries and common performance metrics . . . 114

7.B The effect of the fraction of known positives, known negatives and $\hat{\beta}$ . . . 117

8 Building Classifiers to Predict the Start of Glucose-Lowering Pharmacotherapy Using Belgian Health Expenditure Data 121

8.1 Introduction . . . 122

8.2 Existing Type 2 Diabetes Risk Profiling Approaches . . . 123

8.3 Health Expenditure Data . . . 124

8.3.1 Records Related to Drug Purchases . . . 125

8.3.2 Records Related to Medical Provisions . . . 126

8.3.3 Advantages of Health Expenditure Data . . . 126

8.3.4 Limitations of Health Expenditure Data . . . 126

8.4 Methods . . . 127

8.4.1 Experimental Setup . . . 128

8.4.2 Data Set Construction . . . 131

8.4.3 Learning Methods . . . 135

8.5 Results and Discussion . . . 137

8.5.1 Benchmark of learning methods . . . 137

8.5.2 Performance Curves . . . 140

8.5.3 Feature Importance Analysis for the RESVM Model . . . 140

8.6 Conclusion . . . 141

9 Conclusion 145

9.1 Machine learning contributions . . . 145

9.1.1 Future work . . . 146

9.2 Screening for type 2 diabetes . . . 147

9.2.1 Weaknesses and limitations of our approach . . . 147

9.2.2 Future work 150
9.2.3 Health expenditure data 150
9.2.4 The elephant in the room 151

Bibliography **153**

List of publications **183**

List of Figures

1.1 Diabetes atlas released by the International Diabetes Federation (IDF). Reuse of this material was granted by the IDF. The original is available at `http://www.idf.org/worlddiabetesday/toolkit/gp/facts-figures`. 3

1.2 The stages of the medical diagnostic process: screening is used to identify patients at high risk, which are then forwarded to diagnostic tests. The cost and invasiveness of tests increase as patients move down the funnel, hence each step aims to remove negatives while retaining positives. 4

1.3 Data exchanges between caregivers in Belgian healthcare: mutual health insurers receive information from all stakeholders through claims, while other stakeholders often only have subsets of a patient's health data. 9

1.4 Example of the ATC hierarchy for common GLAs. A brief explanation of these different active substances is given in Appendix 1.E. 11

1.5 Dependencies of the key contributions made to machine learning research during this project. To enable diabetes screening based on Belgian health expenditure data (Chapter 8), we made contributions to semi-supervised learning (Chapters 4 and 7), automated hyperparameter search (Chapters 5 and 6) and open-source machine learning software (Chapters 3 and 6). 14

2.1 Flowchart describing the selection protocol for study and control patients. Patients can move from the bottom right (monotherapy) to the bottom left group (combination therapy), but not vice versa. All listed counts are for unique patients. 30

2.1 5-year survival for increasing age per cohort. 35

2.2 5-year survival for increasing age per cohort. 39

2.3 5-year survival for increasing age per cohort with matched controls. 40

4.1 Contamination of bootstrap resamples for increasing size of resamples when the original sample has 10% contamination. Errorbars indicate the 95% confidence interval (CI) of contamination in resamples. The contamination varies greatly between small resamples as shown by the CIs. 58

4.1 Overview of a single benchmark iteration. 63

4.2 Empirical densities of the `synthetic` data used for training per problem setting (visualized in input space). The supervised densities (top row) are based on samples of the underlying positive and negative classes. The use of high contamination (30%) induces similar empirical densities for $\mathcal{P}$ and $\mathcal{U}$ in the semi-supervised setting (bottom row). 67

4.3 The effect of majority voting in an ensemble Ω with three linear base models (ψ_1, ψ_2, ψ_3). The thick black line represents the overall decision boundary of Ω. The use of majority voting generally induces nonlinear decision boundaries, e.g., when using linear base models the ensemble has a piecewise linear decision boundary. 67

4.1 Performance in semi-supervised setting on `mnist`, digit 7 as positive. 72

4.2 Critical difference diagrams for each setting. Groups of algorithms that are not significantly different at the 5% significance level are connected. 74

4.3 Effect of different levels of contamination in $\mathcal{U}$ and $\mathcal{P}$ on generalization performance. The plots show point estimates of the mean area under the PR curve across experiments and the associated 95% confidence intervals. 76

6.1 Integrating Optunity in non-Python environments. 89

6.1 Critical difference diagrams for 75 and 150 evaluations to tune an SVM with RBF kernel, depicting average rank per optimizer (lower is better). Optimizers without statistically significant performance differences at $\alpha = 5\%$ are linked. 90

7.1 Rank CDF of two sets of positives $\mathcal{P}_1 = \{B, D, A, C\}$ and $\mathcal{P}_2 = \{E, G, F\}$ within an overall ranking $\mathcal{R} = \{B, E, D, G, H, A, F, C, I\}$, with $|\mathcal{P}_1| = 4$ and $|\mathcal{P}_2| = 3$. In practice $\mathcal{R}$ is obtained by sorting the data according to classifier score. The rank CDF of a set $\mathcal{S} \subseteq \mathcal{R}$ is based on the positions of elements of $\mathcal{S}$ in $\mathcal{R}$. 100

7.1 Illustration of Lemma 1: higher TPR at a given rank r implies lower FPR at r for two positive sets of the same size. 102

7.2 Illustration of Lemma 2: $\mathcal{F}(\cdot)$ denotes feasible region. The rank distribution of the union $\mathcal{P}_\Omega$ of two sets of positives $\mathcal{P}_1$ and $\mathcal{P}_2$ lies between their respective rank distributions. 103

7.2 The effect of $|\mathcal{P}_L|$ on estimated AUC. Based on $|\mathcal{U}| = 100,000$, $\mathcal{N}_L = \emptyset$ and $\hat{\beta} = \beta = 0.2$. Bounds on rank CDF were obtained via bootstrap. The depicted confidence intervals are based on 200 repeated experiments. 110

7.3 The effect of $\hat{\beta}$ on estimated ROC curves, based on 2,000 known positives, 100,000 unlabeled instances and $\beta = 0.3$. 110

8.1 Overview of the full learning approach: data set vectorization, normalization and the nested cross-validation setup. Per iteration, hyperparameter optimization and model training is done based exclusively on $\mathbf{X}_{train}^{(outer)}$ 129

8.2 Visualization and vectorization of trees. In the tree representation, the value of internal nodes is the sum of the values of its children. The unnormalized vector representations $\mathcal{V}_A$ and $\mathcal{V}_B$ contain the values per node in the tree representation in some fixed order. Inner products between unnormalized representations $\mathcal{V}_A$ and $\mathcal{V}_B$ are mainly influenced by the top level nodes, since those have the largest value by construction. This undesirable effect can be fixed through feature-wise scaling. The scaling vector $\mathcal{S}$ was constructed using node-wise maxima. The normalized vector representations $\mathcal{V}_A^\star$ and $\mathcal{V}_B^\star$ are obtained by dividing the vector representations ($\mathcal{V}_A$, $\mathcal{V}_B$) element-wise by entries in the scaling vector $\mathcal{S}$. $\mathcal{V}_A^\star$ and $\mathcal{V}_B^\star$ are used as input to classifiers in the remainder of this work. As desired, the inner product of normalized vector representations is increasingly influenced by similarities at higher depths in the tree representations. 133

8.3 Tensor formulation of medical provisions with three components: patients, physicians and provisions. Each entry in the tensor is the frequency of the given tuple. This provision tensor is very sparse. The patient matrix is obtained by summing counts over all physicians (transposed). The physician matrix is obtained by summing counts over all patients. These matrices capture complementary information. 133

8.4 Structure of the provision similarity matrix $\mathbf{S}_{prov}$ based on providing physicians. 135

8.1 Performance curves for RESVM classifier based on ATC | PROVS vectorization, CWSVM based on age and gender and a random model. The lower and upper bounds are estimated using $\hat{\beta}_{lo} = 5\%$ and $\hat{\beta}_{up} = 10\%$, respectively. 142

List of Tables

1.1 Diagnostic criteria for diabetes and related metabolic abnormalities as recommended by the WHO [193]. 6

1.2 High-risk subpopulations according to the Diabetes Liga [4]. . . 7

2.1 Definitions of drug categories and cardiovascular events. 29

2.2 Partitioning of final treatment regimen of patients starting a specific therapy (rows). The final treatment regimen (columns) is based on the last 9 months of individual followup. Patients are censored in all survival analyses after 9 consecutive months of renunciation from metformin, sulfonylurea and insulin. . . . 32

2.1 Baseline characteristics of the study cohorts. Individuals starting starting mono therapy are selected such that they have no prior history of diabetes-related drugs. Individuals starting combination therapy may have a prior history of diabetes-related drugs. All differences in use of associated therapy are statistically significant between study cohorts, except for use of antihypertensives in insulin and sulfonylurea mono cohorts (no significant difference). All associated therapy use is statistically significantly elevated in subgroups with prior cardiovascular events within each study cohort. All comparisons of study group characteristics use significance level $\alpha = 0.05$ and are computed using Tukey's test in conjunction with ANOVA to adjusts for multiple comparison. 36

2.2 Overview of survival for the study cohorts compared to a fully matched control cohort, stratified by cv history. The control group is sampled from the general population and matched for age, gender and use of statins, antihypertensives and antiplatelet drugs. For every patient in the study cohorts, 5 patients with completely matching profiles were used in control. • indicates that the proportional hazards assumption was rejected for the associated hazards ratio ($p < 0.01$). 38

2.3 Analysis of the effect of statins within each study cohort. Presented hazard ratios are associated to the fraction of follow-up on statins. Patients are classified as statin users if they were on statins for at least half the follow-up. The proportional hazards models used here control for age, gender, use of antihypertensive and antiplatelet drugs and an age-gender interaction. • indicates that the proportional hazards assumption was rejected for the associated hazards ratio ($p < 0.01$). 41

2.4 Hazard ratios between statin users in the study group a control group matched for age and gender. The remaining characteristics of the control groups used here follow the distribution of the total NACM member population (after matching for age and gender). The proportional hazard models used to compute these hazard ratios control for age, gender, the use of antihypertensive and antiplatelet drugs and an age-gender interaction. • indicates that the proportional hazards assumption was rejected for the associated hazards ratio ($p < 0.01$). 42

3.1 Summary of benchmark results per data set: test set accuracy, number of support vectors and training time. Accuracies are listed for a single `LIBSVM` model, `LIBLINEAR` model and an ensemble model. 50

4.1 Overview of the data sets used in simulations: number of features, contamination (when applicable), training set size as used in the experiments and test set size. The `mnist` data set consists of 10 classes and the test set is almost uniformly distributed. The `sensit` data set has 3 classes with uneven class distribution in the test set, so we treat it separately here. 66

4.1 95% CIs for mean test set performance in a fully supervised setup, the results of a paired one-tailed Wilcoxon signed-rank test comparing the AUC of `BAG` and `RESVM` with alternative hypothesis $h_1 : AUC^{RESVM} > AUC^{BAG}$ and the number of times each approach had best test set performance. Test result encoding: • $p < 0.05$, • • $p < 0.01$ and • • • $p < 0.001$. . . . 69

4.2 95% CIs for mean test set performance in a PU learning setup, the results of a paired one-tailed Wilcoxon signed-rank test comparing the AUC of `BAG` and `RESVM` with alternative hypothesis $h_1 : AUC^{RESVM} > AUC^{BAG}$ and the number of times each approach had best test set performance. Test result encoding: • $p < 0.05$, • • $p < 0.01$ and • • • $p < 0.001$. 70

4.3 95% CIs for mean test set performance in a semi-supervised setup, the results of a paired one-tailed Wilcoxon signed-rank test comparing the AUC of `BAG` and `RESVM` with alternative hypothesis $h_1 : AUC^{RESVM} > AUC^{BAG}$ and the number of times each approach had best test set performance. Test result encoding: • $p < 0.05$, • • $p < 0.01$ and • • • $p < 0.001$. 71

4.4 Number of wins in simulations for each method per setting. The bottom half shows normalized number of wins, where wins in multiclass data sets (`mnist` and `sensit`) are divided by the number of classes. 75

4.5 Medians of optimal hyperparameters per digit obtained via cross-validation and mean of all medians per setting. The normalized relative weight on positives versus unlabeled instances (w_{pos}) is associated with the relative size and contamination of the positive and unlabeled training sets. 77

6.A.1 The use of hyperparameter optimization methods as reported in NIPS 2014 papers. Methods and packages with 0 recorded uses are omitted from this table. 92

6.B.1 Benchmark results for tuning an SVM classifier with RBF kernel, using an optimization budget of 75 evaluations (best result per data set in bold, worst in gray). Results depict averages across 5 runs of the optimum (i.e., the best found solution across all optimizers), the third quantile (Q_3) of random search results (which indicates the difficulty of the optimization problem: low Q_3 vis-à-vis the optimum indicates the region of strong performance is small within the overall search space) and the relative rank and regret per optimizer. Performance and regret are measured in terms of cross-validated area under the ROC curve and shown in percent. Relative ranks indicate non-parametric global performance within the pool of optimizers (lower is better, the best optimizer has rank 1). 94

6.B.2 Benchmark results for tuning an SVM classifier with RBF kernel, using an optimization budget of 150 evaluations (best result per data set in bold, worst in gray). Results depict averages across 5 runs of the optimum (i.e., the best found solution across all optimizers), the third quantile (Q_3) of random search results (which indicates the difficulty of the optimization problem: low Q_3 vis-à-vis the optimum indicates the region of strong performance is small within the overall search space) and the relative rank and regret per optimizer. Performance and regret are measured in terms of cross-validated area under the ROC curve and shown in percent. Relative ranks indicate non-parametric global performance within the pool of optimizers (lower is better, the best optimizer has rank 1). 95

8.1 Example of the ATC classification system: classification of metformin per level. 125

8.1 Summary of vectorization schemes used for records of drug purchases. 132

8.2 Summary of vectorization schemes used for records of medical provisions. 135

8.1 Average bounds on area under the ROC curve and p-value of the Mann-Whitney U test over all folds for different feature sets per learning approach in a long-term prediction setup. The lower and upper bounds on AUC were computed with $\hat{\beta}_{lo} = 0.05$ and $\hat{\beta}_{up} = 0.10$, respectively. The ATC | PROVS feature set is the concatenation of the best performing sets per aspect, namely ATC 1–5 and PROVS BOTH. Stars ($*$) denote p-values below 0.005. 138

8.2 Level 3 ATC codes with highest normalized feature weight. . . 142

Chapter 1

Introduction

In this work we explored the ability of screening for (type 2) diabetes mellitus based on Belgian health expenditure data from a machine learning perspective. The thesis is organized as a collection of papers concerning various aspects related to this application.[1] This chapter provides some context of the project, including the medical background of diabetes and its treatment, a summary of the Belgian health insurance system and this project's data analysis challenges.

This work aligns with the overall trend towards eHealth and the rising use of all sorts of data for evidence-based medicine. Our work is the first data-driven medical application based on health expenditure records and demonstrates the potential use of this data in clinical applications that might improve patient outcomes while simultaneously reducing healthcare costs. Building useful medical applications based on health expenditure data can be considered a modern interpretation of one of the key missions of Belgian mutual health insurers as defined by law, namely to promote the physical, psychological and social well-being of their members [5].

To meet our objective we tackled various machine learning challenges, of both theoretical and practical nature. This work contains contributions to machine learning, including open-source implementations of all proposed methods, and a detailed description of our steps towards building a reliable screening approach for type 2 diabetes that can be applied on a population-wide scale.

We will first briefly introduce diabetes mellitus in Section 1.1. We proceed to describe early detection and intervention of type 2 diabetes (T2D) – the most common variant of diabetes mellitus – in Section 1.2. Next, the Belgian

[1] Some chapters have minor differences compared to the papers on which they are based.

health insurance landscape is described in Section 1.3. Subsequently, Section 1.4 contains a discussion of the main challenges of this project from a machine learning perspective to explain the necessity of each aspect of our research. Finally, Section 1.5 summarizes the structure of the text and indicates how all chapters (papers) are related to each other.

1.1 Diabetes mellitus

Diabetes mellitus is a metabolic disorder characterized by chronic hyperglycemia, which is primarily caused by insufficient insulin secretion and/or insulin resistance [10]. The worldwide incidence of diabetes has increased dramatically over the last century due to changes in human behaviour and lifestyle [290, 61]. Diabetes is one of the main threats to human health world wide [149, 290, 289] and is projected to be the 7th leading cause of death by 2030 [174]. Some key facts related to diabetes mellitus are summarized in the diabetes atlas made by the International Diabetes Federation (IDF) (Figure 1.1).

An overview of the medical background of diabetes mellitus is described in Appendices 1.A to 1.E, which discuss various aspects of the disease, namely the underlying biological problem, common complications and comorbidities, a classification of diabetes based on etiology, the prevalence and burden of the disorder and finally treatment approaches with an emphasis on pharmacotherapy. We will focus on type 2 diabetes (T2D) in the remainder of the text. T2D accounts for about 90% of diabetes mellitus patients, but early detection of this highly prevalent disease poses significant challenges to contemporary medicine.

1.2 Early detection and intervention in type 2 diabetes

Studies have convincingly shown that early detection and treatment of T2D can prevent or delay complications of the disease [120, 93, 83, 107, 134, 102, 87]. Additionally, treatment of early-stage T2D is often relatively simple and cheap (e.g. lifestyle changes, often specifically targetted towards weight loss) compared to the treatment of progressed T2D, which typically involves strict pharmacological therapy along with the treatment of potential complications [196, 257, 83, 286], indicating the value of early detection. The successive steps of a typical diagnostic process are shown in Figure 1.2.

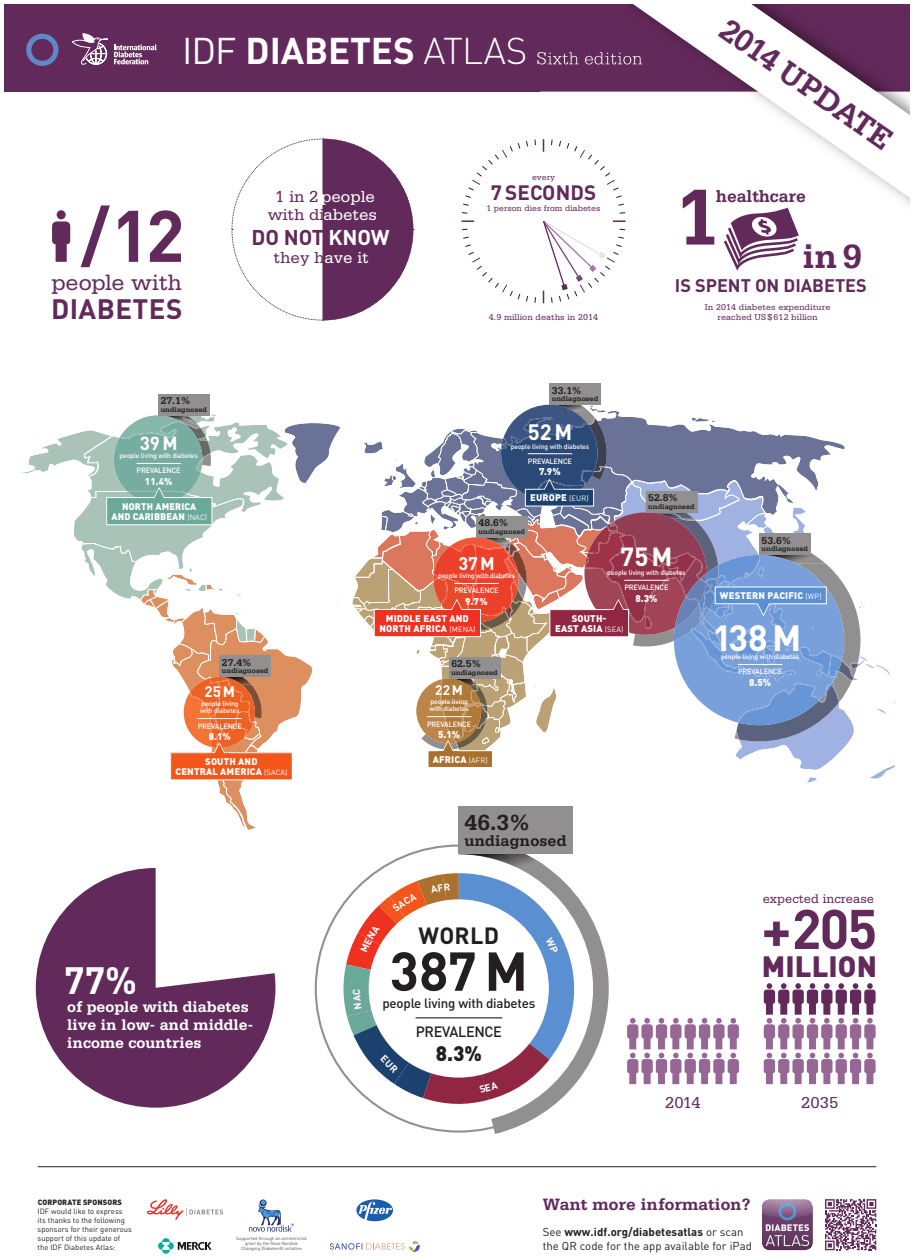


Figure 1.1: Diabetes atlas released by the International Diabetes Federation (IDF). Reuse of this material was granted by the IDF. The original is available at `http://www.idf.org/worlddiabetesday/toolkit/gp/facts-figures`.

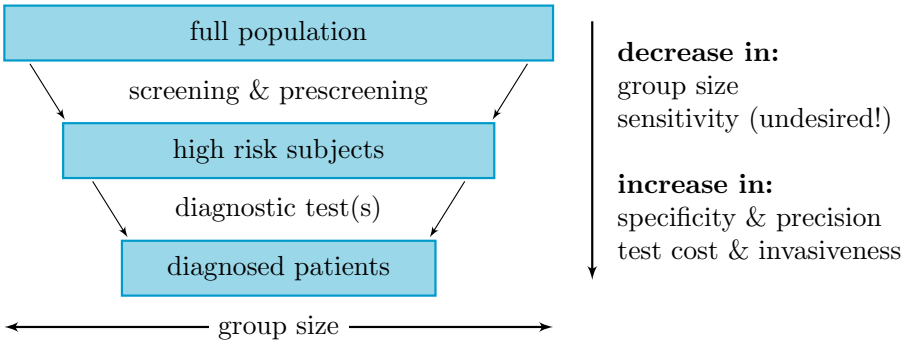


Figure 1.2: The stages of the medical diagnostic process: screening is used to identify patients at high risk, which are then forwarded to diagnostic tests. The cost and invasiveness of tests increase as patients move down the funnel, hence each step aims to remove negatives while retaining positives.

Despite its widely-recognized importance, early detection of T2D proves to be problematic, as one fourth up to one third of T2D patients are estimated to be undiagnosed in developed countries [4, 30, 15] and typically years pass between the onset of T2D and its clinical diagnosis [127]. In fact, the clinical diagnosis of T2D often follows signs of serious complications, which have developed during the latent stage of the disease [210, 124, 136, 15].

Diagnostic inertia for T2D arises in several ways. First, the disease may remain asymptomatic for many years [11], during which unmanaged hyperglycemia may induce serious and irreversible development of micro -and macrovascular complications [100, 30]. Second, health and healthcare information related to a specific patient is often fragmented across databases of individual caregivers and other medical stakeholders. This can induce situations in which various subtle symptoms of diabetes are presented to multiple caregivers, but the diagnosis remains elusive because each individual caregiver receives too little information to spot the slumbering slayer. Finally, universal screening for T2D is cost-prohibitive [270, 93], though many organizations advise opportunistic screening of high-risk subgroups [276, 11, 93, 15].

Certain metabolic abnormalities typically precede T2D and can therefore be used as proverbial miners' canaries by screening approaches, specifically:

- *Impaired fasting glucose (IFG)*, also known as prediabetes, is a condition in which fasting blood glucose levels are consistently higher than normal, but not high enough to warrant a diabetes diagnosis. Some patients with IFG can also be diagnosed with impaired glucose tolerance.

- *Impaired glucose tolerance (IGT)* is a prediabetic state of hyperglycemia which may precede T2D by many years. IGT is detected as an abnormal response to the oral glucose tolerance test (OGTT, cfr. Section 1.2.1). Specifically, patients with IGT exhibit raised glucose levels after 2 hours compared to healthy people, but not high enough to qualify for T2D. Patients with IGT present a higher risk for diabetes than patients with IFG. Approximately 40% of subjects with IGT progress to diabetes over the next decade [290]. Additionally, subjects with IGT have heightened risk of macrovascular disease compared to subjects with IFG [255, 260].

Both IFG and IGT are associated with insulin resistance and increased risk of diabetes and cardiovascular pathologies, with IGT being more strongly associated with cardiovascular outcomes [260]. Although the transition of IFG and/or IGT to diabetes may take many years, the majority of individuals with these pre-diabetic states eventually develop diabetes [257, 83, 183]. Additionally, the risk of complications is known to commence many years before the onset of clinical diabetes [120, 290].

In the remainder of this Section we will discuss current diagnostic tests, existing screening programmes and the Belgian situation and recommendations.

1.2.1 Diagnosis of diabetes

The gold standard to diagnose hyperglycemia is the oral glucose-tolerance test (OGTT), which determines how quickly glucose is cleared from the blood [10, 193]. In this test, patients are administered glucose after fasting for 12 hours and afterwards the patient's blood glucose levels are measured, sometimes at multiple intervals, but typically after 2 hours [4].

Type 1 diabetes has a sufficiently pronounced clinical onset characterized by acute, extreme elevations in glucose concentrations combined with symptoms which make its diagnosis fairly unambiguous and typically timely [70]. Type 2 diabetes, however, has a more gradual onset making its diagnosis less straightforward and causing the diagnostic criteria to be debated regularly [193, 70]. The diagnostic criteria as currently recommended by the WHO are listed in Table 1.1.

The OGTT was widely agreed upon as diagnostic test, though in 2003 the American Diabetes Association (ADA) modified its recommendations in favor of using fasting plasma glucose to diagnose asymptomatic T2D [193]. More recently, the use of the A1C assays for diagnosis was considered, though current point-of-care A1C assays were considered insufficiently accurate [70].

- impaired fasting glucose (IFG):
  - fasting plasma glucose ≥ 6.1 and < 7.0 mmol/l, and
  - 2-hour plasma glucose < 7.8 mmol/l (if measured).
- impaired glucose tolerance (IGT):
  - fasting plasma glucose < 7.0 mmol/l, and
  - 2-hour plasma glucose ≥ 7.8 and < 11.1 mmol/l.
- diabetes:
  - fasting plasma glucose ≥ 7.0 mmol/l, or
  - 2-hour plasma glucose ≥ 11.1 mmol/l.

Table 1.1: Diagnostic criteria for diabetes and related metabolic abnormalities as recommended by the WHO [193].

1.2.2 Existing screening and prescreening approaches

The clinical inertia in diagnosing type 2 diabetes is being tackled by a wide variety of screening and prescreening approaches, which commonly rely on information that is already available or relatively easy to obtain. The main method to implement such screening methods is via questionnaires, possibly paired with clinical information such as parameters recorded in patients' electronic health records or by general practioners.

The Cambridge Risk Score (CRS) was developed to assess the probability of undiagnosed T2D based on data that is routinely available in primary care records, including age, sex, medication use, family history of diabetes, BMI and smoking status [114], The CRS and comparable scores have been shown to be useful on multiple occasions [24, 114, 198, 245]. The FINDRISC score is based on a 10-year follow-up using age, BMI, waist circumference, history of antihypertensive drugs and high blood glucose, physical activity and diet and is used to predict drug-treated diabetes [163]. The strongest reported predictors in this study were BMI, waist circumference, history of high blood glucose and physical activity. Glümer et al. [109] developed a risk score based on age, sex, BMI, known hypertension, physical activity and family history of diabetes. The German diabetes risk score is based on age, waist circumference, height, history of hypertension, physical activity, smoking, and diet [227]. More complex risk scores include various clinical parameters [129, 247, 175].

1.2.3 Situation in Belgium

The IDF estimates over 170,000 undiagnosed diabetes patients in Belgium [2]. The Diabetes Liga estimates that currently one out of three T2D patients are undiagnosed, that one out of ten Belgians will have type 2 diabetes in 2030 and that 8% and 6.5% of the Belgian population currently has diabetes or prediabetes, respectively [4]. Domus Medica[2] advises against population-wide screening, though it recommends case finding in high-risk subpopulations [271], for instance via the risk factors listed in Table 1.2.

- Persons of 18–45 years of age that meet one of the following conditions:
  - prior history of gestational diabetes
  - prior history of stress-induced hyperglycemia
- or two of the following conditions:
  - prior history of giving birth to a baby of over 4.5 kg
  - diabetes in first-line relatives (mother, father, sister, brother)
  - BMI $\geq$ 25 kg/m^2
  - waist circumference $>$ 88 cm (for women) or $>$ 102 cm (for men)
  - treated for high blood pressure or with corticoids
- Persons of 45–64 years of age that meet one of the conditions listed above.
- Persons above 64 years old, regardless of additional risk factors.

Table 1.2: High-risk subpopulations according to the Diabetes Liga [4].

The Belgian Scientific Institute of Public Health (WIV-ISP) reports that screening efforts are increasing in Belgium, but also indicates a need for risk stratification that goes beyond selecting all patients above a given age [132].

1.3 Belgian mutual health insurance

The Belgian health care insurance is a broad solidarity-based form of social insurance. Mutual health insurers are the legally-appointed bodies for managing

[2] A non-profit organization of general practionners that focuses on preventive medicine.

and providing the Belgian compulsory health care and disability insurance. The Belgian sickness fund law of 1990 states that a main goal of mutualities is to promote the physical, psychological and social well-being of their members [5].

Joining one of several mutual health insurers or, alternatively, the relief fund for sickness and disability insurance[3] is obliged for anyone who (i) starts working, (ii) is still studying at the age of 25 years or (iii) receives unemployment benefits. Among other things, mutual health insurers are responsible for refunding medical interventions, drug purchases and payments related to disability and pregnancy leave. To implement their operations, mutual health insurers dispose of large databases containing health expenditure records of all their respective members.

This project was done in close collaboration with the National Alliance of Christian Mutualities (NACM).[4] NACM is the largest Belgian mutual health insurer with records of over 4.4 million persons and over 60% and 40% market share in Flanders and Belgium, respectively. All data extractions and analyses were done in-house at the department of medical management of NACM in its headquarters in Brussels under supervision of and upon request by the Chief Medical Officer.

We developed a screening system based exclusively on basic personal information (i.e., age, gender) and readily-available health expenditure records collected by NACM, without requiring any external input. Our approach is cheap, non-invasive and can be applied on a population-wide scale, making it a suitable initial screening procedure (cfr. Figure 1.2). The relevant patient-centric information embedded in these records belongs to three key classes:

- **Basic biographical information** includes the member's age, gender, place of residence and, if deceased, the date of death. Limited information regarding social status is also available, e.g. whether a member is entitled to increased compensation or suffers from a chronic illness.
- **Medical provisions** are encoded via a national nomenclature comprising over 20,000 unique codes. Each medical act yields one or several of these nomenclature codes.
- **Drug purchases** are registered automatically and are encoded per package or per unit when purchased in retail and hospital pharmacies, respectively. In both cases, the encoding contains information about both volume and active substances.

Figure 1.3 depicts the main data exchanges in Belgian healthcare. Each healthcare provider manages its own subset of a patient's health data, which is

[3] In Dutch: Hulpkas voor Ziekte -en Invaliditeitsuitkering (HZIV).
[4] In Dutch: Landsbond der Christelijke Mutualiteiten (LCM).

usually not fully shared with other caregivers. In principle, the patient's *global medical file* (GMF), which is managed by his or her general practitioner (GP), should be comprehensive. However, GMFs require caregivers to share data, which does not always occur, and puts a burden on GPs. In contrast, mutual health insurers dispose of all reimbursed claims data, regardless of the associated caregiver, which gives them an overview of all healthcare activities. Additionally, claims data are structured while communication between caregivers is often done through plain text. Data sharing is improving through initiatives like Vitalink[5], Hubs and Metahubs[6], though these are still in their infancy.

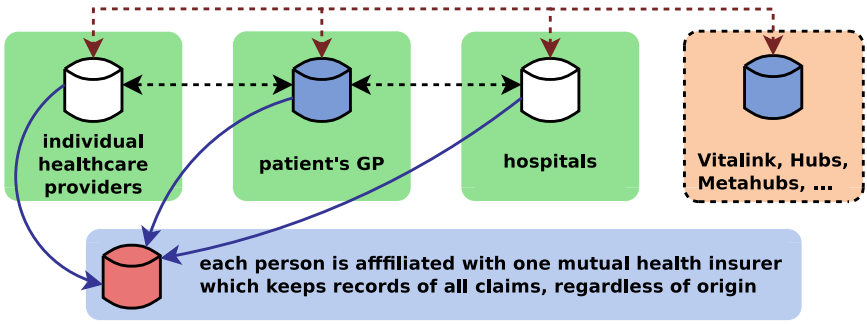


Figure 1.3: Data exchanges between caregivers in Belgian healthcare: mutual health insurers receive information from all stakeholders through claims, while other stakeholders often only have subsets of a patient's health data.

The time-stamped records related to provisions and drug purchases enable constructing a medical resource-use timeline for each patient. As this constitutes the main source of information in our work we will discuss claims records related to provisions and drug purchases in more detail in Sections 1.3.1 and 1.3.2. Finally, we will briefly discuss the overall quality of health expenditure data.

1.3.1 Data related to medical interventions

Each distinct medical intervention is encoded in a national nomenclature that is maintained by the National Institute for Health and Disability Insurance (NIHDI)[7] [264]. After a consultation, patients receive a certificate indicating which provisions were performed (a green, white or blue slip). The patient can then file a claim to get (partially) refunded through his or her mutual health insurer. Refunds can be claimed up to two years after the date of

[5]More information can be found at `http://www.vitalink.be/`.
[6]`https://www.ehealth.fgov.be/nl/zorgverleners/online-diensten/hubs-metahub`
[7]In Dutch: Rijksinstituut voor ziekte -en invaliditeitsverzekering (RIZIV).

the intervention, though most patients do this more swiftly. In some cases, a copayment system enables the caregiver to get paid directly by the health insurer, removing the need for the patient to claim refunds.

The list of nomenclature numbers can be consulted via the website of the NIHDI and currently comprises over 20,000 unique codes. The sheer number of codes indicates the fine granularity at which medical interventions are encoded, making it a valuable source of information. Codes can fall out of use when interventions get deprecated or because they get replaced by other codes that are often more specific in some sense.

However, the codes that identify interventions only carry limited information. Specifically, these codes are sufficiently detailed to know which intervention was performed, but do not contain any information regarding its outcome. For example, there are codes indicating blood tests, but the results of these tests are not available to the mutual health insurer. As such, nomenclature codes often serve as proxies for specific diseases, but essentially carry no direct information regarding diagnoses, indications or clinical parameters.

1.3.2 Data related to drug purchases

Drug purchases work via a copayment system in Belgium, in which the patient only pays his or her share at the time of purchase while the rest is already deducted automatically. As such, drug purchases are automatically recorded and known to health insurers without requiring the patient to explicitly claim refunds and are therefore implicitly complete.

Each drug package carries a *Code Nationale Kode* (CNK) code which indicates the volume in the package and information about the drug itself including its active substances. Hence, these CNK codes carry enough information to map a drug purchase onto one or several codes of the internationally used Anatomical Therapeutic Chemical (ATC) classification system with an associated amount of Defined Daily Doses (DDDs). Tables to map CNK codes onto ATC codes are provided freely by the BCFI[8] and the APB[9].

The ATC classification system is maintained by the World Health Organization and divides active substances into different groups based on the organ or system on which they act and their therapeutic, pharmacological and chemical properties [273]. Each drug is classified in groups at 5 levels in the ATC hierarchy: fourteen main groups (1st level), pharmacological/therapeutic subgroups (2nd level), chemical subgroups (3rd and 4th level) and the chemical substance (5th level).

[8] In Dutch: Belgisch Centrum voor Farmacotherapeutische Informatie.
[9] In Dutch: Algemene Pharmaceutische Bond.

Figure 1.4 illustrates the structure of ATC system for common antidiabetic drugs.

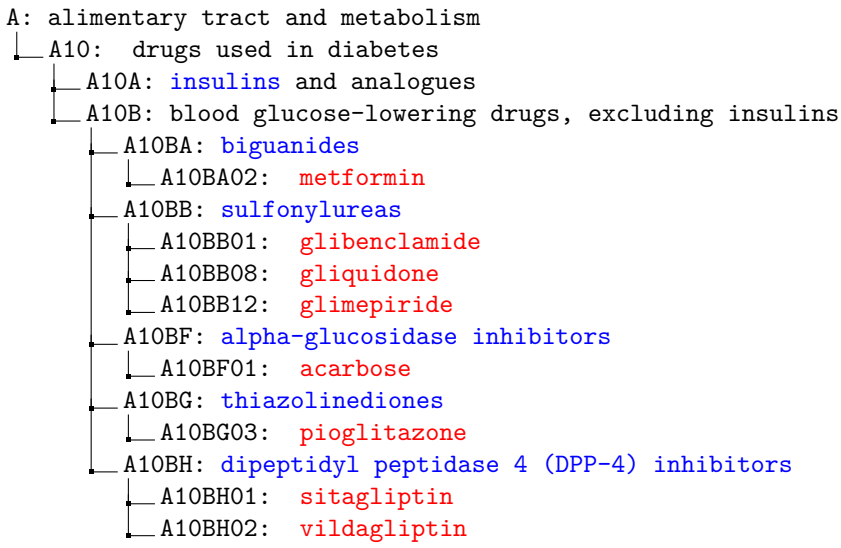


Figure 1.4: Example of the ATC hierarchy for common GLAs. A brief explanation of these different active substances is given in Appendix 1.E.

1.3.3 Quality of health expenditure data

Overall, health expenditure data can be considered complete, due to the clear financial incentive for patients and caregivers to file claims. The automated registration of drug purchases also contributes to this aspect.

A key benefit of health expenditure data is that it integrates resource-use from all medical sources (cfr. Figure 1.3). Patients may consult multiple caregivers and institutions but each patient is affiliated to only one mutual health insurer at a time. Additionally, most Belgians never switch mutual health insurer.

Health expenditure records give a fine-grained overview of patients' medical histories thanks to the detailed encoding of provisions and drug packages. However, the absence of data related to outcomes, diagnoses and clinical parameters constitutes an important limitation. In this regard, it must be noted that a lot of relevant information to screen for T2D is missing, such as glycated hemoglobin levels, lifestyle, BMI and potential genetic predisposition.

Health expenditure records prove extremely useful for retrospective observational studies, as is common in epidemiology. However, a certain lag exists between medical acts and the appearance of associated records in health expenditure databases. For provision records, the maximum lag is two years, while for drug purchases the lag is less than half a year. These lags present problems for applications that require quasi real-time information, such as disease outbreak detection, but are less problematic for screening.

A disadvantage is that expenditure data may be noisy. Most sources of noise can be considered random and hence neglected, but some structural issues exist as well. Specific examples include abuse via overconsumption and fraud through *upcoding*.[10] Such phenomena are known to plague healthcare systems in various countries and likely occur in Belgium as well to some extent [239, 246, 36, 22].

Finally, it is worth noting that the potential of health expenditure data for clinical applications is also being investigated in other countries. A highly visible recent example was the Heritage Health Prize competition to identify patients who will be admitted to a hospital within the next year using historical claims data, with an impressive $3,000,000 prize pool.[11]

1.4 Machine learning challenges and contributions

The previous Sections introduced diabetes mellitus, explained the need for screening approaches and indicated the potential use of Belgian health expenditure data. Identifying individuals at high risk for T2D based on Belgian health expenditure data posed several machine learning challenges, including dealing with missing and noisy information, defining representations that capture the implicit structure of health expenditure data and coping with the size of the learning problem, in terms of number of instances and features alike.

This Section highlights the main machine learning contributions made during this project. We will briefly describe the fundamental problems that were tackled, outline the approach and clarify how it fits into the overarching theme of identifying patients at risk for diabetes based on health expenditure data. Chapters 3 to 8 describe the solutions and methodologies we developed in detail.

We approached the screening task as a binary classification problem. Binary classifiers are models which yield some level of confidence that an instance belongs to the positive class, based on the features of that instance. In our

[10] Upcoding refers to caregivers' wilfull reporting of wrong nomenclature codes, or codes corresponding to provisions that were never performed, in order to obtain higher refunds.

[11] More information is available at `http://www.heritagehealthprize.com/`.

application, every person represents an instance. The associated labels indicate whether a person requires GLA therapy such that persons using GLAs are positive, while all others are unlabeled.[12] The biographic information and resource-use history of each person represent the associated features.

The relationships between all aspects of this project's machine learning research are depicted in Figure 1.5. Our contributions revolved around three focal points: learning from positive and unlabeled data, automated hyperparameter optimization and the development of reusable open-source software to facilitate reproducibility. Sections 1.4.1 to 1.4.3 describe each focal point in more detail.

1.4.1 Learning from positive and unlabeled data

A critical challenge inherent to our application is an infeasibility to ascertain which patients are non-diabetic based only on health expenditure records. This problem originates from several sources, most notably because a significant fraction of diabetic patients is undiagnosed (as discussed in Section 1.2) and additionally because initial diabetes therapies may exclusively consist of lifestyle changes (cfr. Section 1.E) which are not recorded in health expenditure data.

Fortunately, we were able to identify a reasonable set of known diabetics (positives) based on health expenditure data. Positives were identified through the use of pharmacotherapy involving glucose lowering agents (GLAs) over extended periods of time. The thus identified set of positives mainly consists of patients with progressed diabetes (since the treatment involves pharmacotherapy) and omits patients with (potentially diagnosed) prediabetes. This labeling induces a small fraction of false positives, mainly due to the use of GLAs for alternative reasons (e.g. use of metformin for weight loss).

In machine learning, the true class of an instance is commonly called its *label*. Given the labeling issues described previously, we had to learn binary classifiers from positive and unlabeled data to enable screening based exclusively on health expenditure data. This learning scenario is receiving increasing amounts of research attention and is commonly dubbed PU learning. During this project, we improved an existing PU learning method [179] and additionally developed a method to evaluate classifiers without known negatives. The latter aspect is particularly important because it has significant practical implications and was previously uncharted territory.

[12] Persons without records of GLA use should not be treated as negatives because such persons might still need GLA therapy, e.g., undiagnosed diabetes patients.

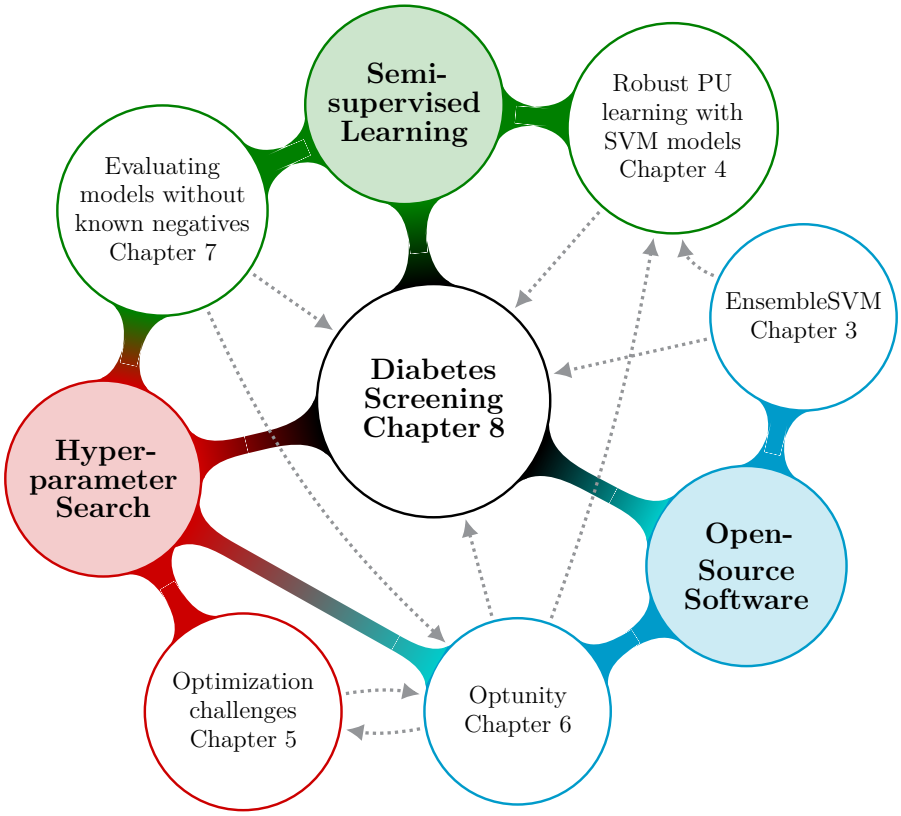


Figure 1.5: Dependencies of the key contributions made to machine learning research during this project. To enable diabetes screening based on Belgian health expenditure data (Chapter 8), we made contributions to semi-supervised learning (Chapters 4 and 7), automated hyperparameter search (Chapters 5 and 6) and open-source machine learning software (Chapters 3 and 6).

Building classifiers with only positive and unlabeled data

This is a common topic within semi-supervised learning, presenting additional complexity compared to fully supervised binary classification.[13] Various methods have been devised to cope with the increased uncertainty, based on one of two fundamental approaches: (i) first attempt to infer a set of likely negatives from the unlabeled data and then train a fully supervised model to distinguish known positives from inferred negatives [167, 282, 161] vis-à-vis (ii) treat unlabeled

[13] In this context, fully supervised means all class labels are known.

instances as negatives with noisy class labels and deal with this directly [92, 159, 166, 179, 168].

The method we developed fits into the latter category and is described in detail in Chapter 4. Our technique achieves state-of-the-art performance in PU learning and is additionally designed for robustness against false positives, which are known to exist in our application. False positives significantly deteriorate the performance of other existing methods, limiting their usability in our project.

Evaluating classifiers with only positive and unlabeled data

Assessing the performance of binary classifiers without known negatives was an open problem at the start of the project. Prior to our work, a few methods have been devised for model selection in PU learning which allow basic pairwise comparisons between classifiers [159]. During our work, some additional related methods were developed by others [230, 121]. However, none of these quantify the performance of a given classifier in terms of commonly used metrics like sensitivity, specificity and area under the ROC curve.

The performance of models for screening must be quantified before their use can even be considered, however no convincing method to quantify performance without known negatives existed. To circumvent this problem we initially considered manually obtaining negative labels by directly asking patients whether or not they had diabetes. Clearly, this is a very sensitive matter and would additionally have been labour intensive to acquire a sufficient amount of negative labels.

Instead of manual labeling, we developed a method to reliably estimate performance of binary classifiers without known negatives (cfr. Chapter 7). This method is the first of its kind and relies only on the reasonable assumption that known positives are sampled completely at random from all positives, which implies that the distributions of known and latent positives are comparable. Our work effectively reduces estimating performance without negatives to estimating the fraction of positives in the unlabeled set, which is often feasible.

1.4.2 Automated hyperparameter optimization

Most machine learning algorithms are parameterized, for example to allow the user to determine an optimal model complexity for a given problem. The coefficients of a trained model are commonly called parameters, and hence the parameters used to describe the training problem itself are referred to as *hyper*parameters. Current research focuses on automatically determining

suitable values for these hyperparameters [139, 35, 242, 32, 33, 90, 254], which essentially boils down to the development of suitable (heuristic) optimizers.

Some of the key challenges in hyperparameter optimization are described in Chapter 5. Several libraries have been developed to automate this process and have proven to be far more efficient than manual tuning or grid search [139, 32, 242, 33]. However, most of these libraries are hard to install (even for seasoned programmers!) and expose a lot of complex configurations, hence effectively limiting their potential userbase to experts. We have developed a cross-platform open-source Python library that provides a variety of optimizers to automate hyperparameter search via a simple, lightweight API to fill this apparant gap of user-friendly tuning software (described in Chapter 6).

1.4.3 Open-source software

Machine learning research requires high-quality, tested and documented software to advance rapidly. Fortunately, several authorities in the machine learning field are appreciative of open-source software [244]. Overall, the field is blessed with a wealth of open-source packages covering all aspects of the learning process and we strongly feel that cultivating this ecosystem is in the best interest of the entire academic community, for reasons such as efficiency, reliability and reproducibility. It is worth noting that every analysis in this project was done using freely available software.

As we recognize the value and importance of a solid open-source ecosystem, we decided to pay it forward by developing two open-source libraries of our own: *EnsembleSVM* and *Optunity*.

EnsembleSVM is a C^{++} package for ensemble learning with support vector machine (SVM) base models (described in Chapter 3). This software enables efficiently computing nonlinear models on large-scale data sets, which would otherwise be infeasible without significant computational resources. The PU learning method we developed (cfr. Chapter 4) is a use-case of EnsembleSVM and was implemented entirely using the API offered by the library.

Optunity is a Python library for automated hyperparameter optimization, with interfaces to R, MATLAB, Octave and Java. An overview of Optunity is given in Chapter 6. At the time of writing, Optunity receives hundreds of downloads each month via the Python Package Index (PyPI). Optunity was used to optimize the hyperparameters of the learning approaches we used to construct models for diabetes screening.

1.5 Structure of the thesis

This Section summarizes all subsequent chapters and reiterates how every aspect is relevant to diabetes screening based on Belgian health expenditure records.

- *Chapter 2* describes a study we performed to quantify the survival of Belgian patients after starting various glucose-lowering pharmacotherapies. Unlike other studies, our study does not focus on relative efficacy of different GLA therapies. Instead, it is the only one that provides an expected survival rate for patients starting a specific therapy, accounting for all possible future therapies commonly seen in the Belgian population.
- *Chapter 3* introduces the EnsembleSVM software package, which provides efficient routines for ensemble learning using SVM base models.
- *Chapter 4* describes a novel algorithm to learn robust binary classifiers from positive and unlabeled data. The key design criterion is robustness to false positives, which was lacking in existing approaches. The implementation is based on EnsembleSVM (see Chapter 3).
- *Chapter 5* discusses the main optimization challenges posed by automated hyperparameter search and summarizes the current state-of-the-art.
- *Chapter 6* describes the Optunity software package, which provides metaheuristic optimization routines for automated hyperparameter optimization. Optunity is available on most commonly used machine learning platforms and tackles the challenges outlined in Chapter 5.
- *Chapter 7* presents a method to evaluate the performance of binary classifiers without negative labels. This method enables estimating most commonly used performance metrics in a semi-supervised setting, which was uncharted territory.
- *Chapter 8* integrates all machine learning aspects into a workflow to predict which patients are likely to start glucose-lowering pharmacotherapy, based exclusively on readily available, individual health expenditure records. This chapter combines all techniques described in previous chapters.
- *Chapter 9* summarizes our work and describes potential use-cases and promising future research avenues. Finally, we conclude with some relevant tradeoffs from a policy perspective regarding the use of health and healthcare data for medical applications.

Appendix

1.A Regulation of blood glucose levels

To allow a better understanding of the underlying problems inherent to diabetes mellitus, we will briefly describe the critical role of insulin in the regulation of blood glucose levels.

Insulin is a peptide hormone which regulates the metabolism of fats, carbohydrates and proteins. In normal circumstances, insulin is released in response to changes in blood glucose concentration to prevent glucose levels from reaching toxic concentrations. Specifically, insulin promotes the absorption of glucose from the blood to skeletal muscles and fat tissue, thereby lowering the glucose level in the bloodstream, and additionally inhibits hepatic glucose output [243]. Insulin is exclusively produced by pancreatic β cells, which are located in clusters known as the islets of Langerhans.

Hyperglycemia occurs when the regulation of the blood glucose level fails and hence toxic concentrations of glucose remain in the bloodstream. Such failures are typically caused by excessive glucose intake, insufficient insulin secretion and/or insulin resistance.

1.B Complications and comorbidities of diabetes

Exposure to chronic hyperglycemia can cause serious damage to many of the body's systems, including dysfunction and failure of various organs.

The leading complication of type 2 diabetes is cardiovascular disease, with about half of type 2 diabetes patient deaths attributable to a cardiovascular cause [281, 38]. Diabetes may lead to severe macro -and microvascular problems. The process of atherosclerosis is the main pathological mechanism leading to

macrovascular complications [31, 47, 100] such as acute vascular infarction [47] and cardiovascular events [31]. Microvascular complications contribute considerably to the morbidity of the disease, specifically diabetes mellitus may lead to the progressive development of retinopathy (which potentially results in blindless), neuropathy (which can induce problems like foot ulcers), nephropathy (which can lead to renal failure) [20] and small vessel vasculopathy causing lower extremity amputation [38]. Finally, patients with diabetes mellitus are at increased risk for peripheral vascular and cerebrovascular disease.

1.C Classification of diabetes mellitus

Diabetes mellitus is a disorder of multiple etiologies and is subdivided into several more specific classes. The primary distinction between subclasses is essentially whether or not external insulin is necessary for survival. The first widely accepted classification was made by the World Health Organization (WHO) in 1980 [190], proposing two main classes of diabetes mellitus:

- **Type 1 diabetes (T1D)** refers to a condition characterized by insufficient insulin secretion caused by the autoimmune-mediated destruction of pancreatic β-cells. T1D patients require insulin for survival. T1D can start at an early age and has a strong genetic component.
- **Type 2 diabetes (T2D)** results from defect(s) in insulin secretion, almost always paired with insulin resistance. T2D includes patients that require insulin for metabolic control and those that don't require insulin at all. The often asymptomatic onset of T2D typically occurs after 50 years of age[14], often as a result of genetic susceptibility combined with chronic obesity, a sedentary lifestyle and overly rich nutrition [290, 241]. The terms *diabesity* and *obesity dependent diabetes mellitus* have been suggested [232, 19] because obesity is a common comorbidity of T2D [241].

In the original proposal, T1D and T2D were aliased insulin-dependent diabetes mellitus (IDDM) and noninsulin-dependent diabetes mellitus (NIDDM), respectively [190]. However, since then the WHO has deprecated the terms IDDM and NIDDM as their use frequently led to patients being classified based on treatment, rather than pathogenesis [10]. Hence, contemporary terminology exclusively uses type 1 and type 2 to denote the main classes of diabetes mellitus.

[14]Though a case-study reported a 3 year-old child diagnosed with T2D at this year's European Association for the Study of Diabetes (EASD) meeting [8, "*A toddler with type 2 diabetes*", pp. 152–153].

Though our work focuses on type 1 and particularly type 2 diabetes mellitus, it must be noted that more forms exist, such as gestational diabetes mellitus which may occur during pregnancy and then disappear or progress into T2D.

T2D accounts for over 90% of diabetes patients and has long been considered an epidemic that affects both developing and developed nations [288, 290, 215, 183, 61, 156] effectively rendering it a pandemic [38]. T2D is often a manifestation of a much broader underlying disorder [212, 288], including the *metabolic syndrome* which is a cluster of cardiovascular disease risk factors that includes hyperinsulinemia, dislipidemia, hypertension, visceral obesity, hypercoagulability and microalbuminuria [12, 290, 98].

1.D Prevalence and burden of diabetes

The number of diabetes patients, particularly type 2 diabetes, is increasing rapidly. In developed countries, this increase is driven by population aging, lifestyle changes (particularly rising levels of obesity and inactivity) but also by greater longevity among diabetes patients [248, 38]. The majority of social and economic burden of type 2 diabetes patients is attributable to vascular complications [38], with pharmacy costs generating the majority of diabetes-related health expenditure [186, 104].

Prevalence In 1995 an estimated 135 million people worldwide had diabetes, which has increased to 285 million patients worldwide in 2010 [235, 61] and is predicted by the WHO to increase further to at least 366 million by 2030 [241]. WHO estimated the global prevalence of diabetes to be 9% among adults over 18 years of age [13]. A recent study estimated the prevalence of diabetes in adults aged 20–79 in Belgium and Europe to be 8% and 6.9%, respectively [235]. Typically, the prevalence of prediabetes is estimated even higher [73, 279, 61].

Mortality The premature mortality attributable to diabetes is widely underestimated because only a minority of persons with diabetes die from a cause that is uniquely attributable to the disease [38]. One study reported about 2.9 million deaths worldwide attributable to diabetes [216] and indicated that this excess mortality accounts for over 8% of deaths in developed countries. More recently, the global excess mortality in adults directly related to diabetes has been estimated to 3.8 million deaths [38]. The main causes of premature deaths in type 2 diabetes patients are due to cardiovascular and renal problems [181, 38]. Chapter 2 reports the survival of patients starting various glucose lowering pharmacotherapies in Belgium and confirms excess mortality in patients

with diabetes compared to the general population. Additionally, our analysis indicates that the excess mortality is significantly associated with the type of pharmacotherapy, which is related to the patient's health status.

Cost Managing diabetes and its complications is expensive, both to the affected individuals and healthcare systems around the world. The International Diabetes Federation (IDF), estimates that diabetes already accounts for one ninth of the total healthcare budget in many countries in 2014 [3]. The IDF further reports an average cost per diabetes patient of 5,679 USD in Belgium [2]. Other sources report comparable numbers: the CoDiM study estimated that in Germany in 2001, annual direct mean costs per diabetic patient are $5,262$ EUR with an additional $5,019$ EUR indirect costs, compared to $2,755$ EUR and $3,691$ EUR for non-diabetics [153]. Köster et al. [153] also note that the direct costs of diabetic patients account for 14.2% of total healthcare costs. Patients of type 2 diabetes with macrovascular complications generate costs that are three times higher than type 2 diabetes patients without macrovascular complications and seven times higher than people with neither type 2 diabetes nor macrovascular diseases [38]. The primary origin of diabetes-related healthcare expenditure are pharmacy costs [186, 104]. The complications of diabetes constitute a large portion of the burden of the disease, with diabetes being a leading cause of blindness, lower limb amputation and kidney failure [38].

1.E Treatment of diabetes mellitus

The fact chronic hyperglycemia may manifest in various ways is reflected in a wide variety of treatments for diabetes mellitus. Treatment of type 1 diabetes patients revolves around timely administration of external insulin, which they need for survival. In contrast, a wide range of treatment options exist for patients with type 2 diabetes.

Management of type 2 diabetes includes several lifestyle interventions, often specifically targetted towards weight loss, including healthy eating (specifically high-fiber, low-fat foods like fruits and vegetables), regular exercise and blood sugar monitoring and management. Pharmacotherapy via glucose lowering agents (GLAs) is used when lifestyle changes alone are insufficient for adequate glycemic control or when diabetes is already in a progressed stage at the time of clinical diagnosis.

We will elaborate on pharmacological treatment of type 2 diabetes, as this has played a crucial role in our work. Pharmacological therapies for (type 2) diabetes may be based on various biological mechanisms:

- **External insulin** is administered when insufficient insulin is secreted by the pancreas. External insulin is always necessary to treat type 1 diabetes but may also be required to treat insulin deficiency in type 2 diabetes. Insulin cannot be taken as a pill because it would be broken down during digestion just like protein in food. Instead, it must be injected or inhaled.

- **Sensitizers** reduce the insulin resistance that is central in type 2 diabetes.

  - Biguanides suppress hepatic glucose output and increase uptake of glucose by the periphery. The most common agent in this class is *metformin* (brand names include *Glucophage*®, *Glucovance*®) [150].

  - Thiazolidinediones (TZDs) enhance the effects of insulin by increasing insulin-dependent glucose disposal and reducing hepatic glucose output (as a result of increased hepatic insulin sensitivity) [222, 280]. An example of TZDs is *pioglitazone* (brand name *Actos*®).

- **Secretagogues** increase insulin output from the pancreas. The main type of secretagogues – sulfonylurea (SU) – stimulate endogenous insulin secretion from pancreatic β-cells [207]. Hypoglycemia is a major concern when using sulfonylureas [43]. The most common SU are *glimepiride* (brand name *Amaryl*®), *glibenclamide* (*Euglucon*® and *Daonil*®), *gliclazide* (*Diamicron*®), *glipizide* (*Glucotrol*®) and *gliquidone* (*Glurenorm*®).

- **Alpha-glucosidase inhibitors** slow down digestion of starch in the small intestine, thereby reducing the rate at which the resulting glucose enters the bloodstream. These agents do not have a direct effect on insulin secretion or sensitivity, but can (i) be sufficiently efficient in early stages of impaired glucose tolerance or (ii) be used in combination with other antidiabetic agents. A common alpha-glucosidase inhibitor is *acarbose* (brand name *Glucobay*®).

- **Incretin-based therapies** use the antidiabetic properties of the incretin hormone glucagon-like peptide 1 (GLP-1), namely that GLP-1 augments glucose-induced insulin secretion in a highly glucose-dependent manner [184, 169]. As this form of insulin secretion occurs in a glucose-dependent manner, incretin-based therapies are less prone to cause hypoglycemia.

  - GLP-1 receptor agonists activate GLP-1 receptors, resulting in increased insulin synthesis and release [85]. Common GLP-1

receptor agonists include *liraglutide* (brand name *Victoza*®), *exenatide* (*Byetta*®) and *lixisenatide* (brand name *Lyxumia*®).

– Dipeptidyl peptidase-4 (DPP-4) inhibitors increase the blood concentration of GLP-1 by inhibiting its degradation caused by the enzyme DPP-4. Common DPP-4 inhibitors include *sitagliptin* (brand name *Januvia*®), *vildagliptin* (brand name *Galvus*®).

Chapter 2

Mortality in individuals treated with glucose lowering agents: a large, controlled cohort study

This chapter has been submitted as:
Claesen, M.*, Gillard, P.*, De Smet, F., Callens, M., De Moor, B. & Mathieu, C. (2015). **Mortality in individuals treated with glucose lowering agents: a large, controlled cohort study**, *Journal of Clinical Endocrinology and Metabolism*.
*: these authors have contributed equally to the manuscript.

Contributions Marc Claesen contributed to the study design and performed all data extractions and statistical analyses.

Abstract

Context Several observational studies and meta-analyses have reported increased mortality of patients taking sulfonylurea and insulin. The impact of patient profiles and concomitant therapies often remains unclear.

Objective To quantify survival of patients after starting glucose-lowering agents (GLAs) and compare it to control subjects, matched for risk profiles and concomitant therapies.

Design Controlled, retrospective cohort study.

Setting The study is based on health expenditure records of the largest Belgian health mutual insurer, covering over 4.4 million people. We analyzed records of 115,896 subjects starting metformin, sulfonylurea or insulin (alone or in combination) between January 2003 and December 2007 and compared them with control subjects without GLA therapy. Controls were matched for age, gender, history of cardiovascular events and therapy with antihypertensives, statins and blood platelet aggregation inhibitors.

Main Outcome Measure 5-year survival after start of GLA.

Results Profiles of patients using different GLAs varied, with patients on sulfonylurea being oldest and patients on insulin having more frequently a history of cardiovascular disease. Excess mortality differed across GLA therapies compared to matched controls without GLAs, even after adjusting for observable characteristics. Only metformin monotherapy was not associated with increased 5-year mortality compared to matched controls, while individuals on combination of sulfonylurea and insulin had highest mortality risks. Age and concomitant use of statins strongly affect survival.

Conclusions Differences exist in 5-year survival of patients on GLA, at least partly driven by the risk profile of the individuals themselves. Metformin use was associated with lowest 5-year mortality risk and statins dramatically lowered 5-year mortality throughout all cohorts.

2.1 Introduction

Glucose lowering therapy in type 2 diabetes is challenging, due to the progressive nature of the disease by the underlying failure of the insulin-secreting beta-cells [204]. Algorithms and guidelines are proposed by international bodies, guiding clinicians through the maze of possibilities of glucose-lowering agents, but these tools are mostly based on evidence from the original UKPDS study, reported in the middle of the 1990's [117]. Evidence on the impact of glucose-lowering agents on the hardest endpoint, survival, is limited. In particular, sulfonylurea and insulin have been associated with higher mortality risks in cross-sectional studies or population studies [116, 218, 76, 141, 180, 259] with criticisms arising that comparing the mortality risk in these individuals to the global population is unfair as the profile of this population may be different, predisposing them to a higher mortality risk.

On the other hand, many studies report a lower mortality risk in type 2 diabetes patients treated with metformin [116, 218, 76, 141, 180, 259, 28] but again, the profile of these people may be different by itself, thus influencing risk. Finally, in the high cardiovascular risk disease that is type 2 diabetes, use of statins has been debated frequently, with doubts being cast over the usefulness of these drugs in this population, in particular in the young or very old age groups.

This study investigated the survival of patients starting therapies involving various glucose-lowering agents (GLAs) compared to fully matched control subjects. We particularly analyzed the effect of age and concomitant use of statins.

This study was performed in collaboration with the largest mutual health insurance fund in Belgium (National Alliance of Christian Mutualities - NACM), which has access to a large database containing health expenditure records of 4.4 million people throughout the country. The Belgian health care insurance is a broad solidarity-based form of social insurance. Mutual health insurers like NACM are the legally-appointed bodies for managing and providing the Belgian compulsory health care and disability insurance. To implement its operations, NACM disposes of a large database containing health expenditure records of all its members. These records hold all financial reimbursements of drugs, procedures and contacts with health care professionals. Long-term follow-up and full matching of the people using GLAs to people identical in age, gender, concomitant medications and start of follow-up are possible. We performed a 5-year survival analysis to assess the excess mortality in patient cohorts defined by their GLA therapy compared to references without GLA therapy but with otherwise similar observable characteristics. Our analysis shows differences in 5-year survival in individuals treated with GLAs, at least

partly driven by the risk profile of the individuals themselves.

2.2 Research design and methods

This study is based on records of the NACM, the largest Belgian mutual health insurer with over 4.4 million members (market shares of over 40% and 60% in Belgium and Flanders, respectively). All data extractions and analyses were performed at the Medical Management Department of the NACM under supervision of the Chief Medical Officer. NACM disposes of a longitudinal overview of its members' medical resource use, embedded in health expenditure records. Only 2% of the subpopulation under study left the NACM to switch to another mutual health insurer, emigration or employment by a foreign employer during the 5-year follow-up period, leading to a retention rate of 98% in our study. Patients that joined NACM after December 1999 were excluded from all analyses to minimize the chance of missing glucose-lowering therapy and/or cardiovascular events prior to starting follow-up.

Medication records were mapped onto the fifth level of the anatomical therapeutic chemical (ATC) classification system via the main chemical substances associated with each drug. The ATC system classifies drugs based on the targeted organ or system and their therapeutic and chemical characteristics [192]. Patients were partitioned into treatment groups based on ATC codes listed in their individual histories. Exact definitions of all pharmacological groups can be consulted in Table 2.1. In addition to pharmacotherapy, we considered a set of cardiovascular events prior to follow-up, which were identified via a combination of medicinal and surgical interventions (also described in Table 2.1). Based on usual prescription behavior in Belgium, exposure of oral glucose lowering drugs was assumed to be uninterrupted between the dates of the first record and up to six months after the final record in the insurance database.

2.2.1 Study cohort selection

The selection process is illustrated in Figure 2.1. 115,896 patients over 18 years old in whom glucose-lowering therapy was prescribed between 1st of January 2003 and 31st of December 2007 were eligible for the study. Eligible patients were assigned to study cohorts based on their glucose-lowering pharmacotherapy: more specifically metformin (MET), sulfonylurea (SU) and insulin (INS). Every combination of these three drug types defines a study cohort. Patients on DPP4

Category	Definition
metformin	ATC codes: A10BA02, A10BD02, A10BD07, A10BD08
sulfonylurea	ATC codes: A10BB01, A10BB08, A10BB09, A10BB12, A10BD02
insulin	ATC codes: A10AB02, A10AB03, A10AB04, A10AB05, A10AB06, A10AB30, A10AC01, A10AC02, A10AC03, A10AC04, A10AC30, A10AD01, A10AD02, A10AD03, A10AD04, A10AD05, A10AD30, A10AE01, A10AE02, A10AE03, A10AE04, A10AE05, A10AE30, A10AF01
statins	ATC codes: all codes under C10AA
antihypertensives	ATC codes: all codes under C02, C03, C07, C08, C09
blood platelet aggregation inhibitors	ATC codes: all codes under B10AC
cardiovascular events	An arterial thrombotic event of the coronary, carotid, vertebral, aortic, iliac or lower extremity arteries necessitating an intervention for revascularization. Open and/or percutaneous interventions included thrombectomy, embolectomy, endarterectomy, artery bypass, vascular endoprosthese, endovascular dilatation, stenting or brinolysis. A positive history of a cardiovascular event was defined as having one or more of those events reimbursed by the NACM based on the Belgian nomenclature of health care provisions.

Table 2.1: Definitions of drug categories and cardiovascular events.

inhibitors or GLP-1 receptor agonists were not included as these were only introduced in Belgium around 2008.

Follow-up started on the first day of therapy intake, based on the patient's purchase of the prescribed agent(s). In each study and control group, subjects were followed until death or censoring over a maximum period of 5 years since inclusion. For control subjects, the start of follow-up was determined at random within the year of inclusion of the associated study subject to avoid bias related to the time of entry into the study.

Monotherapy study cohorts denote the first glucose-lowering therapy consisting of a single type of GLA, given to a patient without prior use of other GLAs (n=74,938), based on historical records from 1990 onwards. Patients are excluded from monotherapy cohorts if they transition to combination therapy within three months. Patients who started a combination therapy during the selection

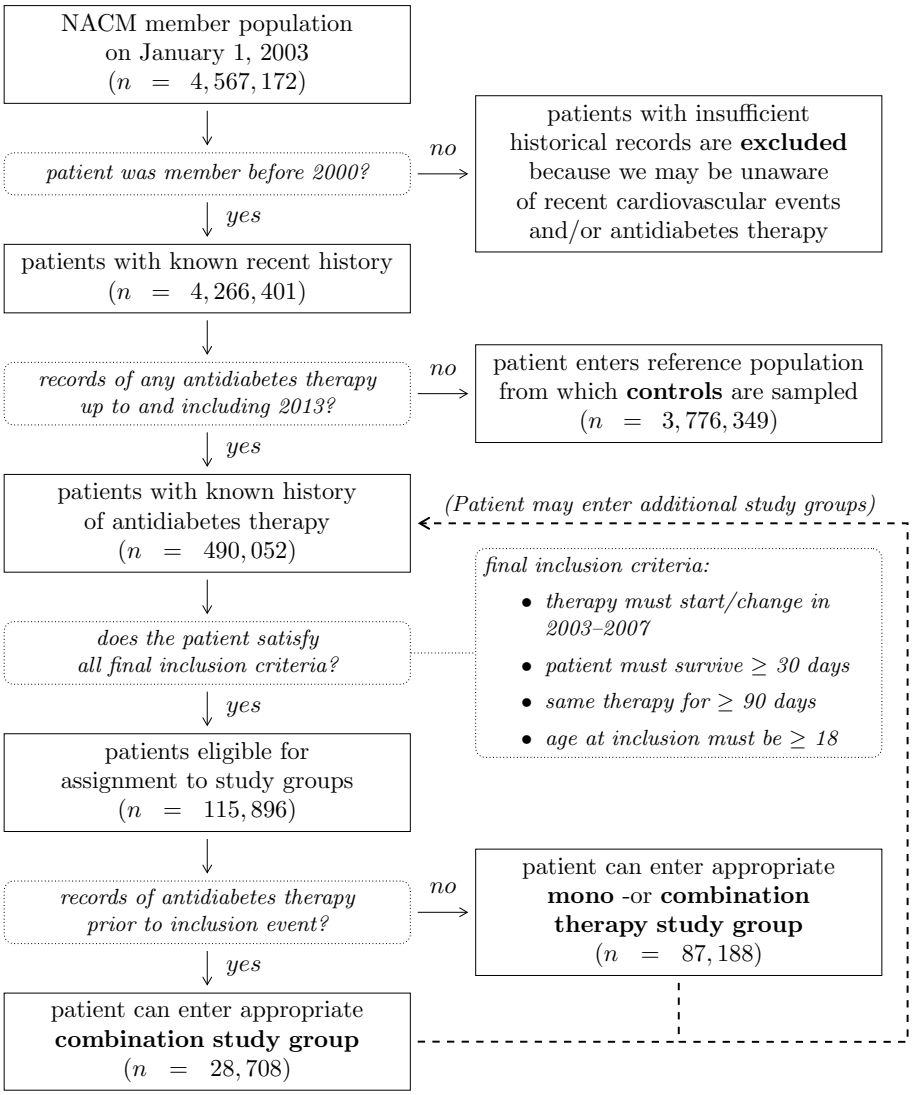


Figure 2.1: Flowchart describing the selection protocol for study and control patients. Patients can move from the bottom right (monotherapy) to the bottom left group (combination therapy), but not vice versa. All listed counts are for unique patients.

interval for at least 3 months (or until death) were included in the associated study cohorts, regardless of potential prior glucose-lowering therapy (n=47,149).

Patients could successively enter multiple study cohorts and be included in multiple cohorts during follow-up. For instance, a patient without prior GLA therapy who started metformin in 2003 and added sulfonylurea in 2005 is included in both the metformin monotherapy and the metformin and sulfonylurea combination therapy cohorts (5-year follow-up starting in 2003 and 2005, respectively), with some period of overlap (2005-2008).

Only patients with at least one month between the first and last purchase of associated GLAs were included in study cohorts, inducing an immortal time of one month. We accounted for potential bias by consistently matching control patients who survived for at least one month [217, 234]. Patients who started treatment and died during a single hospital admission were excluded from the analysis.

2.2.2 Control cohort selection

We compared study groups to controls with similar observable characteristics. Controls were sampled without replacement from the NACM population with matched characteristics to the study cohort, but without records of GLA therapy up to and including 2013. Unless stated otherwise, the control groups contained 5 subjects per subject in the study cohort, matched exactly on age at the start of follow-up, gender, cardiovascular history (had event/no event before the start of the follow-up), associated therapy (use of statins, antiplatelet and antihypertensive drugs) and the year of start of follow-up. Matching based on associated therapy was performed dichotomously (subject has/has not received the therapy for more than half of the individual's effective follow-up period).

2.2.3 Therapy changes within cohorts

The majority of patients remained on the same GLA therapy during the entire follow-up (Table 2.2.4). 15.4 to 28.5% of patients starting on monotherapy moved to a combination therapy by the end of the follow-up. Patients on combination therapy at start were still on the same regimen in 47.7 to 66.5% of cases: changes were often due to stopping of sulfonylurea (9 to 20%) or eliminating metformin from combination regimens that include insulin (15.2 to 18.7%).

	mono therapy			combination therapy			
→ end regimen	metformin	sulfonylurea	insulin	metf+sulf	metf+ins	sulf+ins	metf+sulf+ins
metformin	81.8%	2.0%	0.8%	10.9%	2.9%	0.3%	1.3%
sulfonylurea	5.2%	63.9%	2.4%	20.7%	1.3%	3.9%	2.7%
insulin	2.2%	0.9%	86.2%	0.7%	5.8%	2.6%	1.6%
metf+sulf	9.2%	4.5%	3.2%	66.5%	5.5%	1.7%	9.3%
metf+insulin	9.5%	0.5%	15.2%	1.9%	66.1%	1.3%	5.5%
sulf+insulin	0.9%	11.2%	20.1%	2.9%	3.2%	51.6%	10.2%
metf+sulf+insulin	2.3%	1.7%	11.7%	9.1%	20.6%	7.0%	47.7%

Table 2.2: Partitioning of final treatment regimen of patients starting a specific therapy (rows). The final treatment regimen (columns) is based on the last 9 months of individual followup. Patients are censored in all survival analyses after 9 consecutive months of renunciation from metformin, sulfonylurea and insulin.

2.2.4 Censoring

As we were primarily interested in prognoses for patients starting a certain therapy, no censoring was done based on therapy changes (such as adding additional GLAs) or poor compliance. Censoring based on therapy changes would be informative and hence bias the survival estimates of interest. Patients that discontinued all GLA therapy for nine consecutive months are right censored, as this was considered to indicate that the patient was not using GLAs to manage glucose levels (e.g. using metformin for weight loss). Right censoring also occurred when subjects left the health insurer (lost to follow-up), which was rare (less than 2% of all patients in follow-up in each cohort). Switching health insurer was considered unrelated to a patient's medical condition and can therefore be considered non-informative.

2.2.5 Statistical analysis

Empirical survival curves were obtained using the Kaplan-Meier estimator. The associated 95% CIs were computed using the exponential Greenwood formula [145]. We used Cox proportional hazards (PH) models to quantify excess mortality between study and control cohorts while controlling for all observable patient characteristics. Adjusting for concomitant medication was particularly important, as controls were only matched in a binary fashion. Unless mentioned otherwise, the PH models contained the following set of predictors: continuous covariates describing age at start of follow-up and associated therapy (specifically statins, antiplatelet and antihypertensive drugs) and dichotomous factors for gender and the group a subject belonged to (study or control). Associated therapy-related predictors quantify the fraction of the subject's effective follow-up time during which he/she was exposed to the agent. Finally, an interaction term between age and gender is consistently included. The PH assumption was assessed via the Grambsch-Therneau test on scaled Schoenfeld residuals from the PH models [112]. The proportionality assumption was tested for each reported hazard ratio at the 1% significance level and rejections are indicated in all tables.

Software Statistical analyses were conducted in R using the survival package [252, 253]. Statistical plots were made in R using the ggplot2 package [274].

2.3 Results

2.3.1 Baseline cohort characteristics

An overview of the study cohorts and their baseline characteristics is given in Table 2.3.2. The study group with the youngest patient population was the group on insulin monotherapy without CV history ($p < 0.001$ compared to all other groups), followed by patients on metformin monotherapy without CV history ($p < 0.001$ compared to all remaining groups). The oldest patients were those who received sulfonylurea regardless of CV history ($p < 0.001$ compared to all other groups). Patients with a history of CV disease were consistently older than others ($p < 0.001$ in all pair-wise comparisons to groups without CV history) except in the sulfonylurea-insulin combination group. Patients without insulin in their GLA therapy were less likely to have a history of CV disease (less than 9% percent of the total group) than patients with insulin on board (more than 20% percent of total group) ($p < 0.001$).

The percentage of males and intake of associated therapies (statins, antiplatelet and antihypertensive therapies) were consistently higher in the patients with a history of CV disease than in those without, irrespective of the glucose lowering therapy ($p < 0.001$ for all groups). The majority of patients with a CV history were taking statins for over half the follow-up period, ranging from 58% in the SU + INS group to 79% in the metformin monotherapy group. In contrast, only a minority of patients without CV history were taking statins: ranging from 23% in the insulin monotherapy group to 47% in the MET + INS group.

2.3.2 Five-year survival in individuals on different glucose lowering agents

Compared to their associated matched controls, patients on metformin monotherapy showed no significant excess mortality during the follow-up. In contrast, patients started on SU, and certainly on insulin, did much worse than their respective controls (Figure 2.1). The excess mortality was highest in patients starting on insulin (23.8%), followed by SU (4.1%) and finally metformin (0.3%, though not statistically significant at the 5% significance level). Patients who started with bitherapy (MET + SU or MET + INS) or tritherapy (MET +SU +INS) also exhibited reduced 5-year survival compared to matched controls, with the highest difference in survival (12.9 and 15.6%) when insulin was part of the regimen from the start of follow-up.

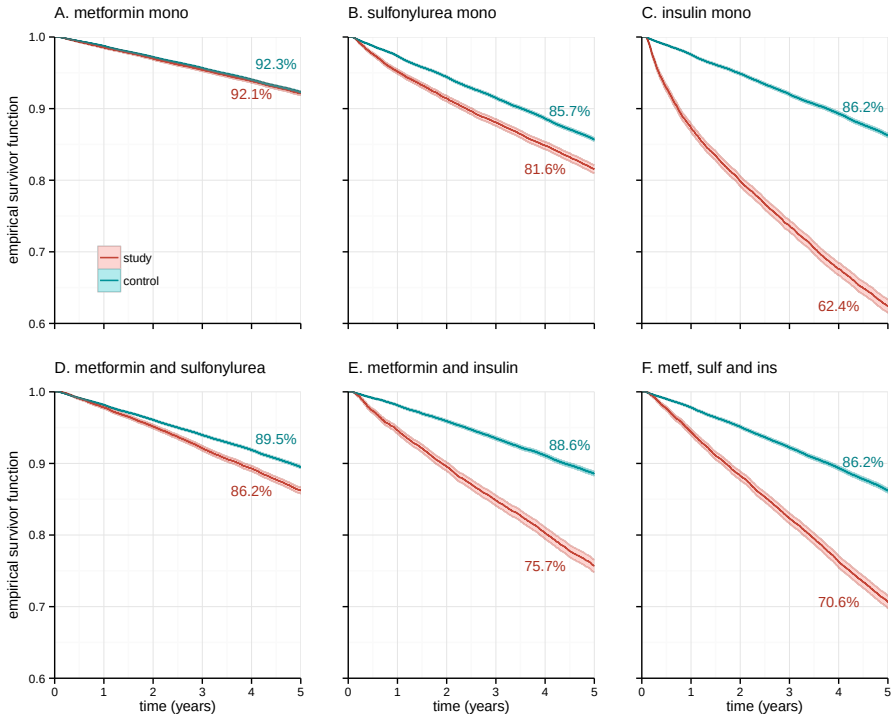


Figure 2.1: 5-year survival for increasing age per cohort.

			gender	associated therapy		
	subjects	age	female	statins	antiplatelet	antihypertensive
study cohort	n	$mean \pm SD$	n (%)	n (%)	n (%)	n (%)
metformin	42,900	62.0 ± 12.3	21,759 (51)	19,747 (46)	7,725 (18)	33,785 (79)
no cv history	39,578	61.6 ± 12.4	20,913 (53)	17,127 (43)	5,579 (14)	30,592 (77)
cv history	3,322	66.8 ± 10.3	846 (25)	2,620 (79)	2,146 (65)	3,193 (96)
sulfonylurea	19,231	68.4 ± 12.6	10,100 (53)	7,479 (39)	3,825 (20)	15,507 (81)
no cv history	17,438	68.0 ± 12.8	9,576 (55)	6,325 (36)	2,739 (16)	13,786 (79)
cv history	1,793	71.8 ± 9.7	524 (29)	1,154 (64)	1,086 (61)	1,721 (96)
insulin	12,807	62.8 ± 17.8	5,818 (45)	3,842 (30)	4,270 (33)	10,214 (80)
no cv history	10,372	61.0 ± 18.7	5,125 (49)	2,395 (23)	2,410 (23)	7,827 (75)
cv history	2,435	70.6 ± 10.2	693 (28)	1,447 (59)	1,860 (76)	2,387 (98)
metf+sulf	25,218	65.8 ± 12.0	12,632 (50)	11,718 (46)	5,521 (22)	20,913 (83)
no cv history	22,830	65.4 ± 12.1	11,966 (52)	9,973 (44)	4,038 (18)	18,612 (82)
cv history	23,88	69.6 ± 9.4	666 (28)	1,745 (73)	1,483 (62)	2,301 (96)
metf+insulin	9,506	64.8 ± 13.9	4,880 (51)	4,891 (51)	3,562 (37)	8,305 (87)
no cv history	7,874	64.0 ± 14.5	4,330 (55)	3,716 (47)	2,333 (30)	6,710 (85)
cv history	1,632	68.7 ± 10.1	550 (34)	1,175 (72)	1,229 (75)	1,595 (98)
sulf+insulin	6,087	74.1 ± 11.0	3,201 (53)	2,285 (38)	2,730 (45)	5,580 (92)
no cv history	4,580	74.1 ± 11.6	2,639 (58)	1,415 (31)	1,584 (35)	4,108 (90)
cv history	1,507	74.1 ± 8.8	562 (37)	870 (58)	1,146 (76)	1,472 (98)
metf+sulf+insulin	10,653	69.1 ± 11.4	5,570 (52)	5,405 (51)	4,680 (44)	9,746 (91)
no cv history	8,380	68.7 ± 12.0	4,800 (57)	3,827 (46)	2,933 (35)	7,520 (90)
cv history	2,273	70.5 ± 9.1	770 (34)	1,578 (69)	1,747 (77)	2,226 (98)

Table 2.1: Baseline characteristics of the study cohorts. Individuals starting starting mono therapy are selected such that they have no prior history of diabetes-related drugs. Individuals starting combination therapy may have a prior history of diabetes-related drugs. All differences in use of associated therapy are statistically significant between study cohorts, except for use of antihypertensives in insulin and sulfonylurea mono cohorts (no significant difference). All associated therapy use is statistically significantly elevated in subgroups with prior cardiovascular events within each study cohort. All comparisons of study group characteristics use significance level $\alpha = 0.05$ and are computed using Tukey's test in conjunction with ANOVA to adjusts for multiple comparison.

Comparable differences were seen in survival of patients without a history of cardiovascular (CV) events, with the lowest survival rates in therapies involving both insulin and SU (up to 29% difference after 5 years) (Table 2.2). Patients with a history of CV events consistently exhibited lower survival than patients without a CV history, but excess mortality compared to matched controls was comparable for both subgroups. Of note, the survival of patients with a CV history on metformin monotherapy was not significantly different from the survival of the associated controls. The observed survival benefit of metformin monotherapy disappeared in combination therapy cohorts (Table 2.2).

2.3.3 Age-dependent 5-year survival of individuals on different glucose lowering agents

Figure 2.3.4 illustrates the 5-year survival of patients as a function of age at the start of follow-up. Compared to the general population, 5-year survival was lower at any age in all cohorts on glucose lowering monotherapy except the metformin monotherapy cohort, which exhibits comparable survival to the general population. At any certain age, survival was highest in patients on metformin, worse in patients on sulfonylurea, and worst in patients on insulin. In patients starting on combination therapy, survival was also lower at any age than associated controls. Again, if the regimen contains insulin, survival is worse at any age category, with or without sulfonylurea on board.

The differences in survival at any age were slightly reduced when comparing to fully matched controls, though they remain large and statistically significant (illustrations are given in Figure 2.3.4). This reduction in excess mortality appears to be mainly attributable to the fact that the fully matched control groups have a higher frequency of prior cardiovascular events than the unmatched general population.

Patients starting metformin monotherapy at a very young age (between 18 and 40 years; n=1,446; 83.3% male) had a 5-year survival rate of 99.2% [98.4%–99.6%] compared to 99.3% [99.1%–99.5%] for fully matched controls (p=0.644). Of note, all females in this study group (n = 242) survived the entire follow-up. In the age category 18 to 40 years, the 5-year survival rate of patients on insulin monotherapy (n = 1,873) was reduced compared to fully matched controls ($p < 0.001$), with survival rates of 94.7% [93.4%–95.6%] and 99.5% [99.3%–99.6%] respectively.

	no history of cardiovasular disease			
	5-year survival (%)		hazard ratio	
study cohort	study cohort	control	$\frac{study}{control}$	
metformin	92.6 [92.3–92.9]	92.9 [92.8–93.0]	1.07 [1.02–1.11]	
sulfonylurea	82.5 [81.9–83.1]	86.5 [86.3–86.8]	1.45 [1.40–1.52]	•
insulin	63.9 [62.9–64.9]	88.1 [87.8–88.3]	4.32 [4.14–4.51]	•
metf+sulf	87.0 [86.5–87.4]	90.3 [90.1–90.5]	1.40 [1.35–1.46]	
metf+insulin	77.1 [76.1–78.0]	89.8 [89.5–90.1]	2.71 [2.56–2.87]	•
sulf+insulin	50.3 [48.8–51.7]	78.4 [77.8–78.9]	3.07 [2.92–3.23]	•
metf+sulf+insulin	71.5 [70.5–72.5]	87.5 [87.2–87.8]	2.71 [2.58–2.85]	

	history of cardiovasular disease			
	5-year survival (%)		hazard ratio	
study cohort	study cohort	control	$\frac{study}{control}$	
metformin	86.7 [85.4–87.8]	85.2 [84.6–85.7]	0.92 [0.83–1.02]	
sulfonylurea	72.5 [70.2–74.6]	77.2 [76.4–78.1]	1.35 [1.22–1.50]	
insulin	56.1 [53.9–58.3]	78.6 [77.9–79.3]	2.69 [2.49–2.90]	
metf+sulf	79.1 [77.4–80.7]	81.8 [81.1–82.5]	1.18 [1.07–1.30]	•
metf+insulin	69.2 [66.9–71.4]	82.7 [81.8–83.5]	2.07 [1.87–2.30]	
sulf+insulin	48.8 [46.2–51.3]	74.3 [73.3–75.2]	2.66 [2.44–2.89]	
metf+sulf+insulin	67.4 [65.5–69.3]	81.5 [80.8–82.2]	2.05 [1.89–2.23]	

Table 2.2: Overview of survival for the study cohorts compared to a fully matched control cohort, stratified by cv history. The control group is sampled from the general population and matched for age, gender and use of statins, antihypertensives and antiplatelet drugs. For every patient in the study cohorts, 5 patients with completely matching profiles were used in control. • indicates that the proportional hazards assumption was rejected for the associated hazards ratio ($p < 0.01$).

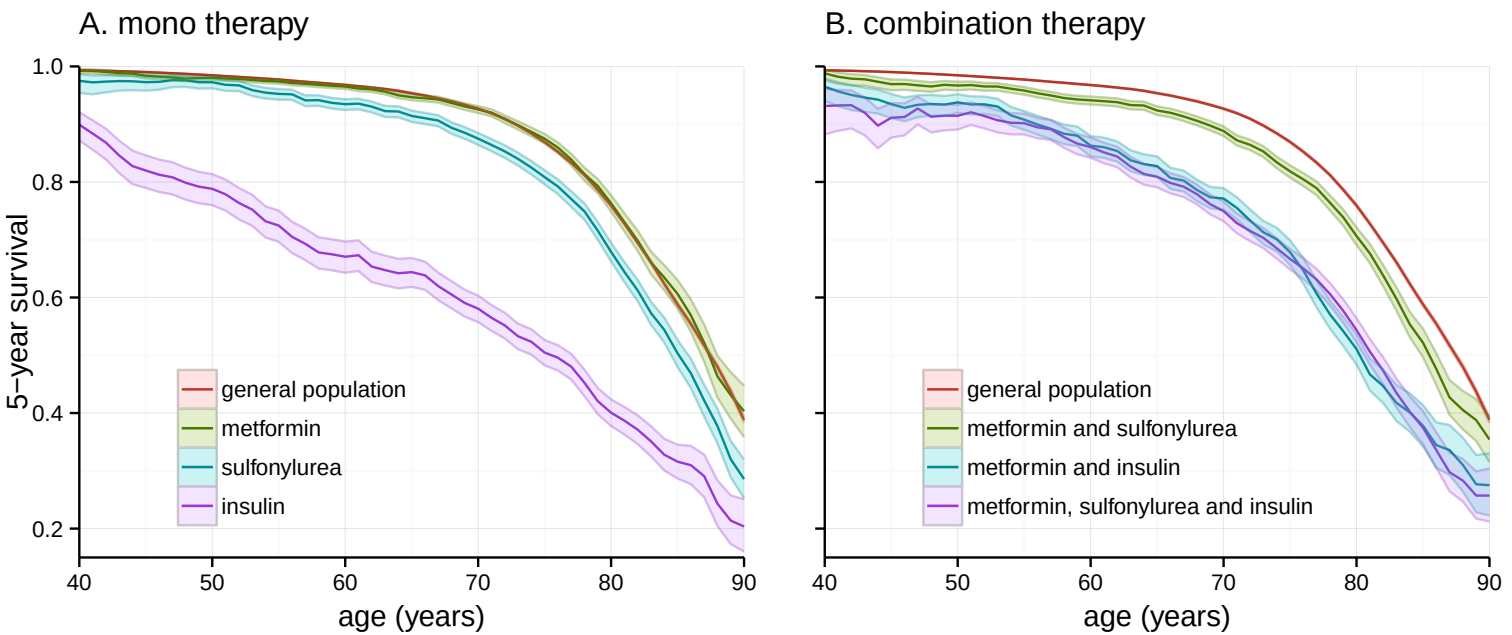


Figure 2.2: 5-year survival for increasing age per cohort.

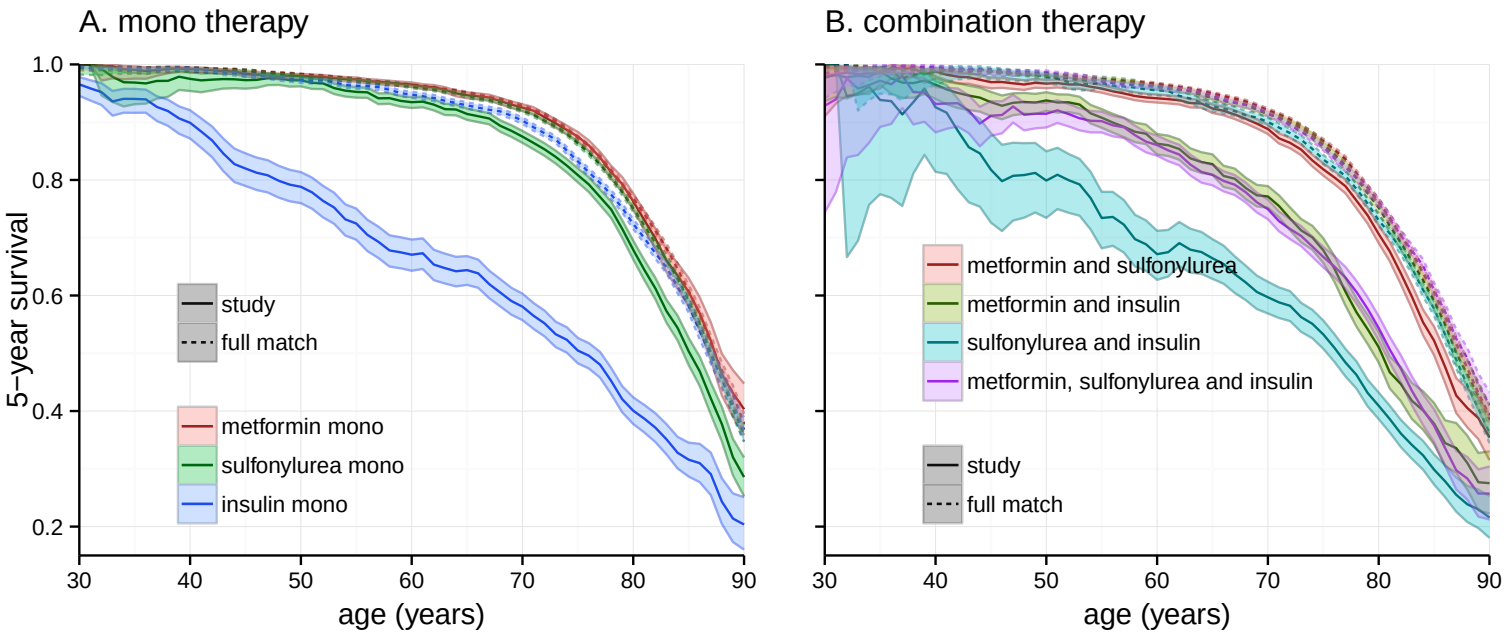


Figure 2.3: 5-year survival for increasing age per cohort with matched controls.

2.3.4 Statins and survival in individuals on different glucose lowering therapy

Survival was compared between patients with and without statins. Survival was consistently higher for patients that used statins in conjunction with GLA therapy (Table 2.3), irrespective of CV history. The observed mortality rate when using statins along with GLAs was 57 to 64% lower in patients without a history of CV disease and by 50 to 68% in patients with a CV history, compared to patients using only GLAs.

	no history of cardiovasular disease			
	5-year survival (%)		hazard ratio	
study cohort	without statins	with statins	$\frac{statins}{no\ statins}$	
metformin	90.2 [89.8–90.6]	95.5 [95.2–95.9]	0.43 [0.39–0.47]	•
sulfonylurea	76.9 [76.1–77.8]	91.7 [91.0–92.4]	0.36 [0.32–0.40]	•
insulin	59.6 [58.4–60.8]	77.3 [75.4–79.0]	0.37 [0.33–0.41]	•
metf+sulf	82.5 [81.8–83.2]	92.6 [92.0–93.1]	0.42 [0.38–0.46]	•
metf+insulin	68.2 [66.7–69.6]	86.8 [85.7–87.9]	0.39 [0.35–0.44]	
sulf+insulin	41.3 [39.6–43.1]	69.9 [67.4–72.3]	0.43 [0.38–0.48]	
metf+sulf+insulin	61.5 [60.0–62.9]	83.4 [82.1–84.5]	0.43 [0.39–0.48]	•
	history of cardiovasular disease			
	5-year survival (%)		hazard ratio	
study cohort	without statins	with statins	$\frac{statins}{no\ statins}$	
metformin	71.3 [67.5–74.6]	90.6 [89.4–91.7]	0.36 [0.29–0.45]	
sulfonylurea	53.1 [48.8–57.2]	82.5 [80.1–84.6]	0.32 [0.26–0.40]	
insulin	40.5 [37.0–43.9]	66.5 [63.7–69.1]	0.45 [0.39–0.53]	
metf+sulf	62.8 [58.8–66.5]	85.0 [83.2–86.6]	0.42 [0.34–0.51]	•
metf+insulin	46.7 [42.0–51.2]	77.9 [75.4–80.2]	0.40 [0.33–0.49]	
sulf+insulin	32.3 [28.6–36.0]	60.8 [57.4–63.9]	0.50 [0.42–0.59]	
metf+sulf+insulin	46.6 [42.8–50.3]	76.6 [74.4–78.6]	0.42 [0.35–0.49]	

Table 2.3: Analysis of the effect of statins within each study cohort. Presented hazard ratios are associated to the fraction of follow-up on statins. Patients are classified as statin users if they were on statins for at least half the follow-up. The proportional hazards models used here control for age, gender, use of antihypertensive and antiplatelet drugs and an age-gender interaction. • indicates that the proportional hazards assumption was rejected for the associated hazards ratio ($p < 0.01$).

In a second analysis, cohorts in which all patients on glucose lowering therapy

were taking statins were compared to the general age and gender matched population. Patients on metformin monotherapy (with and without a CV history) and sulfonylurea mono (without CV history) that were also taking statins exhibited higher survival rates than age and gender matched control groups without glucose lowering therapy (of which resp. only 32,4%, 24.7%, and 29.9% were taking statins during the majority of the follow-up). Patients on the combination of MET and SU and statins had the same survival rate than their controls, irrespective of CV history (Table 2.4).

study cohort	no history of CVD	history of CVD
metformin	0.66 [0.61–0.71] •	0.67 [0.58–0.78]
sulfonylurea	0.88 [0.80–0.97]	0.95 [0.81–1.12]
insulin	2.84 [2.53–3.19] •	2.12 [1.83–2.47]
metf+sulf	0.91 [0.84–0.99] •	0.96 [0.84–1.11] •
metf+insulin	1.91 [1.71–2.14]	1.67 [1.37–2.03]
sulf+insulin	2.40 [2.13–2.71]	2.43 [2.07–2.87]
metf+sulf+insulin	1.83 [1.66–2.01]	1.44 [1.23–1.69]

Table 2.4: Hazard ratios between statin users in the study group a control group matched for age and gender. The remaining characteristics of the control groups used here follow the distribution of the total NACM member population (after matching for age and gender). The proportional hazard models used to compute these hazard ratios control for age, gender, the use of antihypertensive and antiplatelet drugs and an age-gender interaction. • indicates that the proportional hazards assumption was rejected for the associated hazards ratio ($p < 0.01$).

2.4 Conclusions

The main objective of this large controlled cohort study was to investigate the survival of patients on various glucose lowering therapies in comparison to a reference population with similar observable characteristics. It was found that 5-year survival rates vary between glucose lowering therapies, at least partly driven by the risk profile of the individuals themselves, and substantially influenced by the intake of statins and the age at the start of GLA therapy.

Increased 5-year mortality rates were observed in patients on GLAs compared to matched references not on GLAs. This confirms the study of Bannister et al. [28] showing an increased mortality in patients on SU monotherapy and extends the evidence to other groups on insulin monotherapy and different

combination therapies. Although we did not see a better survival rate in patients on metformin monotherapy, our data show that these patients have similar survival rates compared to matched controls, especially if a positive history of CV disease is present.

Our study confirms data from many other observational studies that patients on metformin monotherapy have a lower mortality risk than patients on other glucose lowering therapy [116, 218, 76, 141, 180, 259], characterized by reduced excess mortality compared to matched controls. This study does not determine whether this excess mortality of patients on SU and insulin is mainly caused by the vulnerability of the background population or by negative properties of the therapies themselves. The extra mortality risk can, at least partially, be explained by the risk profile of the individuals themselves and not by using SU or insulin per se. First of all, this might reflect the progressive nature of type 2 diabetes such that patients with less pronounced hyperglycemia are started on metformin monotherapy whereas uncontrolled patients are started on insulin or combination therapies including SU. Age is another important independent predictor of mortality and can explain why younger patient groups (i.e. metformin mono) have better survival rates than older patient groups (i.e. SU mono). Age however does not explain the lower survival rates in younger patients on insulin monotherapy and survival differences throughout all age categories. A positive history of cardiovascular events also increases the background risk of our populations and explains the lower survival rates in any study cohort with a positive CV history. As in Morgan et al. [180], a combination of several other elements will probably play a role such as hypertension and factors that were not available in our study such as presence of chronic kidney disease and albuminuria, the level of glycemic control, smoking and heart failure.

Data from the literature are conflicting concerning differences between agents. On the one hand several studies report no difference in survival when comparing metformin with SU [23, 130, 144] or SU with insulin [130]. Also in the ORIGIN trial, insulin glargine was not associated with higher mortality rates than controls [108] despite the lower use of metformin in the insulin glargine group. On the other hand, many clinical and observational studies have indicated an increased mortality risk associated with the use of SU and insulin compared to metformin [116, 218, 76, 141, 180, 259], although differences were shown to depend on the type of SU [226, 272], and the dose of insulin [103] used. In fact only a well-controlled RCT with sufficient power comparing different treatment strategies might answer this question, but it is very unlikely that these RCT's will ever be undertaken. Observational studies are in that view considered complementary as they do not omit patients on the basis of strict criteria and will usually have enough follow-up time to evaluate hard endpoints such as

mortality risk.

This study is the first to show a beneficial impact of intake of statins on real-life survival data in a large population study of patients on glucose lowering therapy. This is not unexpected, since available evidence from RCT's convincingly showed beneficial effect of statins on survival and prevention of cardiovascular events in secondary prevention (reviewed in [37]). Data in primary prevention are scarce with the only RCT in diabetic patients lacking power to show an overall mortality benefit [68]. Our trial shows a beneficial effect of statins in patients with diabetes, both in primary and secondary prevention, with mortality risks being 60 to 80% lower independent of the type of glucose lowering therapy or presence of a CV disease history. Of note, patients taking statins in combination with metformin or SU monotherapy even showed better survival than the general population.

An asset of this study was the use of health expenditure records to assess the survival of patients on various glucose lowering therapies in comparison with a similar reference cohort from the general population. Claims records constitute a valuable source of information for observational epidemiological studies by embedding long-term longitudinal medical information of a large number of patients. Additionally, claims records aggregate proxies of medical information from various caregivers into a complete patient-wide overview which is often unavailable to individual caregivers and other medical stakeholders.

Through exact pair-wise matching of the reference cohort and regression adjustment in the proportional hazards models we were able to exclude important observable confounders in comparisons of the study cohorts with their respective references [220]. Having access to a large population from which to sample control subjects allowed us to find references with exact matches on key confounding variables. Matching on these observable factors excludes the confounding effect and yields an efficiency gain [155]. Some residual confounding resulting from uncontrolled and unobservable factors may remain. Our study also has limitations. While there are considerable benefits in using claims data for epidemiological research, the absence of detailed clinical parameters prohibits causal inference because we could not control for level of glycemic control (e.g., fasting blood glucose or HbA1c), BMI, or other modifiable cardiovascular risk factors (e.g., smoking). However, we controlled for age, sex, concomitant medication, and presence of history of CV disease. Due to its observational nature our study remains susceptible to confounding by indication [115, 208, 44]. Therefore our study is not suitable to compare GLA therapies directly as the patients' underlying conditions yield indications for their treatment, preventing comparisons [115, 21].

We conclude that 5-year survival in patients on glucose lowering therapy is

lower than in matched controls except for metformin monotherapy. Intake of metformin is associated with lowest 5-year mortality. In all groups, the intake of statins was associated with a reduced mortality rate.

Chapter 3

EnsembleSVM: A Library for Ensemble Learning Using SVMs

This chapter has been previously published as:
Claesen, M., De Smet, F., Suykens, J. A. K., & De Moor, B. (2014). **EnsembleSVM: A library for ensemble learning using support vector machines**. *Journal of Machine Learning Research*, 15(1), 141–145.

Contributions Marc Claesen has developed, tested and documented the software and took the lead in writing the paper.

Abstract

`EnsembleSVM` is a free software package containing efficient routines to perform ensemble learning with support vector machine (SVM) base models. It currently offers ensemble methods based on binary SVM models. Our implementation avoids duplicate storage and evaluation of support vectors which are shared between constituent models. Experimental results show that using ensemble approaches can drastically reduce training complexity while maintaining high predictive accuracy. The `EnsembleSVM` software package is freely available online at `http://esat.kuleuven.be/sista/ensemblesvm`.

3.1 Introduction

Data sets are becoming increasingly large. Machine learning practitioners are confronted with problems where the main computational constraint is the amount of time available. Problems become particularly challenging when the training sets no longer fit into memory. Accurately solving the dual problem for SVM training with nonlinear kernels requires a run time which is at least quadratic in the size of the training set n, thus training complexity is $\Omega(n^2)$ [45, 165].

`EnsembleSVM` employs a divide-and-conquer strategy by aggregating many SVM models, trained on small subsamples of the training set. Through subdivision, total training time decreases significantly, even though more models need to be trained. For example, training p classifiers on subsamples of size n/p, results in an approximate complexity of $\Omega(n^2/p)$. This reduction in complexity helps in dealing with large data sets and nonlinear kernels.

Ensembles consisting of SVM models have been used in various applications [269, 164, 178]. Collobert et al. [69] use ensembles for large scale learning and employ a neural network to aggregate base models. Valentini and Dietterich [261] provide an implementation which allows base models to use different kernels. We require base models to share a single kernel function for efficiency.

While other implementations mainly focus on improving predictive performance, we primarily aim to (i) make nonlinear large-scale learning feasible through complexity reductions and (ii) enable prototyping of novel ensemble algorithms.

The default ensemble learning approach we offer is bagging, which is commonly used to improve the performance of unstable classifiers [50]. In bagging, base models are trained on bootstrap resamples of the training set and their predictions are aggregated through majority voting. A critical aspect of bagging is that base models should have low bias but may exhibit high variance [50, 29, 147], which makes base models like decision trees ideal [52]. Typically, SVM classifiers are considered stable [46] and by implication ill suited for bagging frameworks. However, when using SVM base models in a bagging setup, variance can be promoted while simultaneously reducing bias by using small base model training sets in combination with high misclassification penalties. Effectively, overfitting the base models may positively affect overall performance of the ensemble due to increased efficiency of aggregation. As such, bagging SVM models requires striking a balance between base model performance vis-à-vis aggregation benefits for a given learning task. This may appear counterintuitive as this tradeoff is difficult to make based on domain knowledge alone. However, appropriate hyperparameterizations enable finding the right balance automatically, for instance using Optunity (cfr. Chapter 6).

3.2 Software Description

The `EnsembleSVM` software is freely available online under a LGPL license. `EnsembleSVM` provides ensembles of instance-weighted SVMs, as defined in Equation (3.1).

Base model flexibility is maximized by using instance-weighted binary support vector machine classifiers, as defined in Equation (3.1). This formulation lets users define misclassification penalties per training instance $C_i,\ i = 1, \ldots, n$ and encompasses popular approaches such as C-SVC and class-weighted SVM [72, 195].

$$\min_{\mathbf{w},\xi,\rho} \frac{1}{2}\mathbf{w}^T\mathbf{w} + \sum_{i=1}^{n} C_i\xi_i, \tag{3.1}$$

$$\text{subject to } y_i(\mathbf{w}^T\varphi(\mathbf{x}_i) + \rho) \geq 1 - \xi_i, \qquad i = 1, \ldots, n$$

$$\xi_i \geq 0, \qquad i = 1, \ldots, n$$

When aggregating SVM models, the base models often share support vectors (SVs). The `EnsembleSVM` software intelligently caches distinct SVs to ensure that they are only stored and used for kernel evaluations once. As a result, `EnsembleSVM` models are smaller and faster in prediction than ensemble implementations based on wrappers.

3.2.1 Implementation

`EnsembleSVM` has been implemented in `C++` and makes heavy use of the standard library. The main implementation focus is training speed. We use facilities provided by the `C++11` standard and thus require a moderately recent compiler, such as `gcc` ≥ 4.7 or `clang` ≥ 3.2. A portable Makefile system based on GNU autotools is used to build `EnsembleSVM`.

`EnsembleSVM` interfaces with `LIBSVM` to train base models [57]. Our code must be linked to `LIBSVM` but does not depend on a specific version. This allows users to choose the desired version of the `LIBSVM` software in the back-end.

The `EnsembleSVM` programming framework is designed to facilitate prototyping of ensemble algorithms using SVM base models. We particularly provide extensive support to define novel aggregation schemes, should the available options be insufficient. Key components are extensively documented in the

code and on a wiki, which serves as a high-level guideline.[1] Intuitive APIs are provided for convenient features such as thread pools, command line interface and deserialization to enable users to develop new tools efficiently.

The `EnsembleSVM` library was built with extensibility and user contributions in mind. Major API functions are well documented to lower the threshold for external development. The executable tools provided with `EnsembleSVM` are essentially wrappers for the library itself. The tools can be considered as use cases of the main API functions to help developers.

3.2.2 Tools

The main tools in this package are `esvm-train` and `esvm-predict`, used to train and predict with ensemble models. Both of these are pthread-parallelized. Additionally, the `merge-models` tool can be used to merge standard `LIBSVM` models into ensembles. Finally, `esvm-edit` provides facilities to modify the aggregation scheme used by an ensemble.

`EnsembleSVM` includes a variety of extra tools to facilitate basic operations such as stratified bootstrap sampling, cross-validation, replacing categorical features by dummy variables, splitting data sets and sparsifying standard data sets. We recommend retaining the original ratio of positives and negatives in the training set when subsampling.

3.3 Benchmark Results

To illustrate the potential of our software, `EnsembleSVM` 2.0 has been benchmarked with respect to `LIBSVM` 3.17. To keep the experiments simple, we use majority voting to aggregate predictions, even though more sophisticated methods are offered. For reference, we also list the best obtained accuracy with a linear model, trained using `LIBLINEAR` [95]. Linear methods are common in large-scale learning due to their speed, but may result in significantly decreased accuracy. This is why scalable nonlinear methods are desirable.

We used two binary classification problems, namely the `covtype` and `ijcnn1` data sets.[2] Both data sets are balanced. Features were always scaled to $[0, 1]$. We have used C-SVC as SVM and base models ($\forall\ i : C_i = C$). Reported

[1] The `EnsembleSVM` development wiki is available at `https://github.com/claesenm/EnsembleSVM/wiki`.

[2] Available at: `http://www.csie.ntu.edu.tw/~cjlin/libsvmtools/datasets/binary.html` and UCI.

numbers are averages of 5 test runs to ensure reproducibility. We used the RBF kernel, defined by the kernel function $\kappa(\mathbf{x}_i, \mathbf{x}_j) = \exp\big(-\gamma||\mathbf{x}_i - \mathbf{x}_j||^2\big)$. Optimal parameter selection was done through cross-validation.

The `covtype` data set is a common classification benchmark featuring 54 dimensions [41]. We randomly sampled balanced training and test sets of $100,000$ and $40,000$ instances respectively and classified class 2 versus all others. The `ijcnn1` data set was used in a machine learning challenge during IJCNN 2001 [206]. It contains $35,000$ training instances in 22 dimensions.

data set	**test set accuracy**			**no. of SVs**		**time (s)**	
	`LIBSVM`	`LIBLINEAR`	`ESVM`	`LIBSVM`	`ESVM`	`LIBSVM`	`ESVM`
`covtype`	0.92	0.76	0.89	26516	50590	728	35
`ijcnn1`	0.98	0.92	0.98	3564	7026	9.5	0.3

Table 3.1: Summary of benchmark results per data set: test set accuracy, number of support vectors and training time. Accuracies are listed for a single `LIBSVM` model, `LIBLINEAR` model and an ensemble model.

Results in Table 3.1 show several interesting trends. Training `EnsembleSVM` models is orders of magnitude faster, because training SVMs on small subsets significantly reduces complexity. Subsampling induces smaller kernels per base model resulting in lower overall memory use.

Ensembles can end up with more support vectors than a single SVM. Due to our parallelized implementation, prediction with ensemble models was faster than with `LIBSVM` models in both experiments even though the ensembles comprise twice as many SVs.

The ensembles in these experiments are competitive with a traditional SVM even though we used simple majority voting. For `covtype`, ensemble accuracy is 3% lower than a single SVM and for `ijcnn1` the ensemble is marginally better (0.2%). Linear SVM falls far short in terms of accuracy for both experiments, but is trained much faster (< 2 seconds).

We obtained good results with very basic aggregation. Collobert et al. [69] illustrated that more sophisticated aggregation methods can improve the predictive performance of ensembles. Others have reported performance improvements over standard SVM for ensembles using majority voting [261, 269].

3.4 Conclusions

`EnsembleSVM` provides users with efficient tools to experiment with ensembles of SVMs. Experimental results show that training ensemble models is significantly faster than training standard `LIBSVM` models while maintaining competitive predictive accuracy.

Linear methods are frequently applied in large-scale learning, mainly due to their low training complexity. Linear methods are known to have competitive accuracy for high dimensional problems. As our benchmarks showed, the difference in accuracy may be large for low dimensional problems. As such, fast nonlinear methods remain desirable in large-scale learning, particularly for low dimensional tasks with many training instances. Our benchmarks illustrate the potential of the ensemble approaches offered by `EnsembleSVM`.

Ensemble performance may be improved by using more complex aggregation schemes. `EnsembleSVM` currently offers various aggregation schemes, both linear and nonlinear. Additionally, it facilitates fast prototyping of novel methods through its `Pipeline` framework.[3]

`EnsembleSVM` strives to provide high-quality, user-friendly tools and an intuitive programming framework for ensemble learning with SVM base models. The software will be kept up to date by incorporating promising new methods and ideas when they are presented in the literature. User requests and suggestions are welcome and appreciated.

[3] `https://github.com/claesenm/EnsembleSVM/wiki/Pipeline`

Chapter 4

SVM Ensemble Learning from Positive and Unlabeled Data

This chapter has been previously published as:
Claesen, M., De Smet, F., Suykens, J. A., & De Moor, B. (2015). **A robust ensemble approach to learn from positive and unlabeled data using SVM base models**. *Neurocomputing*, 160, 73-84.

Contributions Marc Claesen designed the learning method and performed all experiments. He took the lead in writing the paper.

Abstract

We present a novel approach to learn binary classifiers when only positive and unlabeled instances are available (PU learning). This problem is routinely cast as a supervised task with label noise in the negative set. We use an ensemble of SVM models trained on bootstrap resamples of the training data for increased robustness against label noise. The approach can be considered in a bagging framework which provides an intuitive explanation for its mechanics in a semi-supervised setting. We compared our method to state-of-the-art approaches in simulations using multiple public benchmark data sets. The included benchmark comprises three settings with increasing label noise: (i) fully supervised, (ii) PU learning and (iii) PU learning with false positives. Our approach shows a marginal improvement over existing methods in the second setting and a significant improvement in the third.

4.1 Introduction

Training binary classifiers on positive and unlabeled data is referred to as PU learning [166]. The absence of known negative training instances warrants appropriate learning methods. Inaccurate label information can be more problematic than attribute noise [287]. Specialised PU learning approaches are recommended when (i) negative labels cannot be acquired, (ii) the training data contains a large amount of false negatives or (iii) the positive set has many outliers.

Practical applications of PU learning typically feature large, imbalanced training sets with a small amount of labeled (positive) and a large amount of unlabeled training instances. The PU learning problem arises in various settings, including web page classification [284], intrusion detection [157] and bioinformatics tasks such as variant prioritization [238], gene prioritization [9, 178] and virtual screening of drug compounds [236].

Though these applications share a common underlying learning problem, the final evaluation criteria may be fundamentally different. For instance, in prioritization one wishes to obtain high precision since highly ranked targets may be subjected to further biological analysis. Intrusion detection, on the other hand, necessitates high recall to ensure that no anomalies go unnoticed.

Following Mordelet and Vert [179], we will use the term *contamination* to refer to the fraction of mislabeled instances in a given set. We will denote the positive and unlabeled training instances by $\mathcal{P}$ and $\mathcal{U}$, respectively. Contamination in $\mathcal{P}$ refers to false positives while contamination in $\mathcal{U}$ refers to the presence of positives in $\mathcal{P}$. Usually $\mathcal{U}$ contains mostly true negative instances (e.g. contamination below 0.5) and $\mathcal{P}$ is assumed to be uncontaminated.

The distributions of the positive and a contaminated unlabeled set overlap even when those of the positive and underlying negative sets do not, which makes classification more difficult compared to a traditional supervised setting. Elkan and Noto [92] and Blanchard et al. [42] report statistical approaches to estimate the contamination of the unlabeled set and additionally show that distinguishing positives from unlabeled instances is a valid proxy for distinguishing positives from negatives.

The assumption in PU learning that $\mathcal{P}$ is uncontaminated may be violated in applications due to various reasons [101]. Additionally, outliers in the positive set may have a similar effect on classification performance [200]. We propose a novel PU learning method that is less vulnerable to potential contamination in $\mathcal{P}$ called the robust ensemble of support vector machines (RESVM). RESVM is compared to other methods in a series of simulations based on several public

data sets.

4.2 Related work

PU learning approaches can be split into two main conceptual categories: (i) approaches that account for the contamination of the unlabeled set explicitly by modeling the label noise and (ii) approaches that try to infer an uncontaminated (negative) subset $\hat{\mathcal{N}}$ from $\mathcal{U}$ and then train supervised algorithms to distinguish $\mathcal{P}$ from $\hat{\mathcal{N}}$. When *very* few labeled examples are available, the structure within the data is the main source of information which can be exploited by semi-supervised clustering techniques [14].

Accounting for the contamination of $\mathcal{U}$ in the modeling process This can be done by weighting individual data points, such as in weighted logistic regression [92, 159]. Another approach is by changing the penalties on misclassification during training, as is done in class-weighted SVM [166], bagging SVM [179] and RT-SVM [168].

Inferring an uncontaminated subset from $\mathcal{U}$ Another class of approaches tries to infer a negative set $\hat{\mathcal{N}}$ from $\mathcal{U}$. After the inferential step, binary classifiers are trained to distinguish $\mathcal{P}$ from $\hat{\mathcal{N}}$ in a supervised fashion. Examples of such two-step approaches include S-EM [167], mapping convergence (MC) [282] and ROC-SVM [161].

Class-weighted SVM and related approaches The approach we suggest belongs to the first class of methods and is closely related to class-weighted SVM and bagging SVM (which uses class-weighted SVM internally). We will discuss both of these approaches in more detail before moving on to the proposed method. We evaluated our method compared to both class-weighted SVM and bagging SVM.

4.2.1 Class-weighted SVM

Class-weighted SVM (CWSVM) is a supervised technique in which the penalty for misclassification differs per class. Liu et al. [166] first applied class-weighted SVM for PU learning by considering the unlabeled set to be negative with noise on its labels. CWSVM is trained to distinguish $\mathcal{P}$ from $\mathcal{U}$. During training,

misclassification of positive instances is penalized more than misclassification of unlabeled instances to emphasize the higher degree of certainty on positive labels. In the context of PU learning, the optimization problem for training CWSVM can be written as:

$$\min_{\alpha,\xi,b} \frac{1}{2}\sum_{i=1}^{N}\sum_{j=1}^{N}\alpha_i\alpha_j y_i y_j \kappa(\mathbf{x}_i,\mathbf{x}_j) + C_{\mathcal{P}}\sum_{i\in\mathcal{P}}\xi_i + C_{\mathcal{U}}\sum_{i\in\mathcal{U}}\xi_i, \tag{4.1}$$

$$\text{s.t. } y_i(\sum_{j=1}^{N}\alpha_j y_j \kappa(\mathbf{x}_i,\mathbf{x}_j) + \rho) \geq 1-\xi_i, \qquad i=1,\ldots,N,$$

$$\xi_i \geq 0, \qquad i=1,\ldots,N,$$

with $\alpha \in \mathbb{R}^N$ the support values, $\mathbf{y} \in \{-1,+1\}^N$ the label vector, $\kappa(\cdot,\cdot)$ the kernel function, ρ the bias term and $\xi \in \mathbb{R}^N$ the slack variables. The misclassification penalties $C_{\mathcal{P}}$ and $C_{\mathcal{U}}$ require tuning (typically $C_{\mathcal{P}} > C_{\mathcal{U}}$ to emphasize known labels). SVM formulations with unequal penalties across classes have been used previously to tackle imbalanced data sets [195].

4.2.2 Bagging SVM

Mordelet and Vert introduce bagging SVM as a meta-algorithm which consists of aggregating classifiers trained to discriminate $\mathcal{P}$ from small, random resamples of $\mathcal{U}$ [179]. They posit that PU learning problems have a particular structure that leads to instability of classifiers, namely the sensitivity of classifiers to the contamination of the unlabeled set. Bagging is a common technique used to improve the performance of instable classifiers [50].

In bagging SVM, random resamples of $\mathcal{U}$ are drawn and CWSVM classifiers are trained to discriminate $\mathcal{P}$ from each resample. By resampling $\mathcal{U}$, the contamination is varied. This induces variability in the classifiers which the aggregation procedure can then exploit. The size of the bootstrap resample of $\mathcal{U}$ is a tuning parameter in bagging SVM. The ratio $C_{\mathcal{P}}/C_{\mathcal{U}}$ is fixed so that the following holds:

$$|\mathcal{P}| \times C_{\mathcal{P}} = n_{\mathcal{U}} \times C_{\mathcal{U}}, \tag{4.2}$$

with $|\mathcal{P}|$ the size of the positive set and $n_{\mathcal{U}}$ the size of resamples from the unlabeled set. This choice of weights is common in imbalanced settings [55, 77].

All base models in bagging SVM classify the full set of positives against a subset of unlabeled instances and use a high misclassification penalty on the positives similar to CWSVM. To our knowledge, bagging SVM was initially designed for

gene prioritization [178], the goal of which is to identify genes that are likely related to some disorder based on genes with known associations [9, 178]. This task often has very few known positives (less than 100) and many unlabeled instances ($\approx$ 20,000), which is probably why bagging SVM consistently uses all positives in every base model by design.

4.3 Robust Ensemble of SVMs

We propose a new technique called the robust ensemble of SVMs (RESVM). RESVM is a bagging method using CWSVM base models as discussed in Section 4.2.1. Base model training sets are constructed by bootstrap resampling both $\mathcal{P}$ and $\mathcal{U}$ separately, both of which may be contaminated.

In the remainder of this text, *bagging SVM* is used to refer to the method by Mordelet and Vert [179] as outlined in Section 4.2.2. The name bagging SVM is somewhat unfortunate since the approach is atypical for bagging frameworks, which usually resample the full training set. Our approach is effectively more similar to standard bagging (using SVM base models) than bagging SVM.

The key difference between RESVM and bagging SVM is that the former resamples $\mathcal{P}$ in addition to $\mathcal{U}$ to increase variability between base models. RESVM additionally features an extra degree of freedom to control the relative misclassification penalty between positive and unlabeled instances, which is fixed in bagging SVM. Mordelet and Vert [179] report no significant changes when varying the relative penalty in bagging SVM, though our experiments show that it is important in RESVM (see w_{pos} in Table 4.5).

Before elaborating on the details of RESVM, we briefly illustrate the effect of resampling contaminated sets. Subsequently we summarize the mechanisms of bagging and why they are advantageous when learning with label noise in the RESVM approach. Finally, we provide the full RESVM training approach and the way ensemble decision values are computed based on the base model decision values.

4.3.1 Bootstrap resampling contaminated sets

The RESVM approach resamples both $\mathcal{P}$ and $\mathcal{U}$, both of which are potentially contaminated. Resampling contaminated sets with replacement induces variability in contamination across the resampled sets (e.g. resamples of $\mathcal{U}$ and $\mathcal{P}$ that are used for training). The variability in contamination between resamples increases for increasing contamination of the original set. We assume

contamination levels below 50%, e.g. less than half the instances in a given set are mislabeled. Due to the law of large numbers the contamination in bootstrap resamples of increasing size converges to the expected contamination, which equals that of the original set that is being resampled. As a result, the variability in contamination decreases for increasing resample size. Figure 4.1 illustrates this property empirically based on 20,000 repeated measurements for each resample size: the expected value (mean) equals the original contamination, but the variability in resample contamination decreases for increasing resample size.

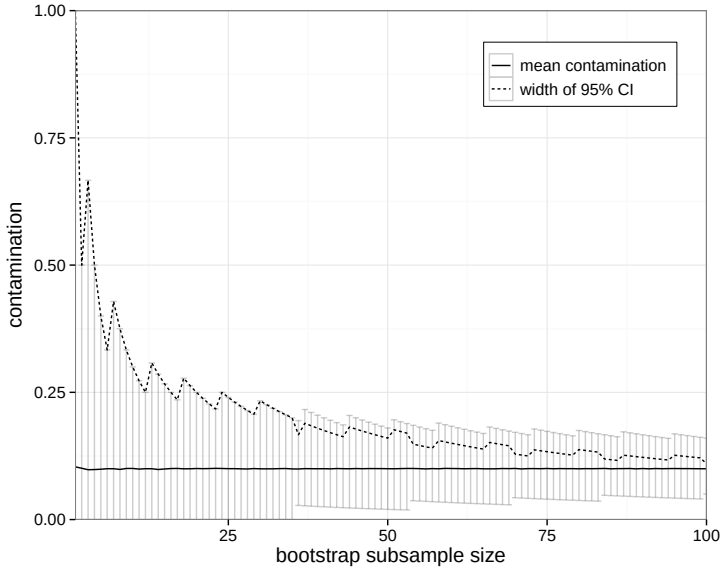


Figure 4.1: Contamination of bootstrap resamples for increasing size of resamples when the original sample has 10% contamination. Errorbars indicate the 95% confidence interval (CI) of contamination in resamples. The contamination varies greatly between small resamples as shown by the CIs.

4.3.2 Bagging predictors

Breiman [50] introduced bagging as a technique to construct strong ensembles by combining a set of base models and stated that "the essential problem in combining classifiers is growing a suitably diverse ensemble of base classifiers" which can be done in various ways [53]. In bagging, the ensemble models use majority voting to aggregate decisions of base models which are trained on

bootstrap resamples of the training set. From a Bayesian point of view, bagging can be interpreted as a Monte Carlo integration over an approximated posterior distribution [211].

In his landmark paper, Breiman [50] noted that base model instability is an important factor in the success of bagging which led to the use of inherently instable methods like decision trees in early bagging approaches [84, 52]. The main mechanism of bagging is often said to be variance reduction [29, 51]. In more recent work, Grandvalet [113] explained that base model instability is not related to the intrinsic variability of a predictor but rather to the presence of influential instances in a data set for a given predictor (so-called *leverage points*). The effect of bagging is explained as equalizing the influence of all training instances, which is beneficial when highly influential instances are harmful for the predictor's accuracy.

4.3.3 Justification of the RESVM algorithm

We have shown the effect of resampling contaminated sets and provided some basic insight into the mechanics of bagging. We will now link these two elements to justify bagging approaches in the context of contaminated training sets. Its usefulness can be considered by both the variance reduction argument of Bauer and Kohavi [29] and equalizing the influence of training points as described by Grandvalet [113].

Variance reduction Resampling a contaminated set yields different levels of contamination in the resamples as explained in Section 4.3.1. Varying the contamination between base model training sets induces variability between base models without increasing bias. This observation enables us to create a diverse set of base models by resampling both $\mathcal{P}$ and $\mathcal{U}$. The variance reduction of bagging is an excellent mechanism to exploit the variability of base models based on resampling [29, 51]. In the context of RESVM, a tradeoff takes place between increased variability (by training on smaller resamples, see Figure 4.1) and base models with increased stability (larger training sets for the SVM models).

Equalizing influence The influence of a training instance on an SVM model can be quantified in terms of its dual weight (the associated α value). Three distinct cases can be distinguished: (i) the training instance is correctly classified and not within the margin ($\alpha = 0$, not a SV), (ii) the training instance lies on the margin and is correctly classified ($\alpha \in [0, C]$, free SV) and (iii) the training

instance is incorrectly classified or within the margin ($\alpha = C$, bounded SV), where C is the misclassification penalty associated to the training instance [45]. Instances that are misclassified during training become bounded SVs, which have the maximal α value and can therefore be considered leverage points of the SVM model. When learning with label noise, the mislabeled training instances are likely to end up as bounded SVs. In a best case scenario, the mislabeled training instances are classified in concordance to their true label by the SVM model (which means they must be a bounded SV as the training procedure identifies this as a misclassification). As such, mislabeled training instances act as leverage points for SVM models. Following Grandvalet [113], bagging equalizes the influence of training instances (e.g. lowers the influence of mislabeled leverage points in comparison to the rest of the data) which yields improved robustness against contamination in the context of RESVM.

4.3.4 RESVM training

RESVM uses CWSVM base models trained on resamples from the original training set, where both $\mathcal{P}$ and $\mathcal{U}$ are being resampled. The technique involves 5 hyperparameters: 3 to define the resampling strategy and 2 for the base models. Additional hyperparameters may be involved, for example γ for the RBF kernel $\kappa(\mathbf{x}_i, \mathbf{x}_j) = \exp(-\gamma\|\mathbf{x}_i - \mathbf{x}_j\|^2)$.

The number of base models to include in the ensemble, $n_{nmodels}$, is the first hyperparameter. Using more base models improves the stability of the ensemble (up to a certain plateau) at a linear increase in computational cost for training and prediction. n_{models} is not a traditional hyperparameter in the sense that a good value can be determined during training, for example based on out-of-bag error estimates [27].[1]

By resampling $\mathcal{P}$, RESVM takes potential contamination of the labeled instances into account by design. Since the contamination between $\mathcal{P}$ and $\mathcal{U}$ can vary, the ability to vary the size of resamples from $\mathcal{P}$ and $\mathcal{U}$ separately is required. This results in two tuning parameters: n_{pos} and n_{unl}. In general, using small base model training sets results in increased base model variability which then necessitates using more base models in the ensemble to obtain a given level of stability. In our experiments, we have tuned n_{pos} and n_{unl} but it is also possible to obtain good values using out-of-bag techniques [173].[1]

RESVM additionally inherits at least 2 hyperparameters from its SVM base models, namely misclassification penalties for both classes and, if applicable,

[1]Note that the error estimates in out-of-bag techniques must account for potential contamination. See our discussion of hyperparameter tuning for a possible score function.

hyperparameters related to the kernel function. We define the CWSVM penalties in see Eq. (4.1) based on 2 hyperparameters $C_{\mathcal{U}}$ and w_{pos}:

$$C_{\mathcal{P}} = C_{\mathcal{U}} \times w_{pos} \times \frac{n_{unl}}{n_{pos}}. \tag{4.3}$$

w_{pos} enables reweighting labeled and unlabeled instances after equalizing class imbalance. In bagging SVM, w_{pos} is always fixed to 1.

The RESVM training approach has been summarised in Algorithm 1. The algorithm uses 5 hyperparameters plus additional kernel parameters.

Algorithm 1: Training procedure for RESVM.

Data: $\mathcal{P}$: the set of positive instances.
$\mathcal{U}$: the set of unlabeled instances.
Input: n_{models}: number of base models to include in the ensemble.
n_{unl}: size of bootstrap resamples of $\mathcal{U}$.
n_{pos}: size of bootstrap resamples of $\mathcal{P}$.
$C_{\mathcal{U}}$: misclassification penalty for $\mathcal{U}$ in class-weighted SVM.
w_{pos}: relative positive misclassification penalty coefficient.
$\kappa(\cdot,\cdot)$: kernel function to be used by base models.
Output: Ω: RESVM with n_{models} base models.
begin
  $\Omega \leftarrow \emptyset$;
  $C_{\mathcal{P}} \leftarrow C_{\mathcal{U}} \times w_{pos} \times \frac{n_{unl}}{n_{pos}}$;
  for $i \leftarrow 1$ **to** n_{models} **do**
    `// create base model training set from` $\mathcal{P}$ `and` $\mathcal{U}$.
    $\mathcal{P}^{(i)} \leftarrow$ sample n_{pos} instances from $\mathcal{P}$ with replacement;
    $\mathcal{U}^{(i)} \leftarrow$ sample n_{unl} instances from $\mathcal{U}$ with replacement;
    `// train CWSVM base model` $\psi^{(i)}$ `and add to ensemble` Ω.
    $\psi^{(i)} \leftarrow$ train CWSVM for $\mathcal{P}^{(i)}$ vs. $\mathcal{U}^{(i)}$ (parameters $C_{\mathcal{P}}$, $C_{\mathcal{U}}$, κ);
    $\Omega \leftarrow \{\Omega, \psi^{(i)}\}$;

4.3.5 RESVM prediction

RESVM uses majority voting to aggregate base model predictions. By default, the returned label is the one predicted by most base models. The fraction of positive votes for a test instance $\mathbf{x}$ can be written as:

$$v(\mathbf{x}) = \frac{n_{models} + \sum_{i=1}^{n_{models}} \mathtt{sgn}(\psi^{(i)}(\mathbf{x}))}{2n_{models}}, \tag{4.4}$$

where $\mathtt{sgn}(\cdot)$ is the sign function and $\psi^{(i)}$ denotes the decision function of SVM base model i with codomain $\mathbb{R}$. $v(\cdot)$ has the interval $[0, 1]$ as codomain.

The RESVM decision value for a test instance $\mathbf{x}$ is defined as the fraction of votes in favor of the positive class $v(\mathbf{x})$ unless the result is unanimous. In the case of a unanimous vote, the ensemble decision value is based on the decision values of its base models to increase the model's ability to differentiate. In case of a unanimous negative vote, the sum of the decision values of the base models is taken (each SVM base model decision value is negative in this case). In case of a unanimous positive vote, the sum of the decision values of the base models (all positive) plus one is taken. The decision value $d(\cdot)$ has codomain $\mathbb{R}$ and is computed as follows:

$$d(\mathbf{x}) = \begin{cases} v(\mathbf{x}) & \text{if } 0 < v(\mathbf{x}) < 1, \\ \sum_{i=1}^{n_{models}} \psi^{(i)}(\mathbf{x}) & \text{if } v(\mathbf{x}) = 0, \\ 1 + \sum_{i=1}^{n_{models}} \psi^{(i)}(\mathbf{x}) & \text{if } v(\mathbf{x}) = 1. \end{cases} \tag{4.5}$$

The resulting label for a given decision threshold T can be written as follows:

$$l(\mathbf{x}) = \mathtt{sgn}\big(d(\mathbf{x}) - T\big). \tag{4.6}$$

The default decision value threshold for positive classification is $T = 0.5$ (this is majority voting, e.g. positive iff more than half of all base models predict positive). Using the modified decision values $d(\mathbf{x})$ instead of the votes $v(\mathbf{x})$ does not affect the predicted labels for typical choices of the threshold T (e.g. $T \in (0, 1)$). It does, however, affect performance measures that use the entire range of decision values such as area under the PR curve. Using $d(\mathbf{x})$ enables us to rank different instances that received all positive or all negative votes by base models (e.g. $v(\mathbf{x}) = 1$ and $v(\mathbf{x}) = 0$, respectively).

4.4 Experimental setup

RESVM has been compared to class-weighted SVM (CWSVM) and bagging SVM (BAG) in a number of simulations to assess the merits of our modifications compared to conceptually comparable algorithms. In this Section we will summarize the experimental setup (training set construction, model selection and performance evaluation) and the data sets we used.

4.4.1 Simulation setup

Our experiments consist of repeated simulations on a variety of data sets under different settings. Briefly, in each iteration hyperparameters were optimized per

approach based on cross-validation on the training set (using identical folds for all approaches). Subsequently, a model with the optimal parameters is trained on the full training set and used to predict an independent test set. An overview of the experiments is shown in Figure 6.1. Every experiment consists of 20 repetitions.

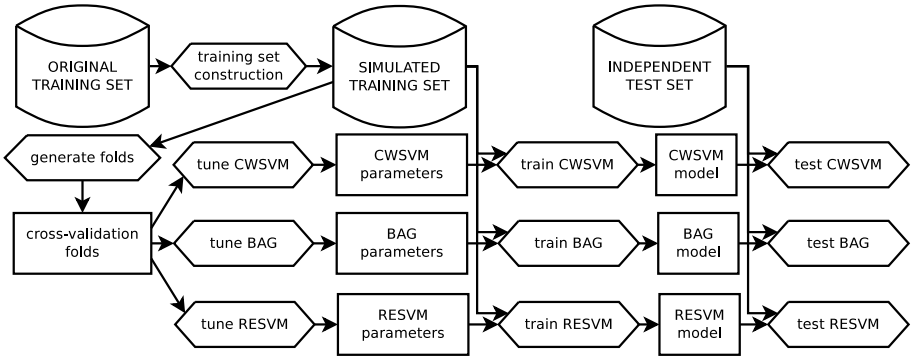


Figure 4.1: Overview of a single benchmark iteration.

To assess what situations are favorable per approach, we have investigated three different settings with distinct label noise configurations. For every data set, we performed 10 iterations per simulation in the following settings:

1. **supervised**: no contamination in $\mathcal{P}$ or $\mathcal{U}$ ($\mathcal{U}$ is the negative class).
2. **PU learning**: contamination in $\mathcal{U}$ but not in $\mathcal{P}$.
3. **semi-supervised**: contamination in both $\mathcal{P}$ and $\mathcal{U}$. The contamination levels in $\mathcal{P}$ and $\mathcal{U}$ were always chosen equal (except in Section 4.5.6).

The contamination levels we used were chosen per data set based on when differences between the three approaches become visible. A summary is available in Table 4.1 in Section 4.4.2. When applicable, contamination was introduced by flipping class labels (e.g. true positives in $\mathcal{U}$ and true negatives in $\mathcal{P}$). This effectively changes the empirical densities of the classes in the training set (illustrated in Figure 4.2 in the next Section).

Every binary learning task was repeated 20 times to get reliable assessments of all methods. Each repetition involves redoing all steps shown in Figure 6.1, including resampling of training sets based on the known true positives and true negatives. Contamination was introduced at random where applicable by flipping class labels.

Hyperparameter selection In every iteration, hyperparameters were tuned per setting using 10-fold cross-validation over a grid of parameter tuples. To ensure a fair comparison, one set of folds is generated in each iteration and used by all methods. We ensured that the optimal values that were found during tuning in any setting were never on the edge of the search grid. The search resolution in comparable parameters between methods was always defined to be identical (for example γ in the case of an RBF kernel).

The same search grids were used in all three settings for a given data set to illustrate that a method can work well in a supervised setting with a given search grid but degrade when label noise is added. Since negative labels are unavailable in PU learning, we used the following score function in all learning settings which only requires positive labels for hyperparameter selection [159]:

$$\texttt{pu_score} = \frac{\texttt{precision} \times \texttt{recall}}{Pr(y=1)} = \frac{\texttt{recall}^2}{Pr(\hat{y}=1)}, \tag{4.7}$$

where $Pr(y=1)$ is the fraction of known positive labels in the predicted set and $Pr(\hat{y}=1)$ is the fraction of positive predictions made by the classifier. Note that this score function is not ideal when $\mathcal{P}$ is contaminated, though we obtained good results even in that setting.

The following parameters were tuned per method: (CWSVM) $C_{\mathcal{P}}$ and $C_{\mathcal{U}}$, (BAG) $C_{\mathcal{U}}$ and $n_{\mathcal{U}}$ and (RESVM) $C_{\mathcal{U}}$, w_{pos}, n_{pos} and n_{unl}. In both ensemble approaches we consistently used 50 base models.

Performance assessment Models are trained with the optimal hyperparameters on the full training set and subsequently tested on the independent test set. We use the known test labels to compute the area under the Precision-Recall curve (AUC) for each model. We opted to use PR curves because they capture the performance of interest of models over their entire operating range and work well for imbalanced data [79].

We used statistical analyses to determine whether one approach trumps another while accounting for the variability between simulations. The nonparametric Wilcoxon signed-rank test is recommended for pairwise comparisons between learning algorithms [81]. In every setting per data set we performed a paired one-tailed Wilcoxon signed-rank test comparing the area under the PR curve of bagging SVM and RESVM with alternative hypothesis h_1 : $AUC^{RESVM} > AUC^{BAG}$ (pairs being iterations). Low p-values indicate a statistically significant improvement.

Implementation details We used the class-weighted SVM implementation available in LIBLINEAR [95] and LIBSVM [57] for models using the linear and RBF kernel, respectively. Bagging SVM and RESVM were implemented using the EnsembleSVM library [65].[2] The decision values of bagging SVM used to compute PR curves were defined in the same way as for RESVM (see Section 4.3.5).

4.4.2 Data sets

We used a synthetic data set and 5 publicly available data sets:[3]

- `synthetic`: a 2-D binary data set. Positive instances are sampled from a standard normal distribution. Negative instances are sampled from a circle centered at the origin with radius 4 with 2-D noise superimposed from a standard normal distribution. Training and testing data was generated in every iteration. Figure 4.2 shows densities for all settings.
- `cancer`: the Wisconsin breast cancer data set related to breast cancer diagnosis. It consists of 10 features and 683 instances without an explicit train/test partitioning so we partitioned it at random in every iteration.
- `ijcnn1`: used for the IJCNN 2001 neural network competition [206], comprising 2 classes, 22 features and $49,990/91,701$ training/testing instances.
- `covtype`: a common classification benchmark about predicting forest cover types based on cartographic information [41]. We used a subsample of $100,000/40,000$ training/testing instances.
- `mnist`: a digit recognition task [158]. This data set contains 10 classes (one for each digit), 780 features, $60,000$ training instances and $10,000$ test instances with an almost uniform class distribution. We performed one-versus-all classification for each digit.
- `sensit`: SensIT Vehicle (combined), vehicle classification [86]. This data set contains 3 classes with an uneven distribution. We performed one-versus-all classification for each class. This data set has 100 features, $78,823$ training instances and $19,705$ testing instances.

Most data sets have a prespecified test set, except for `synthetic` and `cancer`. We used the prespecified test sets when available. We used the RBF kernel for

[2]Python code for RESVM is available at `https://github.com/claesenm/resvm`.
[3]Public data at: `http://www.csie.ntu.edu.tw/~cjlin/libsvmtools/datasets/`.

all data sets except `mnist` (linear kernel). Note that both RESVM and bagging SVM models are always implicitly nonlinear due to their majority voting scheme, even when using linear base models, as illustrated in Figure 4.3.

In every setting each original data set was resampled without replacement to construct training sets to use in the simulations. The resampled training sets are typically significantly smaller than what is available in the original data sets to show that some methods can obtain good models even with few training instances. An overview of the actual training sets we constructed is presented in Table 4.1.

		contamination	training set		test set	
data set	d	in percent	$\lvert\mathcal{P}\rvert$	$\lvert\mathcal{U}\rvert$	$\lvert\mathcal{P}\rvert$	$\lvert\mathcal{N}\rvert$
`synthetic`	2	30	100	200	$5,000$	$5,000$
`cancer`	10	30	50	200	100	100
`ijcnn1`	22	10	100	$10,000$	$8,712$	$82,989$
`covtype`	54	30	100	1,000	20,000	20,000
`mnist`	780	10	50	$2,000$	$\approx 1,000$	$\approx 9,000$
`sensit 1`	100	30	100	$1,000$	$4,575$	$15,130$
`sensit 2`	100	30	100	$1,000$	$5,520$	$14,455$
`sensit 3`	100	30	100	$1,000$	$9,880$	$9,825$

Table 4.1: Overview of the data sets used in simulations: number of features, contamination (when applicable), training set size as used in the experiments and test set size. The `mnist` data set consists of 10 classes and the test set is almost uniformly distributed. The `sensit` data set has 3 classes with uneven class distribution in the test set, so we treat it separately here.

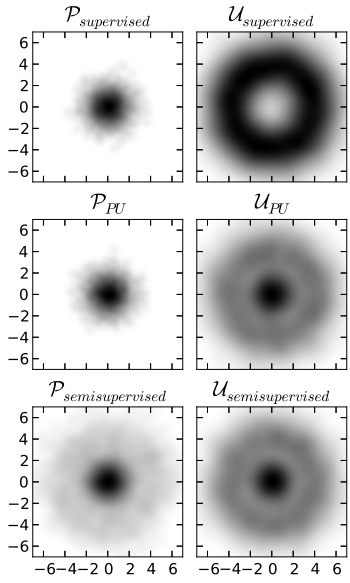


Figure 4.2: Empirical densities of the `synthetic` data used for training per problem setting (visualized in input space). The supervised densities (top row) are based on samples of the underlying positive and negative classes. The use of high contamination (30%) induces similar empirical densities for $\mathcal{P}$ and $\mathcal{U}$ in the semi-supervised setting (bottom row).

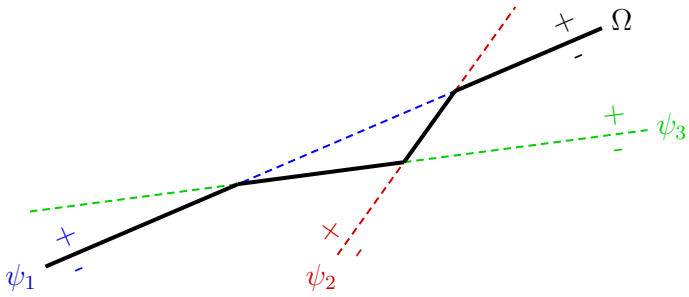


Figure 4.3: The effect of majority voting in an ensemble Ω with three linear base models (ψ_1, ψ_2, ψ_3). The thick black line represents the overall decision boundary of Ω. The use of majority voting generally induces nonlinear decision boundaries, e.g., when using linear base models the ensemble has a piecewise linear decision boundary.

4.5 Results and discussion

We will summarize all results of our simulation experiments comparing class-weighted SVM (CWSVM), bagging SVM (BAG) and the robust ensemble of SVMs (RESVM). First we will show the results of each setting separately. Subsequently we present an overview of the number of wins per setting for each method across all data sets. Section 4.5.6 shows the results of an experiment to assess the effect of contamination in $\mathcal{P}$ and $\mathcal{U}$ on all methods. Finally, we include an interesting observation regarding the optimal hyperparameters of RESVM that were found using cross-validation on the `mnist` data set per setting in Table 4.5.

4.5.1 Results for supervised classification

Table 4.1 summarizes our results in a fully supervised setting. In these experiments both $\mathcal{P}$ and $\mathcal{U}$ are uncontaminated. Based on the number of wins per simulation and the confidence intervals, we can conclude that all methods are competitive in this setting.

The confidence intervals show that all methods obtain comparable results for all simulations except `mnist` digit 8, where CWSVM performs poorly compared to the others. This performance difference could be caused by the fact we used linear class-weighted SVM while both ensemble methods implicitly yield nonlinear decision boundaries. A linear model may be too simple to properly distinguish this digit from the others.

The overall good results in the supervised setting confirm that the score function in Equation (4.7) is a good choice for tuning. In these supervised experiments we could have used a traditional score like accuracy, area under the ROC curve or F-measure, but these would no longer be useful in the other settings. The performance in these supervised experiments can be considered an objective baseline for comparison in the PU learning and semi-supervised setting since only levels of contamination are varied.

4.5.2 Results for PU learning

The results of our experiments in a PU learning setting are shown in Table 4.2. In the pure PU learning setting, $\mathcal{P}$ is uncontaminated but $\mathcal{U}$ is contaminated. Class-weighted SVM tends to suffer from the largest loss in performance between supervised learning and pure PU learning based on area under PR curves. Class-weighted SVM obtains less wins than it did in the supervised simulations (21

data	area under PR curve			p	number of wins		
	CWSVM	BAG	RESVM		CWSVM	BAG	RESVM
synthetic	98.1–98.7	98.7–98.8	98.7–98.8		2	12	6
cancer	98.4–98.8	98.4–98.7	98.3–98.7		8	12	0
ijcnn1	85.3–87.4	79.1–81.6	82.3–86.2	• • •	16	0	4
covtype	77.1–78.3	76.8–78.5	76.8–78.7		8	6	6
mnist (positive = x)							
0	96.9–97.5	96.9–97.4	96.9–97.4		7	8	5
1	98.1–98.3	98.3–98.5	98.2–98.5		0	8	12
2	87.3–89.1	88.5–89.8	89.6–90.5	•	2	6	12
3	83.7–85.9	86.9–88.7	88.8–90.1	• • •	0	5	15
4	88.8–90.2	89.8–91.1	90.8–92.2	• • •	1	3	16
5	78.7–80.9	79.2–81.0	81.4–83.2	• •	3	3	14
6	92.4–93.4	93.9–94.7	94.3–94.9		0	8	12
7	92.2–92.9	92.6–93.2	93.1–93.7	• • •	1	3	16
8	56.5–58.9	74.3–76.1	79.6–80.5	• • •	0	0	20
9	72.5–75.6	77.8–80.3	81.5–82.6	• • •	0	2	18
sensit (positive = x)							
1	80.5–81.4	79.8–80.7	80.5–81.3	•	10	2	8
2	65.7–75.4	72.6–74.0	73.5–74.9	• • •	15	0	5
3	35.5–56.1	92.3–92.7	91.7–92.3		0	15	5

Table 4.1: 95% CIs for mean test set performance in a fully supervised setup, the results of a paired one-tailed Wilcoxon signed-rank test comparing the AUC of BAG and RESVM with alternative hypothesis $h_1 : AUC^{RESVM} > AUC^{BAG}$ and the number of times each approach had best test set performance. Test result encoding: • $p < 0.05$, • • $p < 0.01$ and • • • $p < 0.001$.

wins in PU learning compared to 73 in the supervised setting), except on the cancer data set. Bagging SVM and RESVM maintain strong performance. Bagging SVM obtains a comparable number of wins and RESVM gains many compared to the supervised setting.

On the mnist data, RESVM consistently exhibits the best performance (based on the Wilcoxon signed-rank test), though the effective improvement over bagging SVM is marginal. On sensit with classes 2 or 3 as positive, bagging SVM obtains the majority of wins though the confidence intervals of its area under the PR curve overlap completely with those of RESVM. On the other data sets, no worthwile differences were obtained between both ensemble methods.

data	area under PR curve			p	number of wins		
	CWSVM	BAG	RESVM		CWSVM	BAG	RESVM
synthetic	96.9–98.4	97.9–98.6	98.2–98.5		6	8	6
cancer	98.2–98.5	87.5–98.4	96.1–98.1		10	7	3
ijcnn1	71.2–76.5	73.4–78.2	72.6–80.7	•	1	5	14
covtype	65.2–67.9	70.2–72.2	71.4–73.0		0	6	14
mnist (positive = x)							
0	74.1–77.8	90.5–93.3	94.6–95.5	• • •	0	5	15
1	89.1–91.2	95.2–96.7	96.4–97.3	• •	0	5	15
2	55.2–60.1	75.5–80.0	84.2–86.1	• • •	0	0	20
3	54.6–60.2	74.5–80.3	83.6–86.2	• • •	0	2	18
4	57.8–62.5	73.9–80.3	83.9–85.9	• • •	0	2	18
5	53.3–56.7	63.8–70.3	69.1–72.6	•	0	7	13
6	66.9–71.0	85.9–89.7	90.6–92.5	• •	0	4	16
7	71.4–74.8	84.0–88.0	90.0–91.4	• • •	0	1	19
8	34.8–38.8	63.5–69.1	72.2–74.8	• • •	0	4	16
9	50.5–54.8	66.2–71.0	74.2–76.4	• • •	0	1	19
sensit (positive = x)							
1	61.6–73.0	70.6–75.3	72.5–76.2	•	2	7	11
2	58.6–68.1	68.5–70.5	67.8–70.0		2	10	8
3	33.2–50.2	90.2–91.8	89.7–91.1		0	14	6

Table 4.2: 95% CIs for mean test set performance in a PU learning setup, the results of a paired one-tailed Wilcoxon signed-rank test comparing the AUC of BAG and RESVM with alternative hypothesis $h_1 : AUC^{RESVM} > AUC^{BAG}$ and the number of times each approach had best test set performance. Test result encoding: • $p < 0.05$, • • $p < 0.01$ and • • • $p < 0.001$.

4.5.3 Results of semi-supervised classification

In the semi-supervised setting we deliberately violated the assumption of an uncontaminated positive training set by contaminating $\mathcal{P}$ and $\mathcal{U}$. The results listed in Table 4.3 confirm that both class-weighted and bagging SVM are vulnerable to contamination in $\mathcal{P}$ and experience very large performance losses. We believe this is induced by using high misclassification penalties for training instances in $\mathcal{P}$ without any resampling to account for potential false positives. In bagging SVM this leads to a systematic bias in all base models. The resampling strategy of RESVM prevents systematic bias over all base models.

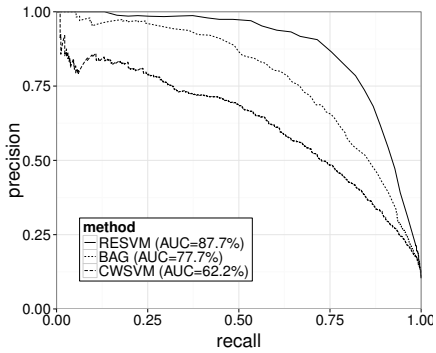
The results clearly show that RESVM is more robust to false positives, evidenced by a much lower drop in predictive performance for almost all data sets. The

data	area under PR curve			p	number of wins		
	CWSVM	BAG	RESVM		CWSVM	BAG	RESVM
synthetic	83.6–90.0	91.9–94.9	96.4–97.4	• • •	3	2	15
cancer	62.5–80.2	91.1–96.7	96.2–97.6	•	1	8	11
ijcnn1	69.8–73.4	67.4–70.4	72.0–75.2	• • •	5	2	13
covtype	58.1–61.8	61.2–64.2	60.4–65.7		4	4	12
mnist (positive = x)							
0	59.9–64.1	72.8–81.1	91.4–93.4	• • •	0	0	20
1	80.3–82.7	90.6–93.4	96.1–97.4	• • •	0	0	20
2	42.3–48.0	55.1–63.7	79.8–83.0	• • •	0	0	20
3	43.8–47.6	59.9–66.0	78.1–81.1	• • •	0	0	20
4	52.4–56.2	66.4–72.8	79.7–83.4	• • •	0	0	20
5	40.5–45.2	56.0–61.1	65.8–69.4	• • •	0	2	18
6	52.4–57.3	72.9–79.3	87.9–90.9	• • •	0	0	20
7	58.7–61.6	69.9–77.3	87.9–90.2	• • •	0	1	19
8	29.7–33.9	48.3–55.3	68.0–71.0	• • •	0	0	20
9	42.1–44.9	52.5–59.0	68.7–72.7	• • •	0	0	20
sensit (positive = x)							
1	34.5–49.4	59.6–69.0	60.6–66.4		3	12	5
2	44.9–53.7	46.4–53.4	50.1–56.7	•	8	4	8
3	44.5–61.1	75.4–83.5	80.5–84.9	•	1	7	12

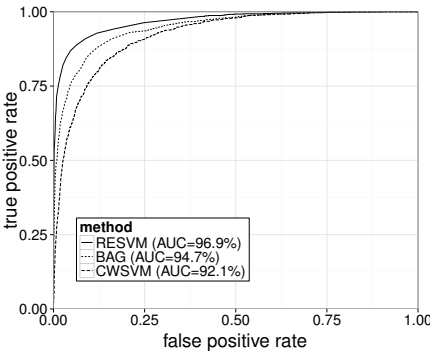
Table 4.3: 95% CIs for mean test set performance in a semi-supervised setup, the results of a paired one-tailed Wilcoxon signed-rank test comparing the AUC of BAG and RESVM with alternative hypothesis $h_1 : AUC^{RESVM} > AUC^{BAG}$ and the number of times each approach had best test set performance. Test result encoding: • $p < 0.05$, • • $p < 0.01$ and • • • $p < 0.001$.

performance difference between bagging SVM and RESVM is statistically significant for all data sets except covtype and sensit. Surprisingly, CWSVM obtains 8 wins on sensit with class 2 as positive. RESVM shows the best and most consistent performance overall.

On the mnist data, RESVM not only achieved consistently higher area under the PR curve, but visual inspection showed that its PR curves almost always dominated the others over the entire range. This means that in this experiment, RESVM models are always better than the others regardless of design priorities (high precision versus high recall). As an illustration, Figure 4.1 shows the PR and ROC curves of a representative simulation with digit 7 as positive. Since the PR curve of RESVM completely dominates the others we know that its ROC curve does too [79].



(a) Precision-Recall curves.



(b) ROC curves.

Figure 4.1: Performance in semi-supervised setting on `mnist`, digit 7 as positive.

Finally, it is worth noting that the confidence intervals of RESVM tend to be narrower than those of both other approaches. Even though RESVM base models have more variability compared to bagging SVM base models, the overall performance of RESVM is more reliable. This constitutes an important practical advantage since assessing different models is not trivial outside of simulation studies (e.g. when no negative labels are available).

4.5.4 A note on the number of repetitions per experiment

The tightness of the confidence intervals of generalization performance allow us to conclude that the number of repetitions (20) is sufficient to demonstrate the merits of RESVM (see Tables 4.1–4.3). Increasing the number of repetitions further would yield even narrower confidence intervals and increase the number of statistically significant results in the Wilcoxon signed-rank test comparing bagging SVM and RESVM (due to increased power). All key conclusions remain valid if the number of repetitions would be increased.

Additional statistically significant results may only be obtained in experiments where the improvement offered by RESVM is too small to be of practical significance (as large improvements already yield significant test results). Failure to reject the null hypothesis ($h_0 : AUC^{BAG} \geq AUC^{RESVM}$) in our current results indicates that (i) bagging SVM is effectively better than RESVM, (ii) they are comparable or (iii) the performance improvement of RESVM is too small to yield a significant test result given the current sample size (number of

repetitions). Increasing the number of repetitions can only lead to additional statistically significant results in the latter situation.

To illustrate our claims, we performed 100 repetitions for `covtype` in the semi-supervised setting. This yielded the following CIs and win counts: CWSVM 59.0–60.5% (8 wins), bagging SVM 62.3–63.5% (21 wins), RESVM 63.8–65.8% (71 wins). The p-value of the Wilcoxon signed-rank test becomes 2×10^{-5}, while the p-value was insignificant with 20 repetitions (Table 4.3).

4.5.5 Trend across data sets

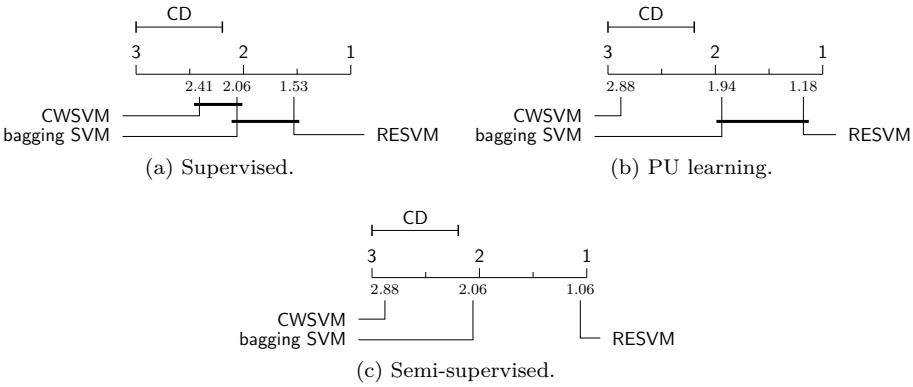
In the previous tables we have shown the results per data set for each setting. In this section we summarize the results across all data sets, using critical difference diagrams [81] in Section 4.5.5 and an overview of win counts in Section 4.5.5.

Critical difference diagrams

In every setting, we compared the performance of the three learning approaches across all data sets using non-parametric statistical tests. For each data set, approaches were ranked based on their mean area under the PR curve across all iterations. Multiclass data sets count once per class. Friedman tests per setting yielded significant evidence of differences between the three learning approaches at the $\alpha = 0.05$ level, though this was marginal in the supervised setting ($p = 0.034$). The Nemenyi post-hoc test [185] was used after each omnibus test to assess differences between all approaches. The critical difference diagrams in Figure 4.2 visualize the results.

Critical difference diagrams were introduced by Demšar [81] to visualize a comparison of multiple learning approaches over multiple data sets. These diagrams depict the average rank of each approach (lower is better) along with the critical difference (CD). The critical difference is the minimum difference in average ranks that yields a significant result in the Nemenyi post-hoc test. It depends on the significance level ($\alpha = 0.05$), the number of learning approaches (3) and the number of data sets (17).

From Figure 4.2 we can conclude that bagging SVM and RESVM are comparable in the PU learning setting (both significantly better than CWSVM). In the semi-supervised setting, bagging SVM is statistically significantly better than CWSVM and RESVM is significantly better than both other approaches across all data sets.



(a) Supervised.

(b) PU learning.

(c) Semi-supervised.

Figure 4.2: Critical difference diagrams for each setting. Groups of algorithms that are not significantly different at the 5% significance level are connected.

Win counts

The number of wins per method across all data sets are summarized in Table 4.4. The top half shows the total number of wins across all data sets, which weighs `mnist` and `sensit` heavier than the other data sets since we performed several one-vs-all experiments. Because RESVM consistently performed very strong on `mnist`, the top half is an overly optimistic representation.

The bottom half of Table 4.4 contains normalized results, where every data set contributes equally. Based on these numbers we can conclude that there is little difference between the three methods in a supervised setting. In the PU learning setting, ensemble methods become favorable over CWSVM (bagging SVM and RESVM being competitive). Finally, in the semi-supervised setting RESVM pulls far ahead of both other methods and obtains 65% of the normalized wins, which is over three times more than bagging SVM and over five times more than class-weighted SVM.

4.5.6 Effect of contamination

In this Section we show the effect of different levels of contamination in $\mathcal{P}$ and $\mathcal{U}$ on the `synthetic` data set. In these simulations, we fixed the contamination level in one part of the training set ($\mathcal{P}$ or $\mathcal{U}$) and the contamination of other was varied. The fixed contamination was set to 30%. Twenty simulations were run per contamination setting.

	CWSVM		bagging SVM		RESVM	
setting	count	win %	count	win %	count	win %
supervised	73	21	93	27	**174**	**51**
PU learning	21	6	88	26	**231**	**68**
semi-supervised	25	7	42	12	**273**	**80**
supervised	**44.8**	**37.3**	40.3	33.6	36.0	30.0
PU learning	18.3	15.3	39.4	32.8	**62.2**	**51.8**
semi-supervised	17.0	14.2	24.0	20.0	**79.0**	**65.8**

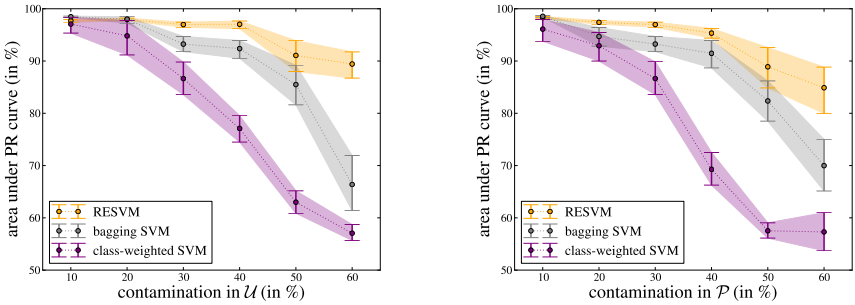
Table 4.4: Number of wins in simulations for each method per setting. The bottom half shows normalized number of wins, where wins in multiclass data sets (`mnist` and `sensit`) are divided by the number of classes.

In these experiments, we used random search to tune hyperparameters of each method [32] using the Optunity package.[4] Briefly, hyperparameters were searched by random sampling 100 tuples uniformly within a given box and subsequently the best tuple was selected as before. We ensured that the optimal hyperparameters were never too close to the edge of the feasible region (if so, the box was expanded). Note that this approach of testing a fixed number of tuples favors methods with less hyperparameters. Even though RESVM has more hyperparameters than the other methods, good models can be obtained at the same search cost.

The results are shown in Figure 4.3. In general, contamination in $\mathcal{P}$ causes larger performance losses than the same level of contamination in $\mathcal{U}$ for all algorithms. As expected, the difference in sensitivity to contamination in $\mathcal{P}$ and $\mathcal{U}$ is smallest for RESVM in which $\mathcal{P}$ and $\mathcal{U}$ are resampled similarly. At high contamination levels, RESVM is the only method that still works well (even at 60%).

Figure 4.3a illustrates that RESVM and bagging SVM behave in a similar fashion at contamination levels of $\mathcal{U}$ up to 50% and both outperform class-weighted SVM. RESVM outperforms bagging SVM for contamination levels of 30–50% but the consistency (width of CI) and performance losses of both methods are comparable. Figure 4.3b shows the increased robustness of RESVM to contamination in $\mathcal{P}$ resulting in reduced loss of generalization performance for increasing contamination.

[4]Optunity is available at: `http://www.optunity.net`.



(a) Effect of contamination in $\mathcal{U}$.

(b) Effect of contamination in $\mathcal{P}$.

Figure 4.3: Effect of different levels of contamination in $\mathcal{U}$ and $\mathcal{P}$ on generalization performance. The plots show point estimates of the mean area under the PR curve across experiments and the associated 95% confidence intervals.

4.5.7 RESVM optimal parameters

As an illustration of the implicit mechanism of RESVM we show some of the optimal tuning parameters for every setting in Table 4.5. These parameters were obtained by performing 10-fold cross-validation on the training set.

An interesting observation is that the size of the training sets that are being used decreases for increasing contamination. Increasing label noise induces RESVM to favor smaller base model training sets for which the variability in contamination is larger (see Figure 4.1). Though this may appear counterintuitive, bagging approaches are known to exhibit a bias-variance tradeoff [29] for which using weaker base models with increased variability may yield better ensembles [147].

The optimal value of the misclassification penalty for positive training instances relative to unlabeled instances, w_{pos}, changes between learning settings (see Equation (4.3)). It exhibits expected behaviour: the maximum value is obtained when the certainty on $\mathcal{P}$ relative to $\mathcal{U}$ is largest (e.g. the pure PU learning setting). This parameter implicitly balances empirical certainty on $\mathcal{P}$ and $\mathcal{U}$ and is an important degree of freedom in RESVM. In bagging SVM, this parameter is implicitly fixed to 1 via Equation (4.2) [179]. Note that w_{pos} need not be larger than 1 (which would place extra emphasisis on the known labels after accounting for class imbalance). In highly imbalanced settings where $n_{unl} \gg n_{pos}$, the optimal value of w_{pos} may well be less than 1.

	0	1	2	3	4	5	6	7	8	9	mean
$\mathbf{n_{pos}}$											
supervised	20	20	20	20	20	20	10	20	20	10	18
PU learn	10	10	10	10	10	15	10	10	10	10	10.5
semi-sup.	10	5	10	10	10	10	10	10	10	10	9.5
$\mathbf{n_{unl}/n_{pos}}$											
supervised	10	10	10	10	10	10	10	10	10	10	10
PU learn	5	5	5	5	5	5	5	5	5	5	5
semi-sup.	5	5	5	8	5	5	5	5	5	5	5.25
$\mathbf{w_{pos}}$											
supervised	1.6	1.6	1.6	3.2	3.2	3.2	3.2	1.6	3.2	2.4	2.48
PU learn	4.8	6.4	3.2	6.4	4.8	6.4	4.8	4.8	6.4	6.4	5.44
semi-sup.	12.8	6.4	4.8	2.1	4.8	6.4	4.8	3.2	3.2	3.2	5.17

Table 4.5: Medians of optimal hyperparameters per digit obtained via cross-validation and mean of all medians per setting. The normalized relative weight on positives versus unlabeled instances (w_{pos}) is associated with the relative size and contamination of the positive and unlabeled training sets.

4.6 Conclusion

We have introduced a new approach for learning from positive and unlabeled data, called the robust ensemble of SVMs (RESVM). RESVM constructs an ensemble model using a bagging strategy in which the positive and unlabeled sets are resampled to obtain base model training sets. By resampling both $\mathcal{P}$ and $\mathcal{U}$, our approach is more robust against false positives than others.

The robustness of our approach to potential contamination in both $\mathcal{P}$ and $\mathcal{U}$ can be attributed to the synergy between our resampling scheme and voting aggregation. The resampling itself strongly resembles a typical bootstrap approach. RESVM uses class-weighted SVM base models though the resampling scheme is likely to work well with other types of base models.

RESVM was compared with class-weighted SVM and bagging SVM on several data sets under different label noise conditions. The trends across data sets show that bagging SVM and RESVM outperform class-weighted SVM in PU learning. In a pure PU learning setting the average improvement over existing methods is modest though RESVM classifiers exhibit lower variance in performance making it more reliable.

In the semi-supervised setting, label noise was introduced in $\mathcal{P}$ to highlight the improved robustness of RESVM compared to the other methods. Our

experimental results show that RESVM remains very strong in the semi-supervised setting while both other approaches degrade dramatically. Statistical analysis showed that RESVM is significantly better than both other approaches across all data sets.

Visual inspection of the PR curves shows that in the majority of experiments the curve for RESVM not only has higher AUC but completely dominates the other curves. As such RESVM models are a good approach regardless of design priorities (high recall versus high precision).

A weakness of RESVM is its amount of hyperparameters (5 plus potential kernel parameters), though RESVM models are less sensitive to accurate tuning of these parameters than standard SVM. Our experiments indicated that although RESVM has more hyperparameters, good models can be obtained at the same search effort than the other approaches (e.g. testing the same number of hyperparameter tuples). An interesting question is whether prior knowledge regarding contamination of $\mathcal{P}$ and $\mathcal{U}$ can help in limiting the search scope for some of the hyperparameters (n_{pos}, n_{unl} and w_{pos} specifically).

Chapter 5

Hyperparameter Search in Machine Learning

This chapter has been previously published as:
Claesen, M., & De Moor, B. (2015). **Hyperparameter Search in Machine Learning**. In *Proceedings of the 11th Metaheuristics International Conference (MIC)*, Agadir, Morocco.
Manuscript available at `http://arxiv.org/abs/1502.02127`.

Contributions Marc Claesen drafted the paper.

Abstract

We describe the hyperparameter search problem in the field of machine learning and discuss its main challenges from an optimization perspective. Machine learning methods attempt to build models that capture some element of interest based on given data. Most common learning algorithms feature a set of hyperparameters that must be determined before training commences. The choice of hyperparameters can significantly affect the resulting model's performance, but determining good values can be complex; hence a disciplined, theoretically sound search strategy is essential.

5.1 Introduction

Machine learning research focuses on the development of methods that are capable of capturing some element of interest from a given data set. Such elements include but are not limited to coherent structures within data (clustering) or the ability to predict certain target values based on given characteristics, which may be discrete (classification) or continuous (regression).

A large variety of learning methods exist, ranging from biologically inspired neural networks [40] over kernel methods [225] to ensemble models [52, 65]. A common trait in these methods is that they are parameterized by a set of hyperparameters λ, which must be set appropriately by the user to maximize the usefulness of the learning approach. Hyperparameters are used to configure various aspects of the learning algorithm and can have wildly varying effects on the resulting model and its performance.

Hyperparameter search is commonly performed manually, via rules-of-thumb [135, 133] or by testing sets of hyperparameters on a predefined grid [201]. These approaches leave much to be desired in terms of reproducibility and are impractical when the number of hyperparameters is large [64]. Due to these flaws, the idea of automating hyperparameter search is receiving increasing attention in machine learning, for instance via benchmarking suites [90] and various initiatives.[1] Automated approaches have already been shown to outperform manual search by experts on several problems [35, 32].

We briefly introduce some key challenges inherent to hyperparameter search in Section 5.2. The combination of all these hurdles make hyperparameter search a formidable optimization task. In Section 5.3 we give a succinct overview of the current state-of-the-art in terms of algorithms and available software.

5.1.1 Example: controlling model complexity

A key balancing act in machine learning is choosing an appropriate level of model complexity: if the model is too complex, it will fit the data used to construct the model very well but generalize poorly to unseen data (overfitting); if the complexity is too low the model won't capture all the information in the data (underfitting). This is often referred to as the bias-variance trade-off [106, 74], since a complex model exhibits large variance while an overly simple one is strongly biased. Most general-purpose methods feature hyperparameters to control this trade-off; for instance via regularization as in support vector machines and regularization networks [94, 128].

[1] Such as `http://www.automl.org/` and `https://www.codalab.org/competitions/2321`.

5.1.2 Formalizing hyperparameter search

The goal of many machine learning tasks can be summarized as training a model $\mathcal{M}$ which minimizes some predefined loss function $\mathcal{L}(\mathbf{X}^{(te)};\ \mathcal{M})$ on given test data $\mathbf{X}^{(te)}$. Common loss functions include mean squared error and error rate. The model $\mathcal{M}$ is constructed by a learning algorithm $\mathcal{A}$ using a training set $\mathbf{X}^{(tr)}$; typically involving solving some (convex) optimization problem. The learning algorithm $\mathcal{A}$ may itself be parameterized by a set of hyperparameters λ, e.g. $\mathcal{M} = \mathcal{A}(\mathbf{X}^{(tr)};\ \lambda)$. An example model $\mathcal{M}$ is a support vector machine classifier with Gaussian kernel [225], for which the training problem $\mathcal{A}$ is parameterized by the regularization constant C and kernel bandwidth σ, i.e. $\lambda = [C, \sigma]$.

The goal of hyperparameter search is to find a set of hyperparameters $\lambda^\star$ that yield an optimal model $\mathcal{M}^\star$ which minimizes $\mathcal{L}(\mathbf{X}^{(te)};\ \mathcal{M})$. This can be formalized as follows [64]:

$$\lambda^\star = \arg\min_{\lambda} \mathcal{L}\big(\mathbf{X}^{(te)};\ \mathcal{A}(\mathbf{X}^{(tr)};\ \lambda)\big) = \arg\min_{\lambda} \mathcal{F}(\lambda;\ \mathcal{A},\ \mathbf{X}^{(tr)}, \mathbf{X}^{(te)},\ \mathcal{L}). \quad (5.1)$$

The objective function $\mathcal{F}$ takes a tuple of hyperparameters λ and returns the associated loss. The data sets $\mathbf{X}^{(tr)}$ and $\mathbf{X}^{(te)}$ are given and the learning algorithm $\mathcal{A}$ and loss function $\mathcal{L}$ are chosen . Depending on the learning task, $\mathbf{X}^{(tr)}$ and $\mathbf{X}^{(te)}$ may be labeled and/or equal to each other. In supervised learning, a data set is often split into $\mathbf{X}^{(tr)}$ and $\mathbf{X}^{(te)}$ using hold-out or cross-validation methods [88, 151].

5.2 Challenges in hyperparameter search

The characteristics of the search problem depend on the learning algorithm $\mathcal{A}$, the chosen loss function $\mathcal{L}$ and the data set $\mathbf{X}^{(tr)}$, $\mathbf{X}^{(te)}$, as shown in Equation (6.1). Hyperparameter search is typically approached as a non-differentiable, single-objective optimization problem over a mixed-type, constrained domain. In this section we will discuss the origins and consequences of challenges in hyperparameter search.

5.2.1 Costly objective function evaluations

Each objective function evaluation requires evaluating the performance of a model trained with hyperparameters λ. Depending on the available computational resources, the nature of the learning algortihm $\mathcal{A}$ and size of the problem ($\mathbf{X}^{(tr)}$, $\mathbf{X}^{(te)}$) each evaluation may take considerable time. Training

times in the order of minutes are considered fast, since days and even weeks are not unheard of [154, 80, 250]. Evaluation time is exacerbated when procedures that train multiple models are employed; for instance to reliably estimate generalization performance [88, 151]. This leads to an increasing need for efficient methods to optimize hyperparameters that require a minimal amount of objective function evaluations.

Additionally, the time required to train and test models can be contingent upon the choice of hyperparameters. Some hyperparameters have an obvious influence on train and/or test time, e.g., the architecture of neural networks [40] and size of ensembles [52, 65]. The influence of hyperparameters can also be subtle, for instance regularization and kernel complexity can significantly affect training time for support vector machines [45].

5.2.2 Randomness

The objective function often exhibits a stochastic component, which can be induced by various components of the machine learning pipeline, for example due to inherent randomness of the learning algorithm (initialization of a neural network, resampling in ensemble approaches, ...) or due to finite sample effects in estimating generalization performance. This stochasticity can sometimes be addressed via machine learning techniques; but unfortunately such solutions typically dramatically increase the time required per objective function evaluation, limiting their usefulness in some settings.

This inherent stochasticity directly implies that the empirical best hyperparameter tuple, obtained after a given set of evaluations, is not necessarily the true optimum of interest $\lambda^\star$. Fortunately, many search methods are designed to probe many tuples close to the empirical best. If the search region surrounding the empirical optimum is densely sampled, we can determine whether the empirical best was an outlier or not in a post-processing phase, for instance by assuming Lipschitz continuity or smoothness.

5.2.3 Complex search spaces

The number of hyperparameters is usually small (≤ 5), but it can range up to hundreds for complex learning algorithms [34] or when preprocessing steps are also subjected to optimization [139]. It has been demonstrated empirically that in many cases only a handful of hyperparameters significantly impact performance, though identifying the relevant ones in advance is difficult [32].

Hyperparameters are usually of continuous or integer type, leading to mixed-type optimization problems. Continuous hyperparameters are commonly related to regularization. Common integer hyperparameters are related to network architecture for neural networks [40], size of ensembles [52, 65] or the parameterization of kernels in kernel methods [225].

Some tasks feature highly complex search spaces, in which the very existence of certain hyperparameters are conditional upon the value of others [139, 35, 33]. A simple example is optimizing the architecture of neural networks [40], where the number of hidden layers is one hyperparameter and the size of each layer induces a set of additional hyperparameters, conditional upon the number of layers.

5.3 Current approaches

A wide variety of optimization methods have been used for hyperparameter search, including particle swarm optimization [176, 162], genetic algorithms [256], coupled simulated annealing [278] and racing algorithms [39]. Surprisingly, randomly sampling the search space was only established recently as a baseline for comparison of optimization methods [32]. Bayesian and related sequential model based optimization techniques using variants of the expected improvement criterion [142] are receiving a lot of attention currently [35, 138, 242, 25, 90], owing to their efficiency in terms of objective function evaluations.

Software packages are being released which implement various dedicated optimization methods for hyperparameter search. Such packages are usually intended to be used in synergy with machine learning libraries that provide learning algorithms [201]. Most of these packages focus on Bayesian methods [139, 242, 33], though metaheuristic optimization approaches are also offered [64]. The increased development of such packages testifies towards the growing interest in automated hyperparameter search.

5.4 Conclusion

A fully automated, self-configuring learning strategy can be considered the holy grail of machine learning. Though the current state-of-the-art still has a long way to go before this goal can be reached, it is evident that hyperparameter search is a crucial element in its pursuit. Automated hyperparameter search is a hot topic within the machine learning community which we believe can benefit greatly from the techniques and lessons learnt in metaheuristic optimization.

Chapter 6

Easy Hyperparameter Search Using Optunity

This chapter has been submitted as:
Claesen, M., Simm, J., Popovic, D., Moreau, Y., & De Moor, B. (2015). **Easy hyperparameter search using Optunity**, *Journal of Machine Learning Research*.

Contributions Marc Claesen has developed, maintained, tested and documented the software in Python, MATLAB and Octave and took the lead in writing the initial draft, the revision and rebuttal of the paper.

Abstract

Optunity is a free software package dedicated to hyperparameter optimization. It contains various types of solvers, ranging from undirected methods to direct search, particle swarm and evolutionary optimization. The design focuses on ease of use, flexibility, code clarity and interoperability with existing software in popular machine learning environments. Optunity is written in Python and contains interfaces to R, Julia, Octave and MATLAB. Optunity uses a BSD license and is available at `http://www.optunity.net`.

6.1 Introduction

Many machine learning tasks involve training a model $\mathcal{M}$ which minimizes some loss function $\mathcal{L}(\mathcal{M} \mid \mathbf{X}^{(te)})$ on given test data $\mathbf{X}^{(te)}$. A model is obtained via a learning algorithm $\mathcal{A}$ which uses a training set $\mathbf{X}^{(tr)}$ and solves some optimization problem. The learning algorithm $\mathcal{A}$ may itself be parameterized by a set of hyperparameters λ, e.g. $\mathcal{M} = \mathcal{A}(\mathbf{X}^{(tr)} \mid \lambda)$. Hyperparameter search – also known as tuning – aims to find a set of hyperparameters λ^*, such that the learning algorithm yields an optimal model $\mathcal{M}^*$ that minimizes $\mathcal{L}(\mathcal{M} \mid \mathbf{X}^{(te)})$:

$$\lambda^* = \arg\min_{\lambda} \mathcal{L}\big(\mathcal{A}(\mathbf{X}^{(tr)} \mid \lambda) \mid \mathbf{X}^{(te)}\big) = \arg\min_{\lambda} \mathcal{F}(\lambda \mid \mathcal{A},\ \mathbf{X}^{(tr)}, \mathbf{X}^{(te)},\ \mathcal{L}). \tag{6.1}$$

In tuning, $\mathcal{F}$ is the objective function and the hyperparameters λ are optimization variables. The learning algorithm $\mathcal{A}$, loss function $\mathcal{L}$ and data sets $\mathbf{X}^{(tr)}$ and $\mathbf{X}^{(te)}$ are known.

Tuning hyperparameters is a recurrent task in machine learning which may significantly affect overall performance. Commonly tuned hyperparameters are related to kernels, regularization, learning rates and network architecture. Some specific challenges associated to hyperparameter optimization are discussed by Claesen and De Moor [63]. General machine learning packages provide only basic tuning methods like grid search [201]. In practice, the most common tuning approaches are grid search and manual tuning, though both are known to fail when the number of hyperparameters grows and manual search is additionally hard to reproduce [32].

The current adoption of dedicated hyperparameter optimizers is limited: we surveyed NIPS 2014 and found that only 2 out of 86 works used suitable approaches while 84 papers reported the use of grid search, random search or manual tuning (cfr. Appendix 6.A).

6.2 Optunity

Optunity offers various optimizers and utility functions to enable efficient hyperparameter optimization using only a few of lines of code and minimal expertise. Our software is complementary to libraries that provide learning algorithms, such as scikit-learn [201]. The package uses a BSD license and is simple to deploy in any environment. Optunity supports Python, R, Octave and MATLAB on Linux, OSX and Windows.

6.2.1 Functional Overview

OPTUNITY provides both simple routines for lay users and expert routines that enable fine-grained control of various aspects of the solving process. Basic tuning requires only an objective function, a maximum number of evaluations and box constraints on the hyperparameters to be optimized. Conditional search spaces in which the existence of some hyperparameters is contingent upon some discrete choice are also supported.

The objective function must be defined by the user. It takes a hyperparameter tuple λ and typically involves three steps: (i) training a model $\mathcal{M}$ with λ, (ii) use $\mathcal{M}$ to predict a test set and (iii) compute some score or loss based on the predictions.

Tuning involves a series of function evaluations until convergence or until a predefined maximum number of evaluations is reached. OPTUNITY is capable of vectorizing evaluations in the working environment to speed up the process at the end user's volition.

OPTUNITY also provides k-fold cross-validation to estimate the generalization performance of supervised modeling approaches. The implementation can account for strata and clusters.[1] Finally, a variety of common quality metrics is available. The snippet below shows how to tune an SVM classifier with RBF kernel using SCIKIT-LEARN and OPTUNITY:[2]

```
1 @optunity.cross_validated(x=data, y=labels, num_folds=10, num_iter=2)
2 def score(x_train, y_train, x_test, y_test, C, gamma):
3     model = sklearn.svm.SVC(C=10**C, gamma=10**gamma).fit(x_train, y_train)
4     decision_values = model.decision_function(x_test)
5     return optunity.metrics.roc_auc(y_test, decision_values)
6
7 hps, _, _ = optunity.maximize(score, num_evals=100, C=[-5, 2], gamma=[-5, 0])
8 svm = sklearn.svm.SVC(C=10**hps['C'], gamma=10**hps['gamma'])
9 svm.fit(data, labels)
```

The objective function as per Equation (6.1) is defined on lines 1 to 5, where $\lambda = (C, \gamma)$, $\mathcal{A}$ is the SVM training algorithm and $\mathcal{L}$ is area under the ROC curve. We use 2× iterated 10-fold cross-validation to estimate area under the ROC curve. Up to 100 hyperparameter tuples are tested in an exponential search space, bounded by $10^{-5} < C < 10^2$ and $10^{-5} < \gamma < 10^0$ on line 7. Finally, an SVM with optimized hyperparameters is trained on lines 8 and 9.

[1] Instances in a stratum should be spread across folds. Clustered instances must remain in a single fold.

[2] We assume the correct imports are made and `data` and `labels` contain appropriate content.

6.2.2 Available Solvers

Optunity provides a wide variety of solvers, ranging from basic, undirected methods like grid search, sobol sequences and random search [32] to evolutionary methods such as particle swarm optimization [148], the covariance matrix adaptation evolutionary strategy (CMA-ES) [123], tree-structured Parzen estimator [35] and the Nelder-Mead simplex. The default solver is particle swarm optimization, which performs well for a large variety of tuning tasks involving various learning algorithms. Additional solvers will be incorporated in the future.

6.2.3 Software Design and Implementation

The design philosophy of Optunity prioritizes code clarity over performance. This is justified by the fact that objective function evaluations constitute the performance bottleneck.

In contrast to typical Python packages, we avoid dependencies to facilitate users working in non-Python environments (sometimes at the cost of performance). To prevent issues for users that are unfamiliar with Python, care is taken to ensure all code in Optunity works out of the box on any Python version above 2.7, without requiring tools like `2to3` to make explicit conversions. Optunity has optional dependencies on DEAP [99] and Hyperopt [33] for the CMA-ES and TPE solvers, respectively.

A key aspect of Optunity's design is interoperability with external environments. This requires bidirectional communication between Optunity's Python back-end ($\mathcal{O}$) and the external environment ($\mathcal{E}$) and roughly involves three steps: (i) $\mathcal{E} \rightarrow \mathcal{O}$ solver configuration, (ii) $\mathcal{O} \leftrightarrow \mathcal{E}$ objective function evaluations and (iii) $\mathcal{O} \rightarrow \mathcal{E}$ solution and solver summary. To this end, Optunity can do straightforward communication with any environment via sockets using JSON messages as shown in Figure 6.1. Only some information must be communicated, big objects like data sets are never exchanged. To port Optunity to a new environment, a thin wrapper must be implemented to handle communication.

6.2.4 Development and Documentation

Collaborative development is organized via GitHub.[3] The project's master branch is kept stable and is subjected to continuous integration tests using

[3]We maintain the following subdomains for convenience: `http://`{builds, docs, git, issues}`.optunity.net`.

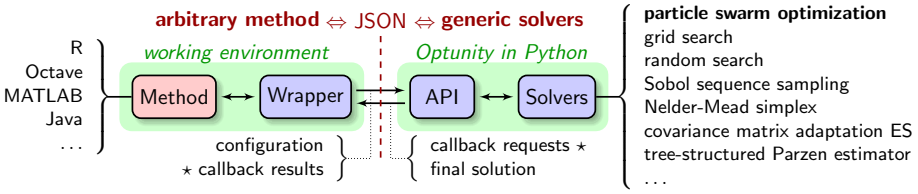


Figure 6.1: Integrating Optunity in non-Python environments.

Travis CI. We recommend prospective users to clone the master branch for the most up-to-date stable version of the software. Bug reports and feature requests can be filed via issues on GitHub. Future development efforts will focus on wrappers for Java and C/C++. We additionally plan to incorporate Bayesian optimizers which have no reference implementation in other packages.

Code is documented using Sphinx and contains many doctests that can serve as both unit tests and examples of the associated functions. Our website contains developer and user documentation and a wide range of examples to illustrate all aspects of the software. The examples involve various packages and environments, including scikit-learn [201], OpenCV [49] and Spark's MLlib [285].

6.3 Related Work

A number of software solutions exist for hyperparameter search. Hyperopt offers random search and sequential model-based optimization [33]. Some packages dedicated to Bayesian approaches include Spearmint [242], DiceKriging [219], SMAC [138] and BayesOpt [172]. Finally, ParamILS provides iterated local search [139].

Optunity distinguishes itself from other packages by exposing a variety of fundamentally different solvers through a lightweight API. Optunity's client-server model facilitates integration in any language and environment and can even be used to run solvers remotely.

6.4 Solver Benchmark

We compared Optunity against BayesOpt [172], Hyperopt [33], SMAC [138], and random search [32]. Implementations of the last three solvers were available

in HPOlib [90]. We optimized 5-fold cross-validated area under the ROC curve for an SVM classifier with an RBF kernel (with continuous hyperparameters $\log C$ and $\log \gamma$), given a fixed search space and a budget of 150 evaluations on 19 pristine real-world problems. All solvers were given identical objective functions. Figure 6.1 summarizes the results using critical difference (CD) diagrams as introduced by Demšar [81]. More details are available in Appendix 6.B.

Optunity and BayesOpt statistically significantly outperformed random search at 75 and 150 evaluations, with BayesOpt winning twice. Optunity improved at 150 evaluations relative to the other optimizers, indicating it is better at local search. Overall, we conclude that all 4 directed optimizers are competitive and convincingly outperform random search.

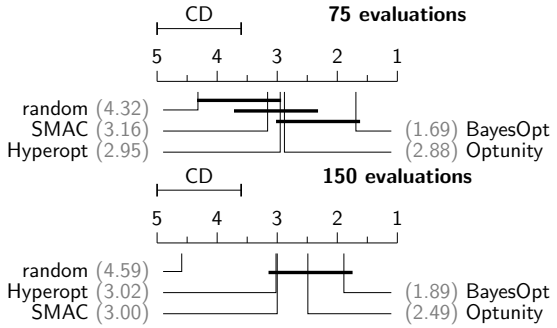


Figure 6.1: Critical difference diagrams for 75 and 150 evaluations to tune an SVM with RBF kernel, depicting average rank per optimizer (lower is better). Optimizers without statistically significant performance differences at $\alpha = 5\%$ are linked.

Appendix

6.A Survey of hyperparameter optimization in NIPS 2014

To objectively assess the current adoption of dedicated hyperparameter optimization techniques, we have surveyed all papers of the NIPS 2014 conference[4] (411 in total).[5] The main question was how many papers reported the use of techniques other than grid search, random search and manual tuning. We counted all papers mentioning cross-validation or hyperparameter optimization (86 papers) and then categorized these papers based on which hyperparameter optimization method was used. Table 6.A.1 summarizes the survey's outcome.[6]

Table 6.A.1 indicates that the adoption of dedicated hyperparameter optimizers remains limited in contemporary machine learning. Grid search remains the head honcho for hyperparameter optimization (used in 82 out of 86 works, or 95%), despite significant evidence that better optimization methods exist. Although automated hyperparameter optimization is a hot topic in contemporary machine learning research, the resulting methods appear to not yet be a part of practitioners' toolkits and workflows (used in 2 out of 86 works, or 2%).

We believe several barriers exist towards the adoption of dedicated hyperparameter optimization methods. First, users must know of their existence

[4]The NIPS 2014 conference homepage is available at `https://nips.cc/Conferences/2014/`.

[5]The full survey with each paper's tags is available at `https://github.com/jaak-s/nips2014-survey`.

[6]To automate the survey and make it reproducible, we scanned all papers for names of well-known hyperparameter optimization packages and techniques along with names of the authors of the corresponding publications. Using this approach, we automatically accounted for random search [32], Spearmint [242], Hyperopt [33], BayesOpt [172], ParamILS [139], SMAC [138] and the Tree of Parzen Estimators (TPE) optimizer [35].

optimization method	number of uses
grid search	82
random search	2
Spearmint [242]	1
predictive entropy search [131]	1
total	**86**

Table 6.A.1: The use of hyperparameter optimization methods as reported in NIPS 2014 papers. Methods and packages with 0 recorded uses are omitted from this table.

and relative benefit compared to conventional methods (we believe this to be the case). Second, these methods must be available in all common machine learning environments. Third, it must be easy for potential users to start using these optimizers and get immediate results, which requires that installation is straightforward and the APIs are intuitive, flexible and well-documented.

Finally, it is worth noting that NIPS is one of the hotspots of automated hyperparameter optimization research, both in terms of publications and related workshops. Hence it is reasonable to assume that the adoption of dedicated hyperparameter optimization methods is elevated within the NIPS community compared to the entire machine learning field and more applied fields such as computer vision and bioinformatics.

6.B Performance benchmark

We created a benchmark to assess the performance of Optunity's default optimizer (particle swarm optimization) against the defaults of SMAC [138], Hyperopt [33] and BayesOpt [172] for real hyperparameter search tasks.[7]

6.B.1 Setup

Our benchmark entails optimizing the 2 continuous hyperparameters of an SVM classifier with RBF kernel on an exponential grid ($10^{-8} < C < 10$ and $10^{-8} < \gamma < 10$). We used 5-fold cross-validation to estimate area under the

[7]The benchmark is based on HPOlib (which provided Hyperopt, SMAC and random search). All code and full results are available at `https://github.com/claesenm/optunity-benchmark` and should work on any linux platform, provided all dependencies are met.

ROC curve to build the objective function. All optimizers used the exact same objective function and a uniform prior to optimize $\log_{10}(C)$ and $\log_{10}(\gamma)$ within the specified bounds (the exponentiation was done within the objective function). Each optimizer was given a budget of 150 function evaluations and we probed their intermediate results at 75 evaluations and the final results at 150 evaluations.

We simulated 19 real-world problems based on the `mnist digits`, `covtype`, `diabetes` and `ionosphere` data sets. Multiclass data sets were used several times in a one-vs-all setting, i.e., `mnist digits` and `covtype` were used to create 10 and 7 optimization problems, respectively. `mnist digits` and `covtype` were used as provided in scikit-learn [201], while we used the scaled versions of the `diabetes` and `ionosphere` data sets as available on the website of LIBSVM.[8]

For some data sets we added random noise on the data matrix to make the learning problems more challenging and enable differentiating between various hyperparameter optimizers. Each task was simulated 5 times to improve consistency. Results of each optimization task at 75 and 150 evaluations are shown in Tables 6.B.1 and 6.B.2, respectively, which show average performance and rank of each solver per data set along with an overall summary.

6.B.2 Results & Discussion

The results of the benchmark are summarized in Figure 6.1 and shown in full for 75 and 150 evaluations in Tables 6.B.1 and 6.B.2, respectively. The tables show averages (across 5 runs per problem) of the optimum across all solvers, the third quantile of random search performance (to indicate problem difficulty) and the relative rank and regret per solver. Regret in this case means the difference between an optimizer's best and the overall best solution in a given experiment and can be considered to measure the cost of using a given optimizer for a given task, with the optimizer that found the best solution inducing 0 regret.

Overall, BayesOpt took the lead in this benchmark at both evaluation counts, followed by Optunity. Optunity and Hyperopt improve in terms of regret and relative rank in evaluations 76–150, with Optunity showing the biggest relative improvement. Since most optimizers have already reached fairly good solutions after 75 evaluations, local search performance is key in the final 75 evaluations. Since Optunity's regret and relative rank amongst optimizers show a noteworthy improvement at 150 evaluations compared to 75 evaluations, we conclude that its local search performance beats that of other optimizers.

[8] Available at `https://www.csie.ntu.edu.tw/~cjlin/libsvmtools/datasets/` and in the GitHub repo.

Table 6.B.1: Benchmark results for tuning an SVM classifier with RBF kernel, using an optimization budget of 75 evaluations (best result per data set in bold, worst in gray). Results depict averages across 5 runs of the optimum (i.e., the best found solution across all optimizers), the third quantile (Q_3) of random search results (which indicates the difficulty of the optimization problem: low Q_3 vis-à-vis the optimum indicates the region of strong performance is small within the overall search space) and the relative rank and regret per optimizer. Performance and regret are measured in terms of cross-validated area under the ROC curve and shown in percent. Relative ranks indicate non-parametric global performance within the pool of optimizers (lower is better, the best optimizer has rank 1).

			Optunity		Hyperopt		SMAC		BayesOpt		random search	
data set	optimum	Q_3	rank	regret	rank	regret	rank	regret	rank	regret	rank	regret
`digits-0`	96.56	95.46	**1.80**	**0.041**	3.20	0.096	3.40	0.145	**1.80**	0.055	4.80	0.340
`digits-1`	91.10	86.69	2.40	0.256	2.60	0.258	3.80	0.562	**1.20**	**0.069**	5.00	1.064
`digits-2`	93.27	91.19	2.60	0.166	3.80	0.376	2.60	0.390	**2.00**	**0.156**	4.00	0.734
`digits-3`	90.82	88.63	2.20	0.316	3.40	0.530	3.40	0.528	**1.80**	**0.093**	4.20	0.651
`digits-4`	94.86	93.50	3.60	0.406	3.20	0.291	2.20	0.222	**1.60**	**0.051**	4.40	0.480
`digits-5`	93.11	90.67	2.60	0.328	3.60	0.570	2.40	0.399	**1.40**	**0.101**	5.00	1.038
`digits-6`	95.97	94.97	3.40	0.325	2.20	0.121	3.20	0.300	**1.60**	**0.098**	4.60	0.516
`digits-7`	95.20	93.52	3.00	0.162	2.80	0.193	2.20	0.130	**2.00**	**0.068**	5.00	0.774
`digits-8`	82.75	73.61	3.00	0.365	2.80	0.370	3.80	0.754	**1.80**	**0.168**	3.60	0.373
`digits-9`	87.92	84.61	2.60	0.260	2.60	0.506	3.20	0.522	**1.60**	**0.164**	5.00	1.143
`covtype-1`	82.41	77.44	**2.00**	0.508	3.20	0.870	3.00	0.868	2.60	**0.442**	4.20	1.491
`covtype-2`	81.97	73.97	2.20	0.649	2.80	0.919	3.80	2.074	**1.60**	**0.262**	4.60	2.906
`covtype-3`	97.91	94.79	3.20	0.263	3.20	0.210	3.60	0.185	**1.60**	**0.012**	3.40	0.182
`covtype-4`	99.76	98.40	3.20	0.130	3.40	0.058	3.20	0.090	**1.60**	**0.019**	3.60	0.067
`covtype-5`	96.84	90.53	4.00	0.797	2.80	0.441	3.00	0.586	**1.20**	**0.023**	4.00	0.744
`covtype-6`	97.40	93.63	4.60	0.595	2.80	0.241	2.40	0.339	**1.40**	**0.083**	3.80	0.498
`covtype-7`	98.51	94.66	2.80	0.183	3.00	0.335	4.80	0.854	**1.00**	**0.000**	3.40	0.440
`diabetes`	84.28	81.87	3.60	0.785	2.00	0.293	2.60	0.220	**1.80**	**0.163**	5.00	1.477
`ionosphere`	83.20	73.90	**2.00**	0.650	2.60	0.681	3.40	1.409	2.60	**0.606**	4.40	1.682
average	N/A	N/A	2.88	0.378	2.95	0.387	3.16	0.557	**1.69**	**0.139**	4.32	0.874

Table 6.B.2: Benchmark results for tuning an SVM classifier with RBF kernel, using an optimization budget of 150 evaluations (best result per data set in bold, worst in gray). Results depict averages across 5 runs of the optimum (i.e., the best found solution across all optimizers), the third quantile (Q_3) of random search results (which indicates the difficulty of the optimization problem: low Q_3 vis-à-vis the optimum indicates the region of strong performance is small within the overall search space) and the relative rank and regret per optimizer. Performance and regret are measured in terms of cross-validated area under the ROC curve and shown in percent. Relative ranks indicate non-parametric global performance within the pool of optimizers (lower is better, the best optimizer has rank 1).

			Optunity		Hyperopt		SMAC		BayesOpt		random search	
data set	optimum	Q_3	rank	regret	rank	regret	rank	regret	rank	regret	rank	regret
digits-0	96.68	95.41	2.40	0.065	3.40	0.110	2.40	0.157	**1.80**	**0.043**	5.00	0.391
digits-1	91.26	86.48	3.20	0.371	**1.80**	0.182	3.20	0.477	2.00	**0.095**	4.80	0.726
digits-2	93.42	91.08	2.40	0.195	3.60	0.380	**1.40**	**0.071**	2.60	0.214	5.00	0.672
digits-3	90.87	88.56	2.20	0.176	3.40	0.236	3.20	0.285	**1.60**	**0.065**	4.60	0.444
digits-4	94.99	93.42	2.80	0.277	3.00	0.211	3.20	0.276	**1.60**	**0.037**	4.40	0.539
digits-5	93.32	90.60	**1.80**	0.278	4.20	0.544	2.80	0.460	**1.80**	**0.064**	4.40	0.586
digits-6	95.97	94.91	3.00	0.205	**1.80**	**0.072**	4.00	0.292	2.20	0.098	4.00	0.280
digits-7	95.30	93.45	**2.00**	**0.064**	3.40	0.209	3.00	0.213	2.40	0.095	4.20	0.516
digits-8	83.24	73.05	**1.80**	**0.220**	3.80	0.737	3.20	0.676	2.60	0.510	3.60	0.581
digits-9	88.00	84.48	**1.80**	**0.033**	3.20	0.447	3.20	0.441	**1.80**	0.206	5.00	0.901
covtype-1	82.75	77.31	2.80	0.220	3.60	0.630	2.20	0.239	**1.40**	**0.000**	5.00	1.864
covtype-2	82.15	73.55	**1.80**	**0.182**	2.60	0.452	3.60	1.356	2.00	0.248	5.00	2.768
covtype-3	97.97	94.12	2.00	0.074	2.80	0.129	3.80	0.178	**1.80**	**0.051**	4.60	0.261
covtype-4	99.78	98.13	2.80	0.119	3.20	0.022	3.60	0.060	**1.20**	**0.000**	4.20	0.084
covtype-5	96.91	89.55	3.40	0.620	2.80	0.463	3.20	0.440	**1.20**	**0.021**	4.40	0.810
covtype-6	97.47	92.72	3.40	0.318	2.80	0.142	3.00	0.332	**1.00**	**0.000**	4.80	0.581
covtype-7	98.56	94.07	2.60	0.163	3.40	0.245	3.20	0.318	**1.20**	**0.026**	4.60	0.499
diabetes	84.38	81.89	2.80	0.374	2.60	0.165	**1.80**	**0.027**	2.80	0.166	5.00	1.166
ionosphere	83.68	74.16	2.40	0.673	**2.00**	**0.390**	3.00	0.658	3.00	1.044	4.60	1.497
average	N/A	N/A	2.49	0.243	3.02	0.303	3.00	0.366	**1.89**	**0.157**	4.59	0.798

Chapter 7

Assessing Binary Classifiers Using Only Positive and Unlabeled Data

This chapter will be submitted to *ACM SIGKDD 2016* as:
Claesen, M., Davis, J., De Smet, F., & De Moor, B. (2015). **Assessing Binary Classifiers Using Only Positive and Unlabeled Data**.

Contributions Marc Claesen has derived the approach, implemented it and created examples. He took the lead in writing the initial draft and revisions.

Abstract

Assessing the performance of a learned model is a crucial part of machine learning. However, in some domains only positive and unlabeled examples are available, which prohibits the use of most standard evaluation metrics. We propose an approach to estimate any metric based on contingency tables using only positive and unlabeled data. Estimating these metrics is essentially reduced to estimating the fraction of (latent) positives in the unlabeled set, assuming known positives are a random sample of all positives. We provide theoretical bounds on the quality of our estimates, illustrate the importance of estimating the fraction of positives in the unlabeled set and demonstrate empirically that we are able to reliably estimate ROC and PR curves on real data.

7.1 Introduction

Model evaluation is a critical step in the learning process. Typically, evaluations either report summary metrics, such as accuracy, F1 score, or area under the receiver operator characteristic (ROC) curve or visually show a model's performance under different operating conditions by using ROC or precision-recall curves. All the aforementioned evaluation approaches require constructing contingency tables (also called confusion matrices), which show how a model's predicted labels relate to an example's ground truth label. Computing a contingency table requires labeled examples. However, for many problems only a few labeled examples and many unlabeled ones are available as acquiring labels can be time-consuming, costly, unreliable, and in some cases impossible.

The field semi-supervised learning [58] focuses on coping with partially labeled data. Positive and unlabeled (PU) learning is a special case of semi-supervised learning where each example's label is either positive or not known [166, 283, 82, 92, 229, 179, 66]. Both semi-supervised and PU learning tend to focus on developing learning algorithms that cope with partially labeled data during training as opposed to evaluating algorithms when the test set is partially labeled. What is less well studied is the effect of partially labeled data on evaluation. Currently, algorithms are evaluated assuming that the test data is fully labeled [111, 187, 60, 54, 59, 179, 66] and if the test data is only partially labeled, sometimes it is assumed that all unlabeled instances are negative when evaluating performance [178, 238, 230].

This paper describes how to incorporate the unlabeled data in the model evaluation process. We show how to compute contingency tables based on only positive and unlabeled examples where the unlabeled set contains both positive and negative examples, by looking at the ranking of examples produced by a model. Theoretically, we establish important relationships between contingency tables and rank distributions, which allow us to provide bounds on the false positive rate at each rank when the ranking contains examples whose ground truth label is unknown. Our findings have important implications for model selection as we show that naively assuming that all unlabeled examples are negative, as is sometimes done in PU learning, could lead to selecting the wrong model. We demonstrate the efficacy of our approach by estimating ROC and PR curves from real-world data.

7.2 Background and definitions

We first review the relevant background on model evaluation and issues caused by partial labeling.

7.2.1 Rank distributions and contingency tables

We focus on binary decision problems, where the goal is to classify examples as either positive or negative. Most learned models (e.g., SVM, logistic regression, naive Bayes) predict a numeric score for each example where higher values imply higher confidence that the instance belongs to the positive class. Typically, a *ranking* $\mathcal{R}$ is produced by sorting examples in descending order by their numeric score such that confident positive predictions are ranked close to the top of $\mathcal{R}$.[1]

Within a ranking $\mathcal{R}$, we treat $\mathcal{P} \subset \mathcal{R}$ as the subset of examples with positive labels, $\bar{\mathcal{P}} = \mathcal{R} - \mathcal{P}$ as the subset of examples with negative labels, and let $\text{rank}(\mathcal{R}, x)$ denote the rank of an instance x in $\mathcal{R}$. Given a cutoff rank r, predictions can be made by assigning the positive class to the r top ranked instances and the negative class to the rest. This decision rule yields a *true positive rate (TPR)*, which is the fraction of positive examples that are correctly labeled as positive, and *false positive rate (FPR)*, which is the fraction of negative examples that are incorrectly labeled as positive:

$$\begin{aligned}\text{TPR}(\mathcal{P}, r) &= \Pr(\text{rank}(\mathcal{R}, x) \leq r \mid x \in \mathcal{P}), \\ &= |\{\ x \in \mathcal{P}\ :\ \text{rank}(\mathcal{R}, x) \leq r\}|\ /\ |\mathcal{P}|, \end{aligned} \tag{7.1}$$

$$\text{FPR}(\mathcal{P}, r) = \Pr(\text{rank}(\mathcal{R}, \bar{x}) \leq r \mid \bar{x} \in \bar{\mathcal{P}}) = \text{TPR}(\mathcal{R} - \mathcal{P}, r). \tag{7.2}$$

Given the number of positives $|\mathcal{P}|$ and negatives $|\mathcal{R} - \mathcal{P}|$, the contingency table for a rank r is:

$$\text{TP}(\mathcal{P}, r) = \text{TPR}(\mathcal{P}, r) \cdot |\mathcal{P}|, \tag{7.3}$$

$$\text{FP}(\mathcal{P}, r) = \text{FPR}(\mathcal{P}, r) \cdot |\mathcal{R} - \mathcal{P}|,$$

$$\text{FN}(\mathcal{P}, r) = |\mathcal{P}| - \text{TP}(\mathcal{P}, r), \tag{7.4}$$

$$\text{TN}(\mathcal{P}, r) = |\mathcal{R} - \mathcal{P}| - \text{FP}(\mathcal{P}, r). \tag{7.5}$$

The rank distribution of a set of instances $\mathcal{P}$ within an overall ranking $\mathcal{R}$ is defined as the distribution of their corresponding ranks within $\mathcal{R}$. The rank cumulative distribution function (CDF) of a set of instances $\mathcal{P}$ is defined as the (empirical) CDF of their ranks, i.e. $\forall\ r \in \{1, \ldots, |\mathcal{R}|\}$:

$$\text{F}(\mathcal{P}, r) = \Pr(\text{rank}(\mathcal{R}, x) \leq r \mid x \in \mathcal{P}). \tag{7.6}$$

[1] Which means a low value for rank in this work, though this is often referred to as *highly ranked* in literature.

The concept of rank CDF is illustrated in Figure 7.1. Note that $\mathrm{F}(\mathcal{P}, r) \equiv \mathrm{TPR}(\mathcal{P}, r)$ (Equations (7.1) and (7.6)), that is, the rank CDF of the set of positives $\mathcal{P}$ at rank r in an overall ranking $\mathcal{R}$ can be interpreted directly as a true positive rate, when labeling the r top ranked instances as positive.

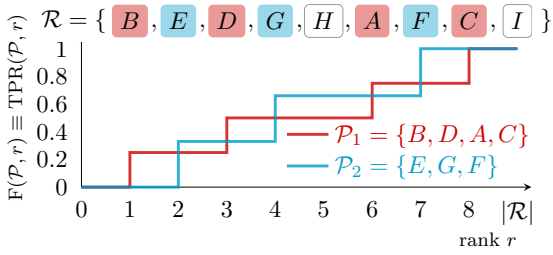


Figure 7.1: Rank CDF of two sets of positives $\mathcal{P}_1 = \{B, D, A, C\}$ and $\mathcal{P}_2 = \{E, G, F\}$ within an overall ranking $\mathcal{R} = \{B, E, D, G, H, A, F, C, I\}$, with $|\mathcal{P}_1| = 4$ and $|\mathcal{P}_2| = 3$. In practice $\mathcal{R}$ is obtained by sorting the data according to classifier score. The rank CDF of a set $\mathcal{S} \subseteq \mathcal{R}$ is based on the positions of elements of $\mathcal{S}$ in $\mathcal{R}$.

We use two convenience functions to partition sets of ranks:

$$\mathrm{head}(X, r) = \{\ \mathrm{rank}(\mathcal{R}, x) \leq r \ :\ x \in X\ \},$$

$$\mathrm{tail}(X, r) = \{\ \mathrm{rank}(\mathcal{R}, x) > r \ :\ x \in X\ \},$$

such that $\mathrm{head}(X, r) \cup \mathrm{tail}(X, r) = X$ and $|\,\mathrm{head}(X, r)| = \mathrm{F}(X, r) \cdot |X|$.

7.2.2 ROC and PR curves

Receiver operator characteristic (ROC) curves are used extensively for evaluating classifiers in machine learning [48] as they illustrate the performance of a model over its entire operating range. ROC curves depict how a model's true positive rate (shown on the y-axis) varies as a function of its false positive rate (shown on the x-axis). Each cutoff rank $r \in \{1, \ldots, |\mathcal{R}|\}$ corresponds to a single point (i.e., (FPR, TPR) pair) in ROC space (Eqs. (7.1) and (7.2)). An (empirical) ROC curve for a ranking $\mathcal{R}$ and set of positives $\mathcal{P} \subset \mathcal{R}$ is constructed by computing $\mathrm{FPR}(\mathcal{P}, r)$ and $\mathrm{TPR}(\mathcal{P}, r)$ at each rank r and interpolating by drawing a straight line between points corresponding to consecutive ranks. The area under an ROC curve (AUROC) is a commonly used summary statistic, typically ranging between 0.5 (random model) and 1 (perfect model). AUROC is a popular criterion in model selection and is often used as the optimization objective in hyperparameter search [48].

Precision-Recall (PR) curves [79] are an alternative to ROC curves that show how a model's precision (y-axis) varies as a function of recall (x-axis). Recall is equivalent to TPR and precision is the fraction of examples classified as positive that are truly positive ($\mathrm{TP}/(\mathrm{TP}+\mathrm{FP})$). PR curves are widely used when there is a skew in the class distributions [78, 66].

7.2.3 Evaluation with partially labeled data

In the partial labeling setting, $\mathcal{R}$ consists of disjoint sets of known positives $\mathcal{P}_L$, known negatives $\mathcal{N}_L$ and unlabeled instances $\mathcal{U}$. The unlabeled set $\mathcal{U}$ consists of latent positives $\mathcal{P}_U$ and latent negatives. The fraction of latent positives in the unlabeled set plays a crucial role in our work, denoted by β:

$$\beta = \Pr(x \in \mathcal{P}_U \mid x \in \mathcal{U}) = |\mathcal{P}_U| \;/\; |\mathcal{U}|. \tag{7.7}$$

Note that computing contingency tables requires fully labeled data. If only a few labeled instances of both classes are available, they can be used to compute rough estimates of predictive performance. However, if only positive labels are available, even a rough approximation of common metrics cannot be estimated directly as we do not know which unlabeled examples are positives and which are negative. A common approach to evaluate models in a PU learning context is to treat the full unlabeled set as negative [178, 238, 230], though we will show that this may lead to spurious results.

7.3 Relationship between the rank CDF of positives and contingency tables

The challenge of incorporating unlabeled data into an evaluation metric is knowing which unlabeled examples are latent positives and which are latent negatives. Our insight is that, if the known positives are sampled completely at random from all positives, the rank distribution of latent positives should follow the rank distribution of known positives. Thus if we know β, which is needed to compute the expected number of latent positives within the unlabeled data, this provides an avenue for building contingency tables that incorporate the unlabeled data. To do so, we first prove relationships between rank CDFs of sets of positives within an overall ranking at a given rank r and the corresponding contingency tables. Then, we use these relationships to prove bounds on the FPR at a given rank r when the ranking includes unlabeled examples, some of which are latent positives.

7.3.1 Rank distributions and contingency tables based on subsets of positives within a ranking

We begin by considering given sets of positives within an overall ranking.

Lemma 1. *Given a rank r and two disjoint subsets of positives $\mathcal{P}_1$ and $\mathcal{P}_2$ within an overall ranking $\mathcal{R}$. If $|\mathcal{P}_1| = |\mathcal{P}_2|$ and $\mathrm{TPR}(\mathcal{P}_1, r) > \mathrm{TPR}(\mathcal{P}_2, r)$, then $\mathrm{FPR}(\mathcal{P}_1, r) < \mathrm{FPR}(\mathcal{P}_2, r)$ (see Figure 7.1). If $\mathrm{TPR}(\mathcal{P}_1, r) = \mathrm{TPR}(\mathcal{P}_2, r)$, then $\mathrm{FPR}(\mathcal{P}_1, r) = \mathrm{FPR}(\mathcal{P}_2, r)$.*

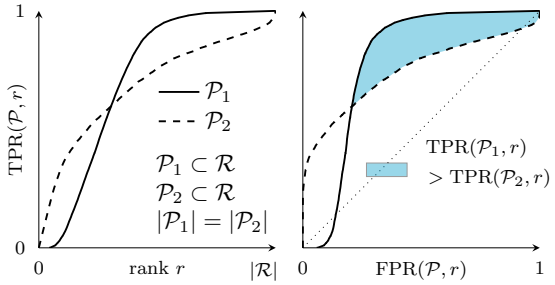


Figure 7.1: Illustration of Lemma 1: higher TPR at a given rank r implies lower FPR at r for two positive sets of the same size.

***Proof**: The numerator of FPR is the number of false positives, this is the number of positive predictions minus the number of true positives. Via Equations* (7.2) *and* (7.3)*, this is r and $\mathrm{TPR}(\mathcal{P}, r) \cdot |\mathcal{P}|$, respectively:*

$$\mathrm{FPR}(\mathcal{P}, r) = \frac{r - \mathrm{TPR}(\mathcal{P}, r) \cdot |\mathcal{P}|}{|\mathcal{R}| - |\mathcal{P}|}. \tag{7.8}$$

Since $|\mathcal{P}_1| = |\mathcal{P}_2|$, the denominators of $\mathrm{FPR}(\mathcal{P}_1, r)$ and $\mathrm{FPR}(\mathcal{P}_2, r)$ are equal, so $\mathrm{TPR}(\mathcal{P}_1, r) > \mathrm{TPR}(\mathcal{P}_2, r) \leftrightarrow \mathrm{FPR}(\mathcal{P}_1, r) < \mathrm{FPR}(\mathcal{P}_2, r)$.

$\mathrm{TPR}(\mathcal{P}_1, r) = \mathrm{TPR}(\mathcal{P}_2, r)$ trivially implies $\mathrm{FPR}(\mathcal{P}_1, r) = \mathrm{FPR}(\mathcal{P}_2, r)$ via Equation 7.8, as all terms in the right hand side are equal for $\mathcal{P}_1$ and $\mathcal{P}_2$. ■

Lemma 2. *Given a rank r and two disjoint sets of positives $\mathcal{P}_1$ and $\mathcal{P}_2$ in a ranking $\mathcal{R}$ and $\mathcal{P}_\Omega = \mathcal{P}_1 \cup \mathcal{P}_2$. If $\mathrm{TPR}(\mathcal{P}_1, r) = t_1 < \mathrm{TPR}(\mathcal{P}_2, r) = t_2$ then $\mathrm{TPR}(\mathcal{P}_1, r) < \mathrm{TPR}(\mathcal{P}_\Omega, r) < \mathrm{TPR}(\mathcal{P}_2, r)$ (see Figure 7.2).*

***Proof**: write $\mathrm{TPR}(\mathcal{P}_\Omega, r)$ in terms of t_1 and t_2:*

$$\mathrm{TPR}(\mathcal{P}_\Omega, r) = \frac{t_1 \cdot |\mathcal{P}_1| + t_2 \cdot |\mathcal{P}_2|}{|\mathcal{P}_1| + |\mathcal{P}_2|}. \tag{7.9}$$

since $t_1 < t_2$, we get $t_1 < \mathrm{TPR}(\mathcal{P}_\Omega, r) < t_2$. ■

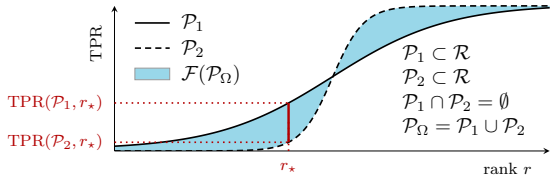


Figure 7.2: Illustration of Lemma 2: $\mathcal{F}(\cdot)$ denotes feasible region. The rank distribution of the union $\mathcal{P}_\Omega$ of two sets of positives $\mathcal{P}_1$ and $\mathcal{P}_2$ lies between their respective rank distributions.

Corollary 1. *Given a rank r and three sets of positives $\mathcal{P}_A$, $\mathcal{P}_B$ and $\mathcal{P}_C$ within a ranking $\mathcal{R}$ such that $\mathcal{P}_A \cap \mathcal{P}_B = \emptyset$ and $\mathcal{P}_A \cap \mathcal{P}_C = \emptyset$ and $|\mathcal{P}_B| = |\mathcal{P}_C|$, then*

$$\mathrm{TPR}(\mathcal{P}_B, r) = t_B < \mathrm{TPR}(\mathcal{P}_C, r) = t_C \quad \leftrightarrow \quad \mathrm{TPR}(\mathcal{P}_A \cup \mathcal{P}_B, r) < \mathrm{TPR}(\mathcal{P}_A \cup \mathcal{P}_C, r).$$

***Proof**: all terms are equal for $\mathrm{TPR}(\mathcal{P}_A \cup \mathcal{P}_B, r)$ and $\mathrm{TPR}(\mathcal{P}_A \cup \mathcal{P}_C, r)$ except $t_B < t_C$ in Eq. (7.9).* ■

7.3.2 Contingency tables based on partially labeled data

Lemmas 1 and 2 describe relationships between rank distributions and contingency tables of different (but known) sets of positives within an overall ranking. We now show how to construct contingency tables corresponding to the greatest-lower and least-upper bound of the FPR at a given rank, accounting for the unknown set of latent positive example from partially labeled data, given β.

Theorem 1. *Given an overall ranking $\mathcal{R}$ consisting of disjoint sets of known positives $\mathcal{P}_L$, known negatives $\mathcal{N}_L$ and unlabeled instances $\mathcal{U}$, where $\mathcal{U}$ contains an unknown set of latent positives $\mathcal{P}_U \subset \mathcal{U}$ of known size $|\mathcal{P}_U| = \beta \cdot |\mathcal{U}|$. Given a rank r and an upper bound $\mathcal{T}_{ub}(r) \geq \mathrm{TPR}(\mathcal{P}_U, r)$, a tight lower bound on $\mathrm{FPR}(\mathcal{P}_\Omega, r)$ with $\mathcal{P}_\Omega = \mathcal{P}_L \cup \mathcal{P}_U$ can be found without explicitly identifying $\mathcal{P}_U$.*

***Proof**: Step 1: assign a set of surrogate positives $\mathcal{P}_U^\star$:*[2]

$$\mathcal{P}_U^\star = \underset{\mathcal{P}_U^* \subset\, \mathcal{U}}{\arg\min}\ \mathrm{TPR}(\mathcal{P}_U^*, r), \tag{7.10}$$

$$\text{subject to}\ \ \mathrm{TPR}(\mathcal{P}_U^*, r) \geq \mathcal{T}_{ub}(r)\ \text{ and }\ |\mathcal{P}_U^*| = \beta \cdot |\mathcal{U}|,$$

then $\mathrm{TPR}(\mathcal{P}_U^\star, r) \geq \mathrm{TPR}(\mathcal{P}_U, r)$ by construction. If $|\,\mathrm{head}(\mathcal{U}, r)| < \beta \mathcal{T}_{ub}(r) \cdot |\mathcal{U}|$, then no $\mathcal{P}_U^\star$ exists that satisfies the constraint $\mathrm{TPR}(\mathcal{P}_U^\star, r) \geq \mathcal{T}_{ub}(r)$ in

[2] A surrogate positive is an example that we treat as if its ground truth label is positive (even though in reality its ground truth label is unknown) when constructing a contingency table.

Equation (7.10).[3] *In this case, treat all instances in* $\text{head}(\mathcal{U}, r)$ *as surrogate positive, which trivially implies* $\text{TPR}(\mathcal{P}_U^\star, r) \geq \text{TPR}(\mathcal{P}_U, r)$.

Step 2: define $\mathcal{P}_\Omega^\star = \mathcal{P}_L \cup \mathcal{P}_U^\star$. *Using Corollary 1 yields* $\text{TPR}(\mathcal{P}_\Omega^\star, r) \geq \text{TPR}(\mathcal{P}_\Omega, r)$. *Since* $|\mathcal{P}_\Omega^\star| = |\mathcal{P}_\Omega|$, *using Lemma 1 yields the lower bound on FPR, i.e.,* $\text{FPR}(\mathcal{P}_\Omega^\star, r) \leq \text{FPR}(\mathcal{P}_\Omega, r)$. ■

Applying Theorem 1 yields a nontrivial lower bound on $\text{FPR}(\mathcal{P}_\Omega, r)$. In Lemma 3 we prove that $\text{FPR}(\mathcal{P}_\Omega^\star, r)$ is the greatest achievable lower bound based on a given $\mathcal{U} \subset \mathcal{R}$.

Lemma 3. *Minimizing* $\text{TPR}(\mathcal{P}_U^\star, r)$ *in Equation* (7.10) *of Theorem 1 ensures* $\text{FPR}(\mathcal{P}_\Omega^\star, r)$ *is the greatest achievable lower bound on* $\text{FPR}(\mathcal{P}_\Omega, r)$ *given* β, $\mathcal{T}_{ub}(r)$, $\mathcal{R}$ *and* $\mathcal{U}$.

Proof *(by contradiction): suppose another set of surrogate positives* $\mathcal{P}_U^\bullet \subset \mathcal{U}$ *exists with* $|\mathcal{P}_U^\bullet| = \beta \cdot |\mathcal{U}|$, *such that* $\mathcal{P}_U^\bullet \neq \mathcal{P}_U^\star$, *and* $\text{TPR}(\mathcal{P}_U^\bullet, r) \geq \mathcal{T}_{ub}(r)$ *and for* $\mathcal{P}_\Omega^\bullet = \mathcal{P}_L \cup \mathcal{P}_U^\bullet$*:*

$$\text{FPR}(\mathcal{P}_\Omega^\star, r) < \text{FPR}(\mathcal{P}_\Omega^\bullet, r) \leq \text{FPR}(\mathcal{P}_\Omega, r).$$

Via Corollary 1 this implies $\text{TPR}(\mathcal{P}_U^\bullet, r) < \text{TPR}(\mathcal{P}_U^\star, r)$, *which contradicts the definition of* $\mathcal{P}_U^\star$ *(Eq.* (7.10)*).* ■

Due to its symmetry, Theorem 1 can also be used to obtain the least achievable upper bound of $\text{FPR}(\mathcal{P}_\Omega, r)$ given a ranking $\mathcal{R}$ and a bound $\mathcal{T}_{lb}(r) \leq \text{TPR}(\mathcal{P}_U^\star, r)$ by assigning $\mathcal{P}_U^\star$ such that:

$$\mathcal{P}_U^\star = \underset{\mathcal{P}_U^* \subset\, \mathcal{U}}{\arg\max}\ \text{TPR}(\mathcal{P}_U^*, r), \tag{7.11}$$

$$\text{subject to}\ \ \text{TPR}(\mathcal{P}_U^*, r) \leq \mathcal{T}_{lb}(r) \text{ and } |\mathcal{P}_U^*| = \beta \cdot |\mathcal{U}|.$$

7.4 Efficiently computing the bounds

We now describe how to use Theorem 1 and Lemma 3 to compute the contingency tables corresponding to the greatest lower and least upper bound on $\text{FPR}(\mathcal{P}_\Omega, r)$ from a finite sample. First, we explain how to compute contingency tables efficiently via Theorem 1. Second, we propose how to obtain the bounds on rank CDF ($\mathcal{T}_{lb}(r)$ and $\mathcal{T}_{ub}(r)$) that are needed to build the contingency table.

[3] An infeasibility implies that $\mathcal{T}_{ub}(r)$ and/or β are too high.

7.4.1 Computing the contingency table with greatest-lower bound on FPR at given rank r

Given β, $\mathcal{R}$ and the sets $\mathcal{P}_L$, $\mathcal{N}_L$, and $\mathcal{U}$, Theorem 1 enables computing contingency tables corresponding to the least upper and greatest lower bound on FPR at a given cutoff rank r. We focus on building the contingency table corresponding to the lower bound on the FPR, the other is analogous.

We decompose the computation to consider the labeled and unlabeled instances separately:

$$\begin{bmatrix} \mathrm{TP}^r_\Omega & \mathrm{FP}^r_\Omega \\ \mathrm{FN}^r_\Omega & \mathrm{TN}^r_\Omega \end{bmatrix} = \begin{bmatrix} \mathrm{TP}^r_L = |\operatorname{head}(\mathcal{P}_L, r)| & \mathrm{FP}^r_L = |\operatorname{head}(\mathcal{N}_L, r)| \\ \mathrm{FN}^r_L = |\operatorname{tail}(\mathcal{P}_L, r)| & \mathrm{TN}^r_L = |\operatorname{tail}(\mathcal{N}_L, r)| \end{bmatrix} + \begin{bmatrix} \mathrm{TP}^r_U & \mathrm{FP}^r_U \\ \mathrm{FN}^r_U & \mathrm{TN}^r_U \end{bmatrix}.$$

Given that at rank r we can directly compute partial contingency tables for the labeled data based on $\mathcal{R}$, $\mathcal{P}_L$ and $\mathcal{N}_L$, we focus on computing the contingency table for the unlabeled instances.

Given $\mathcal{T}_{ub}(r)$, we can use Theorem 1 to determine the values in the contingency table for the unlabeled instances for the greatest lower bound on FPR. Doing so requires inferring a set of surrogate positives $\mathcal{P}^\star_U$ from the unlabeled data, which must be a solution to Equation (7.10). This requires θ surrogate positives in $\operatorname{head}(\mathcal{P}^\star_U, r)$ and the rest in $\operatorname{tail}(\mathcal{P}^\star_U, r)$, where θ is defined as:

$$\theta = \left\lceil \mathcal{T}_{ub}(r) \cdot |\mathcal{P}^\star_U| \right\rceil = \left\lceil \mathcal{T}_{ub}(r) \cdot \beta \cdot |\mathcal{U}| \right\rceil, \tag{7.12}$$

By rounding up in Equation (7.12), we ensure that $\mathrm{TPR}(\mathcal{P}^\star_U, r) \geq \mathcal{T}_{ub}(r)$ as required by Theorem 1.

In practice, two corner cases must be considered. One is if $|\operatorname{head}(\mathcal{U}, r)| < \theta$, then it is impossible to assign θ surrogates below rank r in $\mathcal{U}$. In this case, all of $\operatorname{head}(\mathcal{U}, r)$ is assigned as surrogate positives and the remaining surrogates are in $\operatorname{tail}(\mathcal{U}, r)$ (as discussed in Theorem 1). Two is if $|\operatorname{tail}(\mathcal{U}, r)| < |\mathcal{P}^\star_U| - \theta$, in which case all of $\operatorname{tail}(\mathcal{U}, r)$ is labeled positive and the remaining surrogate positives inevitably end up in $\operatorname{head}(\mathcal{U}, r)$. Hence, any set of surrogate positives $\mathcal{P}^\star_U$ that meets the following criteria solves Equation (7.10) and thus yields a valid bound:

$$\begin{aligned} |\mathcal{P}^\star_U| &= \beta \cdot |\mathcal{U}|, \\ |\operatorname{head}(\mathcal{P}^\star_U, r)| &= \begin{cases} \min\left(|\operatorname{head}(\mathcal{U}, r)|,\ \theta\right) & \text{if } |\mathcal{P}^\star_U| - \theta \leq |\operatorname{tail}(\mathcal{U}, r)|, \\ |\mathcal{P}^\star_U| - |\operatorname{tail}(\mathcal{U}, r)| & \text{if } |\mathcal{P}^\star_U| - \theta > |\operatorname{tail}(\mathcal{U}, r)|. \end{cases} \end{aligned} \tag{7.13}$$

Given a set of surrogate positives $\mathcal{P}_U^\star$, the partial contingency table of interest becomes:

$$\begin{bmatrix} \mathrm{TP}_U^r & \mathrm{FP}_U^r \\ \mathrm{FN}_U^r & \mathrm{TN}_U^r \end{bmatrix} = \begin{bmatrix} |\operatorname{head}(\mathcal{P}_U^\star, r)| & |\operatorname{head}(\mathcal{U} - \mathcal{P}_U^\star, r)| \\ |\operatorname{tail}(\mathcal{P}_U^\star, r)| & |\operatorname{tail}(\mathcal{U} - \mathcal{P}_U^\star, r)| \end{bmatrix}, \tag{7.14}$$

where $\mathcal{U} - \mathcal{P}_U^\star$ is the set of surrogate negatives and $|\mathcal{P}_U^\star|$ and $|\operatorname{head}(\mathcal{P}_U^\star, r)|$ are known via Eq. 7.13.

Note that computing the partial contingency table for the unlabeled data can be done very efficiently since it only requires set sizes as shown in Equation 7.14, without explicitly partitioning the unlabeled set $\mathcal{U}$. That is, we do not need to know which examples are in $\operatorname{head}(\mathcal{P}_U^\star, r)$, $\operatorname{tail}(\mathcal{P}_U^\star, r)$, $\operatorname{head}(\mathcal{U} - \mathcal{P}_U^\star, r)$ and $\operatorname{tail}(\mathcal{U} - \mathcal{P}_U^\star, r)$, we just need to know the number of examples each set contains.

The contingency table with least upper bound on $\mathrm{FPR}(\mathcal{P}_U, r)$ is obtained by replacing Eq. (7.12) by:

$$\theta = \left\lfloor \mathcal{T}_{lb}(r) \cdot |\mathcal{P}_U^\star| \right\rfloor = \left\lfloor \mathcal{T}_{lb}(r) \cdot \beta \cdot |\mathcal{U}| \right\rfloor. \tag{7.15}$$

7.4.2 Bounds on the rank distribution of $\mathcal{P}_U$

Applying Theorem 1 to build a contingency table at rank r requires a bound $\mathcal{T}_{ub}(r) \geq \mathrm{TPR}(\mathcal{P}_U, r)$ for estimating a lower bound on the FPR and a bound $\mathcal{T}_{lb}(r) \leq \mathrm{TPR}(\mathcal{P}_U, r)$ for estimating an upper bound on the FPR. To compute these bounds, we assume known and latent positives have similar rank distributions. This holds when known positives $\mathcal{P}_L$ are selected completely at random from all positives $\mathcal{P}_\Omega$, but is violated if the process of selecting examples for labeling is biased [60].

$\mathrm{TPR}(\mathcal{P}_\Omega, r)$ is estimated via the empirical CDF of $\mathcal{P}_L$, which only approximates the true CDF. To acccount for uncertainty, we construct confidence intervals (CIs) for the rank CDF. Our assumption implies that a CI of the CDF based on $\mathcal{P}_L$ is also a CI of the CDF of $\mathcal{P}_U$. A CI boundary is treated as a function mapping rank r to the estimated bound on the CDF. $\mathcal{T}_{lb}$ and $\mathcal{T}_{ub}$ denote these bounds:

$$0 \leq \mathcal{T}_{lb}(r) \leq \mathrm{TPR}(\mathcal{P}_L, r), \mathrm{TPR}(\mathcal{P}_U, r), \mathrm{TPR}(\mathcal{P}_\Omega, r) \leq \mathcal{T}_{ub}(r) \leq 1, \ \forall\, r. \tag{7.16}$$

We formalize the bounds of the CI of the CDF as functions of rank because an underlying set with that rank distribution does not necessarily exist in the overall ranking $\mathcal{R}$.

The confidence band on rank CDF can be computed based on the known positives in several ways. We use a standard bootstrap approach [89] in our

experiments. Having many known positives yields a tight confidence band on rank CDF, which then translates to tight bounds on performance metrics.

7.5 Constructing ROC and PR curve estimates

Next, we describe how to estimate bounds on the true ROC and PR curves. Though we focus on these two criteria, our approach can be used to estimate any metric based on contingency tables.

ROC curves Given a ranking, instead of constructing a single ROC curve, our approach computes two curves: one corresponding to the upper bound and one corresponding to the lower bound on the CI on rank CDF of known positives $\mathcal{P}_L$, using the methodology outlined in Section 4 to compute two contingency tables for each rank r, corresponding to the greatest lower and least upper bound on $\text{FPR}(\mathcal{P}_\Omega, r)$. The set of contingency tables corresponding to greatest lower bounds on FPR at each rank form an upper bound on the ROC curve of all positives $\mathcal{P}_\Omega$, whereas the set of contingency tables corresponding to the least upper bound on FPR form a lower bound on the ROC curve of $\mathcal{P}_\Omega$.

It is important to understand how these estimates correspond to bounds in ROC space. By computing θ as in Equation (7.12) to obtain the greatest lower bound on $\text{FPR}(\mathcal{P}_U, r)$, the corresponding TPR is higher than $\text{TPR}(\mathcal{P}_U, r)$. As such, the upper bound on the ROC curve is shifted upwards and to the left. Conversely, the lower bound on the ROC curve (based on the least upper bound on FPR at each rank, i.e. θ as in Equation (7.15)) is shifted downward and to the right. This implies that the upper bound on the ROC curve completely dominates the curve of $\mathcal{P}_\Omega$ and the lower bound is completely dominated by the curve of $\mathcal{P}_\Omega$, provided that $\mathcal{T}_{lb}(r) \leq \text{TPR}(\mathcal{P}_U, r) \leq \mathcal{T}_{ub}(r),\ \forall r \in \{1, \ldots, |\mathcal{R}|\}$.

Convergence properties The convergence properties of our bounds are contingent on those of (a CI on) the empirical CDF: via the strong law of large numbers the empirical CDF $\hat{F}_n(x)$ is a consistent pointwise estimator of the true CDF $F(x)$, converging uniformly for increasing n [265].

Figure 7.2 shows the convergence of the bounds on area under the curve for the estimated lower and upper bound of the ROC curve for increasing amounts of known positives in simulated rankings. The range of bounds depends on the width of the CI on rank CDF, which in turn depends on the number of known positives (higher is better) and the size of the total data set (lower is better).

PR curves Given the contingency tables used to generate the least upper bound and greatest lower bound ROC curves, it is straightforward to construct

the corresponding bounds in PR space. Each contingency table contains all the required information for generating a point in PR space.

A key result relating ROC and PR curves is that one curve dominates another in ROC space if and only if it also dominates in PR space [79]. Given this result, mapping the bounds we obtain for ROC curves to PR space directly yields (tight) bounds on the corresponding true PR curve. Since the upper bound in ROC space completely dominates the true curve, and the lower bound in ROC space is completely dominated by it, the same holds for the bounds on PR curves.

7.6 Discussion and Recommendations

Next, we discuss several issues related to using our approach in practice.

7.6.1 Determining $\hat{\beta}$ and its effect

Our approach requires having an estimate $\hat{\beta}$ of β. There are many problems where β is known from domain knowledge (e.g., calculated and published based on a data source you do not have access to), but explicit negatives are scarce or unavailable in the data under analysis. A real-world example where this is true is the task of predicting whether someone has diabetes from health insurance data (cfr. Chapter 8). Some individuals are coded as having diabetes, but many diabetics are undiagnosed and hence it is wrong to assume that all unlabeled patients do not have diabetes. However, the incidence rate of diabetes is known and published in the medical literature. This type of situation characterizes many medical problems. If β is not known from domain knowledge, then it could be estimated from data [92, 229, 224].

In either case, if $\hat{\beta}$ is not exact, the conditions of Lemma 1 are potentially violated where it is used within Theorem 1. The effects of set size on FPR is characterized in Lemma 4, which will help us understand the effect of over or under estimating β.

Lemma 4. *Given two sets of positive labels $\mathcal{P}_1$ and $\mathcal{P}_2$ within an overall ranking $\mathcal{R}$ and a rank r, such that $\mathrm{TPR}(\mathcal{P}_1, r) = \mathrm{TPR}(\mathcal{P}_2, r) = t$ and $|\mathcal{P}_1| > |\mathcal{P}_2|$, then:*

$$(a) \quad \mathrm{FPR}(\mathcal{P}_2, r) < t \rightarrow \mathrm{FPR}(\mathcal{P}_1, r) < \mathrm{FPR}(\mathcal{P}_2, r),$$

$$(b) \quad \mathrm{FPR}(\mathcal{P}_2, r) > t \rightarrow \mathrm{FPR}(\mathcal{P}_1, r) > \mathrm{FPR}(\mathcal{P}_2, r).$$

(a) corresponds to a ranking and cutoff that is better than random (i.e. $\text{TPR}(\mathcal{P}, r) > \text{FPR}(\mathcal{P}, r)$*) whereas (b) corresponds to a ranking and cutoff that is worse than random.*

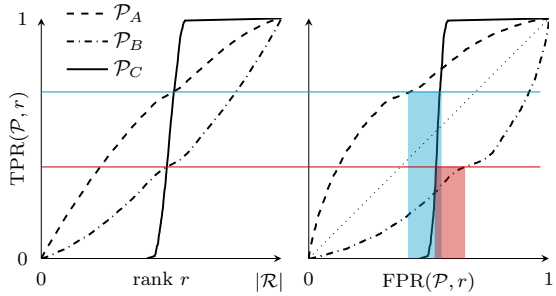


Figure 7.1: Illustration of Lemma 4, with $\mathcal{P}_A \subset \mathcal{R}$, $\mathcal{P}_B \subset \mathcal{R}$, $\mathcal{P}_C \subset \mathcal{R}$, $|\mathcal{P}_A| > |\mathcal{P}_C|$ and $|\mathcal{P}_B| > |\mathcal{P}_C|$. If two sets of positives $\mathcal{P}_1$ and $\mathcal{P}_2$ achieve a given TPR at the same rank r, e.g. $\text{TPR}(\mathcal{P}_1, r) = \text{TPR}(\mathcal{P}_2, r)$ and $|\mathcal{P}_1| > |\mathcal{P}_2|$ then $\text{FPR}(\mathcal{P}_1, r) < \text{FPR}(\mathcal{P}_2, r)$ if $\text{FPR}(\mathcal{P}_2, r) < \text{TPR}(\mathcal{P}_2, r)$ and otherwise $\text{FPR}(\mathcal{P}_1, r) > \text{FPR}(\mathcal{P}_2, r)$.

***Proof**: take the derivative of FPR to $|\mathcal{P}|$ while fixing r, based on Equation* (7.8)*:*

$$\frac{d\,\text{FPR}(\mathcal{P}, r)}{d|\mathcal{P}|} = \frac{r - t \cdot |\mathcal{R}|}{(|\mathcal{R}| - |\mathcal{P}|)^2},$$

$$= \frac{r - t \cdot |\mathcal{P}| - t \cdot |\mathcal{R} - \mathcal{P}|}{(|\mathcal{R}| - |\mathcal{P}|)^2}. \tag{7.17}$$

$r - t \cdot |\mathcal{P}|$ is the number of negatives in the top ranking (false positives) and $t \cdot |\mathcal{R} - \mathcal{P}|$ is the number of false positives at $\text{FPR} = t$*. The derivative is negative if the* FPR *is below t and vice versa, therefore if the ranking is better than random (*$\text{TPR} = t > \text{FPR}$*), increasing $|\mathcal{P}|$ leads to a lower* FPR *at rank r and vice versa.* ■

Lemma 4 has a large practical impact. If the ranking of $\mathcal{P}_L$ is better than random, then over and under estimating $\hat{\beta}$ is useful to obtain a (loose) upper/lower bound on performance curves, respectively. In other words, given bounds or a CI on β, that is $\hat{\beta}_{lo} \leq \beta \leq \hat{\beta}_{up}$, we can use $\hat{\beta}_{lo}$ and $\hat{\beta}_{up}$ to estimate a lower and upper bound on the true ROC or PR curve. Bounds computed based on a CI for β constitute a CI for the performance metric (at the same confidence level), assuming the rank CDF of $\mathcal{P}_U$ is contained by the confidence band on the rank CDF. Tighter bounds on β translate directly to tighter bounds on performance estimates. Finally, treating the full unlabeled set as negative

results underestimates performance, since $\hat{\beta} = 0 < \beta$. The effect of varying $\hat{\beta}$ is shown in Figure 7.3.

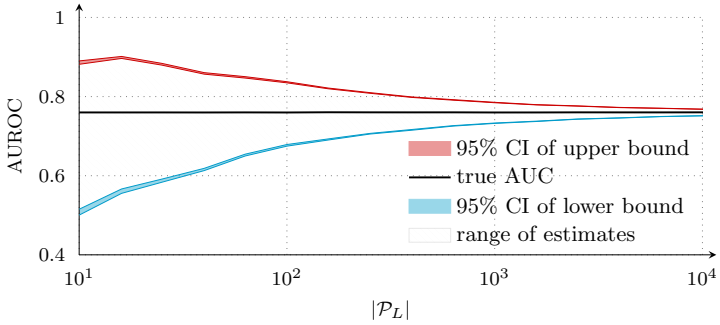


Figure 7.2: The effect of $|\mathcal{P}_L|$ on estimated AUC. Based on $|\mathcal{U}| = 100,000$, $\mathcal{N}_L = \emptyset$ and $\hat{\beta} = \beta = 0.2$. Bounds on rank CDF were obtained via bootstrap. The depicted confidence intervals are based on 200 repeated experiments.

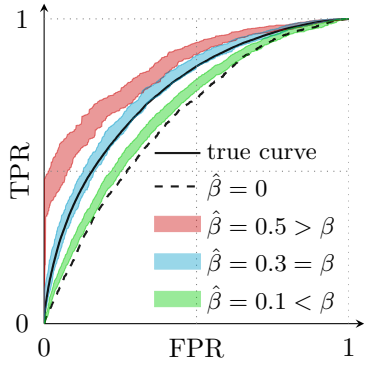


Figure 7.3: The effect of $\hat{\beta}$ on estimated ROC curves, based on 2,000 known positives, 100,000 unlabeled instances and $\beta = 0.3$.

7.6.2 Model selection

Often evaluation metrics are used to select the best model from a set of candidates. If model A's ROC (PR) curve dominates model B's ROC (PR) curve, then for all β model A is better than model B (leaving aside significance testing). However, in most cases one model does not dominate another model and there exists a point where the two curves cross. Surprisingly, the ordering in

terms of both AUROC and AUPR are dependent on $\hat{\beta}$ when this happens. This means that the ordering of models according to these metrics can switch when $\hat{\beta}$ changes. Figure 7.4 depicts an example that illustrates this. This demonstrates that $\hat{\beta}$ can play a crucial role in model selection. In the likely event that the curves cross, it is important to look at the range of possible values for $\hat{\beta}$ that represent different operating conditions when selecting among different models.

A more formal explanation of why this occurs can be made based on partial derivatives of each entry of the partial contingency table and TPR, FPR and precision based on unlabeled instances to $\hat{\beta}$:[4]

$$\frac{\partial \operatorname{TPR}_U^r}{\partial \hat{\beta}} = 0, \tag{7.18}$$

$$\frac{\partial \operatorname{FPR}_U^r}{\partial \hat{\beta}} = \frac{|\operatorname{head}(\mathcal{U}, r)| - \mathcal{T}(r) \cdot |\mathcal{U}|}{(1-\hat{\beta})^2}, \tag{7.19}$$

$$\frac{\partial \operatorname{PRE}_U^r}{\partial \hat{\beta}} = \frac{\mathcal{T}(r) \cdot |\mathcal{U}|}{|\operatorname{head}(\mathcal{U}, r)|} \geq 0. \tag{7.20}$$

The partial derivative of TPR is exactly 0 because our approach is based on rank CDFs (that is TPR at each rank). Interestingly, the partial derivatives of FPR and precision to $\hat{\beta}$ are dependent on the value of the rank CDF $\mathcal{T}(r)$ that is being used to infer surrogate positives. Since TPR is not a function of $\hat{\beta}$ and the partial derivatives of FPR/precision to $\hat{\beta}$ are functions of $\mathcal{T}(r)$, distinct segments of an ROC/PR curve are moved differently when $\hat{\beta}$ changes, inducing a non-uniform scaling of AUC across the TPR range. Such scaling potentially changes the ordering of models based on AUC.

7.6.3 Empirical quality of the estimates

We illustrate the quality of our estimated bounds on ROC and PR curves using a model trained in a PU learning setting [66] on the `covtype` data set [41]. The model was evaluated on a fully labeled test set of $20,000$ positive and $20,000$ negative examples. To estimate performance, we randomly selected 5% of positive examples to serve as our labeled set and treated all other examples as unlabeled, which yields $|\mathcal{P}_L| = 1,000$, $|\mathcal{U}| = 39,000$ and $\beta \approx 49\%$. We present ROC and PR curves with bounds for $\hat{\beta} = \beta$, $\hat{\beta} = 0$, and a confidence interval $\hat{\beta}_{lo} = 0.8\beta \leq \hat{\beta} \leq \hat{\beta}_{up} = 1.2\beta$. Finally, as we have the ground truth, we present true curves as a reference.[5]

[4] We made some simplifications, the details are described in Appendix 7.A.

[5] Python code to reproduce all results (and modify the configuration) is available at `https://github.com/claesenm/semisup-metrics`.

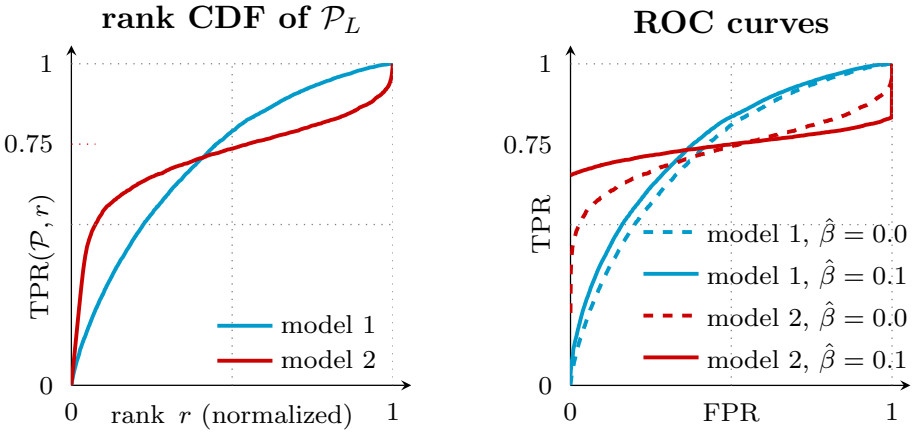


Figure 7.4: The effect of $\hat{\beta}$ on ROC curves. Setup: $|\mathcal{U}| = 45,000$, $|\mathcal{P}_L| = 5,000$.

Corresponding AUROC (best in bold):

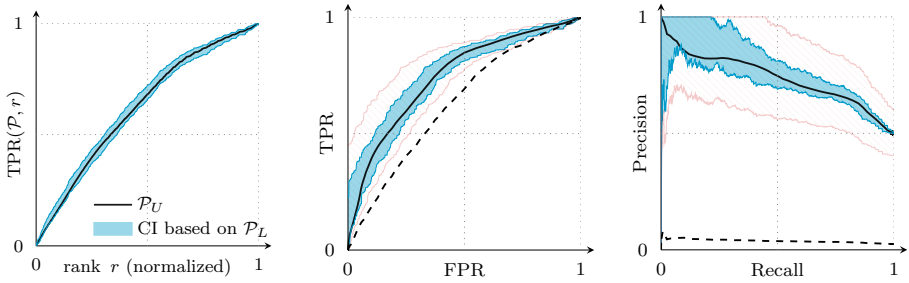
estimated $\hat{\beta}$	model 1	model 2
0.0	72.5%	**73.2**%
0.1	**75.5**%	74.7%

Figure 7.5 presents the rank CDF and estimated bounds on ROC and PR curves. Figure 7.5a shows the true rank CDF of $\mathcal{P}_U$ along with an estimated 95% CI on the rank CDF using the $\mathcal{P}_L$ via a standard bootstrap approach with 2,000 resamples. In this case, the CI contains the true rank CDF of latent positives.[6] Figures 7.5b and 7.5c show that the bounds closely approximate the true performance curves. The estimated bounds are wider in PR space than in ROC space, particularly at low recall. Note that estimated PR curves are sensitive to the estimation error in $\hat{\beta}$, as precision is directly affected by class balance, limiting their usefulness if only a rough estimate of β is available.

7.6.4 Relative importance of known negatives compared to known positives

As our approach can incorporate known negatives, a natural question is how their presence influences the estimates. In practice, a test set is of fixed size, so known negatives essentially reduce the size of the unlabeled subset, which in turn reduces the number of degrees of freedom in assigning surrogate positives.

[6]The rank CDF of $\mathcal{P}_U$ is unknown in practice, but assumed to be comparable to the rank CDF of $\mathcal{P}_L$.



(a) Rank CDF. (b) ROC curves. (c) PR curves.

Figure 7.5: Results for `covtype` showing rank CDF, ROC and PR curves, with $\beta \approx 49\%$. Performance curve legend:
—— true curve, - - - $\hat{\beta} = 0$, $\hat{\beta} = \beta$ and $0.8\beta \leq \hat{\beta} \leq 1.2\beta$.

Using the same setup as in Subsection 7.6.3, we varied the proportion of known positives and negatives and found known negatives provide some benefit, though this is small in practice. However, our approach can also be reversed given a large amount of negatives, that is flip known class labels, use $\bar{\beta} = 1 - \beta$ and adjust the resulting contingency tables accordingly, which can improve performance bounds. The benefits of known negatives are further discussed in Appendix 7.B.

7.7 Conclusion

We presented an approach to construct contingency tables corresponding to a lower and upper bound on FPR using only partially labeled, which enables computing many commonly used performance metrics in a semi-supervised setting. Our approach relies on knowing the fraction of latent positives in the unlabeled data, and we discussed its effect on determing the bounds and model selection. We have seen that our approach can yield good estimates in practice.

Appendix

7.A Effect of $\hat{\beta}$ on contingency table entries and common performance metrics

To study the effect of imprecise estimates of β, we start by computing partial derivatives of each entry of the partial contingency table based on unlabeled instances to $\hat{\beta}$ (see Section 7.4.1). Subsequently, we will compute partial derivatives of TPR, FPR and precision to $\hat{\beta}$ to describe the effect of estimating β on (area under) ROC and PR curves.

For ease of notation, we base all subsequent calculations on $\tilde{\theta} = \hat{\beta}\mathcal{T}(r) \cdot |\mathcal{U}| \approx \theta$ which ignores the discrete effect of rounding in the real definition of θ (Eq. 7.12). We additionally assume it is possible to assign the desired amount $\tilde{\theta}$ of surrogate positives in $\text{head}(\mathcal{U}, r)$, which holds for ranks r that are not too close to the top or bottom of $\mathcal{R}$, given reasonable values of $\hat{\beta}$ and CDF bounds $\mathcal{T}(r)$.[7] If this does not hold, that is when there is clipping in Eq. 7.13, then (small) changes in $\hat{\beta}$ do not affect TP_U^r and hence the partial derivatives of *all* entries in the contingency table to $\hat{\beta}$ are effectively 0.

[7] $\mathcal{T}(r)$ represents a bound on rank CDF, that is either $\mathcal{T}_{lb}(r)$ or $\mathcal{T}_{ub}(r)$ as used in the manuscript.

Given these simplifications, the partial contingency table based on unlabeled instances becomes:

$$\begin{aligned}
\mathrm{TP}_U^r &= \tilde{\theta} = \hat{\beta}\mathcal{T}(r) \cdot |\mathcal{U}| \\
\mathrm{FN}_U^r &= |\mathcal{P}_U^\star| - \mathrm{TP}_U^r = \hat{\beta} \cdot |\mathcal{U}| - \hat{\beta}\mathcal{T}(r) \cdot |\mathcal{U}| = \hat{\beta}\big(1 - \mathcal{T}(r)\big) \cdot |\mathcal{U}| \\
\mathrm{FP}_U^r &= |\operatorname{head}(\mathcal{U}, r)| - \mathrm{TP}_U^r = |\operatorname{head}(\mathcal{U}, r)| - \hat{\beta}\mathcal{T}(r) \cdot |\mathcal{U}|, \\
\mathrm{TN}_U^r &= |\mathcal{U}| - |\mathcal{P}_U^\star| - \mathrm{FP}_U^r = |\mathcal{U}| - \hat{\beta} \cdot |\mathcal{U}| - |\operatorname{head}(\mathcal{U}, r)| + \hat{\beta}\mathcal{T}(r) \cdot |\mathcal{U}|, \\
&= \big(1 - \hat{\beta} + \hat{\beta}\mathcal{T}(r)\big) \cdot |\mathcal{U}| - |\operatorname{head}(\mathcal{U}, r)|.
\end{aligned}$$

The partial derivatives of each entry of the partial contingency table then become:

$$\frac{\partial\, \mathrm{TP}_U^r}{\partial \hat{\beta}} = \mathcal{T}(r) \cdot |\mathcal{U}| \geq 0, \qquad \frac{\partial\, \mathrm{FP}_U^r}{\partial \hat{\beta}} = -\mathcal{T}(r) \cdot |\mathcal{U}| \leq 0,$$

$$\frac{\partial\, \mathrm{FN}_U^r}{\partial \hat{\beta}} = \big(1 - \mathcal{T}(r)\big) \cdot |\mathcal{U}| \geq 0, \qquad \frac{\partial\, \mathrm{TN}_U^r}{\partial \hat{\beta}} = \big(\mathcal{T}(r) - 1\big) \cdot |\mathcal{U}| \leq 0.$$

Partial derivatives for TPR, TPR and precision are a little more involved:

$$\frac{\partial \operatorname{TPR}_U^r}{\partial \hat{\beta}} = \frac{\frac{\partial \operatorname{TP}_U^r}{\partial \hat{\beta}} |\mathcal{P}_U^\star| - \operatorname{TP}_U^r \frac{\partial |\mathcal{P}_U^\star|}{\partial \hat{\beta}}}{|\mathcal{P}_U^\star|^2} = \frac{\mathcal{T}(r)\hat{\beta} \cdot |\mathcal{U}|^2 - \mathcal{T}(r)\hat{\beta}|\mathcal{U}|^2}{\hat{\beta}^2 |\mathcal{U}|^2}$$

$$= \frac{\mathcal{T}(r) - \mathcal{T}(r)}{\hat{\beta}} = 0 \tag{7.21}$$

$$\frac{\partial \operatorname{FPR}_U^r}{\partial \hat{\beta}} = \frac{\frac{\partial \operatorname{FP}_U^r}{\partial \hat{\beta}} \cdot (|\mathcal{U}| - |\mathcal{P}_U^\star|) - \operatorname{FP}_U^r \frac{\partial (|\mathcal{U}| - |\mathcal{P}_U^\star|)}{\partial \hat{\beta}}}{(|\mathcal{U}| - |\mathcal{P}_U^\star|)^2}$$

$$= \frac{-\mathcal{T}(r) \cdot |\mathcal{U}| \cdot (|\mathcal{U}| - |\mathcal{P}_U^\star|) + \operatorname{FP}_U^r \cdot |\mathcal{U}|}{(|\mathcal{U}| - |\mathcal{P}_U^\star|)^2}$$

$$= \frac{-\mathcal{T}(r)(1-\hat{\beta}) \cdot |\mathcal{U}|^2 + \operatorname{FP}_U^r \cdot |\mathcal{U}|}{(1-\hat{\beta})^2 \cdot |\mathcal{U}|^2}$$

$$= \frac{-\mathcal{T}(r)}{1-\hat{\beta}} + \frac{(|\operatorname{head}(\mathcal{U}, r)| - \hat{\beta}\mathcal{T}(r) \cdot |\mathcal{U}|) \cdot |\mathcal{U}|}{(1-\hat{\beta})^2 \cdot |\mathcal{U}|^2}$$

$$= \frac{-\mathcal{T}(r)}{(1-\hat{\beta})^2} + \frac{|\operatorname{head}(\mathcal{U}, r)|}{(1-\hat{\beta})^2 \cdot |\mathcal{U}|} = \frac{|\operatorname{head}(\mathcal{U}, r)| - \mathcal{T}(r) \cdot |\mathcal{U}|}{(1-\hat{\beta})^2} \tag{7.22}$$

$$\frac{\partial \operatorname{PRE}_U^r}{\partial \hat{\beta}} = \frac{\frac{\partial \operatorname{TP}_U^r}{\partial \hat{\beta}} \cdot (\operatorname{TP}_U^r + \operatorname{FP}_U^r) - \operatorname{TP}_U^r \frac{\partial (\operatorname{TP}_U^r + \operatorname{FP}_U^r)}{\partial \hat{\beta}}}{(\operatorname{TP}_U^r + \operatorname{FP}_U^r)^2}$$

$$= \frac{\mathcal{T}(r) \cdot |\mathcal{U}| \cdot (\operatorname{TP}_U^r + \operatorname{FP}_U^r)}{(\operatorname{TP}_U^r + \operatorname{FP}_U^r)^2}$$

$$= \frac{\mathcal{T}(r) \cdot |\mathcal{U}|}{(\operatorname{TP}_U^r + \operatorname{FP}_U^r)} = \frac{\mathcal{T}(r) \cdot |\mathcal{U}|}{|\operatorname{head}(\mathcal{U}, r)|} \geq 0 \tag{7.23}$$

Both $\partial \operatorname{FPR}_U^r / \partial \hat{\beta}$ and $\partial \operatorname{PRE}_U^r / \partial \hat{\beta}$ are a function of $\mathcal{T}(r)$, while $\partial \operatorname{FPR}_U^r / \partial \hat{\beta} = 0$. This implies that the ordering of rankings in terms of area under the ROC curve can change when the estimate of β changes, as proven by example in Figure 7.4.

7.B The effect of the fraction of known positives, known negatives and $\hat{\beta}$

Known negatives can be incorporated in our approach as described in Section 7.4.1. Given a fixed ranking $\mathcal{R}$, having known negatives essentially reduces the size of the unlabeled subset $\mathcal{U}$, which in turn reduces the number of degrees of freedom in assigning surrogate positives. As such, known negatives provide some benefit, though this is small in practice. Table 7.B.1 illustrates the effect of increasing amounts of known positives and known negatives: known positives significantly tighten bounds on AUROC, while known negatives only do so marginally (cfr. bounds with 10% known positives and 40/60/80% known negatives).

However, when the number of known negatives is large, it may be useful to reverse our approach, i.e., start from the rank distribution of known negatives. To do so, we can essentially flip all known class labels, use $\bar{\beta} = 1 - \beta$ and adjust the resulting contingency tables accordingly.

Table 7.B.2 shows bounds when based on known positives or known negatives (whichever are tightest). It is important to see that $|\mathcal{N}_L| > |\mathcal{P}_L|$ does not guarantee that performance bounds based on known negatives are tighter, because β also affects the bounds. When computing performance bounds based on known negatives, overestimating $\hat{\beta}$ leads to underestimated bounds (since we use $\bar{\beta} = 1 - \hat{\beta}$) and vice versa. The effect of errors in $\hat{\beta}$ is opposite in bounds based on $\mathcal{N}_L$.

Hence, bounds on performance metrics can be computed based primarily on known positives $\mathcal{P}_L$ *or* known negatives $\mathcal{N}_L$. The width of the bounds depends on the combination of $|\mathcal{P}_L|$ (or $|\mathcal{N}_L|$) and β (or $\bar{\beta}$) in a nontrivial way: depending on β, it is possible to obtain wider bounds based on known negatives, even if $|\mathcal{N}_L| > |\mathcal{P}_L|$ (or vice versa). In practice, we can estimate metrics based on $\mathcal{P}_L$ and $\mathcal{N}_L$ separately and then use whichever yields the tightest bounds, as shown in Table 7.B.2.

configuration			bounds on area under the ROC curve (true AUROC=76.8%)		
$\frac{\lvert\mathcal{P}_L\rvert}{\lvert\mathcal{P}_\Omega\rvert}$	$\frac{\lvert\mathcal{N}_L\rvert}{\lvert\mathcal{N}_\Omega\rvert}$	β	$\hat{\beta}$ / $\beta = 0.8$	$\hat{\beta}$ / $\beta = 1.0$	$\hat{\beta}$ / $\beta = 1.2$
10	0	15			
	20	18			
	40	23			
	60	31			
	80	47			
			67% 76.8% 87%	67% 76.8% 87%	67% 76.8% 87%
30	0	12			
	20	15			
	40	19			
	60	26			
	80	41			
			67% 76.8% 87%	67% 76.8% 87%	67% 76.8% 87%
50	0	9			
	20	11			
	40	14			
	60	20			
	80	33			
			67% 76.8% 87%	67% 76.8% 87%	67% 76.8% 87%
70	0	6			
	20	7			
	40	9			
	60	13			
	80	23			

Table 7.B.1: Estimated bounds on AUROC under different configurations. The total data set comprises 2,000 positives and 10,000 negatives. We varied the fraction of known positives and known negatives, which also implies changing β. All entries in the table are in percentages. We used three estimates for $\hat{\beta}$, namely an underestimate, the correct value and an overestimate (left to right). Legend: - - - true AUROC, ▭ bounds based on known positives.

configuration			bounds on area under the ROC curve (true AUROC=76.8%)		
$\frac{\lvert\mathcal{P}_L\rvert}{\lvert\mathcal{P}_\Omega\rvert}$	$\frac{\lvert\mathcal{N}_L\rvert}{\lvert\mathcal{N}_\Omega\rvert}$	β	$\hat{\beta}$ / $\beta = 0.8$	$\hat{\beta}$ / $\beta = 1.0$	$\hat{\beta}$ / $\beta = 1.2$
10	0	15			
	20	18			
	40	23			
	60	31			
	80	47			
			67% 76.8% 87%	67% 76.8% 87%	67% 76.8% 87%
30	0	12			
	20	14			
	40	18			
	60	25			
	80	41			
			67% 76.8% 87%	67% 76.8% 87%	67% 76.8% 87%
50	0	9			
	20	11			
	40	14			
	60	20			
	80	33			
			67% 76.8% 87%	67% 76.8% 87%	67% 76.8% 87%
70	0	5			
	20	6			
	40	9			
	60	13			
	80	23			

Table 7.B.2: Estimated bounds on AUROC under different configurations. The total data set comprises 2,000 positives and 10,000 negatives. We varied the fraction of known positives and known negatives, which also implies changing β. All entries in the table are in percentages. We used three estimates for $\hat{\beta}$, namely an underestimate, the correct value and an overestimate (left to right). In this table, we computed bounds based on known positives and known negatives (separately) and report the tightest confidence interval each time. Legend: - - - true AUROC, bounds based on known positives and known negatives.

Chapter 8

Building Classifiers to Predict the Start of Glucose-Lowering Pharmacotherapy Using Belgian Health Expenditure Data

This chapter has been submitted as:
Claesen, M., De Smet, F., Gillard, P., Mathieu, C.& De Moor, B. (2015). **Building Classifiers to Predict the Start of Glucose-Lowering Pharmacotherapy Using Belgian Health Expenditure Data**. *Journal of Machine Learning Research: special issue on Learning from Electronic Health Data*.

Contributions Marc Claesen has performed all data extractions and preprocessing and developed the learning pipeline. He took the lead in writing the corresponding paper.

Abstract

Early diagnosis is important for type 2 diabetes (T2D) to improve patient prognosis, prevent complications and reduce long-term treatment costs. We present a novel risk profiling approach based exclusively on health expenditure data that is available to Belgian mutual health insurers. We used expenditure data related to drug purchases and medical provisions to construct models that predict whether a patient will require glucose-lowering pharmacotherapy in the coming years, based on that patient's recent medical expenditure history. The design and implementation of the modeling strategy are discussed in detail and several learning methods are benchmarked for our application. Our best performing model obtains between 74.9% and 76.8% area under the ROC curve, which is comparable to state-of-the-art risk prediction approaches for T2D based on questionnaires. In contrast to other methods, our approach can be implemented on a population-wide scale at virtually no extra operational cost. Possibly, our approach can be further improved by additional information about some risk factors of T2D that is unavailable in health expenditure data.

8.1 Introduction

Type 2 diabetes mellitus (T2D) is a chronic metabolic disorder characterized by hyperglycemia and is considered one of the main threats to human health [290]. In developed countries, T2D makes up about 85% of diabetes mellitus patients and occurs when either insufficient insulin is produced, the body becomes resistant to insulin or both [276]. Prediabetes and less severe cases of T2D are initially managed by lifestyle changes, specifically increasing physical exercise, dietary change and smoking cessation [257, 83, 15]. If this yields insufficient glycemic control, pharmacotherapy with glucose-lowering agents (GLAs) like metformin or insulin is started [258, 15].

Several studies have indicated that one third to one half of T2D patients are undiagnosed [125, 149, 221]. Additionally, patients often remain undiagnosed for extended periods of time, with average diagnose-free intervals ranging from 4 to 7 years [127]. The prognosis of untreated patients can deteriorate rapidly as prolonged hyperglycemia can cause serious damage to many of the body's systems. Timely diagnosis of T2D proves challenging in contemporary medicine, as many patients already present signs of complications of the disease at the time of clinical diagnosis of T2D [126, 210, 152, 26, 124, 136].

Earlier diagnosis and subsequent treatment is believed to prevent or delay complications and improve prognosis [199, 93]. When impaired glucose tolerance

is diagnosed early, initial treatment can often be limited to lifestyle changes [196, 257, 83]. Compared to pharmacotherapy, lifestyle changes are simple, fully manageable by the patient and far less likely to cause serious treatment-induced complications like hypoglycemia [231, 286]. Complementary to health benefits, early diagnosis and prediction of future T2D pose a health economical advantage, as patients that do not require acute or intensive long-term treatment are far less demanding on the health care system.

Universal screening for T2D is cost-prohibitive [270, 93], but many organizations advise opportunistic screening of high-risk subgroups [276, 11, 93, 15]. Several risk profiling strategies have been developed to aid in the timely diagnosis of T2D [24, 247, 163, 175, 109, 129, 228]. Risk profiling is typically done by assessing some of the key risk factors for T2D, which include obesity [177], genetic predisposal [233, 140], lifestyle [213] and various clinical parameters. Existing risk profiling approaches are implemented via questionnaires, potentially augmented with clinical information that is available to the patient's general practitionner [114, 245, 163, 109, 227, 129]. Commonly required information includes BMI, family history, exercise and smoking habits and various clinical parameters.

In this work, we present an alternative approach for risk profiling which only requires data that is already available to Belgian mutual health insurers. This work was done in collaboration with the National Alliance of Christian Mutualities (NACM). NACM is the largest Belgian mutual health insurer with over four million members. Our approach does not require any questionnaires or additional clinical information and predicts whether a patient will require GLAs in the next few years. Interestingly, our approach works well despite the fact that Belgian health insurer data contains little direct information regarding key risk factors of T2D, that is weight, lifestyle and family history are all unavailable.

8.2 Existing Type 2 Diabetes Risk Profiling Approaches

The Cambridge Risk Score (CRS) was developed to assess the probability of undiagnosed T2D based on data that is routinely available in primary care records, including age, sex, medication use, family history of diabetes, BMI and smoking status [114], The CRS has been shown to be useful on multiple occasions [114, 198, 245], though its AUC seems to depend heavily on the population in which it is used, ranging between 67% [245] and 80% [114]. The

information used in the CRS is comparable to the approach of Baan et al. [24] which obtained AUCs ranging between 70% and 78%.

The FINDRISC score is based on a 10-year follow-up using age, BMI, waist circumference, history of antihypertensive drugs and high blood glucose, physical activity and diet with reported AUCs of 85% and 87% in predicting drug-treated diabetes [163]. The strongest reported predictors in this study were BMI, waist circumference, history of high blood glucose and physical activity. Glümer et al. [109] developed a risk score based on age, sex, BMI, known hypertension, physical activity and family history of diabetes with AUC ranging from 72% to 87.6%. The German diabetes risk score reached AUCs ranging from 75% to 83% on validation data and is based on age, waist circumference, height, history of hypertension, physical activity, smoking, and diet [227].

Heikes et al. [129] developed a decision tree for risk prediction achieving 82% AUC in a cross-validation setting, based on weight, age, family history and various clinical parameters. Various other approaches based on routine clinical information have demonstrated similarly accurate predictions of type 2 diabetes [247, 175].

8.3 Health Expenditure Data

The Belgian health care insurance is a broad solidarity-based form of social insurance. Mutual health insurers such as NACM are the legally-appointed bodies for managing and providing the Belgian compulsory health care and disability insurance, among other things. To implement their operations, Belgian mutual health insurers dispose of large databases containing health expenditure records of all their respective members.

These expenditure records hold all financial reimbursements of drugs, procedures and contacts with health care professionals. Each record comprises a timestamp, financial details and a description of the claim. The financial aspect is irrelevant from a medical point of view, but the type of resource-use as indicated by the description can contain medical information about the patient. These types belong to one of two main categories:

1. **Drug purchases** are recorded per package. The coding of packages contains information about the active substances in the drug along with the volume of the package.

2. **Medical provisions** are identified by a national encoding along with an identifier of the associated medical caregiver. Each provision has a

distinct code number.

In addition to resource-use data, some biographical information is available about each patient including age, gender, place of residence and social parameters. In the remainder of this Section we will elaborate on expenditure records related to drugs and provisions as used in our models. Subsequently we will briefly summarize the main strengths and limitations of using health expenditure data for predictive modeling.

8.3.1 Records Related to Drug Purchases

Expenditure records concerning drug purchases contain information about the active substances in the drug and the purchased volume. We mapped all active substances onto the anatomical therapeutic chemical (ATC) classification system maintained by the WHO [273]. The ATC classification system divides active substances into different groups based on the organ or system on which they act and their therapeutic, pharmacological and chemical properties. Each drug is classified in groups at 5 levels in the ATC hierarchy: fourteen main groups (1st level), pharmacological/therapeutic subgroups (2nd level), chemical subgroups (3rd and 4th level) and the chemical substance (5th level).

After mapping records onto the ATC classification system, a patient's medication history consists of specific ATC codes (5th level) along with the associated number of defined daily doses (DDD). In the period of interest, purchases of 4,580 distinct active substances were recorded in the NACM database. Table 8.1 shows an example of the classification of active substance on all levels in the ATC system.

level	ATC code	description
1	A	alimentary tract and metabolism
2	A10	drugs used in diabetes
3	A10B	blood glucose lowering drugs, excluding insulins
4	A10BA	biguanides
5	A10BA02	metformin

Table 8.1: Example of the ATC classification system: classification of metformin per level.

8.3.2 Records Related to Medical Provisions

Expenditure records concerning medical provisions can be considered tuples containing time-stamped identifiers of the patient, physician and medical provision. A single patient-physician interaction may yield multiple such records, one for each specific provision that occurred.

In the Belgian health care system, medical provisions are encoded via the Belgian nomenclature of medical provisions [264], which is maintained by the National Institute for Health and Disability Insurance (NIHDI).[1] This nomenclature is an unstructured list of unique codes (numbers) for each provision that is being refunded. Nomenclature numbers are added when new provisions are defined or when revisions are made. A single provision may correspond to multiple numbers for various reasons.

8.3.3 Advantages of Health Expenditure Data

The key benefit of expenditure databases is that they centralize structured medical information across all medical stakeholders to yield a comprehensive, longitudinal overview of each patient's medical history. Other health data sources are commonly fragmented, e.g., medical records maintained by the patient's general practitioner or hospital often contain only a subset of the patient's medical history. This fragmentation hampers the identification of patterns that may indicate elevated risk for diseases like type 2 diabetes. The NACM database comprises claims records of over four million Belgians, which enables complex modeling. Additionally, claims data have few omissions due to the financial incentive for patients and medical stakeholders (e.g., hospitals) to claim refunds. While other health data sources may contain more detailed information, the strength of NACM's data is in its volume, both in terms of number of patients and the amount of information that is recorded per individual. Finally, as most people tend to stay affiliated with the same mutual health insurer, their expenditure records provide long-term information.

8.3.4 Limitations of Health Expenditure Data

Belgian health expenditure data is strictly limited to what is required for mutual health insurers to implement their operations, which are mainly administrative in nature. Detailed health information such as diagnoses and test results are not directly available. In some other countries, health insurers dispose

[1] The website of NIHDI is available at `http://www.riziv.fgov.be`.

of more detailed information, such as ICD-10 codes which include diagnoses and symptoms [277]. Including such information is out of scope of this work as we focus exclusively on data that is already available to Belgian mutual health insurers. Biographical information about patients does not contain direct information about some important risk factors such as lifestyle, family history and BMI, though this may be partially embedded indirectly in medical resource-use.

8.4 Methods

In this Section we define the prediction task and describe all its aspects: the overall setup (Section 8.4.1), the data and its representation (Section 8.4.2) and the learning algorithms (Section 8.4.3). Briefly, our aim is to predict which patients will start glucose-lowering pharmacotherapy within the next 4 years, based on expenditure records of the previous 4 years.

Our key hypothesis is that patients with increased risk for T2D or those that are already afflicted but not diagnosed have a different medical expenditure history than patients without impaired glycemic control. We essentially use the start of GLA therapy as a proxy for diagnosis of (advanced) type 2 diabetes. This is reasonable since most patients that start GLA therapy above 40 years old have T2D [276].

We posed this task as a binary classification problem. Our classifiers produce a numeric level of confidence that a given patient will start glucose-lowering pharmacotherapy. When predicting a population, the outputs can be used to rank patients according to decreasing confidence that the patients will start glucose-lowering therapy. Highly ranked patients represent a high-risk subgroup which can be targetted for clinical screening. Briefly, we used nested cross-validation to obtain unbiased estimates of the predictive performance of each vectorization and learning approach. Predictive performance of all models was quantified via (area under) receiver operating characteristic (ROC) curves.

Data Our work is based on a subset of the expenditure records of NACM. All data extractions and analyses were performed at the Medical Management Department of the NACM under supervision of the Chief Medical Officer. The other research partners received no personally identifiable information (including small cells) from NACM. The patient selection protocol and vector representations are described in detail in Section 8.4.2.

Class definitions The positive class was defined as patients that require GLAs for long-term glycemic control.[2] The negative class is then defined as patients that do not need GLAs. Expenditure records related to GLAs were used to identify a set of known positives. However, the absence of such records in a patient's resource use history is not proof that this patient has no need for GLAs. This subtle difference is crucial, because it is well known that patients with impaired glycemic control or T2D often remain undiagnosed and hence untreated for a very long time [125, 149, 15]. As we cannot identify negatives, we had to build models from positive and unlabeled data.

PU learning Learning binary classifiers from positive and unlabeled data (PU learning) is a well-studied branch of semi-supervised learning [159, 92, 179, 66]. PU learning is more challenging than fully supervised binary classification, since it requires special learning approaches and quality metrics for hyperparameter optimization that account for the lack of known negatives. We benchmarked three PU learning methods, which are discussed in more detail in Section 8.4.3.

Software The entire data analysis pipeline was implemented using open-source software. For general data transformations and preprocessing we used *SciPy* and *NumPy* [143, 266]. The learning algorithms we used are available in *scikit-learn* and *EnsembleSVM* [201, 65] . Finally, we used *Optunity* for automated hyperparameter optimization [64].

8.4.1 Experimental Setup

We gathered all expenditure records during the 4-year interval of 2008 up to 2012 and labeled patients that used GLA therapy in $[2012, 2014]$ as positive. The selection protocol and representations of patients' medical resource-use are discussed in detail in Section 8.4.2. All vector representations of patients include age (in years), an indicator variable for gender and positive entries related to the patient's medical resource-use. A patient vector $\mathbf{p}$ can be written in the following general form, where d_{meds} and d_{provs} denote the number of features in the vectorization of medication and provision use, respectively:

$$\mathbf{p} \in \mathbb{R}_+^{2+d_{\text{meds}}+d_{\text{provs}}} = \begin{bmatrix} age & gender & medication & provisions \\ \mathbb{R}_+ & \{0,1\} & \mathbb{R}_+^{d_{\text{meds}}} & \mathbb{R}_+^{d_{\text{provs}}} \end{bmatrix}. \tag{8.1}$$

In Sections 8.4.2 and 8.4.2 we explain how records related to medication purchases and provisions were represented in vector form. All entries in the

[2] GLAs are defined as any drug in ATC category `A10`, which includes metformin, sulfonylurea and insulin.

vector representations were consistently normalized to the interval $[0, 1]$ by dividing feature-wise by the 99^{th} percentile and subsequently clipping where necessary. These normalized vector representations are used as inputs for the learning algorithms described in Section 8.4.3.

Figure 8.1 summarizes the full machine learning pipeline, which starts from expenditure records and ends with models to predict whether a patient will start glucose-lowering pharmacotherapy along with an estimate of their generalization performance. We used nested cross-validation to estimate generalization performance of different learning configurations [267]. The outer 3-fold cross-validation is used to estimate generalization performance of the full learning approach. Internally, twice iterated 10-fold cross-validation was used to find optimal hyperparameters for every learning method.

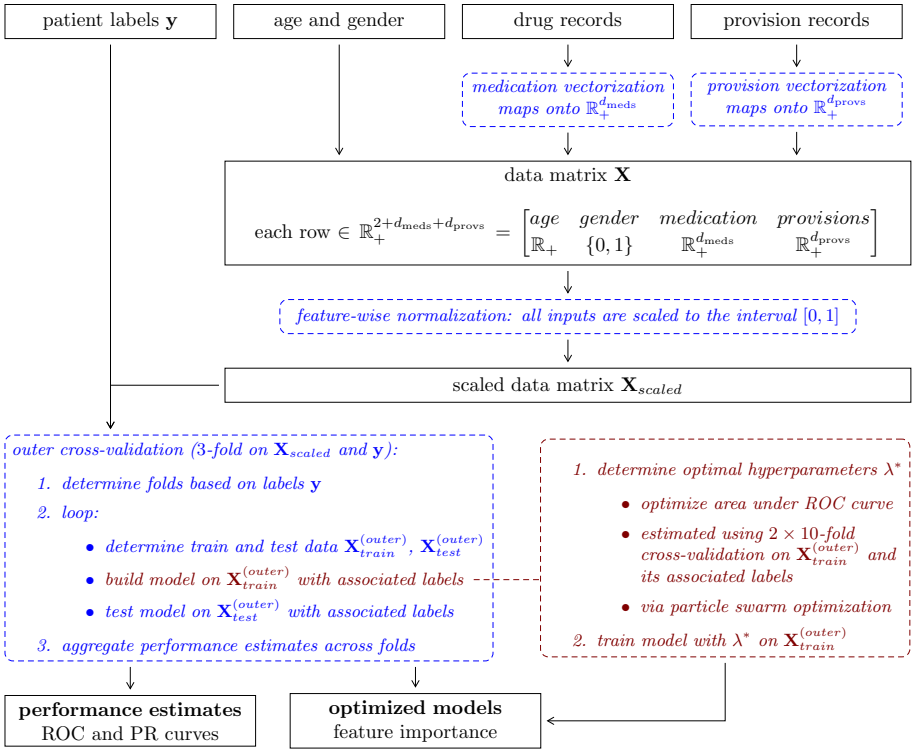


Figure 8.1: Overview of the full learning approach: data set vectorization, normalization and the nested cross-validation setup. Per iteration, hyperparameter optimization and model training is done based exclusively on $\mathbf{X}_{train}^{(outer)}$.

Model evaluation Models are compared based on area under the ROC curve. ROC curves visualize a classifier's performance spectrum by depicting its true positive rate (TPR)[3] as a function of its false positive rate (FPR)[4] while varying the decision threshold to decide on positives. Area under the ROC curve (AUROC) is a useful summary statistic of a classifier's performance. AUROC is equal to the probability that the classifier ranks a random positive higher than a random negative and is known to be equivalent to the Wilcoxon test of ranks [122].

Hyperparameter search We used Optunity's particle swarm optimizer to identify suitable hyperparameters for each approach based on the given training set as defined by the outer cross-validation procedure [64]. Every tuple of hyperparameters was evaluated using twice iterated 10-fold cross-validation on the training set. Per technique, the hyperparameters that maximized cross-validated area under the ROC curve were selected and used to train a model on the full training set.

Computing ROC curves Full label knowledge is required to compute ROC curves. In previous work, we introduced a method to compute bounds on ROC curves based on positive and unlabeled data [62]. Briefly, it is based on the positions of known positives in a ranking produced by a given classifier and requires two things:

- The rank distributions of labeled and latent positives must be comparable. This holds when known and latent positives follow the same distribution in input space (ie. the vector representation of patients). This is a fair assumption in our application, since we specifically ignore records after the start of glucose-lowering pharmacotherapy while identifying the set of positives (see Section 8.4.2), so the medication regimen of known positives has not yet diverged from the regimen of untreated patients.
- An estimate $\hat{\beta}$ of the fraction of latent positives in the unlabeled set is needed, that is the fraction of members that have never used GLAs but are likely to start glucose-lowering pharmacotherapy. In the period 2010–2014 roughly 8% of members of NACM aged 40 or higher started using GLAs.[5] Underestimating $\hat{\beta}$ results in an underestimated ROC curve and vice versa [62]. We opted to be conservative and used $\hat{\beta}_{lo} = 5\%$ to estimate lower bounds and $\hat{\beta}_{up} = 10\%$ for upper bounds.

[3]TPR measures the fraction of true positives that are correctly identified by the classifier.
[4]FPR measures the fraction of true negatives that are incorrectly identified by the classifier.
[5]The true value of β is higher than 8%, as this estimate omits all undiagnosed patients.

We consistently used the *lower* bounds for hyperparameter search. All our performance reports contain lower and upper bounds, based on $\hat{\beta}_{lo}$ and $\hat{\beta}_{up}$, respectively.

Diagnosing overfitting In addition to measuring performance, we diagnosed overfitting via the concept of rank distributions as defined by Claesen et al. [62]. The rank distribution of a subset of test instances is defined as the distribution of the positions of these test instances in a ranking of the full test set based on a model's predicted decision values. We diagnose overfitting based on the rank distributions of known positive training instances ($\mathcal{P}_{train}$) and known positives in the independent test fold ($\mathcal{P}_{test}$) after predicting the full data set. If the model overfits, the rank distribution of $\mathcal{P}_{train}$ is inconsistent with the rank distribution of $\mathcal{P}_{test}$. Specifically, ranks in $\mathcal{P}_{test}$ are worse than those in $\mathcal{P}_{train}$ when the model overfits. This can be quantified via the Mann-Whitney U test [170] based on ranks of $\mathcal{P}_{train}$ and $\mathcal{P}_{test}$ after predicting the full data set (that is all outer folds). The Mann-Whitney U test is expected to yield a non-significant result when the rank distributions of $\mathcal{P}_{train}$ and $\mathcal{P}_{test}$ are comparable. We report the average p-values of the test across outer cross-validation folds for each model (low p-values indicate overfitting).

8.4.2 Data Set Construction

We constructed a data set containing records of patients born before 1973 (e.g. 40 or more years old in 2012). Patients with records of glucose-lowering agents (GLAs) during less than 30 days were discarded. Patients with records of glucose-lowering therapy prior to 2012 were discarded. Patients that joined NACM after 2005 were also discarded, as we cannot determine whether these patients used GLAs in the recent past.

All patients that started glucose-lowering pharmacotherapy in 2012 or later are included as known positives ($n = 31,066$), along with unlabeled patients that were sampled at random from the remaining NACM members ($n = 79,243$). Known positives have a minimum of 30 days between the first and last purchase of GLAs to avoid contaminating the data set with false positives, for instance due to insulin use in surgical and medical ICUs [263, 262]. It must be noted that some false positives remain, that is patients that use GLAs but not for glycemic control.

In Sections 8.4.2 and 8.4.2 we describe the vector representations of records regarding medication and medical provisions, respectively.

Representation of Medication Records

The simplest way to represent medication purchases during a time interval is by having one input dimension per active substance (level 5 ATC codes) and counting the purchased volume in terms of DDDs. This representation is easy to construct but fails to capture any similarity between active substances, such as the system or organ on which they act.

Imposing structure We can directly use the hierarchical structure of the ATC system to define a measure of similarity between drugs. To impose structure between drugs we included input dimensions related to more generic levels of the ATC hierarchy (levels 1 to 4). On more generic levels we summed all DDD counts of active substances per category (level 5). This redundancy allowed us to express similarity between different active substances with a standard inner product. By normalizing every feature to the unit interval, we obtained the desired effect that patients with comparable drug use on ATC level 5 are more similar than patients that only share coefficients on more generic levels. Figure 8.2 illustrates this vector representation of trees and the effect of normalization.

Summary All vectorizations related to drug purchases are described in Table 8.1.

vectorization	description	d_{meds}
ATC 5	counts of DDDs per medication class in ATC level 5	4,580
ATC 1–4	counts of DDDs per medication class in ATC levels 1–4	1,257
ATC 1–5	counts of DDDs per medication class in ATC levels 1–5	5,837

Table 8.1: Summary of vectorization schemes used for records of drug purchases.

Representation of Provision Records

When considering a specific time period, we can describe records by a (sparse) three-dimensional tensor containing frequency counts as illustrated in Figure 8.3. We filtered all provisions with a description containing *diabetes*, *insulin* and *glucose* and provisions not recorded with a physician identifier. After filtering, 5,799 distinct provision codes remain (denoted by *#provisions*).

Each patient is modelled by a histogram of their provisions in the period of interest. This essentially means we compute the sum over the *physician-*

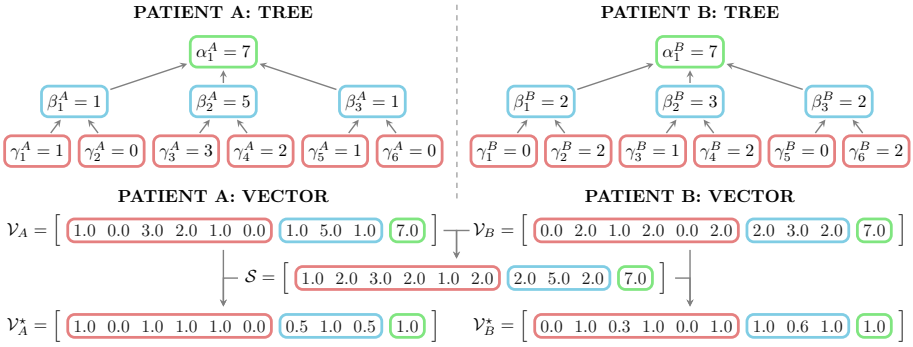


Figure 8.2: Visualization and vectorization of trees. In the tree representation, the value of internal nodes is the sum of the values of its children. The unnormalized vector representations $\mathcal{V}_A$ and $\mathcal{V}_B$ contain the values per node in the tree representation in some fixed order. Inner products between unnormalized representations $\mathcal{V}_A$ and $\mathcal{V}_B$ are mainly influenced by the top level nodes, since those have the largest value by construction. This undesirable effect can be fixed through feature-wise scaling. The scaling vector $\mathcal{S}$ was constructed using node-wise maxima. The normalized vector representations $\mathcal{V}_A^\star$ and $\mathcal{V}_B^\star$ are obtained by dividing the vector representations ($\mathcal{V}_A$, $\mathcal{V}_B$) element-wise by entries in the scaling vector $\mathcal{S}$. $\mathcal{V}_A^\star$ and $\mathcal{V}_B^\star$ are used as input to classifiers in the remainder of this work. As desired, the inner product of normalized vector representations is increasingly influenced by similarities at higher depths in the tree representations.

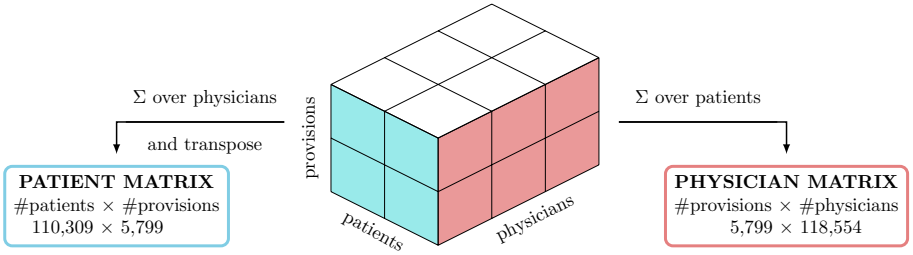


Figure 8.3: Tensor formulation of medical provisions with three components: patients, physicians and provisions. Each entry in the tensor is the frequency of the given tuple. This provision tensor is very sparse. The patient matrix is obtained by summing counts over all physicians (transposed). The physician matrix is obtained by summing counts over all patients. These matrices capture complementary information.

component of the tensor representation to obtain a matrix, in which rows and columns represent patients and provisions, respectively. Unfortunately, the encoding of provisions has no medically relevant structure in contrast to the ATC hierarchy for drugs as discussed in Section 8.4.2.

Imposing structure In order to define a reasonable similarity measure between patients, we first had to impose a structure onto the nomenclature that captures similarity between provisions. To structure provisions, we should not use information originating from the patient matrix, as this may cause information leaks (since the patient matrix is used directly in our models for prediction). Instead, we used the complementary physician matrix as a basis to define similarity between provisions, which essentially serves as a proxy for the medical specializations to which each provision belongs.

First, we computed cosine similarity between provisions based on the physician matrix. We used cosine similarity because it is known to work well for text mining with bag-of-words representations, which is comparable to our use case as it also features sparse, high dimensional input spaces. The cosine similarity κ_{cos} between two column vectors $\mathbf{u}$ and $\mathbf{v}$ is defined as:

$$\kappa_{cos}(\mathbf{u}, \mathbf{v}) = \frac{\langle \mathbf{u}, \mathbf{v} \rangle}{\|\mathbf{u}\| \cdot \|\mathbf{v}\|} = \frac{\mathbf{u}^T \mathbf{v}}{\|\mathbf{u}\| \cdot \|\mathbf{v}\|}. \tag{8.2}$$

Using cosine similarity we can construct a pair-wise similarity matrix $\mathbf{S}_{prov}$ between provisions based on the rows of the physician matrix $\mathbf{x}_i, i = 1..\#provisions$:

$$\mathbf{S}_{prov} = \left(\kappa_{cos}(\mathbf{x}_i, \mathbf{x}_j)\right)_{ij} \in \mathbb{R}^{\#provisions \times \#provisions}. \tag{8.3}$$

$\mathbf{S}_{prov}$ expresses similarity between provision codes based on the physicians that provide them and can be regarded as a proxy for the medical subdomain each provision frequently occurs in. In our context, its entries range from 0 (completely orthogonal) to +1 (exact similarity). To impose sparsity we set all entries of $\mathbf{S}_{prov}$ below 0.05 to 0. Its structure is visualized in Figure 8.4, which clearly indicates that our approach successfully identifies some coherent groups of provisions.

Finally, the structured representation of provisions $\mathbf{P}_{struct}$ is defined as the matrix product between the patient matrix $\mathbf{P}_{flat}$ and the provision similarity matrix $\mathbf{S}_{prov}$:

$$\mathbf{P}_{struct} = \mathbf{P}_{flat} \times \mathbf{S}_{prov} \in \mathbb{R}^{\#patients \times \#provisions}. \tag{8.4}$$

$\mathbf{P}_{struct}$ approximately captures which provisions occur in a patient's history with redundancy based on medical specializations.

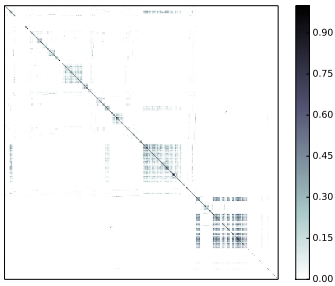


Figure 8.4: Structure of the provision similarity matrix $\mathbf{S}_{prov}$ based on providing physicians.

Summary All vectorizations related to medical provisions are described in Table 8.2.

vectorization	symbol	description	d_{provs}
PROVS FLAT	$\mathbf{P}_{flat}$	entries taken from the patient matrix	5,799
PROVS STRUCT	$\mathbf{P}_{struct}$	captures similarity between provisions	5,799
PROVS BOTH	$\mathbf{P}_{flat} \mid \mathbf{P}_{struct}$	concatenation of flat & structured	11,598

Table 8.2: Summary of vectorization schemes used for records of medical provisions.

8.4.3 Learning Methods

Having only positive and unlabeled data (PU learning) presents additional challenges for learning algorithms. Two broad classes of approaches exist to tackle these problems: (i) two-phase methods that first attempt to identify likely negatives from the unlabeled set and then train a supervised model on the positives and inferred negatives [167, 282] and (ii) approaches that treat the unlabeled set as negatives with label noise [92, 159, 179, 66].

We have tested three approaches from the latter category in this work, namely class-weighted SVM [166], bagging SVM [179] and the robust ensemble of SVM models [66]. All of these approaches are based on support vector machines. We used the linear kernel on vector representations of patients as described

in Section 8.4.2.[6] We will briefly introduce each method in the following subsections.

Class-weighted SVM

Class-weighted SVM (CWSVM) uses a misclassification penalty per class. CWSVM was first applied in a PU learning context by Liu et al. [166], by considering the unlabeled set to be negative with noise on its labels. A CWSVM is trained to distinguish positives ($\mathcal{P}$) from unlabeled instances ($\mathcal{U}$), leading to the following optimization problem:

$$\min_{\alpha,\xi,b} \frac{1}{2}\sum_{i=1}^{N}\sum_{j=1}^{N}\alpha_i\alpha_j y_i y_j \kappa(\mathbf{x}_i,\mathbf{x}_j) + C_{\mathcal{P}}\sum_{i\in\mathcal{P}}\xi_i + C_{\mathcal{U}}\sum_{i\in\mathcal{U}}\xi_i, \tag{8.5}$$

$$\text{s.t. } y_i(\sum_{j=1}^{N}\alpha_j y_j \kappa(\mathbf{x}_i,\mathbf{x}_j) + b) \geq 1-\xi_i, \qquad i=1,\ldots,N,$$

$$\xi_i \geq 0, \qquad i=1,\ldots,N,$$

where $\alpha \in \mathbb{R}^N$ are the support values, $\mathbf{y} \in \{-1,+1\}^N$ is the label vector, $\kappa(\cdot,\cdot)$ is the kernel function, b is the bias term and $\xi \in \mathbb{R}^N$ are the slack variables for soft-margin classification. The misclassification penalties $C_{\mathcal{P}}$ and $C_{\mathcal{U}}$ require tuning. We used the implementation available in scikit-learn [201] based on LIBSVM [57].

Bagging SVM

In bagging SVM, random resamples are drawn from the unlabeled set and CWSVM classifiers are trained to discriminate all positives from each resample [179]. Resampling the unlabeled set induces variability in the base models which is exploited via bagging. Base model predictions are aggregated via majority voting.

Bagging SVM with linear base models has two hyperparameters, namely the size of resamples of the unlabeled set $n_{\mathcal{U}}$ and the misclassification penalty on unlabeled instances $C_{\mathcal{U}}$. The misclassification penalty on positives $C_{\mathcal{P}}$ is fixed via the following rule:

$$C_{\mathcal{P}} = \frac{n_{\mathcal{U}} \times C_{\mathcal{U}}}{|\mathcal{P}|}, \tag{8.6}$$

[6] Though it must be noted that the ensemble methods are always implicitly nonlinear.

where $|\mathcal{P}|$ denotes the number of known positives. The heuristic rule in Equation 8.6 is common in imbalanced settings [55, 77]. We implemented bagging SVM using the EnsembleSVM library [65].

Robust Ensemble of SVM models

The robust ensemble of SVM models (RESVM) is a modified version of bagging SVM in which both the positive and unlabeled sets are resampled when constructing base model training sets [66]. The extra resampling induces additional variability between base models which improves performance when combined with a majority vote aggregation scheme. Claesen et al. [66] demonstrated that resampling the positive set provides robustness against false positives, which makes RESVM appealing for our application since our data set is known to contain a small fraction of false positives (as explained in Section 8.4.2).

When using linear base models, the RESVM approach has four hyperparameters that must be tuned, namely resample sizes and misclassification penalties per class. This approach was implemented based on EnsembleSVM [65].

8.5 Results and Discussion

Section 8.5.1 shows the predictive performance per learning configuration and compares these performances to the current state-of-the-art in large-scale risk assessment for T2D. Section 8.5.2 shows performance curves of the best configuration, which enable us to determine suitable cutoffs to identify target groups in practice. Finally, Section 8.5.3 describes a simple approach to assess which features contribute most to risk according to our best models.

8.5.1 Benchmark of learning methods

Table 8.1 summarizes the performance of each learning configuration. The AGE,GENDER feature set provides a baseline for comparison, all other feature sets include these as well. As shown in the results, this two-dimensional representation already carries some information.

Based on Table 8.1 we can conclude that a patient's medication history is highly informative to predict the start of GLA therapy. Using features based on ATC level 5, the RESVM model obtained an AUC between 72.55% and 74.43%. By adding redundancy as described in Section 8.4.2 the performance based on

	RESVM		bagging SVM		class-weighted SVM	
features	AUROC (%)	p	AUROC (%)	p	AUROC (%)	p
AGE, GENDER	55.74–56.64	$*$	58.61–59.67	$*$	**60.96–62.21**	0.04
ATC 5	**72.55–74.43**	0.17	70.83–72.62	0.09	71.89–73.74	0.01
ATC 1–4	**73.12–75.07**	0.07	69.57–71.24	$*$	73.05–74.91	0.04
ATC 1–5	**74.34–76.27**	0.13	71.50–73.27	0.05	72.13–73.94	$*$
PROVS FLAT	58.45–59.51	$*$	60.74–61.92	$*$	**63.01–64.31**	$*$
PROVS STRUCT	57.40–58.39	0.02	59.53–60.58	0.01	**62.53–63.81**	0.01
PROVS BOTH	58.89–59.75	$*$	61.72–62.87	$*$	**63.45–64.75**	$*$
ATC | PROVS	**74.89–76.82**	0.04	69.72–71.40	$*$	73.77–75.64	$*$

Table 8.1: Average bounds on area under the ROC curve and p-value of the Mann-Whitney U test over all folds for different feature sets per learning approach in a long-term prediction setup. The lower and upper bounds on AUC were computed with $\hat{\beta}_{lo} = 0.05$ and $\hat{\beta}_{up} = 0.10$, respectively. The ATC | PROVS feature set is the concatenation of the best performing sets per aspect, namely ATC 1–5 and PROVS BOTH. Stars ($*$) denote p-values below 0.005.

medication history alone was further increased to between 74.34% and 76.27% for the best learning approach (RESVM).

Predictive performance based on provisions alone turned out fairly poor, showing only a mild improvement compared to models based exclusively on age and gender for all learning algorithms. Interestingly, the best approach for representations based on provisions was class-weighted SVM, with RESVM being worst of all three learning methods. It appears that for these representations, large training sets are more important than base model variability: class-weighted SVM uses the full training set, bagging SVM uses all positives and a subset of unlabeled instances per base model and RESVM uses (small) subsets of both positives and unlabeled instances per base model.

The best representation included age, gender, and structured information about the drugs and provision history of each patient. The best learning method on this representation was RESVM, achieving an AUC between 74.89% and 76.82%. In Section 8.5.1 we compare the performance of our approach to competing screening methods.

Finally, RESVM appears most resistant to overfitting in the hyperparameter optimization stage as it consistently exhibits the highest average p-values in our diagnostic test (higher is better, see Section 8.4.1). We believe this to be attributable to the use of small resamples of both positives and unlabeled instances when training base models in RESVM, since this makes it unlikely to obtain a structural overfit of the ensemble model on the full training set. In contrast, bagging SVM is far more prone to overfitting because every base

model is trained on all positives.

Comparison to State-of-the-art

Our best approach obtained cross-validated AUC between 74.89% and 76.82% (exact numbers are unknown due to the lack of known negatives). This is comparable to many competing approaches, based on questionnaires and some clinical information such as the Cambridge Risk Score (AUC 67%–80%, [245, 114]), the Danish risk score (AUC 72%–87.6%, [109]), the German diabetes risk score (AUC 75%–83%, [227]) and a Dutch approach (AUC 74%, [24]). Approaches using detailed clinical information generally perform better, but are more expensive to maintain [247, 175, 163, 129]. The key advantage of our approach is the fact it is easy to implement on a population wide scale at virtually no operational cost.

The target class we used in this work is stricter than in the risk prediction methods mentioned in Section 8.2, namely patients that require GLAs for glycemic control versus patients with impaired glycemic control, respectively (except for Lindström and Tuomilehto [163], which also predicted drug-treated T2D). It is reasonable to assume that our models generally rank patients with impaired glycemic control but without a need for GLAs higher than patients without impaired glycemic control. In our performance assessment both of these patient groups are essentially treated as negatives, in contrast to the screening programmes mentioned previously which treat patients with impaired glycemic control as positives. Hence, we believe the performance of our models would appear higher when evaluated against a target class comprising all patients with impaired glycemic control, as is done in the evaluation of other screening approaches. Unfortunately, we are unable to accurately identify patients with impaired glycemic control but without need for GLAs.

All competing methods use either clinical information or direct knowledge of risk factors that is unavailable to us. Furthermore, some of the characteristics that are lacking in our data have been reported to be the most informative to assess risk for T2D [163, 247, 175]. We obtained generalization performances that are comparable to existing approaches, despite these missing predictors. Finally, our approach is the only one that is based exclusively on existing data that is always available, without requiring additional patient contacts or clinical tests.

8.5.2 Performance Curves

The RESVM model based on ATC | PROVS vectorization had the best overall performance. Figure 8.1 shows bounds on the ROC and PR curves for this model and includes curves for the CWSVM model based on age and gender and a random model for reference. These bounds were computed using the technique described in Chapter 7. The true curve is unknown because we do not dispose of negative labels.

ROC curves enable us to determine a cutoff to use in practice, based on a suitable balance between true and false positive rate (sensitivity and 1-specificity, respectively). Determining a suitable balance requires a tradeoff between the relative importance of identifying undiagnosed patients (true positives) vis-à-vis increased amounts of screening tests on patients that are in fact healthy (false positives).

It should be noted that precision depends on class balance, and therefore the PR curve shown in Figure 8.1b is not representative for screening an overall population, since the overall population has a higher fraction of negatives than our custom data set (i.e. precision would be lower in practice). In contrast, the bounds in ROC space are representative because ROC curves are insensitive to changes in class distribution [96]. What matters in the PR curves is the shape of the curve for RESVM, which peaks at low recall, while the curves for CWSVM and a random model do not. The CWSVM approach is similar to the existing guidelines outlined in Table 1.2, which essentially identify persons at high risk through age and a handful additional risk factors. The performance curves indicates that the RESVM model is good for case finding (which requires high precision) and far outperforms screening based on only age and gender.

8.5.3 Feature Importance Analysis for the RESVM Model

The RESVM model is implicitly nonlinear due to its majority voting rule to aggregate base model decisions, which poses problems in assessing the importance of each predictor. However, our use of linear base models enables a simple approximation. The decision value for base model $i \in \{1, \ldots, n_{\text{models}}\}$ for a test instance $\mathbf{z}$ can be written as follows:

$$f_i(\mathbf{z}) = \langle \mathbf{w}_i, \mathbf{z} \rangle + \rho_i = \mathbf{w}_i^T \mathbf{z} + \rho_i,$$

where $\mathbf{w}_i$ is the separating hyperplane and ρ_i is a bias term. A simple linear approximation of such ensemble models can be computed as the average of all

base model hyperplanes:

$$\bar{\mathbf{w}} = \sum_{i=1}^{n_{\text{models}}} \mathbf{w}_i / n_{\text{models}}. \tag{8.7}$$

Feature importance can then be determined based on the coefficients in $\bar{\mathbf{w}}$. The range of every feature is comparable, since we normalized all features to the unit interval $[0, 1]$. This allows us to conclude that the features with largest (positive) coefficients in $\bar{\mathbf{w}}$ contribute most to risk according to our model.

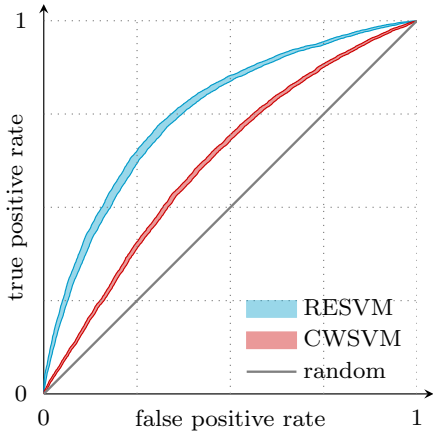
Table 8.2 depicts the level 3 ATC codes that contribute most to diabetes risk based on the metric outlined above. As expected, cardiovascular medication (ATC `C*`) is identified as a clear risk indicator [146, 118, 136]. However, a number of less obvious indicators are also revealed, specifically antipsychotics (`N05A`), antidepressants (`N06A`) and antigout preparations (`M04A`), for which associations with T2D are known [67, 16, 177]. The relative importance of features and associated medical implications will be discussed in detail in a forthcoming medical paper.

8.6 Conclusion

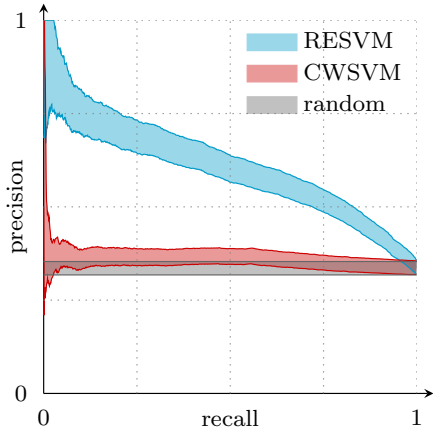
In this work we have demonstrated the ability to predict clinical outcomes based solely on readily available health expenditure data. We successfully built proof-of-concept classifiers to predict the start of glucose-lowering pharmacotherapy in patients above 40. Our experiments show that accurate predictions can be made based on historical medication purchases. These predictions can be further improved by incorporating information about medical provisions and the use of appropriate vectorization schemes.

Since adult patients starting glucose-lowering pharmacotherapy are mainly afflicted with type 2 diabetes (T2D), our models can be used for T2D risk assessment. Our approach presents a novel method for case finding which can be easily incorporated in modern healthcare, since all required data is already available. The associated operational costs are very low as the entire workflow can be fully automated without any need for patient contacts or medical tests. As such, our work provides an efficient and cost-effective method to identify a high risk subgroup, which can then be screened using decisive clinical tests.

Interestingly, our approach works well even though health expenditure data contains very limited direct information on some important known risk factors. In that sense, our approach is fundamentally different from the current state-of-the-art which mainly focuses on quantifying known risk factors directly, either



(a) Receiver Operating Characteristic curve.



(b) Precision-Recall curve.

Figure 8.1: Performance curves for RESVM classifier based on ATC | PROVS vectorization, CWSVM based on age and gender and a random model. The lower and upper bounds are estimated using $\hat{\beta}_{lo} = 5\%$ and $\hat{\beta}_{up} = 10\%$, respectively.

feature	normalized weight as per Equation (8.7)
C09B	788.3
C09D	653.8
C10A	503.0
N05A	434.3
C03E	412.7
C03C	404.2
N06A	403.1
M04A	397.0
A02B	378.5
C09A	340.1

Table 8.2: Level 3 ATC codes with highest normalized feature weight.

by asking the patient or through clinical tests. The performance of our approach is expected to improve further when additional information about these risk factors can be obtained, e.g., family history and lifestyle.

Chapter 9

Conclusion

We conclude by summarizing the main insights and implications of the project, along with interesting avenues for future research. We will discuss machine learning-specific aspects in Section 9.1 and the screening application in Section 9.2.

9.1 Machine learning contributions

The machine learning research in this project focused on learning from positive and unlabeled data and the construction of high-quality, reusable tools that allow easy reproduction of our results, fast prototyping of novel ideas and the partial automation of machine learning pipelines.

One of the main hurdles we had to overcome was learning classifiers from positive and unlabeled data, where the set of labeled positives is known to be contaminated with some false positives (Chapter 4). Existing approaches were sensitive to false positives, often to such an extent that they became unreliable. Our approach addresses this weakness by resampling known positives within a bagging framework, which was a natural extension to the already-existing bagging SVM that used the same idea on the unlabeled set [179].

The major issue we tackled in semi-supervised learning was evaluating binary classifiers without known negatives (Chapter 7). Prior to our work, a lack of negatives prohibited the quantification of classifier performance in terms of traditional metrics, which in turn prohibited the use of (potentially very good) models for many applications (e.g., the performance of models used for

screening or diagnosis must be quantified before their use is even considered). Our contribution solves an important problem that plagues many practical applications. Specifically, the ability to evaluate models without known negatives saved us a considerable amount of time, as the only alternative would have been to acquire negative labels manually. Additionally, we have shown that existing model selection approaches are prone to errors in some practical cases.

The software packages we developed (described in Chapters 3 and 6) provide easy access to our methods to other researchers and enable them to reuse and extend our work, rather than having to reinvent the wheel. With these packages we gave heed to the call of several prominent journals regarding the need and value of open-source software in scientific research [244, 205]. Optunity specifically tackles a common element of practical machine learning (Chapter 6), as most methods feature hyperparameters that must be optimized somehow. Optunity's usefulness is evidenced by its popularity, with hundreds of monthly downloads through the Python Package Index at the time of writing.[1]

9.1.1 Future work

Based on the experience gathered and results obtained during our work, we see opportunities for future machine learning research in automated hyperparameter optimization and learning from positive and unlabeled data.

Fully automated machine learning is becoming popular, evidenced by competitions like the ChaLearn AutoML challenge [119]. A key element of such pipelines is automated hyperparameter optimization, which is receiving a lot of research attention [35, 242, 32, 34, 90, 172, 64, 91]. Current research focuses on Bayesian optimization based on the somewhat dogmatic belief that these optimizers converge faster than others. We are skeptical towards this claim, as meta-heuristic techniques have been shown competitive in recent publications [197] as well as our own experiments (see Chapter 6) and because the famous no free lunch theorem applies [275]. We believe that meta-heuristic techniques for hyperparameter optimization are currently underdeveloped but promising.

In Chapter 7 we described how to compute any contingency table-based metric based on only positive and unlabeled data. This is the first approach to compute commonly known metrics, and hence an important contribution, though it does not directly enable computing probablistic performance metrics in general and strictly proper scoring rules like log loss or Brier score in particular. Strictly proper scoring rules [110] are especially useful for model selection and calibration

[1] Statistics can be found at `https://pypi.python.org/pypi/Optunity`.

as they are more sensitive than metrics like AUROC and AUPR, so extending our approach to enable approximation of these metrics would be useful.

9.2 Screening for type 2 diabetes

We set out to investigate the extent to which health expenditure data enables clinical applications like screening for T2D, and thereby improve healthcare. During this research we have successfully developed a proof-of-concept screening method for type 2 diabetes, based exclusively on readily-available health expenditure data collected by the largest Belgian mutual health insurer. Our performance benchmarks have indicated competitiveness to existing screening approaches for T2D that have proven useful in international contexts. Our work can serve as the basis for cost-effective population-wide screening for type 2 diabetes which would strengthen early detection of the disease.

Principally, our screening method identifies patients that will require glucose lowering agents. Given the way we approached the task, we likely have problems identifying patients suffering from mild (pre)diabetes. That said, we treated such patients as negatives in all evaluations, and hence all reported performance estimates are conservative. In fact, our performance estimates are conservative under the reasonable assumption that claims histories of patients with mild diabetes are somewhere between claims histories of healthy patients and those of patients that require GLAs. Interestingly, additional experiments indicate that our approach can identify patients years before GLA therapy is or needs to be initiated, which further adds to the potential of our approach.

Finally, the screening models can also be used to identify drugs and provisions that indicate diabetes risk. This information can then be used to create new medical guidelines or finetune existing ones. Additionally, small subsets of these indictors may be used to create alerts for physicians to help them in screening for diabetes. An example would be to add alerts in the software used by general practitioners when certain combinations of drugs/provisions occur.

9.2.1 Weaknesses and limitations of our approach

The screening approach we developed has a number of weaknesses, related to the labeling of NACM members, limitations of health expenditure data and limitations of machine learning in general.

Labeling issues

The quality of learned models hinges upon the quality of the ground truth on which they are based, that is the representativeness of the sets of known positives and (ideally) known negatives for the positive and negative class, respectively. Any labeling bias will perpetuate throughout the modeling process and bias resulting models and performance estimates to some extent.

Known positives have progressed T2D We identified diabetes patients (positives) based on the routine use of GLA therapy. This labeling omits patients that are exclusively on lifestyle interventions and hence only identifies more severe cases of diabetes. By implication, our models are able to identify patients with profiles that are similar to those on GLA therapy, i.e., patients that likely require GLA therapy, while identifying early stage patients is problematic.

False positives Our labeling can flag type 1 diabetes patients, however these patients are usually diagnosed at a young age [18]. Hence, any bias caused by T1D patients is low when screening in adults above 30. A more severe problem is that we might also flag patients on GLA therapy for alternative reasons (e.g., weight loss [182]). This is problematic because a significant amount of false positives prohibits reliably estimating performance using the technique outlined in Chapter 7. Fortunately, the number of false positives in our setting can reasonably be assumed negligible, though an exact estimate remains unavailable.

No known negatives As explained in Section 1.4.1, we had to use semi-supervised learning approaches because it is impossible to directly identify negatives (persons without diabetes). A fully supervised dataset with both positive and negative labels would facilitate learning better models. One way to reliably identify negatives would be to contact individual NACM members to inquire about their health, though this approach may be cost-prohibitive.

Limitations of health expenditure data

An important weakness of screening for type 2 diabetes based on health expenditure records is the fact this data source lacks direct indicators for several key risk factors, including lifestyle, diet and genetic predisposition. Luckily, some of this information may nonetheless be available via proxies, e.g., obesity may be subtlely indicated by treatments of hypertension [209], asthma [240, 249], joint diseases [251, 71] and many more health issues.

Additional problems arise when relevant information is omitted from health expenditure databases, e.g., when patients forget to claim refunds. Finally, we must be aware of potentially relevant biases against certain population segments. For example, poverty, lower health literacy and social exclusion are known barriers to accessing healthcare [137, 203, 191, 237] while unfortunately the affected population segments are often exposed to elevated health risks [137, 223, 171]. These increased risks include diseases like obesity and diabetes [214, 223].

Machine learning limitations

Machine learning approaches have shown impressive performance on a wide variety of tasks, but it is important to note that machine learning is not a silver bullet that can solve all problems in data analysis. Contemporary machine learning is constrained by limitations which are similar to those imposed on computing in general since the early days of Babbage's Analytical Engine:

> "*The Analytical Engine has no pretensions whatever to originate anything. It can only do whatever we know how to order it to perform. It can follow analysis, but it has no power of anticipating any analytical revelations or truths. Its province is to assist us in making available what we are already acquainted with.*" – Ada Byron, Countess of Lovelace, 1815 – 1852

The notion of generalization performance in machine learning does not defy Lady Lovelace's statement, since generalization performance of learned models is entirely contingent upon the degree to which the assumptions underpinning the learning approach hold. These assumptions are made when designing learning algorithms and object representations. An additional crucial factor is the informativeness of the training data and quality of prior knowledge (if any), as is aptly summarized by the mantra of "*garbage in, garbage out*".

The key assumption underlying this entire work is that the health expenditure profiles of undiagnosed diabetes patients are similar in some sense to the health expenditure profiles of patients that started glucose-lowering pharmacotherapy. Furthermore, as we used linear SVM (base) models, the assumed similarity should be captured in the input space representation of persons (cfr. Section 8.4.2). The performance of our approach indicates that our assumptions are reasonable, though our method is not fit to identify atypical diabetes patients. Such limitations can only be overcome by universal screening.

9.2.2 Future work

Our research has shown that health expenditure data can effectively be used as a basis for T2D screening programmes with state-of-the-art performance, despite the fact it lacks information on known risk factors for diabetes which are heavily used by other screening approaches (e.g., lifestyle, BMI, genetic predisposition, ...). This suggests a lot of potential in screening methods that combine both of these types of information, that is health expenditure data *and* lifestyle, BMI and various clinical parameters, though the potential improvement in predictive performance by linking data sources is difficult to estimate a priori.

Health expenditure data unifies information across caregivers and provides a fairly complete long-term overview, while other data sources include crucial parameters about lifestyle, genetics and clinical measurements. As such, it is reasonable to assume that these types of data are complementary, and hence their union may allow for screening approaches that far outperform existing approaches. A lot of this information could simply be obtained via patient questionnaires (e.g. BMI, lifestyle, family history, ...), though more detailed clinical parameters are harder to procure. Overall, this is a very promising direction for future research, though coupling health expenditure data with other types of information is a sensitive subject from a privacy point of view, so strict adherence to all guidelines and regulations is of paramount importance.

9.2.3 Health expenditure data

The screening method itself is a proof-of-concept which showcases the potential clinical value of administrative databases such as claims databases maintained by mutual health insurers. The results of the project yield a few conclusions regarding the use of health expenditure data for clinical applications:

- It is a valuable source of information to build screening programmes for diseases like type 2 diabetes, which prove challenging to detect in contemporary medicine. Its key strengths are that it integrates healthcare information across all caregivers and provides a reliable longitudinal overview of a patient's medical resource-use history. However, resource-use histories are not as detailed as clinical databases maintained by caregivers.
- It is difficult to find or replicate these strengths elsewhere. Particularly, Belgium does not yet have EHRs that record information from all medical stakeholders into a central, comprehensive database. Implementing such EHRs would be complex for technological, legal, political and psychological

reasons. Initiatives like Vitalink[2] and the shared pharmaceutical file[3] envision parts of this functionality, though these projects are currently in their infancy. For now, claims records remain the sole source of complete, long-term information across medical stakeholders and time.

Health expenditure data is already widely used for epidemiology [202, 160, 105, 272] and, more recently, to assess quality of care [268]. Our work shows that claims data can additionally be used pro-actively to improve healthcare, rather than only in retrospective, descriptive studies. The wealth of information in these databases can likely improve healthcare in many aspects.

9.2.4 The elephant in the room

Our work demonstrated the technological possibility of screening for T2D based on health expenditure data. However, we have not touched upon the ethical, legal and psychological perspectives of data-driven applications in the health and healthcare domain. We conclude this work by briefly discussing some key barriers and open questions concerning applications such as ours.

Population-wide screening

The approach outlined in this thesis enables population-wide screening for T2D at a very low operational cost, since we exclusively use readily-available health expenditure data. A major practical question for any population-wide screening approach is how it should be put to use in the real world.

The first option is to perform risk assessment on the whole population (all members of NACM in our context) and actively contact persons identified to be at high risk. From a medical perspective, such a *push* model seems most appropriate since this has the potential to help a maximal amount of people.

On the other hand, many people may have qualms about inferences of their health status without the concerned person's explicit prior request and/or approval. A push model as described above can raise issues from a psychological point of view, as it can induce a "*Big Brother*" feeling that will surely be resisted by some. Additionally, the *right not to know* has experienced a revived interest from an ethical point of view due to advances in genetic research [194, 17, 56], and many of the arguments raised in that discussion essentially also apply to push models which involve proactively notifying patients identified at high risk

[2]More info about Vitalink is available at http://www.vitalink.be/.
[3]In Dutch: gedeeld farmaceutisch dossier (GFD).

for some disease.[4] A *pull* model, which allows everyone to request the results of a personalized risk analysis at their own leisure, may prove to be more popular.

Use of personal data

Principally, health and healthcare data is considered personal information owned by the involved patient, though often this patient has limited or no access to his or her data and may even be unaware of its existence. This highly sensitive type of personal data is rightfully protected from unpermitted use [6, 1].

Several models exist for patients to permit the usage of personal data for research and various applications after obtaining informed consent. The main distinction is between *opt-in* models, in which data usage is permitted after explicit approval of the patient, and *opt-out* models, in which data can be used unless patients explicitly prohibit it. Opt-in models are most common due to their conservative nature from a privacy point of view, but these may prohibit applications that require a lot of data to create a minimum viable product.

The use of health and healthcare data is a sensitive matter and policymakers in Belgium and Europe understandably err on the side of conservatism [6, 1], though this inevitably constrains both research and potentially beneficial applications. Recently, the proposal for European data protection regulation raised a lot of criticism, as researchers in health and healthcare worried that an increased amount of conservatism could significantly impede scientific research [188, 75, 97, 7, 189]. Our project chimes in on this discussion with a proof-of-concept clinical application based on health expenditure data.

In the end, policymakers must strike a tradeoff between patient privacy vis-à-vis potential healthcare improvements through the use of personal data. This sensitive matter is the subject of ongoing debate in both Belgium and Europe.

[4]The right not to know entails whether patients must be informed regarding some (potentially serious) health problems, even if the patients themselves do not want to know.

Bibliography

[1] Directive 95/46/EC of the European parliament and of the council of 24 october 1995 on the protection of individuals with regard to the processing of personal data and on the free movement of such data, OJ L 281, 23.11.1995, p.31. pages 152

[2] IDF diabetes atlas. http://www.idf.org/sites/default/files/Atlas-poster-2014_EN.pdf. Accessed: 2015-08-30. pages 7, 21

[3] IDF diabetes: facts and figures. http://www.idf.org/worlddiabetesday/toolkit/gp/facts-figures. Accessed: 2015-08-30. pages 21

[4] Preventie van type 2 diabetes bij volwassenen. http://www.diabetes.be/sites/default/files/13/diabetesliga_kernboodschappendiabetespreventie.pdf. Accessed: 2015-09-01. pages xxv, 4, 5, 7

[5] Wet van 6 augustus 1990 betreffende de ziekenfondsen en de landsbonden van ziekenfondsen, BS 28 september 1990, 18475. pages 1, 8

[6] Wet van 8 december 1992 tot bescherming van de persoonlijke levenssfeer ten opzichte van de verwerking van persoonsgegevens, BS 8 december 1992, 5801. pages 152

[7] Impact of the draft European Data Protection Regulation and proposed amendments from the rapporteur of the LIBE committee on scientific research. http://www.wellcome.ac.uk/stellent/groups/corporatesite/@policy_communications/documents/web_document/wtvm054713.pdf, 2013. [Online; accessed 2015-09-19]. pages 152

[8] Abstracts of 51st EASD annual meeting. *Diabetologia*, 58(1):1–607, 2015. pages 19

[9] Stein Aerts, Diether Lambrechts, Sunit Maity, Peter Van Loo, Bert Coessens, Frederik De Smet, Leon-Charles Tranchevent, Bart De Moor, Peter Marynen, Bassem Hassan, Peter Carmeliet, and Yves Moreau. Gene prioritization through genomic data fusion. *Nature Biotechnology*, 24(5):537–544, May 2006. pages 54, 57

[10] Kurt George Matthew Mayer Alberti and Paul Zimmet. Definition, diagnosis and classification of diabetes mellitus and its complications. part 1: diagnosis and classification of diabetes mellitus. provisional report of a who consultation. *Diabetic medicine*, 15(7):539–553, 1998. pages 2, 5, 19

[11] Kurt GMM Alberti, Mayer B Davidson, Ralph A DeFronzo, Allan Drash, Saul Genuth, Maureen I Harris, Richard Kahn, Harry Keen, William C Knowler, and Harold Lebovitz. Report of the expert committee on the diagnosis and classification of diabetes mellitus. *Diabetes Care*, 21:S5, 1998. pages 4, 123

[12] Kurt GMM Alberti, Paul Zimmet, Jonathan Shaw, and IDF Epidemiology Task Force Consensus Group. The metabolic syndrome – a new worldwide definition. *The Lancet*, 366(9491):1059–1062, 2005. pages 20

[13] Ala Alwan. *Global status report on noncommunicable diseases 2010.* World Health Organization, 2011. pages 20

[14] Carlos Alzate and Johan A. K. Suykens. A semi-supervised formulation to binary kernel spectral clustering. In *2012 IEEE World Congress on Computational Intelligence (IEEE WCCI/IJCNN 2012)*, Brisbane, Australia, June 2012. pages 55

[15] American Diabetes Association. Standards of medical care in diabetes–2014. *Diabetes Care*, 37(Supplement 1):S14–S80, 2014. pages 4, 122, 123, 128

[16] Ryan J Anderson, Kenneth E Freedland, Ray E Clouse, and Patrick J Lustman. The prevalence of comorbid depression in adults with diabetes a meta-analysis. *Diabetes Care*, 24(6):1069–1078, 2001. pages 141

[17] Roberto Andorno. The right not to know: an autonomy based approach. *Journal of Medical Ethics*, 30(5):435–439, 2004. pages 151

[18] American Diabetes Association. Diagnosis and classification of diabetes mellitus. *Diabetes Care*, 33(Supplement 1):S62–S69, 2010. pages 148

[19] A Astrup and N Finer. Redefining type 2 diabetes: 'diabesity' or 'obesity dependent diabetes mellitus'? *Obesity Reviews*, 1(2):57–59, 2000. pages 19

[20] Robert C Atkins and Paul Zimmet. Diabetic kidney disease: Act now or pay later—world kidney day, 11 march 2010. *Therapeutic Apheresis and Dialysis*, 14(1):1–4, 2010. pages 19

[21] Peter C Austin, Muhammad M Mamdani, Therese A Stukel, Geoffrey M Anderson, and Jack V Tu. The use of the propensity score for estimating treatment effects: administrative versus clinical data. *Statistics in medicine*, 24(10):1563–1578, 2005. pages 44

[22] Guoda Azguridienė and Corinna Delkeskamp-Hayes. Public health care in Europe: Moral aspirations, ideological obsessions, and structural pitfalls in a post-enlightenment culture. *Journal of Medicine and Philosophy*, 2015. pages 12

[23] Laurent Azoulay, Verena Schneider-Lindner, Sophie Dell'Aniello, Alicia Schiffrin, and Samy Suissa. Combination therapy with sulfonylureas and metformin and the prevention of death in type 2 diabetes: a nested case-control study. *Pharmacoepidemiology and drug safety*, 19(4):335–342, 2010. pages 43

[24] Caroline A Baan, Johannes B Ruige, Ronald P Stolk, JC Witteman, Jacqueline M Dekker, Robert J Heine, and EJ Feskens. Performance of a predictive model to identify undiagnosed diabetes in a health care setting. *Diabetes Care*, 22(2):213–219, 1999. pages 6, 123, 124, 139

[25] François Bachoc. Cross validation and maximum likelihood estimations of hyper-parameters of gaussian processes with model misspecification. *Computational Statistics & Data Analysis*, 66:55–69, 2013. pages 83

[26] David J Ballard, Linda L Humphrey, L Joseph Melton, Peter P Frohnert, Chu-Pin Chu, W Michael O'Fallon, and Pasquale J Palumbo. Epidemiology of persistent proteinuria in type II diabetes mellitus: population-based study in Rochester, Minnesota. *Diabetes*, 37(4):405–412, 1988. pages 122

[27] Robert E Banfield, Lawrence O Hall, Kevin W Bowyer, and W Philip Kegelmeyer. A comparison of decision tree ensemble creation techniques. *Pattern Analysis and Machine Intelligence, IEEE Transactions on*, 29(1):173–180, 2007. pages 60

[28] Christian A Bannister, Sarah E Holden, S Jenkins-Jones, C Ll Morgan, JP Halcox, G Schernthaner, J Mukherjee, and CJ Currie. Can people with type 2 diabetes live longer than those without? a comparison of mortality in people initiated with metformin or sulphonylurea monotherapy and matched, non-diabetic controls. *Diabetes, Obesity and Metabolism*, 16(11):1165–1173, 2014. pages 27, 42

[29] Eric Bauer and Ron Kohavi. An empirical comparison of voting classification algorithms: Bagging, boosting, and variants. *Machine learning*, 36(1-2):105–139, 1999. pages 47, 59, 76

[30] Jessica Beagley, Leonor Guariguata, Clara Weil, and Ayesha A Motala. Global estimates of undiagnosed diabetes in adults. *Diabetes research and clinical practice*, 103(2):150–160, 2014. pages 4

[31] Joshua A Beckman, Mark A Creager, and Peter Libby. Diabetes and atherosclerosis: epidemiology, pathophysiology, and management. *Jama*, 287(19):2570–2581, 2002. pages 19

[32] James Bergstra and Yoshua Bengio. Random search for hyper-parameter optimization. *Journal of Machine Learning Research*, 13(1):281–305, 2012. pages 16, 75, 80, 82, 83, 86, 88, 89, 91, 146

[33] James Bergstra, Dan Yamins, and David D Cox. Hyperopt: A Python library for optimizing the hyperparameters of machine learning algorithms. In *Proceedings of the 12th Python in Science Conference*, pages 13–20. SciPy, 2013. pages 16, 83, 88, 89, 91, 92

[34] James Bergstra, Daniel Yamins, and David Cox. Making a science of model search: Hyperparameter optimization in hundreds of dimensions for vision architectures. In *Proceedings of The 30th International Conference on Machine Learning*, pages 115–123, 2013. pages 82, 146

[35] James S Bergstra, Rémi Bardenet, Yoshua Bengio, and Balázs Kégl. Algorithms for hyper-parameter optimization. In *Advances in Neural Information Processing Systems*, pages 2546–2554, 2011. pages 16, 80, 83, 88, 91, 146

[36] Paolo Berta, Giuditta Callea, Gianmaria Martini, and Giorgio Vittadini. The effects of upcoding, cream skimming and readmissions on the italian hospitals efficiency: a population-based investigation. *Economic Modelling*, 27(4):812–821, 2010. pages 12

[37] D John Betteridge. Lipid control in patients with diabetes mellitus. *Nature Reviews Cardiology*, 8(5):278–290, 2011. pages 44

[38] Joline WJ Beulens, Diederick E Grobbee, and Bruce Nealb. The global burden of diabetes and its complications: an emerging pandemic. *European Journal of Cardiovascular Prevention & Rehabilitation*, 17(1 suppl):s3–s8, 2010. pages 18, 19, 20, 21

[39] Mauro Birattari, Zhi Yuan, Prasanna Balaprakash, and Thomas Stützle. F-race and iterated f-race: An overview. In *Experimental methods for the*

analysis of optimization algorithms, pages 311–336. Springer, 2010. pages 83

[40] Christopher M Bishop. Neural networks for pattern recognition. 1995. pages 80, 82, 83

[41] Jock A. Blackard and Denis J. Dean. Comparative accuracies of artificial neural networks and discriminant analysis in predicting forest cover types from cartographic variables. *Computers and Electronics in Agriculture*, 24(3):131–151, December 1999. pages 50, 65, 111

[42] Gilles Blanchard, Gyemin Lee, and Clayton Scott. Semi-supervised novelty detection. *Journal of Machine Learning Research*, 11:2973–3009, 2010. pages 54

[43] Michael Bodmer, Christian Meier, Stephan Krähenbühl, Susan S Jick, and Christoph R Meier. Metformin, sulfonylureas, or other antidiabetes drugs and the risk of lactic acidosis or hypoglycemia a nested case-control analysis. *Diabetes Care*, 31(11):2086–2091, 2008. pages 22

[44] Jaclyn LF Bosco, Rebecca A Silliman, Soe Soe Thwin, Ann M Geiger, Diana SM Buist, Marianne N Prout, Marianne Ulcickas Yood, Reina Haque, Feifei Wei, and Timothy L Lash. A most stubborn bias: no adjustment method fully resolves confounding by indication in observational studies. *Journal of clinical epidemiology*, 63(1):64–74, 2010. pages 44

[45] Léon Bottou and Chih-Jen Lin. Support Vector Machine Solvers. In Léon Bottou, Olivier Chapelle, Dennis DeCoste, and Jason Weston, editors, *Large Scale Kernel Machines*, pages 301–320, Cambridge, MA, USA, 2007. MIT Press. pages 47, 60, 82

[46] Olivier Bousquet and André Elisseeff. Stability and generalization. *The Journal of Machine Learning Research*, 2:499–526, 2002. pages 47

[47] Patrick J Boyle. Diabetes mellitus and macrovascular disease: mechanisms and mediators. *The American journal of medicine*, 120(9):S12–S17, 2007. pages 19

[48] AP Bradley. The use of the area under the ROC curve in the evaluation of machine learning algorithms. *Pattern Recognition*, 30(7):1145–1159, July 1997. pages 100

[49] G. Bradski. The OpenCV library. *Dr. Dobb's Journal of Software Tools*, 2000. pages 89

[50] Leo Breiman. Bagging predictors. *Machine Learning*, 24(2):123–140, August 1996. pages 47, 56, 58, 59

[51] Leo Breiman. Randomizing outputs to increase prediction accuracy. *Machine Learning*, 40(3):229–242, 2000. pages 59

[52] Leo Breiman. Random forests. *Machine learning*, 45(1):5–32, 2001. pages 47, 59, 80, 82, 83

[53] Gavin Brown, Jeremy Wyatt, Rachel Harris, and Xin Yao. Diversity creation methods: a survey and categorisation. *Information Fusion*, 6(1):5–20, 2005. pages 58

[54] Borja Calvo, Pedro Larrañaga, and Jose A Lozano. Learning Bayesian classifiers from positive and unlabeled examples. *Pattern Recognition Letters*, 28(16):2375–2384, 2007. pages 98

[55] Gavin C Cawley. Leave-one-out cross-validation based model selection criteria for weighted LS-SVMs. In *Neural Networks, 2006. IJCNN'06. International Joint Conference on*, pages 1661–1668. IEEE, 2006. pages 56, 137

[56] Ruth Chadwick, Mairi Levitt, and Darren Shickle. *The right to know and the right not to know: genetic privacy and responsibility*. Cambridge University Press, 2014. pages 151

[57] Chih-Chung Chang and Chih-Jen Lin. LIBSVM: A library for support vector machines. *ACM Transactions on Intelligent Systems and Technology*, 2:27:1–27:27, 2011. Software available at `http://www.csie.ntu.edu.tw/~cjlin/libsvm`. pages 48, 65, 136

[58] Olivier Chapelle, Bernhard Schölkopf, and Alexander Zien. *Semi-supervised learning*, volume 2. MIT press Cambridge, 2006. pages 98

[59] Olivier Chapelle, Vikas Sindhwani, and Sathiya Keerthi. Optimization techniques for semi-supervised support vector machines. *Journal of Machine Learning Research*, 9:203–233, 2008. pages 98

[60] Nitesh V Chawla and Grigoris Karakoulas. Learning from labeled and unlabeled data: An empirical study across techniques and domains. *Journal of Artificial Intelligence Research*, 23:331–366, 2005. pages 98, 106

[61] Lei Chen, Dianna J Magliano, and Paul Z Zimmet. The worldwide epidemiology of type 2 diabetes mellitus—present and future perspectives. *Nature Reviews Endocrinology*, 8(4):228–236, 2012. pages 2, 20

[62] Marc Claesen, Jesse Davis, Frank De Smet, and Bart De Moor. Assessing binary classifiers using only positive and unlabeled data. *arXiv preprint arXiv:1504.06837*, 2015. pages 130, 131

[63] Marc Claesen and Bart De Moor. Hyperparameter search in machine learning. In *Proceedings of the 11th Metaheuristics International Conference (MIC'2015)*, 2015. arXiv preprint arXiv:1502.02127, available at `http://arxiv.org/abs/1502.02127`. pages 86

[64] Marc Claesen, Jaak Simm, Dusan Popovic, Yves Moreau, and Bart De Moor. Easy hyperparameter search using Optunity. *Journal of Machine Learning Research (submitted)*, 2015. Available at `http://arxiv.org/abs/1412.1114`. Homepage: `http://www.optunity.net`. pages 80, 81, 83, 128, 130, 146

[65] Marc Claesen, Frank De Smet, Johan A.K. Suykens, and Bart De Moor. EnsembleSVM: A library for ensemble learning using support vector machines. *Journal of Machine Learning Research*, 15:141–145, 2014. pages 65, 80, 82, 83, 128, 137

[66] Marc Claesen, Frank De Smet, Johan A.K. Suykens, and Bart De Moor. A robust ensemble approach to learn from positive and unlabeled data using SVM base models. *Neurocomputing*, 160(0):73 – 84, 2015. pages 98, 101, 111, 128, 135, 137

[67] Nathanial G Clark. Consensus development conference on antipsychotic drugs and obesity and diabetes. *Diabetes Care*, 27(2):596, 2004. pages 141

[68] Helen M Colhoun, D John Betteridge, Paul N Durrington, Graham A Hitman, H Andrew W Neil, Shona J Livingstone, Margaret J Thomason, Michael I Mackness, Valentine Charlton-Menys, and John H Fuller. Primary prevention of cardiovascular disease with atorvastatin in type 2 diabetes in the collaborative atorvastatin diabetes study (cards): multicentre randomised placebo-controlled trial. *The Lancet*, 364(9435):685–696, 2004. pages 44

[69] Ronan Collobert, Samy Bengio, and Yoshua Bengio. A parallel mixture of SVMs for very large scale problems. *Neural Computation*, 14(5):1105–1114, 2002. pages 47, 50

[70] International Expert Committee. International expert committee report on the role of the A1C assay in the diagnosis of diabetes. *Diabetes Care*, 32(7):1327–1334, 2009. pages 5

[71] Cyrus Cooper, Shelagh Snow, Timothy E McAlindon, Samantha Kellingray, Brenda Stuart, David Coggon, and Paul A Dieppe. Risk factors for the incidence and progression of radiographic knee osteoarthritis. *Arthritis & Rheumatism*, 43(5):995, 2000. pages 148

[72] Corinna Cortes and Vladimir Vapnik. Support-vector networks. *Machine Learning*, 20(3):273–297, September 1995. pages 48

[73] Catherine C Cowie, Keith F Rust, Earl S Ford, Mark S Eberhardt, Danita D Byrd-Holt, Chaoyang Li, Desmond E Williams, Edward W Gregg, Kathleen E Bainbridge, and Sharon H Saydah. Full accounting of diabetes and pre-diabetes in the us population in 1988–1994 and 2005–2006. *Diabetes Care*, 32(2):287–294, 2009. pages 20

[74] Felipe Cucker and Steve Smale. Best choices for regularization parameters in learning theory: on the bias-variance problem. *Foundations of Computational Mathematics*, 2(4):413–428, 2002. pages 80

[75] Richard Cumbley and Peter Church. Is "*Big Data*" creepy? *Computer Law & Security Review*, 29(5):601–609, 2013. pages 152

[76] Craig J Currie, Chris D Poole, Marc Evans, John R Peters, and Christopher Ll Morgan. Mortality and other important diabetes-related outcomes with insulin vs other antihyperglycemic therapies in type 2 diabetes. *Mortality*, 98(2), 2013. pages 27, 43

[77] Anneleen Daemen, Olivier Gevaert, Fabian Ojeda, Annelies Debucquoy, Johan A.K. Suykens, Christine Sempoux, Jean-Pascal Machiels, Karin Haustermans, and Bart De Moor. A kernel-based integration of genome-wide data for clinical decision support. *Genome Medicine*, 1(4):39, 2009. pages 56, 137

[78] Jesse Davis and Pedro Domingos. Deep transfer via second-order Markov logic. In *Proceedings of the 26th International Conference on Machine Learning (ICML)*, pages 217–224, 2009. pages 101

[79] Jesse Davis and Mark Goadrich. The relationship between precision-recall and ROC curves. In *Proceedings of the 23rd international conference on Machine learning*, ICML '06, pages 233–240, New York, NY, USA, 2006. ACM. pages 64, 71, 101, 108

[80] Jeffrey Dean, Greg Corrado, Rajat Monga, Kai Chen, Matthieu Devin, Mark Mao, Andrew Senior, Paul Tucker, Ke Yang, and Quoc V Le. Large scale distributed deep networks. In *Advances in Neural Information Processing Systems*, pages 1223–1231, 2012. pages 82

[81] Janez Demšar. Statistical comparisons of classifiers over multiple data sets. *Journal of Machine Learning Research*, 7:1–30, 2006. pages 64, 73, 90

[82] François Denis, Rémi Gilleron, and Fabien Letouzey. Learning from positive and unlabeled examples. *Theoretical Computer Science*, 348(1):70–83, 2005. pages 98

[83] Diabetes Prevention Program Research Group. Reduction in the incidence of type 2 diabetes with lifestyle intervention or metformin. *The New England Journal of Medicine*, 346(6):393, 2002. pages 2, 5, 122, 123

[84] Thomas G Dietterich. An experimental comparison of three methods for constructing ensembles of decision trees: Bagging, boosting, and randomization. *Machine learning*, 40(2):139–157, 2000. pages 59

[85] Daniel J Drucker, Jacques Philippe, Svetlana Mojsov, William L Chick, and Joel F Habener. Glucagon-like peptide I stimulates insulin gene expression and increases cyclic AMP levels in a rat islet cell line. *Proceedings of the National Academy of Sciences*, 84(10):3434–3438, 1987. pages 22

[86] Marco F Duarte and Yu Hen Hu. Vehicle classification in distributed sensor networks. *Journal of Parallel and Distributed Computing*, 64(7):826–838, 2004. pages 65

[87] Justin B Echouffo-Tcheugui, Mohammed K Ali, Simon J Griffin, and KM Venkat Narayan. Screening for type 2 diabetes and dysglycemia. *Epidemiologic reviews*, 33(1):63–87, 2011. pages 2

[88] Bradley Efron and Gail Gong. A leisurely look at the bootstrap, the jackknife, and cross-validation. *The American Statistician*, 37(1):36–48, 1983. pages 81, 82

[89] Bradley Efron and Robert J Tibshirani. *An introduction to the bootstrap*. CRC press, 1994. pages 106

[90] Katharina Eggensperger, Matthias Feurer, Frank Hutter, James Bergstra, Jasper Snoek, Holger Hoos, and Kevin Leyton-Brown. Towards an empirical foundation for assessing Bayesian optimization of hyperparameters. In *NIPS workshop on Bayesian Optimization in Theory and Practice*, 2013. pages 16, 80, 83, 90, 146

[91] Katharina Eggensperger, Frank Hutter, Holger H Hoos, and Kevin Leyton-Brown. Efficient benchmarking of hyperparameter optimizers via surrogates. 2015. pages 146

[92] Charles Elkan and Keith Noto. Learning classifiers from only positive and unlabeled data. In *Proceedings of the 14th ACM SIGKDD International Conference on Knowledge Discovery and Data Mining*, KDD '08, pages 213–220, New York, NY, USA, 2008. ACM. pages 15, 54, 55, 98, 108, 128, 135

[93] Michael M Engelgau, KM Narayan, and William H Herman. Screening for type 2 diabetes. *Diabetes Care*, 23(10):1563–1580, 2000. pages 2, 4, 122, 123

[94] Theodoros Evgeniou, Massimiliano Pontil, and Tomaso Poggio. Regularization networks and support vector machines. *Advances in Computational Mathematics*, 13(1):1–50, 2000. pages 80

[95] Rong-En Fan, Kai-Wei Chang, Cho-Jui Hsieh, Xiang-Rui Wang, and Chih-Jen Lin. LIBLINEAR: A library for large linear classification. *Journal of Machine Learning Research*, 9:1871–1874, June 2008. pages 49, 65

[96] Tom Fawcett. An introduction to ROC analysis. *Pattern Recognition Letters*, 27(8):861–874, June 2006. pages 140

[97] Robin Fears, Helmut Brand, Richard Frackowiak, P-P Pastoret, Robert Souhami, and Beth Thompson. Data protection regulation and the promotion of health research: getting the balance right. *QJM*, 107(1):3–5, 2014. pages 152

[98] Internation Diabetes Federation. IDF worldwide definition of the metabolic syndrome, 2010. pages 20

[99] Félix-Antoine Fortin, De Rainville, Marc-André Gardner Gardner, Marc Parizeau, and Christian Gagné. DEAP: Evolutionary algorithms made easy. *Journal of Machine Learning Research*, 13(1):2171–2175, 2012. pages 88

[100] Michael J Fowler. Microvascular and macrovascular complications of diabetes. *Clinical diabetes*, 26(2):77–82, 2008. pages 4, 19

[101] Benoît. Frenay and Michel Verleysen. Classification in the presence of label noise: A survey. *Neural Networks and Learning Systems, IEEE Transactions on*, 25(5):845–869, May 2014. pages 54

[102] Peter Gæde, Henrik Lund-Andersen, Hans-Henrik Parving, and Oluf Pedersen. Effect of a multifactorial intervention on mortality in type 2 diabetes. *New England Journal of Medicine*, 358(6):580–591, 2008. pages 2

[103] John-Michael Gamble, Scott H Simpson, Dean T Eurich, Sumit R Majumdar, and Jeff A Johnson. Insulin use and increased risk of mortality in type 2 diabetes: a cohort study. *Diabetes, Obesity and Metabolism*, 12(1):47–53, 2010. pages 43

[104] Shravanthi R Gandra, Lesa W Lawrence, Bhash M Parasuraman, Robert M Darin, Justin J Sherman, and Jerry L Wall. Total and component health care costs in a non-Medicare HMO population of patients with and without type 2 diabetes and with and without macrovascular disease. *Journal of Managed Care Pharmacy: JMCP*, 12(7):546–554, 2006. pages 20, 21

[105] Rajesh Garg, William Chen, and Merri Pendergrass. Acute pancreatitis in type 2 diabetes treated with exenatide or sitagliptin a retrospective observational pharmacy claims analysis. *Diabetes Care*, 33(11):2349–2354, 2010. pages 151

[106] Stuart Geman, Elie Bienenstock, and René Doursat. Neural networks and the bias/variance dilemma. *Neural computation*, 4(1):1–58, 1992. pages 80

[107] S Genuth, R Eastman, R Kahn, R Klein, J Lachin, H Lebovitz, D Nathan, F Vinicor, and American Diabetes Association. Implications of the United Kingdom prospective diabetes study. *Diabetes Care*, 26:S28, 2003. pages 2

[108] Hertzel C Gerstein, Jackie Bosch, Gilles R Dagenais, Rafael Díaz, Hyejung Jung, Aldo P Maggioni, Janice Pogue, Jeffrey Probstfield, Ambady Ramachandran, and Matthew C Riddle. Basal insulin and cardiovascular and other outcomes in dysglycemia. *New England Journal of Medicine*, 367(4):319–328, 2012. pages 43

[109] Charlotte Glümer, Bendix Carstensen, Annelli Sandbæk, Torsten Lauritzen, Torben Jørgensen, and Knut Borch-Johnsen. A Danish diabetes risk score for targeted screening – the Inter99 study. *Diabetes Care*, 27(3):727–733, 2004. pages 6, 123, 124, 139

[110] Tilmann Gneiting and Adrian E Raftery. Strictly proper scoring rules, prediction, and estimation. *Journal of the American Statistical Association*, 102(477):359–378, 2007. pages 146

[111] Sally Goldman and Yan Zhou. Enhancing supervised learning with unlabeled data. In *Proceedings of the 17th International Conference on Machine Learning (ICML)*, pages 327–334, 2000. pages 98

[112] Patricia M Grambsch and Terry M Therneau. Proportional hazards tests and diagnostics based on weighted residuals. *Biometrika*, 81(3):515–526, 1994. pages 33

[113] Yves Grandvalet. Bagging equalizes influence. *Machine Learning*, 55(3):251–270, 2004. pages 59, 60

[114] Simon J Griffin, PS Little, CN Hales, AL Kinmonth, and NJ Wareham. Diabetes risk score: towards earlier detection of type 2 diabetes in general practice. *Diabetes/metabolism research and reviews*, 16(3):164–171, 2000. pages 6, 123, 139

[115] Diederick E Grobbee and Arno W Hoes. Confounding and indication for treatment in evaluation of drug treatment for hypertension. *BMJ: British Medical Journal*, 315(7116):1151, 1997. pages 44

[116] UK Prospective Diabetes Study (UKPDS) Group. Effect of intensive blood-glucose control with metformin on complications in overweight patients with type 2 diabetes (UKPDS 34). *The Lancet*, 352(9131):854–865, 1998. pages 27, 43

[117] UK Prospective Diabetes Study (UKPDS) Group. Intensive blood-glucose control with sulphonylureas or insulin compared with conventional treatment and risk of complications in patients with type 2 diabetes (UKPDS 33). *The Lancet*, 352(9131):837–853, 1998. pages 27

[118] Scott M Grundy, Ivor J Benjamin, Gregory L Burke, Alan Chait, Robert H Eckel, Barbara V Howard, William Mitch, Sidney C Smith, and James R Sowers. Diabetes and cardiovascular disease a statement for healthcare professionals from the American Heart Association. *Circulation*, 100(10):1134–1146, 1999. pages 141

[119] Isabelle Guyon, Kristin Bennett, Gavin Cawley, Hugo Jair Escalante, Sergio Escalera, Tin Kam Ho, Núria Macia, Bisakha Ray, Mehreen Saeed, and Alexander Statnikov. Design of the 2015 chalearn automl challenge. pages 146

[120] Steven M Haffner, Michael P Stern, Helen P Hazuda, Braxton D Mitchell, and Judith K Patterson. Cardiovascular risk factors in confirmed prediabetic individuals: does the clock for coronary heart disease start ticking before the onset of clinical diabetes? *Jama*, 263(21):2893–2898, 1990. pages 2, 5

[121] Siamak Hajizadeh, Zili Li, Rolf PBJ Dollevoet, and David MJ Tax. Evaluating classification performance with only positive and unlabeled samples. In *Structural, Syntactic, and Statistical Pattern Recognition*, pages 233–242. Springer, 2014. pages 15

[122] James A Hanley and Barbara J McNeil. The meaning and use of the area under a receiver operating characteristic (ROC) curve. *Radiology*, 143(1):29–36, 1982. pages 130

[123] Nikolaus Hansen and Andreas Ostermeier. Completely derandomized self-adaptation in evolution strategies. *Evolutionary computation*, 9(2):159–195, 2001. pages 88

[124] Maureen I Harris and Richard C Eastman. Early detection of undiagnosed diabetes mellitus: a US perspective. *Diabetes/metabolism research and reviews*, 16(4):230–236, 2000. pages 4, 122

[125] Maureen I Harris, Katherine M Flegal, Catherine C Cowie, Mark S Eberhardt, David E Goldstein, Randie R Little, Hsiao-Mei Wiedmeyer, and Danita D Byrd-Holt. Prevalence of diabetes, impaired fasting glucose, and impaired glucose tolerance in US adults: the Third National Health and Nutrition Examination Survey, 1988–1994. *Diabetes Care*, 21(4):518–524, 1998. pages 122, 128

[126] Maureen I Harris, Ronald Klein, Catherine C Cowie, Michael Rowland, and Danita D Byrd-Holt. Is the risk of diabetic retinopathy greater in non-hispanic blacks and mexican americans than in non-hispanic whites with type 2 diabetes?: A US population study. *Diabetes Care*, 21(8):1230–1235, 1998. pages 122

[127] Maureen I Harris, Ronald Klein, Tim A Welborn, and Matthew W Knuiman. Onset of NIDDM occurs at least 4–7 yr before clinical diagnosis. *Diabetes Care*, 15(7):815–819, 1992. pages 4, 122

[128] Trevor Hastie, Saharon Rosset, Robert Tibshirani, and Ji Zhu. The entire regularization path for the support vector machine. In *Journal of Machine Learning Research*, pages 1391–1415, 2004. pages 80

[129] Kenneth E Heikes, David M Eddy, Bhakti Arondekar, and Leonard Schlessinger. Diabetes risk calculator a simple tool for detecting undiagnosed diabetes and pre-diabetes. *Diabetes Care*, 31(5):1040–1045, 2008. pages 6, 123, 124, 139

[130] Bianca Hemmingsen, Søren S Lund, Christian Gluud, Allan Vaag, Thomas Almdal, Christina Hemmingsen, and Jørn Wetterslev. Targeting intensive glycaemic control versus targeting conventional glycaemic control for type 2 diabetes mellitus. *The Cochrane Library*, 2011. pages 43

[131] José Miguel Hernández-Lobato, Matthew W Hoffman, and Zoubin Ghahramani. Predictive entropy search for efficient global optimization of black-box functions. In *Advances in Neural Information Processing Systems 27*, pages 918–926. 2014. pages 92

[132] Edith Hesse. Screening van suikerziekte. *Wetenschap ten dienste van Volksgezondheid, Voedselveiligheid en Leefmilieu*, 2008. pages 7

[133] Geoffrey E Hinton. A practical guide to training restricted Boltzmann machines. In *Neural Networks: Tricks of the Trade*, pages 599–619. Springer, 2012. pages 80

[134] Rury R Holman, Sanjoy K Paul, M Angelyn Bethel, David R Matthews, and H Andrew W Neil. 10-year follow-up of intensive glucose control in type 2 diabetes. *New England Journal of Medicine*, 359(15):1577–1589, 2008. pages 2

[135] Chih-Wei Hsu, Chih-Chung Chang, and Chih-Jen Lin. A practical guide to support vector classification, 2003. pages 80

[136] Frank B Hu, Meir J Stampfer, Steven M Haffner, Caren G Solomon, Walter C Willett, and JoAnn E Manson. Elevated risk of cardiovascular disease prior to clinical diagnosis of type 2 diabetes. *Diabetes Care*, 25(7):1129–1134, 2002. pages 4, 122, 141

[137] Manfred Huber, Anderson Stanciole, Kristian Wahlbeck, Nicoline Tamsma, Federico Torres, Elisabeth Jelfs, and Jeni Bremner. Quality in and equality of access to healthcare services, study report for European Commission, Directorate-General for Employment, Social Policy and Equal Opportunities, 2008. [Online; accessed 2015-11-08; `www.euro.centre.org/data/1237457784_41597.pdf`]. pages 149

[138] Frank Hutter, Holger H Hoos, and Kevin Leyton-Brown. Sequential model-based optimization for general algorithm configuration. In *Learning and Intelligent Optimization*, pages 507–523. Springer, 2011. pages 83, 89, 91, 92

[139] Frank Hutter, Holger H Hoos, Kevin Leyton-Brown, and Thomas Stützle. ParamILS: an automatic algorithm configuration framework. *Journal of Artificial Intelligence Research*, 36(1):267–306, 2009. pages 16, 82, 83, 89, 91

[140] InterAct Consortium. The link between family history and risk of type 2 diabetes is not explained by anthropometric, lifestyle or genetic risk factors: the EPIC-InterAct study. *Diabetologia*, 56(1):60–69, 2013. pages 123

[141] Jeffrey A Johnson, Sumit R Majumdar, Scot H Simpson, and Ellen L Toth. Decreased mortality associated with the use of metformin compared with sulfonylurea monotherapy in type 2 diabetes. *Diabetes Care*, 25(12):2244–2248, 2002. pages 27, 43

[142] Donald R Jones, Matthias Schonlau, and William J Welch. Efficient global optimization of expensive black-box functions. *Journal of Global optimization*, 13(4):455–492, 1998. pages 83

[143] Eric Jones, Travis Oliphant, and Pearu Peterson. SciPy: Open source scientific tools for Python, 2001. [Online; accessed 2015-04-16]. pages 128

[144] Kristijan H Kahler, Mangala Rajan, George G Rhoads, Monika M Safford, Kitaw Demissie, Shou-En Lu, and Leonard M Pogach. Impact of oral antihyperglycemic therapy on all-cause mortality among patients with diabetes in the veterans health administration. *Diabetes Care*, 30(7):1689–1693, 2007. pages 43

[145] John D Kalbfleisch and Ross L Prentice. *The statistical analysis of failure time data*, volume 360. John Wiley & Sons, 2011. pages 33

[146] WB Kannel and DL McGee. Diabetes and cardiovascular disease: The Framingham study. *JAMA*, 241(19):2035–2038, 1979. pages 141

[147] Maarten Keijzer and Vladan Babovic. Genetic programming, ensemble methods and the bias/variance tradeoff – introductory investigations. In Riccardo Poli, Wolfgang Banzhaf, William B. Langdon, Julian Miller, Peter Nordin, and Terence C. Fogarty, editors, *Genetic Programming*, volume 1802 of *Lecture Notes in Computer Science*, pages 76–90. Springer Berlin Heidelberg, 2000. pages 47, 76

[148] James Kennedy. Particle swarm optimization. In *Encyclopedia of Machine Learning*, pages 760–766. Springer, 2010. pages 88

[149] Hilary King, Ronald E Aubert, and William H Herman. Global burden of diabetes, 1995–2025: prevalence, numerical estimates, and projections. *Diabetes Care*, 21(9):1414–1431, 1998. pages 2, 122, 128

[150] Dmitri Kirpichnikov, Samy I McFarlane, and James R Sowers. Metformin: an update. *Annals of internal medicine*, 137(1):25–33, 2002. pages 22

[151] Ron Kohavi. A study of cross-validation and bootstrap for accuracy estimation and model selection. In *International Joint Conference on Artificial Intelligence*, volume 14, pages 1137–1145, 1995. pages 81, 82

[152] Eva M Kohner, Stephen J Aldington, Irene M Stratton, Susan E Manley, Rury R Holman, David R Matthews, and Robert C Turner. United Kingdom Prospective Diabetes Study, 30: diabetic retinopathy at diagnosis of non–insulin-dependent diabetes mellitus and associated risk factors. *Archives of Ophthalmology*, 116(3):297–303, 1998. pages 122

[153] I Köster, Liselotte Von Ferber, Peter Ihle, I Schubert, and Hans Hauner. The cost burden of diabetes mellitus: the evidence from germany—the CoDiM study. *Diabetologia*, 49(7):1498–1504, 2006. pages 21

[154] Alex Krizhevsky, Ilya Sutskever, and Geoffrey E Hinton. ImageNet classification with deep convolutional neural networks. In *Advances in neural information processing systems*, pages 1097–1105, 2012. pages 82

[155] Lawrence L Kupper, John M Karon, David G Kleinbaum, Hal Morgenstern, and Donald K Lewis. Matching in epidemiologic studies: validity and efficiency considerations. *Biometrics*, pages 271–291, 1981. pages 44

[156] David W Lam and Derek LeRoith. The worldwide diabetes epidemic. *Current Opinion in Endocrinology, Diabetes and Obesity*, 19(2):93–96, 2012. pages 20

[157] Ar Lazarevic, Aysel Ozgur, Levent Ertoz, Jaideep Srivastava, and Vipin Kumar. A comparative study of anomaly detection schemes in network intrusion detection. In *Proceedings of the Third SIAM International Conference on Data Mining*, 2003. pages 54

[158] Yann LeCun, Léon Bottou, Yoshua Bengio, and Patrick Haffner. Gradient-based learning applied to document recognition. In *Proceedings of the IEEE*, pages 2278–2324, 1998. pages 65

[159] Wee Sun Lee and Bing Liu. Learning with positive and unlabeled examples using weighted logistic regression. In *Proceedings of the Twentieth International Conference on Machine Learning (ICML)*, pages 448–455, 2003. pages 15, 55, 64, 128, 135

[160] Won Chan Lee, Sanjeev Balu, David Cobden, Ashish V Joshi, and Chris L Pashos. Medication adherence and the associated health-economic impact among patients with type 2 diabetes mellitus converting to insulin pen therapy: an analysis of third-party managed care claims data. *Clinical therapeutics*, 28(10):1712–1725, 2006. pages 151

[161] Xiaoli Li and Bing Liu. Learning to classify texts using positive and unlabeled data. In *IJCAI'03: Proceedings of the 18th international joint conference on Artificial intelligence*, pages 587–592, San Francisco, CA, USA, 2003. Morgan Kaufmann Publishers Inc. pages 14, 55

[162] Shih-Wei Lin, Kuo-Ching Ying, Shih-Chieh Chen, and Zne-Jung Lee. Particle swarm optimization for parameter determination and feature selection of support vector machines. *Expert systems with applications*, 35(4):1817–1824, 2008. pages 83

[163] Jaana Lindström and Jaakko Tuomilehto. The diabetes risk score a practical tool to predict type 2 diabetes risk. *Diabetes Care*, 26(3):725–731, 2003. pages 6, 123, 124, 139

[164] Bin Linghu and Bing-Yu Sun. Constructing effective SVM ensembles for image classification. In *Knowledge Acquisition and Modeling (KAM), 2010 3rd International Symposium on*, pages 80–83, 2010. pages 47

[165] Nikolas List and Hans Ulrich Simon. SVM-optimization and steepest-descent line search. In *Proceedings of the 22nd Annual Conference on Computational Learning Theory*, 2009. pages 47

[166] Bing Liu, Yang Dai, Xiaoli Li, Wee Sun Lee, and Philip S. Yu. Building text classifiers using positive and unlabeled examples. In *Proceedings of the Third IEEE International Conference on Data Mining*, ICDM '03, pages 179–186, Washington, DC, USA, 2003. IEEE Computer Society. pages 15, 54, 55, 98, 135, 136

[167] Bing Liu, Wee Sun Lee, Philip S. Yu, and Xiaoli Li. Partially supervised classification of text documents. In *ICML '02: Proceedings of the Nineteenth International Conference on Machine Learning*, pages 387–394, San Francisco, CA, USA, 2002. Morgan Kaufmann Publishers Inc. pages 14, 55, 135

[168] Zhigang Liu, Wenzhong Shi, Deren Li, and Qianqing Qin. Partially supervised classification – based on weighted unlabeled samples support vector machine. In *Proceedings of the First international conference on Advanced Data Mining and Applications*, ADMA'05, pages 118–129, Berlin, Heidelberg, 2005. Springer-Verlag. pages 15, 55

[169] Julie A Lovshin and Daniel J Drucker. Incretin-based therapies for type 2 diabetes mellitus. *Nature Reviews Endocrinology*, 5(5):262–269, 2009. pages 22

[170] Henry B Mann and Donald R Whitney. On a test of whether one of two random variables is stochastically larger than the other. *The annals of mathematical statistics*, pages 50–60, 1947. pages 131

[171] Michael Marmot, Sharon Friel, Ruth Bell, Tanja AJ Houweling, Sebastian Taylor, and Commission on Social Determinants of Health. Closing the gap in a generation: health equity through action on the social determinants of health. *The Lancet*, 372(9650):1661–1669, 2008. pages 149

[172] Ruben Martinez-Cantin. BayesOpt: A Bayesian optimization library for nonlinear optimization, experimental design and bandits. *arXiv preprint arXiv:1405.7430*, 2014. pages 89, 91, 92, 146

[173] Gonzalo Martínez-Muñoz and Alberto Suárez. Out-of-bag estimation of the optimal sample size in bagging. *Pattern Recognition*, 43(1):143–152, 2010. pages 60

[174] Colin D Mathers and Dejan Loncar. Projections of global mortality and burden of disease from 2002 to 2030. *PLOS Medicine*, 3(11):e442, 2006. pages 2

[175] Marguerite J McNeely, Edward J Boyko, Donna L Leonetti, Steven E Kahn, and Wilfred Y Fujimoto. Comparison of a clinical model, the oral glucose tolerance test, and fasting glucose for prediction of type 2 diabetes risk in Japanese Americans. *Diabetes Care*, 26(3):758–763, 2003. pages 6, 123, 124, 139

[176] Michael Meissner, Michael Schmuker, and Gisbert Schneider. Optimized particle swarm optimization (OPSO) and its application to artificial neural network training. *BMC bioinformatics*, 7(1):125, 2006. pages 83

[177] Ali H Mokdad, Earl S Ford, Barbara A Bowman, William H Dietz, Frank Vinicor, Virginia S Bales, and James S Marks. Prevalence of obesity, diabetes, and obesity-related health risk factors, 2001. *JAMA*, 289(1):76–79, 2003. pages 123, 141

[178] Fantine Mordelet and Jean-Philippe Vert. ProDiGe: Prioritization of disease genes with multitask machine learning from positive and unlabeled examples. *BMC bioinformatics*, 12(1):389, 2011. pages 47, 54, 57, 98, 101

[179] Fantine Mordelet and Jean-Philippe Vert. A bagging SVM to learn from positive and unlabeled examples. *Pattern Recognition Letters*, 37:201–209, 2014. pages 13, 15, 54, 55, 56, 57, 76, 98, 128, 135, 136, 145

[180] C Ll Morgan, J Mukherjee, S Jenkins-Jones, SE Holden, and CJ Currie. Association between first-line monotherapy with sulphonylurea versus metformin and risk of all-cause mortality and cardiovascular events: a retrospective, observational study. *Diabetes, Obesity and Metabolism*, 16(10):957–962, 2014. pages 27, 43

[181] Nick J Morrish, Shu-Li Wang, LK Stevens, JH Fuller, H Keen, and WHO Multinational Study Group. Mortality and causes of death in the who multinational study of vascular disease in diabetes. *Diabetologia*, 44(2):S14–S21, 2001. pages 20

[182] John A Morrison, Elizabeth M Cottingham, and Bruce A Barton. Metformin for weight loss in pediatric patients taking psychotropic drugs. *American Journal of Psychiatry*, 2014. pages 148

[183] David M Nathan, Mayer B Davidson, Ralph A Defronzo, Robert J Heine, Robert R Henry, Richard Pratley, and Bernard Zinman. Impaired fasting glucose and impaired glucose tolerance implications for care. *Diabetes Care*, 30(3):753–759, 2007. pages 5, 20

[184] Michael A Nauck, Tina Vilsbøll, Baptist Gallwitz, Alan Garber, and Sten Madsbad. Incretin-based therapies viewpoints on the way to consensus. *Diabetes Care*, 32(suppl 2):S223–S231, 2009. pages 22

[185] Peter Nemenyi. Distribution-free multiple comparisons. In *Biometrics*, volume 18, page 263, 1962. pages 73

[186] Gregory A Nichols and Jonathan B Brown. The impact of cardiovascular disease on medical care costs in subjects with and without type 2 diabetes. *Diabetes Care*, 25(3):482–486, 2002. pages 20, 21

[187] Kamal Nigam, Andrew K McCallum, Sebastian Thrun, and Tom Mitchell. Text classification from labeled and unlabeled documents using EM. *Machine Learning*, 39(2-3):103–134, 2000. pages 98

[188] Federation of European Academies of Medicine (FEAM). FEAM statement on data protection regulation. `http://www.feam-site.eu/cms/docs/publications/FEAMDataProtectionStatementJune2012.pdf`, 2012. [Online; accessed 2015-09-20]. pages 152

[189] Federation of European Academies of Medicine (FEAM). Joint statement on ensuring a healthy future for scientific research through the data protection regulation 2012/0011(COD). `http://www.feam-site.eu/cms/docs/publications/DPR/Data_Protection_jointstatement_July2015.pdf`, 2015. [Online; accessed 2015-09-20]. pages 152

[190] WHO Expert Committee on Diabetes Mellitus. Second report. 1980. Technical Report Series 646. pages 19

[191] World Health Organization. Poverty, social exclusion and health systems in the who european region, 2010. pages 149

[192] World Health Organization. *Guidelines for ATC classification and DDD assignment*. World Health Organization, 2015. pages 28

[193] World Health Organization and International Diabetes Federation. Definition and diagnosis of diabetes mellitus and intermediate hyperglycaemia: report of a WHO/IDF consultation. 2006. pages xxv, 5, 6

[194] David E Ost. The 'right' not to know. *Journal of Medicine and Philosophy*, 9(3):301–312, 1984. pages 151

[195] Edgar Osuna, Robert Freund, and Federico Girosi. Support Vector Machines: Training and Applications. Technical Report AIM-1602, 1997. pages 48, 56

[196] Xiao-Ren Pan, Guang-wei Li, Ying-Hua Hu, Ji-Xing Wang, Wen-Ying Yang, Zuo-Xin An, Ze-Xi Hu, Jina-Zhong Xiao, Hui-Bi Cao, and Ping-An Liu. Effects of diet and exercise in preventing NIDDM in people with impaired glucose tolerance: the Da Qing IGT and Diabetes Study. *Diabetes Care*, 20(4):537–544, 1997. pages 2, 123

[197] João P Papa, Gustavo H Rosa, Aparecido N Marana, Walter Scheirer, and David D Cox. Model selection for Discriminative Restricted Boltzmann Machines through meta-heuristic techniques. *Journal of Computational Science*, 9:14–18, 2015. pages 146

[198] PJ Park, Simon J Griffin, L Sargeant, and NJ Wareham. The performance of a risk score in predicting undiagnosed hyperglycemia. *Diabetes Care*, 25(6):984–988, 2002. pages 6, 123

[199] Stephen G Pauker. Deciding about screening. *Annals of internal medicine*, 118(11):901–902, 1993. pages 122

[200] Mykola Pechenizkiy, Alexey Tsymbal, Seppo Puuronen, and Oleksandr Pechenizkiy. Class noise and supervised learning in medical domains: The effect of feature extraction. In *Computer-Based Medical Systems, 2006. CBMS 2006. 19th IEEE International Symposium on*, pages 708–713. IEEE, 2006. pages 54

[201] Fabian Pedregosa, Gaël Varoquaux, Alexandre Gramfort, Vincent Michel, Bertrand Thirion, Olivier Grisel, Mathieu Blondel, Peter Prettenhofer, Ron Weiss, and Vincent Dubourg. Scikit-learn: Machine learning in Python. *Journal of Machine Learning Research*, 12:2825–2830, 2011. pages 80, 83, 86, 89, 93, 128, 136

[202] Manel Pladevall, L Keoki Williams, Lisa Ann Potts, George Divine, Hugo Xi, and Jennifer Elston Lafata. Clinical outcomes and adherence to medications measured by claims data in patients with diabetes. *Diabetes Care*, 27(12):2800–2805, 2004. pages 151

[203] John R Pleis, Jacqueline W Lucas, and Brian W Ward. Summary health statistics for us adults: National health interview survey, 2008. *Vital and health statistics. Series 10, Data from the National Health Survey*, (242):1–157, 2009. pages 149

[204] Marc Prentki and Christopher J Nolan. Islet β cell failure in type 2 diabetes. *Journal of Clinical Investigation*, 116(7):1802, 2006. pages 27

[205] Andreas Prlić and James B Procter. Ten simple rules for the open development of scientific software. *PLoS computational biology*, 8(12):e1002802, 2012. pages 146

[206] Danil Prokhorov. IJCNN 2001 neural network competition. *Slide presentation in IJCNN*, 2001. pages 50, 65

[207] Peter Proks, Frank Reimann, Nick Green, Fiona Gribble, and Frances Ashcroft. Sulfonylurea stimulation of insulin secretion. *Diabetes*, 51(suppl 3):S368–S376, 2002. pages 22

[208] Bruce M Psaty, Thomas D Koepsell, Danyu Lin, Noel S Weiss, David S Siscovick, Frits R Rosendaal, Marco Pahor, and Curt D Furberg. Assessment and control for confounding by indication in observational studies. *Journal of the American Geriatrics Society*, 47(6):749–754, 1999. pages 44

[209] Kamal Rahmouni, Marcelo LG Correia, William G Haynes, and Allyn L Mark. Obesity-associated hypertension: new insights into mechanisms. *Hypertension*, 45(1):9–14, 2005. pages 148

[210] Ulla Rajala, Mauri Laakso, Qing Qiao, and Sirkka Keinänen-Kiukaanniemi. Prevalence of retinopathy in people with diabetes, impaired glucose tolerance, and normal glucose tolerance. *Diabetes Care*, 21(10):1664–1669, 1998. pages 4, 122

[211] J Sunil Rao and Robert Tibshirani. The out-of-bootstrap method for model averaging and selection. *University of Toronto*, 1997. pages 59

[212] Gerald M Reaven. Role of insulin resistance in human disease. *Diabetes*, 37(12):1595–1607, 1988. pages 20

[213] Jared P Reis, Catherine M Loria, Paul D Sorlie, Yikyung Park, Albert Hollenbeck, and Arthur Schatzkin. Lifestyle factors and risk for new-onset diabetes: a population-based cohort study. *Annals of internal medicine*, 155(5):292–299, 2011. pages 123

[214] Lisa Riste, Farida Khan, and Kennedy Cruickshank. High prevalence of type 2 diabetes in all ethnic groups, including europeans, in a british inner city relative poverty, history, inactivity, or 21st century europe? *Diabetes Care*, 24(8):1377–1383, 2001. pages 149

[215] Albert P Rocchini. Childhood obesity and a diabetes epidemic. *New England Journal of Medicine*, 346(11):854–855, 2002. pages 20

[216] Gojka Roglic, Nigel Unwin, Peter H Bennett, Colin Mathers, Jaakko Tuomilehto, Satyajit Nag, Vincent Connolly, and Hilary King. The burden of mortality attributable to diabetes realistic estimates for the year 2000. *Diabetes Care*, 28(9):2130–2135, 2005. pages 20

[217] Kenneth J Rothman, Sander Greenland, and Timothy L Lash. *Modern epidemiology*. Lippincott Williams & Wilkins, 2008. pages 31

[218] Christianne L Roumie, Adriana M Hung, Robert A Greevy, Carlos G Grijalva, Xulei Liu, Harvey J Murff, Tom A Elasy, and Marie R Griffin. Comparative effectiveness of sulfonylurea and metformin monotherapy on cardiovascular events in type 2 diabetes mellitus: a cohort study. *Annals of internal medicine*, 157(9):601–610, 2012. pages 27, 43

[219] Olivier Roustant, David Ginsbourger, and Yves Deville. DiceKriging, DiceOptim: Two R packages for the analysis of computer experiments by kriging-based metamodeling and optimization. 2012. pages 89

[220] Donald B Rubin. Using multivariate matched sampling and regression adjustment to control bias in observational studies. *Journal of the American Statistical Association*, 74(366a):318–328, 1979. pages 44

[221] Robert J Rubin, William M Altman, and Daniel N Mendelson. Health care expenditures for people with diabetes mellitus, 1992. *The Journal of Clinical Endocrinology & Metabolism*, 78(4):809A–809F, 1994. pages 122

[222] Alan R Saltiel and Jerrold M Olefsky. Thiazolidinediones in the treatment of insulin resistance and type II diabetes. *Diabetes*, 45(12):1661–1669, 1996. pages 22

[223] Dean Schillinger, Kevin Grumbach, John Piette, Frances Wang, Dennis Osmond, Carolyn Daher, Jorge Palacios, Gabriela Diaz Sullivan, and Andrew B Bindman. Association of health literacy with diabetes outcomes. *JAMA*, 288(4):475–482, 2002. pages 149

[224] Bernhard Schölkopf, John C Platt, John Shawe-Taylor, Alex J Smola, and Robert C Williamson. Estimating the support of a high-dimensional distribution. *Neural computation*, 13(7):1443–1471, 2001. pages 108

[225] Bernhard Schölkopf and Alexander J Smola. *Learning with kernels: support vector machines, regularization, optimization, and beyond*. MIT press, 2002. pages 80, 81, 83

[226] Tina Ken Schramm, Gunnar Hilmar Gislason, Allan Vaag, Jeppe Nørgaard Rasmussen, Fredrik Folke, Morten Lock Hansen, Emil Loldrup Fosbøl, Lars Køber, Mette Lykke Norgaard, and Mette Madsen. Mortality

and cardiovascular risk associated with different insulin secretagogues compared with metformin in type 2 diabetes, with or without a previous myocardial infarction: a nationwide study. *European heart journal*, 32(15):1900–1908, 2011. pages 43

[227] Matthias B Schulze, Kurt Hoffmann, Heiner Boeing, Jakob Linseisen, Sabine Rohrmann, Matthias Möhlig, Andreas FH Pfeiffer, Joachim Spranger, Claus Thamer, and Hans-Ulrich Häring. An accurate risk score based on anthropometric, dietary, and lifestyle factors to predict the development of type 2 diabetes. *Diabetes Care*, 30(3):510–515, 2007. pages 6, 123, 124, 139

[228] Peter EH Schwarz, Jiang Li, Manja Reimann, Alta E Schutte, Antje Bergmann, Markolf Hanefeld, Stefan R Bornstein, Jan Schulze, Jaakko Tuomilehto, and Jaana Lindstrom. The Finnish Diabetes Risk Score is associated with insulin resistance and progression towards type 2 diabetes. *The Journal of Clinical Endocrinology & Metabolism*, 94(3):920–926, 2009. pages 123

[229] Clayton Scott and Gilles Blanchard. Novelty detection: Unlabeled data definitely help. In *Proc. of the 12th International Conference on Artificial Intelligence and Statistics*, pages 464–471, 2009. pages 98, 108

[230] Konstantinos Sechidis, Borja Calvo, and Gavin Brown. Statistical hypothesis testing in positive unlabelled data. In *Machine Learning and Knowledge Discovery in Databases*, pages 66–81. Springer, 2014. pages 15, 98, 101

[231] Holbrooke S Seltzer. Drug-induced hypoglycemia. a review of 1418 cases. *Endocrinology and metabolism clinics of North America*, 18(1):163–183, 1989. pages 123

[232] E Shafrir. Development and consequences of insulin resistance: lessons from animals with hyperinsulinaemia. *Diabetes & metabolism*, 22(2):122–131, 1996. pages 19

[233] Iris Shai, Rui Jiang, JoAnn E Manson, Meir J Stampfer, Walter C Willett, Graham A Colditz, and Frank B Hu. Ethnicity, obesity, and risk of type 2 diabetes in women a 20-year follow-up study. *Diabetes Care*, 29(7):1585–1590, 2006. pages 123

[234] Salimah Z Shariff, Meaghan S Cuerden, Arsh K Jain, and Amit X Garg. The secret of immortal time bias in epidemiologic studies. *Journal of the American Society of Nephrology*, 19(5):841–843, 2008. pages 31

[235] Jonathan E Shaw, Richard A Sicree, and Paul Z Zimmet. Global estimates of the prevalence of diabetes for 2010 and 2030. *Diabetes research and clinical practice*, 87(1):4–14, 2010. pages 20

[236] Brian K. Shoichet. Virtual screening of chemical libraries. *Nature*, 432(7019):862–865, December 2004. pages 54

[237] Dorota Sienkiewicz. Access to health services in Europe. [Online; accessed 2015-11-08; `http://www.socialwatch.eu/wcm/access_to_health_services.html`]. pages 149

[238] Alejandro Sifrim, Dusan Popovic, Léon-Charles Tranchevent, Amin Arderschirdavani, Ryo Sakai, Peter Konings, Joris Vermeesch, Jan Aerts, Bart De Moor, and Yves Moreau. eXtasy: Variant prioritization by genomic data fusion. *Nature Methods*, 10:1083–1084, 2013. pages 54, 98, 101

[239] Elaine Silverman and Jonathan Skinner. Medicare upcoding and hospital ownership. *Journal of health economics*, 23(2):369–389, 2004. pages 12

[240] DD Sin and ER Sutherland. Obesity and the lung: 4 · obesity and asthma. *Thorax*, 63(11):1018–1023, 2008. pages 148

[241] Simon Smyth and Andrew Heron. Diabetes and obesity: the twin epidemics. *Nature medicine*, 12(1):75–80, 2006. pages 19, 20

[242] Jasper Snoek, Hugo Larochelle, and Ryan P Adams. Practical Bayesian optimization of machine learning algorithms. In *Advances in Neural Information Processing Systems*, pages 2951–2959, 2012. pages 16, 83, 89, 91, 92, 146

[243] P Sonksen and J Sonksen. Insulin: understanding its action in health and disease. *British journal of anaesthesia*, 85(1):69–79, 2000. pages 18

[244] Soren Sonnenburg, Mikio L Braun, Cheng Soon Ong, Samy Bengio, Leon Bottou, Geoffrey Holmes, Yann LeCun, Klaus-Robert Müller, Fernando Pereira, and Carl E Rasmussen. The need for open source software in machine learning. *Journal of Machine Learning Research*, 2007. pages 16, 146

[245] Annemieke MW Spijkerman, Matthew F Yuyun, Simon J Griffin, Jacqueline M Dekker, Giel Nijpels, and Nicholas J Wareham. The performance of a risk score as a screening test for undiagnosed hyperglycemia in ethnic minority groups data from the 1999 health survey for England. *Diabetes Care*, 27(1):116–122, 2004. pages 6, 123, 139

[246] Paul JM Steinbusch, Jan B Oostenbrink, Joost J Zuurbier, and Frans JM Schaepkens. The risk of upcoding in casemix systems: a comparative study. *Health policy*, 81(2):289–299, 2007. pages 12

[247] Michael P Stern, Ken Williams, and Steven M Haffner. Identification of persons at high risk for type 2 diabetes mellitus: do we need the oral glucose tolerance test? *Annals of Internal Medicine*, 136(8):575–581, 2002. pages 6, 123, 124, 139

[248] Henrik Støvring, Morten Andersen, Henning Beck-Nielsen, Anders Green, and Werner Vach. Rising prevalence of diabetes: evidence from a danish pharmacoepidemiological database. *The Lancet*, 362(9383):537–538, 2003. pages 20

[249] Tim JT Sutherland, Jan O Cowan, Sarah Young, Ailsa Goulding, Andrea M Grant, Avis Williamson, Karen Brassett, G Peter Herbison, and D Robin Taylor. The association between obesity and asthma: interactions between systemic and airway inflammation. *American journal of respiratory and critical care medicine*, 178(5):469–475, 2008. pages 148

[250] Ilya Sutskever, Oriol Vinyals, and Quoc VV Le. Sequence to sequence learning with neural networks. In *Advances in Neural Information Processing Systems*, pages 3104–3112, 2014. pages 82

[251] Deborah PM Symmons, Clare R Bankhead, Beverley J Harrison, Paul Brennan, Alan J Silman, Elizabeth M Barrett, and David GI Scott. Blood transfusion, smoking, and obesity as risk factors for the development of rheumatoid arthritis. results from a primary care-based incident case-control study in norfolk, england. *Arthritis & Rheumatism*, 40(11):1955–1961, 1997. pages 148

[252] R Core Team. R: A language and environment for statistical computing. r foundation for statistical computing, vienna, austria, 2012, 2014. pages 33

[253] Terry Therneau. A package for survival analysis in s. r package version 2.37-4. *http://CRAN.R-project.org/package=survival*, 980032:23298–0032, 2013. pages 33

[254] Chris Thornton, Frank Hutter, Holger H Hoos, and Kevin Leyton-Brown. Auto-weka: Combined selection and hyperparameter optimization of classification algorithms. In *Proceedings of the 19th ACM SIGKDD international conference on Knowledge discovery and data mining*, pages 847–855. ACM, 2013. pages 16

[255] Makoto Tominaga, Hideyuki Eguchi, Hideo Manaka, Kimiko Igarashi, Takeo Kato, and Akira Sekikawa. Impaired glucose tolerance is a risk factor for cardiovascular disease, but not impaired fasting glucose. The Funagata Diabetes Study. *Diabetes Care*, 22(6):920–924, 1999. pages 5

[256] Jinn-Tsong Tsai, Jyh-Horng Chou, and Tung-Kuan Liu. Tuning the structure and parameters of a neural network by using hybrid taguchi-genetic algorithm. *Neural Networks, IEEE Transactions on*, 17(1):69–80, 2006. pages 83

[257] Jaakko Tuomilehto, Jaana Lindström, Johan G Eriksson, Timo T Valle, Helena Hämäläinen, Pirjo Ilanne-Parikka, Sirkka Keinänen-Kiukaanniemi, Mauri Laakso, Anne Louheranta, and Merja Rastas. Prevention of type 2 diabetes mellitus by changes in lifestyle among subjects with impaired glucose tolerance. *New England Journal of Medicine*, 344(18):1343–1350, 2001. pages 2, 5, 122, 123

[258] Robert C Turner, Carole A Cull, Valeria Frighi, Rury R Holman, and UK Prospective Diabetes Study (UKPDS) Group. Glycemic control with diet, sulfonylurea, metformin, or insulin in patients with type 2 diabetes mellitus: progressive requirement for multiple therapies (UKPDS 49). *JAMA*, 281(21):2005–2012, 1999. pages 122

[259] Ioanna Tzoulaki, Mariam Molokhia, Vasa Curcin, Mark P Little, Christopher J Millett, Anthea Ng, Robert I Hughes, Kamlesh Khunti, Martin R Wilkins, and Azeem Majeed. Risk of cardiovascular disease and all cause mortality among patients with type 2 diabetes prescribed oral antidiabetes drugs: retrospective cohort study using uk general practice research database. *Bmj*, 339, 2009. pages 27, 43

[260] N Unwin, Jonathan Shaw, Paul Zimmet, and Kurt GMM Alberti. Impaired glucose tolerance and impaired fasting glycaemia: the current status on definition and intervention. *Diabetic medicine*, 19(9):708–723, 2002. pages 5

[261] Giorgio Valentini and Thomas G Dietterich. Low bias bagged support vector machines. In *ICML*, pages 752–759, 2003. pages 47, 50

[262] Greet Van den Berghe, Alexander Wilmer, Greet Hermans, Wouter Meersseman, Pieter J Wouters, Ilse Milants, Eric Van Wijngaerden, Herman Bobbaers, and Roger Bouillon. Intensive insulin therapy in the medical ICU. *New England Journal of Medicine*, 354(5):449, 2006. pages 131

[263] Greet Van den Berghe, Pieter Wouters, Frank Weekers, Charles Verwaest, Frans Bruyninckx, Miet Schetz, Dirk Vlasselaers, Patrick Ferdinande,

Peter Lauwers, and Roger Bouillon. Intensive insulin therapy in critically ill patients. *New England Journal of Medicine*, 345(19):1359–1367, 2001. pages 131

[264] R Van den Oever and C Volckaert. Financing health care in Belgium. The nomenclature: from fee-for-service to budget-financing. *Acta chirurgica Belgica*, 108(2):157, 2008. pages 9, 126

[265] Aad W Van der Vaart. *Asymptotic Statistics*, volume 3. Cambridge university press, 2000. pages 107

[266] Stefan Van Der Walt, S Chris Colbert, and Gael Varoquaux. The NumPy array: a structure for efficient numerical computation. *Computing in Science & Engineering*, 13(2):22–30, 2011. pages 128

[267] Sudhir Varma and Richard Simon. Bias in error estimation when using cross-validation for model selection. *BMC bioinformatics*, 7(1):91, 2006. pages 129

[268] Joan Vlayen, Cindy De Gendt, Sabine Stordeur, Viki Schillemans, Cécile Camberlin, France Vrijens, Elizabeth Van Eycken, and Toni Lerut. Quality indicators for the management of upper gastrointestinal cancer. *Good Clinical Practice (GCP), Belgian Health Care Knowledge Centre (KCE)*, 2013. KCE Reports 200 D/2013/10.273/15. pages 151

[269] Shi-jin Wang, Avin Mathew, Yan Chen, Li-feng Xi, Lin Ma, and Jay Lee. Empirical analysis of support vector machine ensemble classifiers. *Expert Systems with Applications*, 36(3, Part 2):6466 – 6476, 2009. pages 47, 50

[270] Nicholas J Wareham and Simon J Griffin. Should we screen for type 2 diabetes? evaluation against national screening committee criteria. *BMJ: British Medical Journal*, 322(7292):986, 2001. pages 4, 123

[271] Johan Wens, Patricia Sunaert, Frank Nobels, Paul Van Crombrugge, Hilde Bastiaens, and Paul Van Royen. Aanbeveling voor goede medische praktijkvoering: Diabetes mellitus type 2. *Berchem/Gent: Domus Medica*, 2005. pages 7

[272] S Wheeler, K Moore, CW Forsberg, K Riley, JS Floyd, NL Smith, and EJ Boyko. Mortality among veterans with type 2 diabetes initiating metformin, sulfonylurea or rosiglitazone monotherapy. *Diabetologia*, 56(9):1934–1943, 2013. pages 43, 151

[273] WHO Collaborating Centre for Drug Statistics Methodology. *Guidelines for ATC classification and DDD assignment*. World Health Organization, 2015. pages 10, 125

[274] Hadley Wickham. *ggplot2: elegant graphics for data analysis*. Springer Science & Business Media, 2009. pages 33

[275] David H Wolpert and William G Macready. No free lunch theorems for optimization. *Evolutionary Computation, IEEE Transactions on*, 1(1):67–82, 1997. pages 146

[276] World Health Organization. Prevention of diabetes mellitus: report of a WHO study group [meeting held in geneva from 16 to 20 november 1992]. (WHO technical report number 844), 1994. pages 4, 122, 123, 127

[277] World Health Organization. International classification of diseases (ICD). 2012. pages 127

[278] Samuel Xavier-de Souza, Johan AK Suykens, Joos Vandewalle, and Désiré Bollé. Coupled simulated annealing. *Systems, Man, and Cybernetics, Part B: Cybernetics, IEEE Transactions on*, 40(2):320–335, 2010. pages 83

[279] Wenying Yang, Juming Lu, Jianping Weng, Weiping Jia, Linong Ji, Jianzhong Xiao, Zhongyan Shan, Jie Liu, Haoming Tian, and Qiuhe Ji. Prevalence of diabetes among men and women in china. *New England Journal of Medicine*, 362(12):1090–1101, 2010. pages 20

[280] Hannele Yki-Järvinen. Thiazolidinediones. *New England Journal of Medicine*, 351(11):1106–1118, 2004. pages 22

[281] Lawrence H Young, J Th Frans, Deborah A Chyun, Janice A Davey, Eugene J Barrett, Raymond Taillefer, Gary V Heller, Ami E Iskandrian, Steven D Wittlin, and Neil Filipchuk. Cardiac outcomes after screening for asymptomatic coronary artery disease in patients with type 2 diabetes: the diad study: a randomized controlled trial. *Jama*, 301(15):1547–1555, 2009. pages 18

[282] Hwanjo Yu. Single-class classification with mapping convergence. *Machine Learning*, 61(1-3):49–69, November 2005. pages 14, 55, 135

[283] Hwanjo Yu, Jiawei Han, and KC-C Chang. PEBL: Web page classification without negative examples. *IEEE Transactions on Knowledge and Data Engineering*, 16(1):70–81, 2004. pages 98

[284] Hwanjo Yu, Jiawei Han, and Kevin C. Chang. PEBL: positive example based learning for web page classification using SVM. In *KDD '02: Proceedings of the eighth ACM SIGKDD international conference on Knowledge discovery and data mining*, pages 239–248, New York, NY, USA, 2002. ACM Press. pages 54

[285] Matei Zaharia, Mosharaf Chowdhury, Michael J Franklin, Scott Shenker, and Ion Stoica. Spark: cluster computing with working sets. In *Proceedings of the 2nd USENIX conference on Hot topics in cloud computing*, pages 1–7, 2010. pages 89

[286] Nicola N Zammitt and Brian M Frier. Hypoglycemia in type 2 diabetes pathophysiology, frequency, and effects of different treatment modalities. *Diabetes Care*, 28(12):2948–2961, 2005. pages 2, 123

[287] Xingquan Zhu and Xindong Wu. Class noise vs. attribute noise: A quantitative study. *Artificial Intelligence Review*, 22(3):177–210, 2004. pages 54

[288] Paul Zimmet. Diabetes epidemiology as a tool to trigger diabetes research and care. *Diabetologia*, 42(5):499–518, 1999. pages 20

[289] Paul Zimmet. Globalization, coca-colonization and the chronic disease epidemic: can the doomsday scenario be averted? *Journal of internal medicine*, 247(3):301–310, 2000. pages 2

[290] Paul Zimmet, Kurt GMM Alberti, and Jonathan Shaw. Global and societal implications of the diabetes epidemic. *Nature*, 414(6865):782–787, 2001. pages 2, 5, 19, 20, 122

List of publications

International journal papers (published)

- Claesen, M., De Smet, F., Suykens, J. A. K., & De Moor, B. (2014). "*EnsembleSVM: A library for ensemble learning using support vector machines*". Journal of Machine Learning Research, 15(1), 141–145.
- Claesen, M., De Smet, F., Suykens, J. A. K., & De Moor, B. (2015). "*A robust ensemble approach to learn from positive and unlabeled data using SVM base models*". Neurocomputing, 160, 73-84.

International journal papers (submitted)

- Claesen, M., De Smet, F., Gillard, P., Mathieu, C. & De Moor, B. (2015). "*Building Classifiers to Predict the Start of Glucose-Lowering Pharmacotherapy Using Belgian Health Expenditure Data*".
  Submitted to Journal of Machine Learning Research.
- Claesen, M., Gillard, P., De Smet, F., Callens, M., De Moor, B. & Mathieu, C. (2015). "*Mortality in individuals treated with glucose lowering agents: a large, controlled cohort study*".
  Submitted to Journal of Clinical Endocrinology and Metabolism.
- Claesen, M., Simm, J., Popovic, D., Moreau, Y., & De Moor, B. (2015). "*Easy hyperparameter search using Optunity*".
  Submitted to Journal of Machine Learning Research.

International conference papers (published)

- Claesen, M., & De Moor, B. (2015). "*Hyperparameter Search in Machine Learning*". In Proceedings of the 11th Metaheuristics International Conference (MIC), Agadir, Morocco.
  Manuscript available at `http://arxiv.org/abs/1502.02127`.

International conference papers (to be submitted)

- Claesen, M., Davis, J., De Smet, F., & De Moor, B. (2015). "*Assessing Binary Classifiers Using Only Positive and Unlabeled Data*",
  Will be submitted to the 22nd ACM SIGKDD Conference on Knowledge Discovery and Data Mining (ACM SIGKDD 2016).

Conference abstracts

- Claesen, M. & De Moor, B. (2013). "*An overview of the EnsembleSVM software package*". In International Workshop on Technical Computing for Machine Learning and Mathematical Engineering. Leuven, Belgium.
- Claesen, M, Simm, J., Popovic, D. (2013). & De Moor, B. "*Hyperparameter tuning in Python using Optunity*". In International Workshop on Technical Computing for Machine Learning and Mathematical Engineering. 2014. Leuven, Belgium.
- Claesen, M. & De Moor, B. (2014). "*Efficient Ensemble Learning With Support Vector Machines*" BENELEARN. Brussels, Belgium.



FACULTY OF ENGINEERING SCIENCE
DEPARTMENT OF ELECTRICAL ENGINEERING
STADIUS CENTER FOR DYNAMICAL SYSTEMS, SIGNAL PROCESSING AND DATA ANALYTICS
Kasteelpark Arenberg 10, bus 2446
B-3001 Leuven
marc.claesen@esat.kuleuven.be
http://esat.kuleuven.be/stadius